Università degli Studi di Cagliari

DOTTORATO DI RICERCA

Ciclo XXIX

Natural and Nature Inspired Compounds Targeting the Replication Cycle of RNA Viruses and GABA$_A$ Receptor

Settore scientifico disciplinare di afferenza

CHIM/08

Presentata da:	Mr. Vijay Prakash Sonar
Coordinatore Dottorato	Prof. Enzo Tramontano
Tutor	Dr. Filippo Cottiglia

Esame finale anno accademico 2015-2016

Tesi discussa nella sessione d'esame marzo – aprile 2017

Table of Contents

ACKNOWLEDGEMENTS

ABBREVIATIONS

ABTS   2,2-Azino-bis (3-ethylbenzothiazoline-6-sulfonic acid) diammonum salt

AIDS   Acquired Immuno Deficiency Syndrome

AZT   Azidothymidine

CC   Column Chromatography

CNS   Central Nervous System

DCM   Dichloromethane

DMAP   Dimethyl Amino pyridine

DNA   Deoxyribose Nucleic Acid

DPPH   1, 1- Diphenyl-2- picrylhydrazyl

DQF-COSY   Double Quantum Filtered-COrrelation SpectroscopY

ELISA   Enzyme linked immune sorbent assay

ESI MS   Electron Spray Ionization mass spectrometry

GABA γ-Amino Butyric Acid

HAART   Highly active antiretroviral therapy

HIV   Human immuno deficiency virus

HMBC   Heteronuclear Multiple Bond Correlation

HPLC   High Performance Liquid Chromatography

HRV   Human Rhinovirus

HSQC   Heteronuclear Single Quantum Coherence spectroscopy

ICAM-1   Intracellular Adhesion Molecule-1

IPSC   Inhibitory Postsynaptic Currents

LDLR   Low Density Lipoprotein Receptor

MeOH   Methanol

NMR	Nuclear Magnetic Resonance
NNRTI	Non-Nucleoside Reverse Transcriptase Inhibitor
NRTI	Nucleoside/ Nucleotide reverse transcriptase inhibitor
QMPL	QM-Polarized Ligand
RDDP	RNA-dependent DNA polymerase
RNA	Ribonucleic acid
RNase H	Ribonuclease H
ROESy	Rotating-frame Overhauser SpectroscoPY
RT	Reverse Transcriptase
SIV	Simian Immuno Deficiency Virus
SPE	Solid Phase Extraction
TEA	Triethylamine
TFAA	Trifluroacetic acid
TLC	Thin Layer Chromatography
VLC	Vacuum Liquid Chromatography
WHO	World Health Organization
WSe	*Withania somnifera* extract

SUMMARY

A bioassay-guided approach was used to isolate bioactive secondary metabolites from four different plants. Two Indian plants namely, *O. sanctum* and *T. cordifolia* were studied targeting HIV-1 RT associated RNase H function. Among the twenty secondary metabolites isolated from these plants, the triterpenoids **Ursolic acid** (**2**) and **Lupeol** (**22**) were the most potent inhibitors of RNase H function with a IC_{50} of 5.5 µM and 5.9 µM, respectively. **Rabdosiin** (**19**), from *O. sanctum*, was found as a most potent natural compound against RNase H (IC_{50}= 2.16 µM). Also, Rabdosiin was able to inhibit RDDP function (IC_{50}= 4.0 µM) of reverse transcriptase, resulted as a dual inhibitor of HIV-1 RT. Using **tetradecyl ferulate** (**8**) as lead compound, a series of esters and amides of ferulic and caffeic acid were synthesized. Newly synthesized compounds resulted as dual inhibitor of HIV-1 RT. Molecular modeling studies, together with Yonetani-Theorell analysis, demonstrated that one of the most active compounds, ***n*-oleyl caffeamide** (**18f**), is able to bind both RNase allosteric site and NNRTI binding pocket.

Bioguided isolation of the anti-Human Rhinovirus (HRV) DCM extract of *Bupleurum fruticosum* L., a plant growing in Sardinia, gave ten compounds. Among all, **Fruticotriol** (**31**) and (-)-**Eucamanol** (**40**) are new to the literature. An ester of 3,4-dimethoxycinnamyl alcohol (**34**) was found the most active metabolite inhibiting the replication of HRV 39 serotype with an EC_{50} of 0.9 µg/ml with moderate toxicity (CC_{50} = 7.6 µg/ml). A time-of-drug addition assay suggested that the ester of 3,4-dimethoxycinnamyl alcohol behave as capsid binder towards HRV39 and also acts by another mode of action, probably based on the uncoating of viral genome.

The methanol extract of *Withania somnifera* was studied for its $GABA_A$ modulation activity. Two new compounds named Withasomniferolide A (**41**) and Withasomniferolide B (**42**) have been isolated besides seven known compounds. Among all, docosanyl ferulate (**46**) showed positive modulation of $GABA_A$ receptor while octadecyl ferulate (**44**) and withasomniferolide B have shown negative modulation.

In summary, this PhD work permitted to discover some natural and natural-derived compounds that may offer a new class of interesting lead compounds for further optimization.

Chapter 1 Introduction

1.1 Herbal medicine

Plants have fulfilled all needs of mankind throughout the ages. Humans have relied on nature for food, shelter, cloths, flavors and fragrance etc. and not the least, medicines. Plants have been utilized as medicines for thousands of years. The use of natural products with therapeutic potential is as old as human civilization. These natural medicines have given the foundation to traditional medicine system which is still exists and continues to serve mankind and by providing new remedies. Initially herbal medicines were taken in crude form. For example, crude powder, intact leaves, fruits, flowers, roots, tinctures, poultices and other formulations. With the progression of human society and civilization the use of the plants as medicine has evolved. Isolation of bioactive compounds from the plants was a milestone in the history of drug discovery. Purified bioactive compounds have proven themselves as an effective drug and have given lead to the drug development process.

Herbal drugs have been used since ages in the treatment of several diseases. In the context of medicine herbs are defines as, *crude drugs of vegetable origin utilized for the treatment of disease states, often of a chronic nature, or to attain or to maintain a condition of improved health* [1]. Pharmaceutical preparations made by extracting herbs with various solvents to yield tinctures, fluid extracts, extracts, or the like are known as phytomedicinals (plant medicines) [1]. According to the World Health Organization (WHO) definition; herbal drugs are those which contain, as active ingredients, plant parts or plant materials in the crude or processed state plus certain excipients, i.e., solvents, diluents or preservatives [2].

Plants served as sources of drug and drug discovery in different forms like -

➢ Extracts prepared from herbs as botanical drugs, e.g. green tea.
➢ Bioactive compounds isolated from plants, like digoxin.
➢ Chemical structure of bioactive compounds may be useful as a lead compound for development of more potent compounds e.g Paclitaxel from *Taxus brevifolia*.
➢ A novel chemophore that can be engineered into drug.

➢ Pure form of phytochemical can be used as a pharmacological tool and as a marker compound for standardization of crude plant material and extracts.

In the recent era of herbal revitalization, the demand of herbal medicines is increasing steadily. Medicinal plants have been used therapeutically all around the world, being an important aspect of various traditional medicine systems. Traditional medicine may contrtibute to the treatment of several diseases. In high-income countries, the extensive use of phytotherapy declined due to the development and production of synthetic medicines. During the past few decades, however, phytotherapy has started to be increasingly used even in industrialized countries. In low and middle income countries, phytotherapy never stopped being important, often signifying the only therapeutic system to which certain people could refer. The World Medicines Situation report of WHO estimates that 70 to 95% of the population in developing countries consume traditional medicines and that every country in the world uses them in some capacity [3].

Research of herbal medicines has always given a boost to modern system of medicine. Before the invention of high throughput techniques and modern methods of drug discovery, more than 80% of the drug substances were purely natural products or were inspired from naturally derived molecule [4]. It is estimated that about 25% of the modern medicines are directly or indirectly derived from higher plants [2,5,6]. An analysis report on sources of new drugs during the period of 1981-2007 revealed that almost half of the drugs approved since 1994 were based on natural products [4]. According to WHO 65-80% of the world's population, living in developing countries uses herbal medicine as their source of primary health care [2]. The consumption of plant-based medicines and other botanicals in the western world has increased manifold in recent years. For example, between 1990 and 2000, an increase of over 380 % in sales in the United States was recorded [7]. India and China are the countries with great varieties of medicinal plant. Traditional Chinese medicine uses over 5000 plant species; The Indian system of traditional medicine uses about 7000 plant species [8].

1.1.1 Economy of herbal medicine

The potential of *phytomedicine*s or herbal medicines is very large. According to an estimation of WHO (1980) world traded amount of herbal medicine is about $500 million per year [9]. According to WHO estimates, the present demand for medicinal plants is approximately US $80 billion a year and by the year 2050 it would raise to US $5 trillion. It is estimated that the European market alone reached about $7 billion in 1997. The German market corresponds to about 50% of the European market, about $3.5 billion which represents about $42.90 per capita. This market is followed by France, $1.8 billion; Italy, $700 million; the United Kingdom, $400 million; Spain, $300 million; the Netherlands, about $100 million [10]. The herbal medical database indicates that the herbal medicine markets in Asia and Japan reach $2.3 and 2.1 billion, respectively [11]. However, in no other country has the herbal medicine marketplace grown more than it has in USA. A few years ago, this was a non-existent category of medicine. According to Grünwald, the *phytomedicinel*s market has grown at an expressive rate from 5% to 18% a year worldwide since 1985 [11].

Statistics mentioned above indicate the growth and potential input of herbal medicine to the world economy as well as its contribution to healthcare of mankind. Several important factors have contributed to the growth of the phytomedicine market. Synthetic medicines are costly and have undesirable side effects. On the contrary *phytomedicine*s are relatively cheaper and are believed to be free from side effects or to have less. The belief that herbal medicine could be alternative to some critical diseases where modern medicine have failed to perform is yet another reason. In countries like India and China with huge population, traditional systems of medicines are based on use of natural medicines and people have faith over them. Ease of availability at fair price etc. are some of the reasons.

1.1.2 The importance of natural products as source of new drugs

In the past herbal drugs were applied in the form of crude plant or parts of plant. Some were taken orally in the form of powder, tincture, extracted juices etc. In the 19th century, with the isolation of morphine from opium, it was begun to employ the pure active ingredients rather than whole extracts [12]. The isolation of morphine marked a new period during which the use of

pure compounds was preferred to whole plant. After the discovery of morphine a lot of plant-originated drugs have been discovered and various secondary metabolites are currently in use such as, for example, quinine from *Cinchona* species, cardiac glycosides from *Digitalis purpurea*, vinblastine and vincristine from *Catharanthus roseus*, taxol from *Taxus brevifolia* and the antimalarial compound, artemisinin, from *Artemisia annua*.

Natural products have high structural diversity and complexity with well organized three dimensional chemical and sterric properties. This offers many advantages in terms of efficacy and selectivity of molecular target. Natural products still represent a rich source in the discovery and development of new medicines and a significant part of the therapeutic armamentarium of doctors is represented by natural medicines or natural-derived products. Even at the dawn of 21st century, 11% of the 252 drugs considered as basic and essential by the WHO were exclusively of flowering plant origin [13]. 54% of the total anti-cancer drugs approved during the time frame of about 1940-2002 were naturally derived or inspired from the knowledge of natural products [14]. 64% of the newly synthesized anti-hypertensive drugs during the period of 1981-2002 have their origin from natural products [14]. Among the 69 new drug approved worldwide during the time frame of 2005-2007, 13 were natural products or originated from natural products [14-16].

Following are some of the examples of approved drugs from natural sources.

Galanthamine is an alkaloid isolated from the bulbs and flowers of *Galanthus caucasicus*. It is used in treatment of mild to moderate Alzheimers disease and other memory impairmnet problems. Galanthamine was discovered in early 1950's but it is approved by USFDA and was first marketed in USA in 2001 [17].
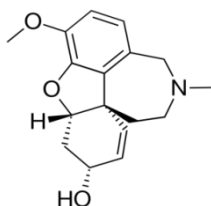
Galanthamine

Nitisinone is a derivative of leptospermone, a natural phytotoxin obtained from the Australlian bottle brush plant (*Callistemon citrinus*). Nitisinone was approved by FDA in 2002 for the treatment of hereditary tyrosinemia type-1 [18].
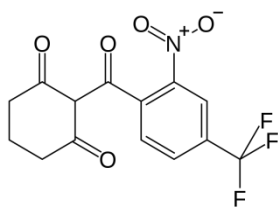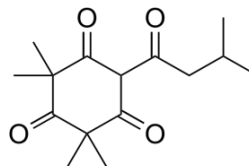
Nitisinone   Leptospermone

Apomorphine, a synthetic derivative of morphine, is a short acting dopamine D_1 and D_2 receptor agonist [19]. In 2004 Apomorphine was approved by FDA as an injectable drug for the treatment of Parkinson's disease, for patients with episodes of hypomobility [20].
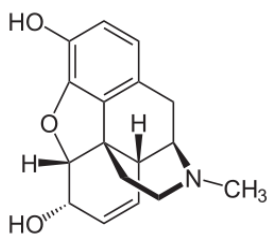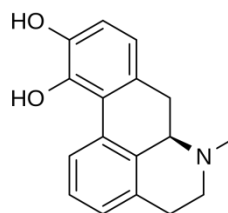
Morphine   Apomorphine

Tiotropium bromide is an analogue of Atropin, was approved by FDA in 2005 for the treatment COPD associated bronchospasm and chronic bronchitis [21].
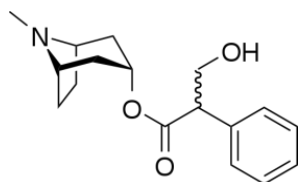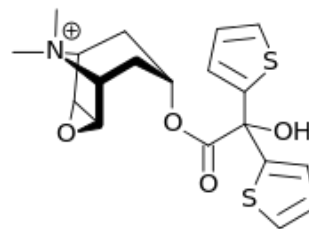
Atropine   Tiotropium bromide

Powerful new technologies such as high-throughput screening and combinatorial chemistry dramatically increase the possibility of drug discovery. Nevertheless, natural products still offer unmatched structural variety when compared to synthetic compounds. For example, natural products (NP) are more likely to be rich in stereochemistry and concatenated rings than the structures obtained by the combinatorial libraries. Nevertheless, the number of the approved natural drug by FDA between 1981 and 2014 is relatively low (64), representing the 4% of the drug entity [22].

This fact may be explained with the following reasons:

➢ Very often NP show a low efficacy and selectivity for the target
➢ Very often NP possess poor pharmacokinetic and pharmacodynamic properties
➢ Sometimes the toxicity of NP is a limiting factor for a medical use

Besides, considering the approved drugs derived from natural products (usually semi-synthetically) and natural product–inspired pharmacophores (that could be considered natural-product analogs), the number of the new entities in the same period dramatically increased with 26% of total drugs [22]. Natural products provide a rich source of potentially attractive scaffolds and molecular building blocks for synthesis. Hence, natural products could provide new starting points in drug discovery. Some natural products can be used as small molecule drug precursors which could be modified to the desired compound.

Following are some of the examples of natural product inspired pharmacophore,

Paclitaxel is an antitumor compound isolated from *Taxus brevifolia*, but the yield is very low. Total synthesis of Paclitaxel can also be possible but the market demand of this compound still not fulfilled. **10-deacetylbaccatin** is a natural compound isolated from *Taxus baccata* L. It can be converted chemically in several steps into paclitaxel [23,24]. Bristol-MyersSquibb, adopted the semisynthetic method developed by the Holton research group to produce paclitaxel from 10-deacetylbaccatin [18,24].
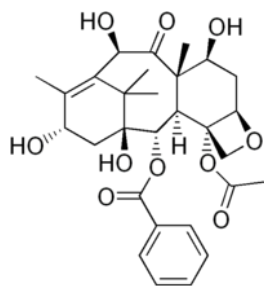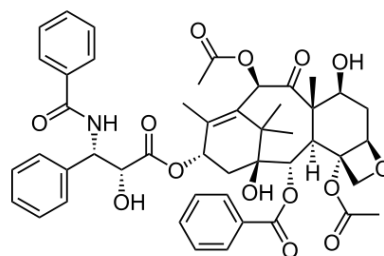
10-deacetylbaccatin	Paclitaxel

Shikimic acid is an important biochemical intermediate in many plants and microorgnism. It is the starting material for the synthesis of **Oseltamivir phosphate**.
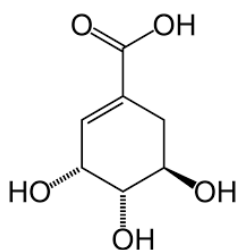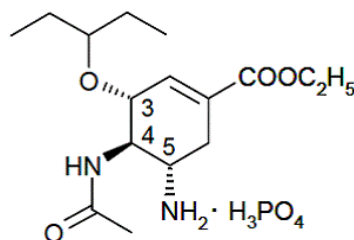
Shikimic acid	Oseltamivir phosphate

Podophyllotoxin is a non alkaloidal toxin lignan extracted from roots and rhizomes of *Podophyllum* species. Camptothecin is a cytotoxic quinoline alkaloid isolated from the bark and stem of *Camptotheca acuminata.* Both, Podophyllotoxin and Camptothecin, have good anticancer avtivity but they are too toxic and have solubility problem. This was a major impediment in clinical use of these compounds as anticancer drugs. Etoposide and topotecan are analogues of these compound with better therapeutic index [25,26].
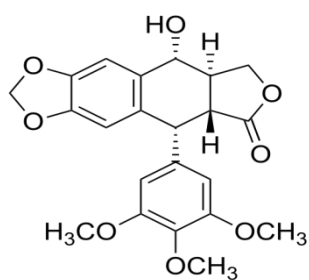
Podophyllotoxin
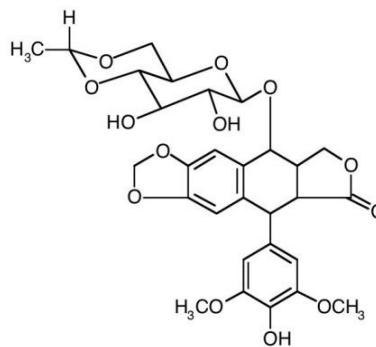
Etoposide
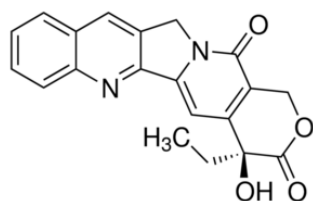
Camptothecin
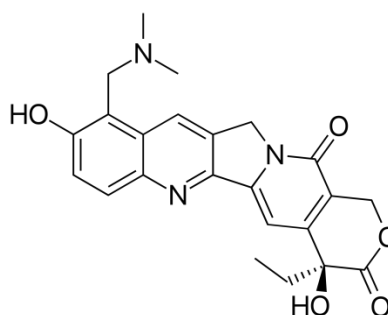
Topotecan

Irinotecan is a drug used in treatment of cancer and is a semisynthetic analogue of natural alkaloid Camptothecin.
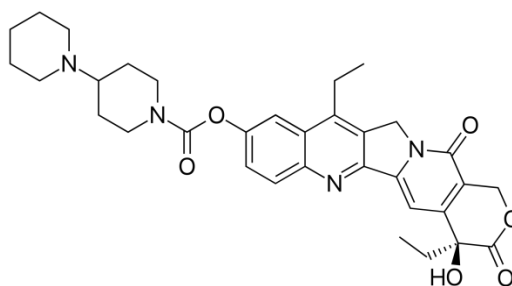
Irinotecan

Guanidine is a natural hypoglycemic compound isolated from *Galega officinalis* L. It has limitations in clinical use because of its toxicity. Metformin is a derivative of guanidine and is being in clinical use for type II diabetes [27].

Guanidine   Metformine
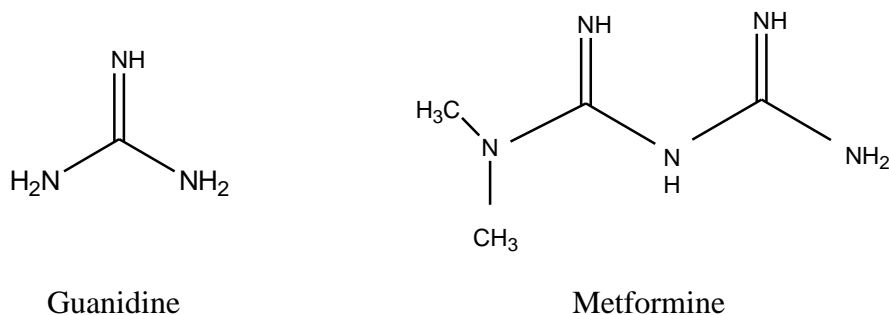
1.1.3 Limitations of herbal medicines

Although, phytomedicines have great potential in curing and preventing the ailment and diseases, they are capturing global market of healthcare; still the use of herbal medicines has some problems as follow:

➢ Active principles are often unknown.

➢ Formulations of *phytomedicine*s are complex combination of two or more plants which makes it difficult for standardization, stability and quality control studies.

➢ Availability of authentic raw material is a big problem.

➢ Problems in identification of accurate species and adulteration and substitution with other plants. More expensive the plant material is, the more likely is to be inferior because of adulteration [28].

➢ Although they are claimed to have no side effects, scientific studies and clinical trials have revealed that some secondary metabolites present in plant may produce undesirable side effects [29]. There is a common misconception that natural means always safe and remedies form natural origin are harmless; but some plants are toxic because of their own inherent toxins [30].

➢ Many herbal drugs currently in use are not fully explored for their chemical constitution, characterization and mechanism of action.

➢ Constituents of plant vary with plant species which could lead to dosage inaccuracy. Origin of the plant, geographical conditions, temperature, light exposure, availability of nutrients and water, time and period of collection, method of collection, drying, packing, storage and transportation etc. greatly affect the quality and therapeutic value of drug [10].

➢ Lack of standardization and quality control of herbal drugs.

To overcome all above hurdles and make phytomedicines as alternative to modern medicines and to acquire benefits of god gifted wealth of herbal medicine; it is important to focus on quality parameters. Detailed study of plant chemistry, its chemical content, characterization of active principles, mechanism of action, safety and efficacy study etc. will ensure the effective and safe utilization of medicinal plants. Traditional system of healthcare, as an alternative to or in combination with, modern medicine, would serve to mankind.

Isolation and characterization of bioactive compounds from plants is foundation of the phytomedicine research. As discussed above, few examples, bioactive compounds and their semisynthetic derivatives have proven themselves as therapeutic agent with great potential. Nature is gifted with variety of herbs and plants, many of them posse's medicinal property. However, *phytomedicine*s area of research is still poorly explored. Among the 250,000-500,000 existing plants species very little percentage have been studied scientifically for their medicinal use [15]. Even a tiny portion has been properly studied in terms of their phytochemical investigation and pharmacological properties. Therefore there is still great potential to discover new chemical constituents and their new type of action related to novel drug discovery. Use of medicinal plants was a tradition of yesterday and it could be a drug for tomorrow.

In present PhD thesis we aimed to isolate, elucidate the structure and evaluate the biological activity of secondary metabolites from some Indian and Sardinian (Italy) plants. Details of the studied plants and their targets are discussed in next sections.

1.2 Ayurveda

Ayurveda (pronounced ah-yur-vee-duh) is one of the most ancient, indigenous and well known traditional systems of medicine in India. It is holistic system of treatment which includes herbal medicine, special diets, Yoga & relaxation methods and lifestyle management. Ayurveda encompasses not only science but also religion and philosophy and it considers entire life to be sacred. Ayurveda has proven itself as an alternative and effective means of treatment for some critical diseases, whereas modern systems of medicine have failed to find a permanent solution.

The term Ayurveda consists of two words; *Ayur* means "Life" and *Veda* referring to "Knowledge", together they mean the "science of life and longevity" [31]. The theory of Ayurvedic medicine has been a part of history for the last 5000 years. The origin of Ayurveda is considered to be divine and it is believed that *Brahma*, the Hindu god, who is believed to be the creator of the universe, passed on this holistic knowledge for the well being of mankind [32]. This knowledge about herbal remedies and their healing properties was composed in the form of poems called *Shlokas* [33]. The knowledge of traditional medicine was passed on from teacher/ guru/rishi to disciple in the form of oral lessons without any written books. The ancient Hindu system of curing the diseases is believed to be based on four literatures called *Veda's*, they are called as *Rig veda, Yajur veda, Sam veda and Atharva veda* [33]. The Rig Veda is the most well known of all the four Vedas and describes 67 plants and 1028 Shlokas. The Atharva Veda and Yajur Veda describe 293 and 81 medicinally useful plants. The practice of Ayurveda is based upon the knowledge gained from these Vedas. The writings in Rig Veda and Atharva Veda are attributed to "*Atreya*" who is believed to have been conferred with this knowledge from Lord *Indra*, who initially received it from Lord *Brahma* [34,35].

In ancient time the way of transforming of the knowledge was *Maukhik* means oral lessons of *Shloka*. Rishi or guru or teachers used to teach the lessons orally in *Ashrams* (traditional schools). Later on, around 1000 BC, the knowledge was transformed into text [36]. Rishi *Agnivesha* compiled the knowledge from the Vedas, and it was edited by Charaka and some other experts. It is presently called as "Charaka Samhita". Charaka Samhita describes all aspects of Ayurvedic medicine and Sushruta Samhita describes the Science of Surgery [37,38]

Wisdom of Ayurveda is documented in *Sanskrit*, the ancient language of India. Following are some credible texts,

1) Charak Samhita (1st century A.D, internal medicine)
2) Sushruta Samhita (4-5 century BC, surgery) and
3) Ashtanga Hridayam Samhita (8th century A.D.)

Charaka samhita is considered as leading resource in regards to depth and extent of content. Charaka is considered as exceptional author among all other writers of ancient Indian medical texts.

1.2.1 Basic principles of Ayurveda

Ayurveda is a different science of medicine, it not only cures the disease but also deals with different levels of a person's body complex like physical, emotional, mental and spiritual [39]. Ayurveda believes that human beings is multidimensional and have conscious and unconscious aspects. According to Ayurveda, health is considered a prerequisite for achieving the goals of life, *dharams, artha, kama and moksha* (salvation) [36]. Ayurveda considers the human being as a combination of three *doshas*, five elements, seven body tissues (*Sapta-dhatu*), five senses (*Panch-indriyas*) with sensory and motor functions, mind (*Manas*), intellect (*Budhi*) and Soul (*Atman*) [36].

I] Panchmahabhuta

The philosophy of Ayurveda is based on the theory of *Panchmahabhutas* (Five great-element theory). It is believed that all the objects of living bodies are composed of panchmahabhuta. Following are the *Panchmahabhuta* (Five great elements), Prithvi (Earth), ap or soma or jala (water), agni (fire), vayu (air), akasha (space). Each element has relation to the body senses [40]. These five elements, in varying combination, are believed to form three basic humors of human body. They are collectively called as *Tridosha* [33,40]. e.g., *Vata* (Ether + Air), *Pitta* (Fire) and *Kaph* (Water + Earth). These three 'Doshas' are physiological entities in living beings.

II] Tridosha

As stated earlier *panchmahbhuta* (five great elements in varying combination form three basic humors of human body and controls the basic physiological functions of the body. According to Ayurveda basic requirement while treating a patient is to understand these *Tridosha.* The catabolism of the body is believed to be governed by *Vata,* metabolism by Pitta and anabolism by *Kapha* [38]. For healthy state of human body a balance between the three doshas and other factor is essential, any imbalance between these three causes' illness and disease [41].

III] Saptdhatu

Ayurveda believes that human body consists of seven basic and vital tissues known as *dhatu,* means "constructing element". These elements are essential for maintaing function of different organs, systems and vital body parts [31]. *Rasa* (tissue fluids), *Meda* (fat and connective tissue), *Rakta* (blood), *Asthi* (bones), *Majja* (marrow), Mamsa (Muscle), and *Shukra* (Semen) are the *saptdhatu*.

IV] Panch-indriya

Panch-indriya are five sense organs (Eyes, ear, tounge, nose, skin) of human body which accepts the external stimuli and transmit signals to brain.

V] Three *mala*

Mala are the waste products of the body. *Mutra* (urine), *Purisa* (faeces), and *Sveda* (sweat) are the three kinds of waste products of body. Ayurveda explains that if balance between *Triodsha* is not maintained then waste products. Any imbalance in generation and elimination leads to health complications.

The mental and spiritual attributes are described as *Satva, Rajas* and *Tamas.* Various permutations and combinations of *Satva, Rajas* and *Tamas* constitute human temperament and personality [36]. The doctrine of Ayurveda aims to keep these structural and functional entities in a functional state of equilibrium which signifies good health. Any imbalance due to internal or external factors causes disease and restoring the equilibrium through various techniques,

procedures, regimen, diet and medicine constitute the treatment. In Ayurveda, diagnosis include questioning and eight examinations, viz., Pulse, Urine, Faces, Tongue, Eyes, Visual / sensual examinations and inferences.

Ayurveda describes in detail the principles of preservation and promotion of health as well as prevention and cure of diseases. It treats man as a whole. The science of Ayurveda guides us to maintain the balance in *Tridosha,* three biological forces, as the imbalance in these is the cause of all the diseases. Ayurveda considers the human being as a microcosm, a replica of macrocosm (Universe) [33]. The treatment in Ayurveda system is individualized.

Treatment in Ayurveda has two components; (a) preventive and (b) curative.

Preventive aspect of Ayurveda is called *Syasth-Vritt* and includes personal hygiene, regular daily routine, appropriate social behaviour and *Rasayana Sevana*, i.e. use of rejuvenative materials / food and drugs. The curative treatment consists of use of drugs, specific diet and life style.

Ayurveda has rich history, but still has some demerits that prevented the growth unlike western system of medicine. Hidden identity of active constituent is the major hurdle. Even today many herbal drugs are not fully explored for their active constituent, characterization and its mechanism of action. Herbal formulations are mixtures of many drugs; this adds complexity to the analysis of each component. Variation of the plant constituent with different species, incorrect identification of species, adulteration, non-uniform quality standards etc are the reasons that this traditional system of medicine lags behind with modern medicine. Though Ayurveda has some hurdles, but it is still serving mankind in countries like India with 1.25 billion populations. In past few decades it is also becoming popular in western world. As Ayurveda targets each individual as a prime focus of treatment, it is proving itself as an alternative to modern medicine. Ayurveda has gained upper hand over modern medicine in treating some critical diseases.

1.3 AIDS (Acquired Immuno Deficiency Syndrome)

AIDS is an infectious disease caused by transmission of virus called HIV (Human Immune Deficiency Virus), represents the second most important cause of mortality in low-income countries and one of the ten leading causes of death worldwide. HIV attacks the immune system and destroys cellular component, the T cells, resulting in immunity collapse. Patients having AIDS do not die because of AIDS itself but dies because of other opportunistic diseases as HIV weakens the immunity and reduces ability to fight. Studies suggest that HIV is more concentrated in blood and semen, it is also reported to be found in saliva and tears but transmission through is not evidenced. HIV or AIDS is becoming major threat to world. According to report on global summary of the AIDS epidemics (15 June, 2016) by WHO- HIV department, there are approximately 36.7 million people living with HIV, 17 million people are on antiretroviral therapy, 1.1 million people died in the year of 2015 because of AIDS.

The first case of HIV was recorded in USA in 1981. In 1983 Luc Montagnier and his colleagues from the Pasture institute, Paris claimed to have discovered the virus HIV, by 1984 it was universally accepted to be cause of AIDS [42,43]. It was also accepted that HIV is a type of retrovirus which has an enzyme called reverse transcriptase (RT) [43]. The origin of this virus is form Africa; causative agent existed in Africa before the emergence of the epidemics in Central Africa and North America in the 1970s. It is believed that HIV has transmitted to human from non human primates; it is tempting to consider AIDS as a zoonosis, resulting of the transmission to human of related viruses infecting primate species without causing disease [43].

1.3.1 HIV

The virus was first discovered in 1983 by Montegnier and colleagues [44]. HIV belongs to the group of retrovirus called lentivirus [45]. Origin of the HIV is believed to be in central Africa, in early 20th or late 19th century, when killing of animals for food was a common practice [46,47]. Transmission of the virus to human is by multiple zoonotic transfers. HIV is known to be transmitted from chimpanzees, gorilla, and sooty mangabeys [42,46,48].

In 1986, after the discovery of HIV-1, a virus morphologically similar but antigenically different was found in Western Africa, causing AIDS. This virus named as HIV-2 [46,49]. HIV-

2 was closely related to a virus which causes immunodeficiency in captive macaques [46,50]. In later period other viruses were found in various different primates like African green monkey, sooty mangabeys, mandrills, chimpanzees etc. This viruses collectively referred as SIV (Simian Immuno deficiency Virus) [46]. Interestingly these viruses are nonpathogenic to their natural hosts. The SIV-simian lentivirus, previously referred to as simian T-cell lymphotropic virus type III (STLV-III), is related to HIV by the antigenicity of its proteins and in its main biological properties, such as cytopathic effect and tropism for CD4-bearing cells [50]. HIV-1 and HIV-2 are closely related and were originated from chimpanzees and sooty mangabeys, respectively [51,52]. The relation between HIV-1 and AIDS was accepted by scientist in 1984, same has been confirmed after the isolation of HIV-2.

1.3.1.1 Morphology of HIV

HIV virus particle is spherical in shape with about 145nm (95-166 nm range) in diameter [53]. The virus has cone-shaped core surrounded by lipid matrix containing key surface antigens and glycoprotein. Genome of HIV is made of RNA and each virus has two single chains of RNA. The genome is composed of 9 genes encoding 15 viral proteins [54]. Three major genes are *gag, pol,* and *env,* code for structural protein, enzymes and envelope proteins. Gag encodes the matrix, capsid and nucleocapsid proteins. Pol encodes protease, reverse transcriptase. Env encodes a key HIV surface antigen gp160 consisting of gp120 and gp41. The remaining genes code for regulatory (*Tat, Rev)* and accessory *(Vif, Vpr, Vpu/Vpx, Nef)* protein [54].

As HIV buds out of the host cell during replication, it acquires a phospholipid envelope. Protruding from the envelope are peg-like structures that the viral RNA encodes. Each peg consists of three or four gp41 glycoproteins (the stem), capped with three or four gp120 glycoproteins. Inside the envelope the bullet-shaped nucleocapsid of the virus is composed of protein, and surrounds two single strands of RNA. Three enzymes important to the virus's life cycle- reverse transcriptase, integrase, and protease - are also within the nucleocapsid.
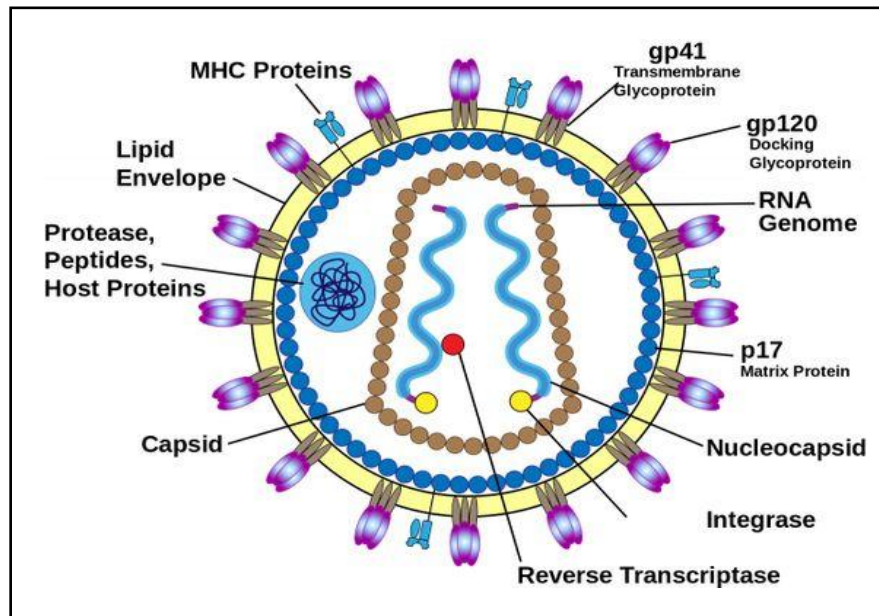
Fig.1: Structure of HIV

1.3.1.2 Replication of HIV

Entry of HIV into the host cell requires the binding of one or more gp120 molecules on the virus to CD4 molecules on the host cell's surface. Binding to a second receptor is also required. Entry of virus to host cell and its replication is depicted in the figure 2.

Step1- Envelope (Env) glycoprotein spikes binds to CD4 receptor

Step 2- Fusion of the viral and cellular membrane and viral particle enters inside the cell

Step 3-Partial core shell uncoating

Step 4- Reverse transcription to form pre-integration complex (PIC)

Step 5- PIC enters into nucleus

Step 6- Formation of integrated provirus

Step 7- Proviral transcription

Step 8- Generation of viral mRNA of different size, larger mRNA leaves the nucleus

Step 9- mRNA helps in production of protein

Step 10- Incorporation of genome length RNA into viral particles with protein component

Step11- Viral particle budding

Step12- Release of viral particle from the cell

Step13- Protease mediated maturation to create an infectious particle
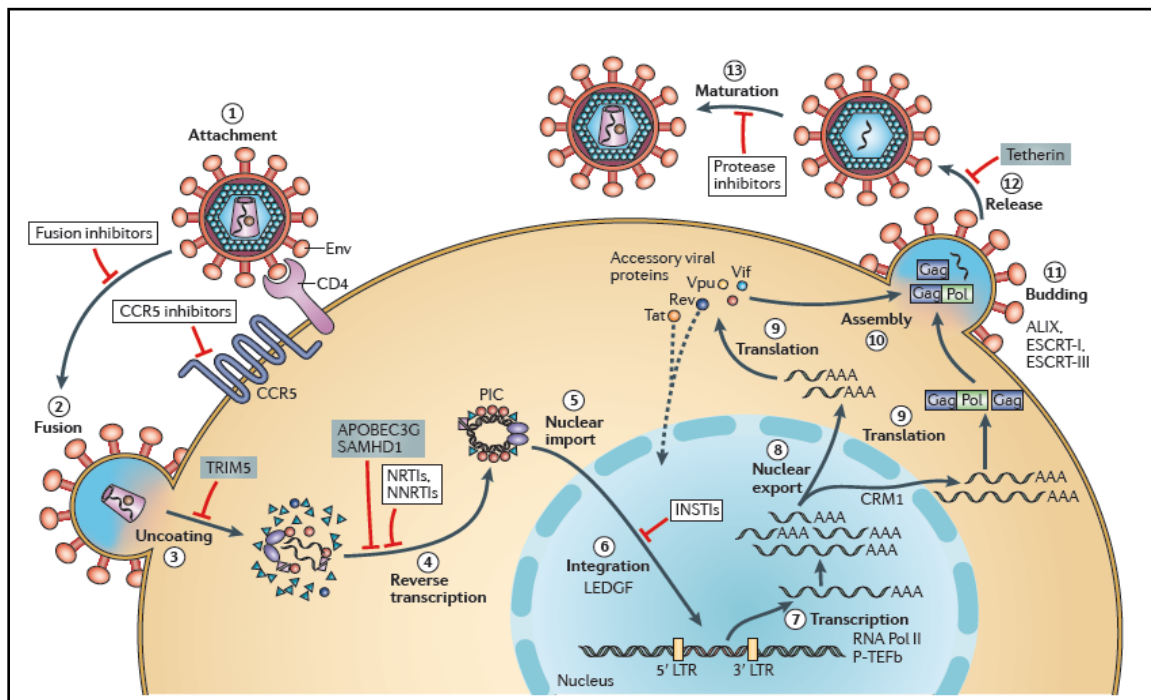
Fig. 2: HIV-1 replication cycle (Source- Nature Review)

1.3.1.3 Transmission of HIV

HIV is present only in five body fluids in enough amount to infect someone; blood, semen, vaginal fluid, rectal fluid and breast milk. HIV can only be transmitted by these fluids from infected person to the blood stream of healthy person. Entry of HIV could be through broken skin, opening of the penis, vaginal opening, and rectum. Unprotected sex is the major cause of transmission, thus AIDS is primarily considered as sexually transmitted disease [46]. Blood transfusion, sharing of needle or equipment to inject drugs, razor, and needle of tattooing can also cause infection. HIV can also be transmitted from mother to fetus during pregnancy or to baby during breast feeding.

HIV cannot be transmitted by talking, shaking hands, working or eating together, hugs or kisses, cough or sneezes, swimming pools, utensils etc.

1.3.1.4 Diagnosis

HIV infection is diagnosed based on: positive HIV antibody testing (rapid or laboratory-based enzyme immunoassay). This is confirmed by a second HIV antibody test (rapid or laboratory-based enzyme immunoassay) relying on different antigens or of different operating characteristics [55]. CD4 + T lymphocyte count is important clinical biomarker in diagnosis of HIV infection. Primary test to detect HIV is ELISA (Enzyme linked immune sorbent assay). If ELISA is positive then Western blot test is done to confirm the diagnosis. HIV infection is detected through the test of blood or oral mucosa.

1.3.2 Anti HIV drugs

It has been generally acknowledged that prevention is the best cure in case of HIV as there is no medical cure to HIV and there are no vaccines to prevent HIV. But there is treatment available and one can live long and healthy with proper medication. Treating viruses is always critical as viruses uses translational machinery of the host cell. Most common anti HIV drugs block key step in viral replication that is interference with reverse transcriptase [42,54,56].

Anti HIV drugs are classified as:

1. Nucleoside/Nucleotide reverse transcriptase inhibitors
2. Non-nucleoside reverse transcriptase inhibitors
3. Protease inhibitors
4. Integrase inhibitors
5. Fusion inhibitors
6. Entry inhibitors

1] Nucleoside/ Nucleotide reverse transcriptase inhibitor (NRTI)

All drugs of these class target to reverse transcriptase and prevents new virus production. All NRTI are 2', 3'-dideoxynucleoside analogues and have similar mechanism of action. They act as chain terminator after their phosphorylation to the 5'-TP [57,58]. NRTIs are not administered alone in treatment of HIV because of low genetic barrier to the development of drug resistant mutations [59]. They are administered in combination with other drugs in highly active antiretroviral therapy (HAART) [60].

Zidovudine (AZT), discovered in 1985, is the first approved drug for treatment of HIV and was licensed for clinical use in 1987 [56]. It is also the first drugs in the group of NRTIs which target HIV reverse transcriptase. After the discovery of AZT, six other drugs were approved in treatment of HIV and HBV

➢ Didanosine (ddI [2',3'-dideoxyinosine])
➢ Zalcitabine (ddC [2',3'-dideoxycytidine])
➢ Stavudine (d4T [2',3'-didehydro-3'-deoxythymidine])
➢ Lamivudine (3TC [2',3'-dideoxy-3'-thiacytidine])
➢ Abacavir (ABC) [(1*S*, 4R)-4-(2-amino-6-(cyclopropylamino)- 9H-purin-9-yl)-2-cyclopentene-1-methanol]
➢ Emtricitabine [(-)FTC (2',3'-dideoxy-5-fluoro-3'-thiacytidine).
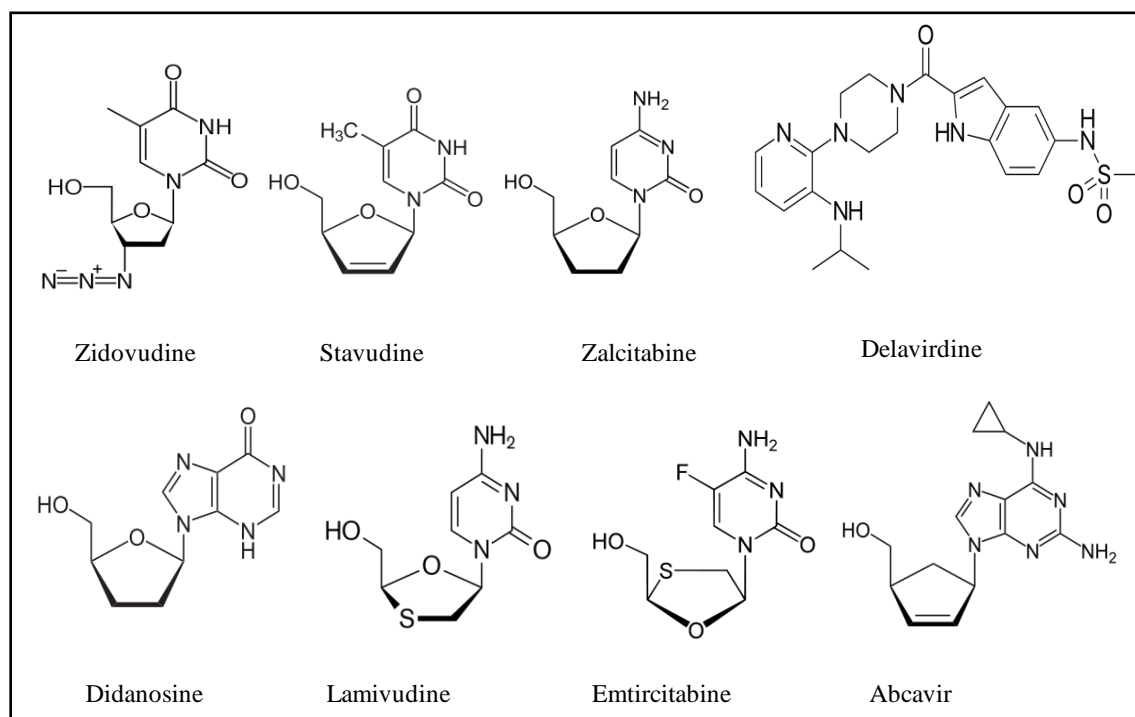
Fig. 3: Nucleoside/Nucleotide reverse transcriptase inhibitor (NRTI)

2] Non-Nucleoside Reverse Transcriptase Inhibitor (NNRTI)

NNRTIs were discovered in late 1980's, originated from 2 different classes of compounds. 1-[(2-hydroxy-ethoxy) methyl]-6-phenylthiothymine (HEPT) analogues and tetrahydro-imidazo[4,5,1-jk][1,4]-benzodiazepine-2(1H)-one and -thione (TIBO) analogues [61,62].

Also these class of compounds target HIV-1 reverse transcriptase but, unlike NRTIs, NNRTIs do not need any metabolic processing to inhibit HIV reverse transcription. Instead, they serve as non-competitive inhibitors that target the allosteric site of HIV-1 RT, situated a short distance (15 Å) from the RT catalytic site. This binding induces conformation changes to impair the catalytic activity of HIV-1 RT, thus interrupting viral replication [63-65]. NNRTIs acts specifically against HIV-1, HIV-2 is naturally resistant to all NNRTIs [66]. NNRTI includes five approved drugs as follows, Nevirapine, Delavirdine, Efavirenz, Etravirine, and Rilpivirine.
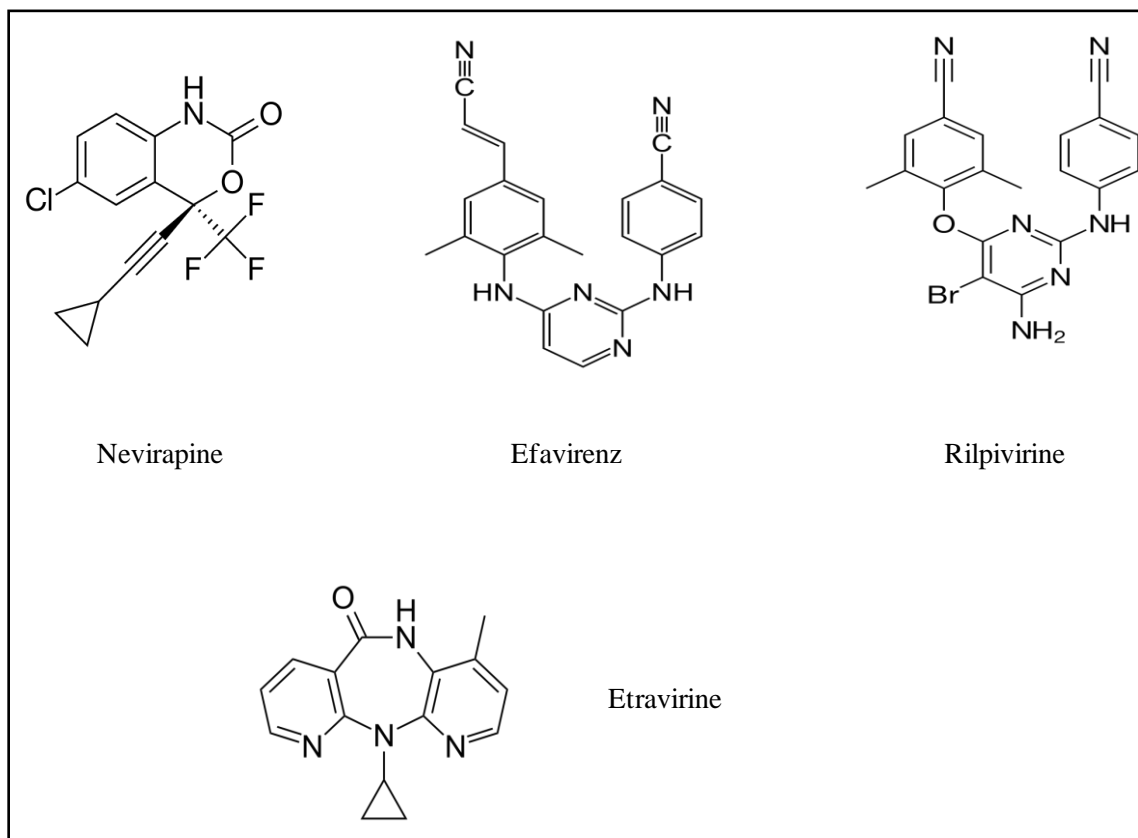
Fig. 4: Non-nucleoside reverse transcriptase inhibitor (NNRTI)

3] Protease inhibitors

This class of compounds blocks the action of protease enzyme. The effectiveness of these protease inhibitors is usually boosted by taking them with a small dose of another protease inhibitor called ritonavir (*Norvir*). Saquinavir is the first approved compound (1995) of this class. Protease inhibitors are important element of HAART in treatment of both HIV-1 and HIV-2. Saquinavir, Ritonavir, Indinavir, Nelfinavir, Amprenavir, Lopinavir, Atazanavir, Fosamprenavir, Darunavir, and Tipranavir: these are approved protease inhibitors.
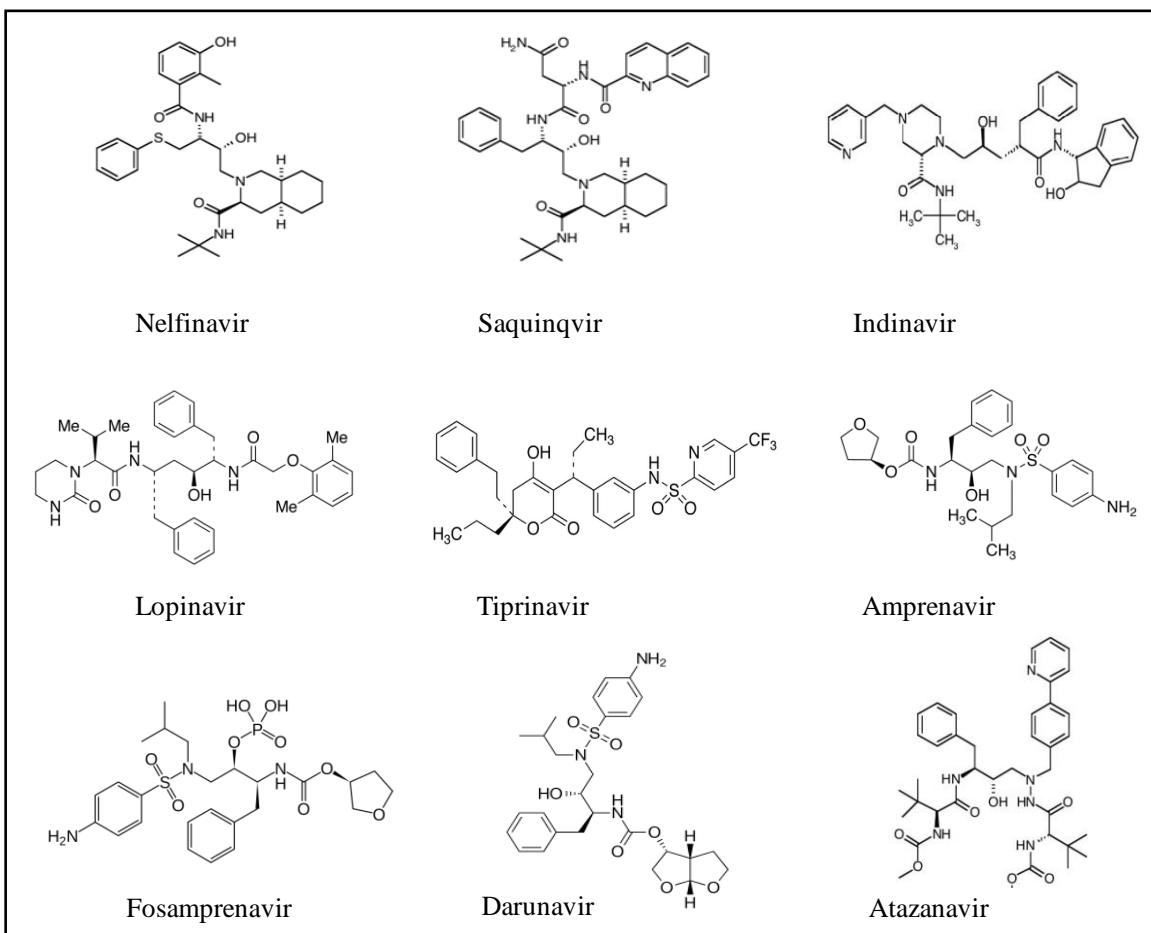
Fig. 5: Protease inhibitors

4] Integrase inhibitors

The first HIV integrase inhibitor was approved in 2007; subsequently two other integrase inhibitors were approved and are being used in HAART [58]. Raltegravir, Dolutegravir, and Elvitegravir are the approved one.

a) Raltegravir is the first integrase inhibitor which prevents integration; it blocks the catalytic site of HIV integrase [52]. It is better for both kinds of patients; one who are about to start HIV treatment and other who have taken anti-HIV regimen in past and possibly be resistant

to other drugs. For patient with HIV-1 who had virological failure Raltegravir could be co-administered along with two nucleoside derivative or with lopinavir [67].

b) Elvitegravir is a new integrase inhibitor which inhbits DNA strand transfer process of HIV-1 integrase [68]. Along with HIV-1; Elvitegravir also inhibits the strains of HIV-2, SIV, murine leukemia virus [69]. Currently, it is available in a combination drug called *Stribild*. Stribild contains Elvitegravir, Cobicistat, FTC and TDF [58]. Genvoya is yet another combination, approved in 2015, of elvitegravir with cobicistat, FTC, and tenofovir alafenamide [70,71].

c) Dolutegravir was approved by FDA in 2013 [56]. It is similar to Raltegravir in terms of safety and efficacy but Dolutegravir exhibits a higher genetic barrier to drug resistance development [72]. Dolutegravir, in combination with up to two other antiretroviral drugs, once daily, provides a better virologic response than twice-daily raltegravir in antiretroviral experienced patients [73]. Two combinations of dolutegravir are in use now, Triumeq (Dolutegravir, Abacavir, Lamivudine), and Dutrebis (Dolutegravir, Lamividine).

5] Entry and fusion inhibitors

a) Enfuvirtide is a peptide inhibitor also known as T20. It's a polypeptide with 36 aminoacids. It is the only anti HIV drug that has to be injected subcutaneously, 2 times in a day [74]. Its use has some limits as it has to be given subcutaneously and having very high cost.

b) Maraviroc is a chemokine receptor antagonist. It targets to chemokine CCR5 receptor on the CD4 cell surface and macrophages [75].

1.3.3 Inhibition of HIV-1 RT-associated RNase H function- (A new approach to target retro transcription of HIV)

Since the discovery of zidovudine (AZT), reverse transcriptase has been a prime target in treatment of HIV and it led to the development of antiretroviral therapy. RT inhibitors used to treat HIV-1 infection are a part of treatment strategy known as HAART (highly active antiretroviral therapy). Although, HAART has great contribution in HIV treatment, associated undesirable side effects of RT inhibitors and development of drug resistance strains limits the use of this therapy. To address this problem, new inhibitors must be developed that can block the replication of the existing drug-resistant viruses. There is need of continuous search of new lead molecule with new target.

Reverse transcriptase (RT), a virus coded enzyme, catalyzes an important event in replication cycle of HIV [76]. RT has two functions, first, RNA dependant and DNA dependant polymerase activity and second, ribonuclease H activity. Synthesis of double stranded DNA form single stranded RNA viral genome is essential step in replication cycle. HIV-1 reverse transcriptase (RT) catalyzes the conversion of single-stranded RNA into double-stranded viral DNA. This retro transcription is mediated through an RNA/DNA duplex intermediate [77,78]. RNA of the duplex intermediate must be removed to allow synthesis of double stranded DNA. This RNA removal is performed by the RT-associated RNase H through a sequence of highly specific hydrolytic events [79]. Since the RNase H is essential for cleavage of RNA: DNA heteroduplex viral replication; it could be an important target. As on today, all of the RT inhibitors that have been approved for clinical use target the polymerase activity of RT and not its RNase H activity. As discussed earlier RNase H activity is essential for viral replication; RNase H inhibitors have considerable potential as anti-HIV agents.

1.3.3.1 Structure and activity of HIV-1 RT RNase H

HIV-1 reverse transcriptase is an asymmetric heterodimer which consists of two subunits; p66 subunit (66kDa) and p51 subunit (51kDa). These subunits are derived from the Gag-Pol polyprotein precursor by the viral protease mediated cleavage. The first 440 residues of p66 and p51 are identical. Both subunits have four polymerase subdomains viz. thumb, palm, finger, and

connection [80,81]. C-terminal residues 427-560 of p66 forms the domain of RNase H. p66 subunit is responsible for all RT enzymatic activity; it contains both polymerase and RNase H sites. Amino acid residues directly responsible for both enzymatic activities are present exclusively in p66 subunit. Both the active sites are separated from each other by a distance of 40 A° which is corresponding to 17-18 base pair of RNA: DNA duplex [82-84]. p51 subunit is catalytically inactive and serve as a structural scaffold for p66subunit. Polymerase and RNase H domains are linked via connection domain of p66 subunit which is critical for RT-nucleic acid interaction [84].
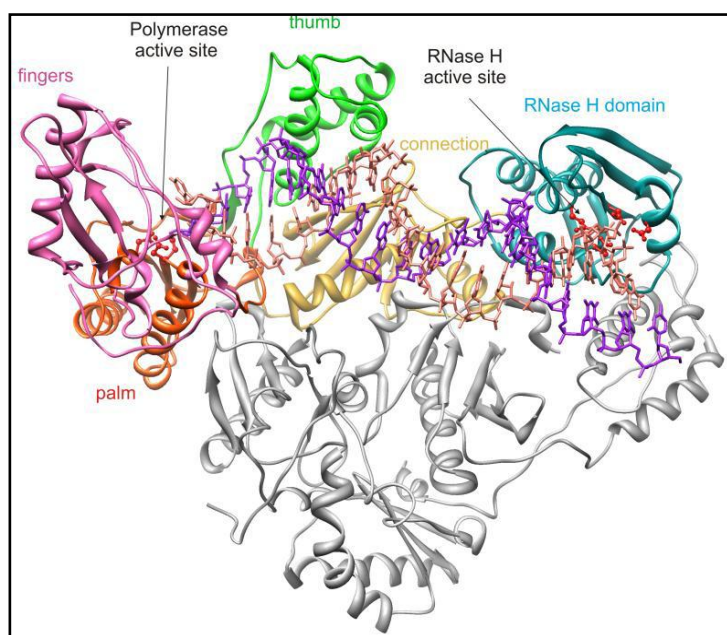
Fig.6: Structure of HIV-1 p66/p51 heterodimeric reverse transcriptase in complex with nucleic acid [85]

RNase H has a tertiary structure which is similar to all known RNase H enzyme, including human RNase H1, with significant difference in primary sequence. Active site of RNase contains 4 catalytic acidic residues: D443, E478, D498, and D549 (Fig.7) located in a cavity which also includes essential H539 [86]. The catalytic acidic residues coordinate with two Mg^{2+} cations which are essential for enzyme function.
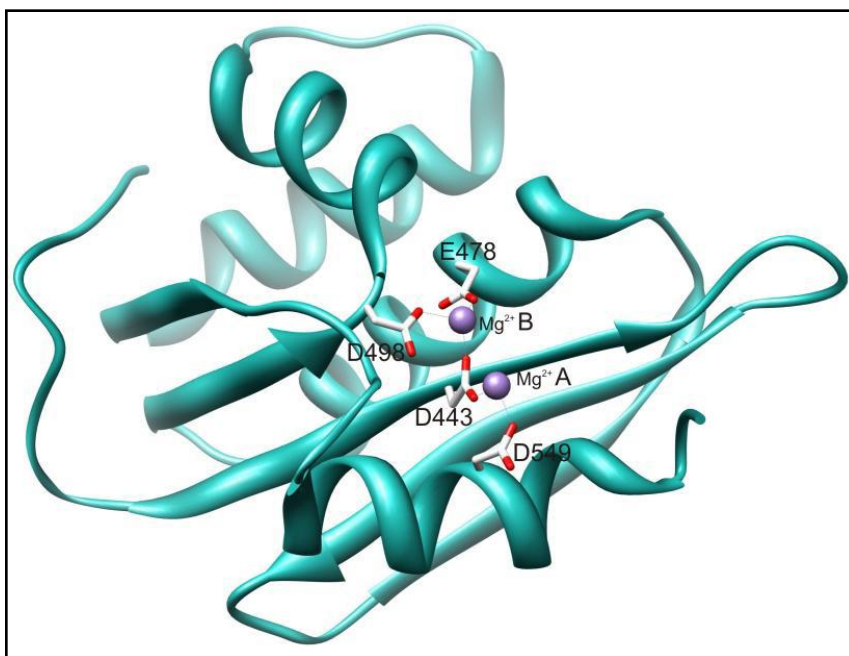
Fig.7: Structure of the RNase H domain of HIV-1 RT [85]

1.3.3.2 Inhibitors of RNase H

All RT inhibitors, currently in use or under clinical trial, inhibit polymerase activity and none of them inhibit RNase H function [87]. RNase H inhibitors that specifically bind in or near the RT RNase H domain would therefore likely retain potency against clinically significant drug-resistant HIV variants, including multidrug resistant viruses. Up to now only few molecules have been described and most RNase H inhibitors have not been studied thoroughly for their mechanism of action. RNase H inhibitors are likely to be classify as, active site directed inhibitors and allosteric inhibitors.

I) Active site directed inhibitors **-**All active site directed inhibitors are enabled to interact with two metal cations in the RNase H active site. This interaction blocks the access of the metal to phopsphodiester bond in the RNA strand and therefore prevents the metal catalyzed hydrolysis reaction [88].

Diketo acids- DKAs were initially developed as integrase inhibitors. As they posses active site metal cation and due to structural similarities between HIV integrase and HIV-1RT RNase H, they were evaluated for inhibition of RNase H [89].

E.g 4-[5-(Benzoylamino) thien-2-yl]-2,4-dioxobutanoic acid (BTDBA)；6-[1-(4-fluorophenyl) methyl-1H-pyrrol-2-yl)]-2,4-dioxo-5-hexenoic acid ethyl ester (RDS-1643)
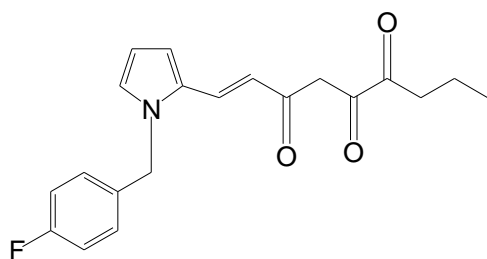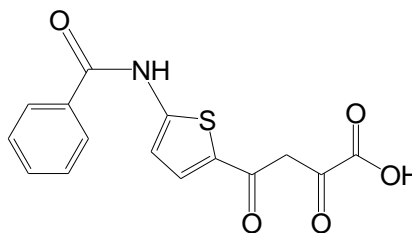
RDS1643   BTDBA

II) Allosteric RNase H Inhibitors- This type of compounds do not bind directly to active site; instead they bind to an allosteric site. Computational studies have revealed the potential allosteric binding pocket for RNase H inhibitors

N-(4-tert-Butylbenzoyl)-2-hydroxy-1-naphthaldehyde hydrazone (BBNH) is a dual function inhibitor and a metal binding compound [90]. It inhibits both the RNase H and DNA polymerase activities of RNase H. Kinetic and biophysical studies have suggested that the dual inhibition of BBNH is due to the fact that they interact with two different sites on RT [90]. **Dihydroxybenzoyl naphthyl hydrazone (DHBNH)** is an analogue of BBNH and it inhibits only RNase H function of RT and has no effect on RT catalyzed DNA synthesis [91].
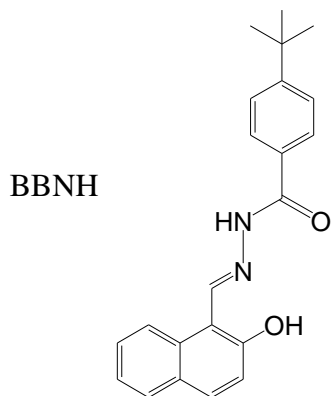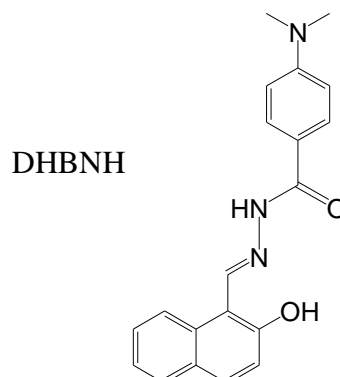
BBNH   DHBNH

1.3.3.3 Natural products as RNase H inhibitors

β-Thujaplicinol (2,7-dihydroxy-4-(propan-2-yl)-cyclohepta-2,4,6-trien-1-one). It is a natural compound from *western red cedar.* Le Grice and co-workers reported that this compound inhibits RNase H by chelating the metal ion at the active site of RNase H. [92].

Illimaquinone. It's a secondary metabolite isolated from Red Sea sponge *Smenospongia sp.* Illimaquinone, a sesquiterpenoid quinone, is reported to inhibit RNase H and RDDP activities [93].
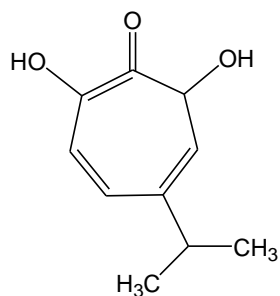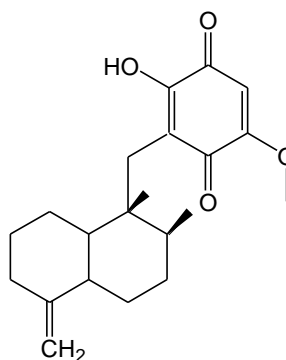
β-Thujaplicinol   Illimaquinone

Considering the pandemic of HIV (1.1 million people died in 2015), it still needs attention and continuous research for new anti HIV compounds. HIV-1 RT associated RNase H is among the less explored target. Numerous compounds with good RNase H inhibitory potential (*in vitro*) are reported. All RNase H inhibitors, identified as of now, inhibits RNase H by chelating active site metal ion at the RNase H active site, also they can inhibit HIV integrase and RT DNA polymerase. Unfortunately very few RNHIs have shown antiviral activity in cell based HIV replication. At present RDS 1643 (diketoacid), selective inhibitor of RNase H and DHBNH (hydrazone derivative) are the two promising compounds [94]. We can postulate that HIV-1 RNase H will be the next target in the field of anti viral drugs.

1.3.4 Herbal medicines as anti-HIV drugs

Since the discovery of zidovudine (1986), the first approved drug for HIV treatment, many other drugs were discovered and approved. Use of ART (Anti retroviral therapy), combination of two or more drugs, to treat HIV patient has provided stable suppression of virus. Although, HAART (Highly active anti retroviral therapy) has great contribution as an anti-HIV regimen, still it has some limitations.

➢ They have undesirable side effect, especially in case of long term treatment.

➢ Emergence of multidrug resistance is yet another problem.

➢ The treatment is very expensive.

Complete eradication of virus with no or minimal side effects demands exploration of other possible targets and sources. Keeping in mind the history of natural medicines and their potential to deal with several diseases, they could be useful as an anti-HIV. This fact provides an idea to explore the plants and study their phytochemistry.

Many research groups are working to explore biodiversity of herbal medicines to find a new lead for HIV treatment. Basic challenge for the new lead compound is to target replication cycle, less toxicity and less resistance profile. Some of the medicinal plants have shown to possess anti-HIV properties. WHO (1989), in the bulletin on *"In vitro screening of traditional medicines for anti-HIV activity"*, had declared the necessity of ethno medicines. A large number of plants are being used by AIDS patient, but lack of experimental evidence makes it difficult to get knowledge about these plants [95]. WHO (1989) report on informal consultation on traditional medicine and AIDS: in vitro screening for anti-HIV activity gives some database about ongoing activities in the area of natural products and AIDS [95]. Following are some examples as per report of WHO (1989);

Garlic- *Allivum sativum*	Shiitake mushrooms- *Lentinus edodes*
Papaya- *Carica papaya*	Ginseng (Panax species)
Ukrain- *Chelidonium majus*	Japanese pine cone extract

1.3.4.1 Selection of plants for anti-viral screening

There are four basic methods available for selection of plants for anti-HIV screening;

- ➤ Ethnobotanical approach- Search from traditional medicines that are being used by indigenous people. It is based on knowledge of traditional medicines and their use. Information can be obtained from the practitioner of traditional medicine.
- ➤ Literature reports- Study of scientific literature in which database is provided for anti-HIV screening.
- ➤ Random collection followed by bioassay- It is based on random screening of great number of plants which could possibly give some clue and some plant may have anti-HIV activity.
- ➤ Chemotaxonomic approach- Plants which are botanically related, probably has similar chemical constituents. If it is known that a plant possesses anti-HIV action, chemo taxonomically similar plants can be studied.

1.3.5 Anti-HIV compounds from natural origin

Calanolides (coumarins), Betulinic acid (triterpene), Baicalin (flavonoid), Polucitone A (alkaloid), lithospemic acid (polyphenol) are mentioned as promising anti-HIV agent [96]. Calanolides are coumarin derivatives; isolated from *calophyllum* spp. It is reported to have action like NNRTI [97]. Furanocoumarins (psolaren and bergapten), isolated from *Prangos tschimganica*, also reported to inhibit HIV-1 replication [98]. Triterpenoids (betulinic acid, plantanic acid and oleanolic acid), when tested in H9 lymphocyte cells, have shown HIV inhibition [99,100]. Lithospermic acid has shown strong anti-HIV activity in H9 cells [101].

Flavonoids and polyphenols have been proved to have antiviral activity in cell culture [102]. Many flavonoids are able to inhibit reverse transcriptase and viral protease [103]. Baicalin is an anti-HIV flavonoid extracted from *Scutellaria baicalensis* [104]. Taxifolin, a flavonoid isolated from stem bark of *Juglans mandshurica* is reported to have potent inhibition of HIV; it has cytopathic activity against MT-4 [99,100]. Thalassiolins (A, B, and C) isolated from *Thalassia testudinum,* a Caribbean Sea grass, are potent inhibitor of HIV integrase [105].

Kaempferol and quercetin from the leaves of *Thevetia peruviana* has good HIV-1 RT associated RDDP inhibitory activity [105,106].

Some Indian plants were also studied for anti-HIV activity. S. Sabde *et al.* has done screening of various extracts prepared form Indian medicinal plants. *Aegle marmelos, Argemone mexicana, Asparagus racemosus, Coleus forskohlii, and Rubia cordifolia* have shown anti-HIV activity measured in CD4+ T-cell line [107]. *O.sanctum, A officinalis and R. mucronata* (Indian traditional medicinal plants) have shown in-vitro anti-HIV activity. The inhibition is by two mechanisms; interference with gp 120/CD4 interaction and inhibition of reverse transcriptase [108]. Ethanolic extract of *O. sanctum and T. cordifolia* were studied as a HIV-protease inhibitor [109].

Several plants have been studied to seek their anti-HIV potential. **Table 1** gives the summary of some medicinal plants, their possible target or mechanism of action, and origin.

Table 1: Summary of some medicinal plants screened as anti-HIV

Name of the plant	Target/ action	Reference	Origin
Smilax corbularia	HIV-1 integrase	Supinya Tewtrakul *et al.*	Thai
Dioscorea birmanica	HIV-1 integrase	Supinya Tewtrakul *et al.*	Thai
Dioscorea membranacea	HIV-1 Protease	Supinya Tewtrakul *et al.*	Thai
Boesenbergia pandurata	HIV-1 Protease	Sarot Cheenpracha *et al.*	Thai
Eclipta prostrata	HIV-1 Protease and Integrase	Supinya Tewtrakul *et al.*	Tropical areas of Asia
Lindera chunii	HIV- 1 Integrase	Chao-feng ZHANG	China
Calophyllum spp	Reverse transcriptase	Xiao-Hui Su	Asia and Africa

Tuberaria lignosa and *Sanguisorba minor magnolii*	MTT assay	L.M. Bedoya	Western Mediterranean region.
Litsea verticillata	Inhibition of HIV replication	Zhang *et al.*, 2003	China
Aristolochia manshuriensis	Inhibition of HIV replication	Wu *et al.*, 2003	China
Anisomeles indica	Inhibited the cytoprothic effects of HIV-1 infection	Shahidul Alam *et al.*, 2000	Eastern Asia
Agastache rugosa	HIV-1 PRa	Min *et al.*, 1999	Korea and China
Crataegus pinnatifida	HIV-1 PR	Min *et al.*, 1999	
Garcinia speciosa	HIV-1 RTb	Rukachaisirikul *et al.*, 2003	
Vatica cinerea	Inhibited HIV-1 replication	Zhang *et al.*, 2003	Cambodiya, Malaysia, Burma, Thialand
Kadsura lancilim	Inhibited HIV replication	Chen *et al.*, 1999	
Tieghemella heckelii	Inhibited HIV-1 syncytium formation	Gosse *et al.*, 2002	Cameroon, Ivory Coast, Gabon, Ghana, Liberia, Nigeria
Cimicifuga racemosa	Inhibited HIV-1 replication	Sakurai *et al.*, 2004	
Valerianae fauriei	Inhibited Rev-mediated nuclear transport	Murakami *et al.*, 2002	Native of Europe

	Inhibited HIV-p24 production		
Terminalia arjuna	CD4 + T cell line	Sudeep Sabde *et al.*, 2011	India
Tinospora cordifolia	CD4 + T cell line	Sudeep Sabde *et al.*, 2011	India
Withania somnifera	CD4 + T cell line	Sudeep Sabde *et al.*, 2011	India
Tinospora cordifolia	HIV-1 RT	Mamidala Estari *et al.*, 2012	India
Ocimum sanctum	Interferance of with 120/CD4 interaction and inhibition of viral RT	Anuya A Rege *et al.*, 2009	India
Rhizophora mucronata	Inhibition of HIV-1 RT	Anuya A Rege *et al.*, 2009	India

1.3.6 Advanced stage anti-HIV natural products

Many research groups in different parts of the world are working with aim to find novel anti-HIV compounds. Few compounds are well studied and are now under clinical trial. Following are some of the natural products in advanced stage.

Calanolide A- It is a coumarin derivative isolated from *Calophyllum lanigerum.* It is selective inhibitor of recombinant HIV-1 RT [110]. Studies revealed that it binds near the active site of reverse transcriptase and interferes with dNTP binding. Now under phase I stage of clinical trial [111].

Calanolide A
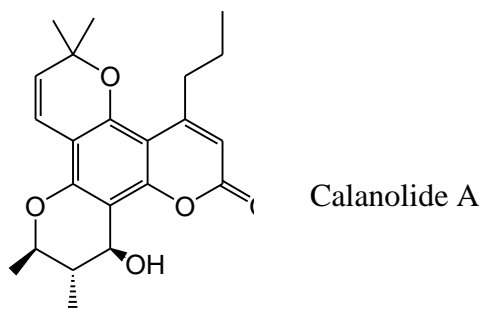
Bevirimat- Bevirimat, (3-O-[3′, 3′-dimethylsuccinyl] betulinic acid, is a semisynthetic derivative of aliphatic tirterpenic acid with two carboxylic groups [112]. It blocks the HIV-1 maturation; mechanism of action is different from other antiretrovirals. Studies revealed that bevirimat inhibits the processing of the viral Gag polyprotein at a specific step, namely the conversion of the capsid precursor p25 to mature capsid protein p24. This inhibition led to the production of non-infectious and immature viral particles [111,112]. It is now under phase IIb clinical trial.
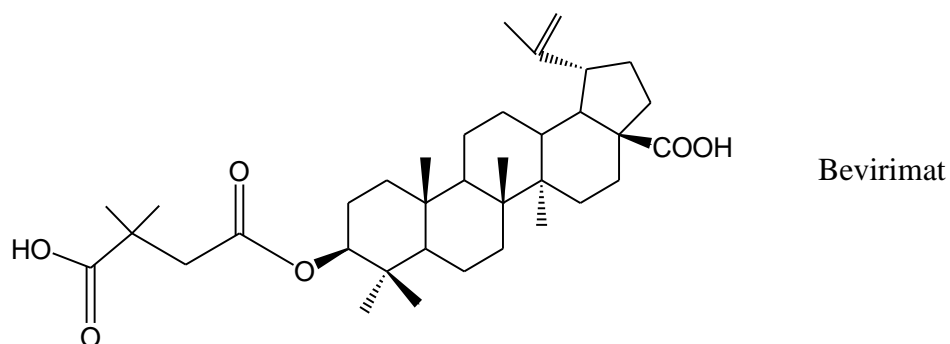
Bevirimat

PA-1050040- It is an analog of bevirimat, mechanism of action is same kind, maturation inhibitor. Now under phase I clinical trial

DCK- 3'R,4'R-di-O-(-)-camphanoyl-(+)-cis-khellactone, synthesized from suksdorfin [111]. Preliminary studies show that it selectively inhibits HIV-1replication and has no inhibitory effect on RT, protease and integrase. Currently it is under preclinical trial.

DCQA- Dicaffeoylquinic acids were found to inhibit HIV-1 replication in T-cell lines. Studies reveal the possible mechanism of action of DCQA is inhibition of HIV-integrase [113]. Currently it is under preclinical trial.

Dicaffeoylquinic acid
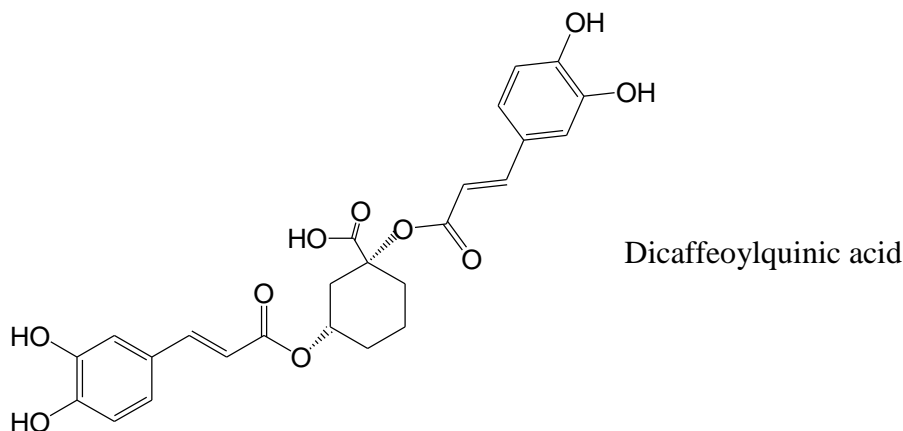
Curcumin- It is yellow pigment of *Curcuma longa* (turmeric). Curcumin has shown inhibitory activity on HIV-1 integrase [114]. Inhibition of HIV integrase is may be result from coordination of hydroxyl groups of curcumin to the acidic residues in the active site [114]. It was also reported that it inhibits p24 antigen production and Tat-mediated transcription at higher concentration [115]. Now it is under preclinical phase of clinical trial.

Curcumin
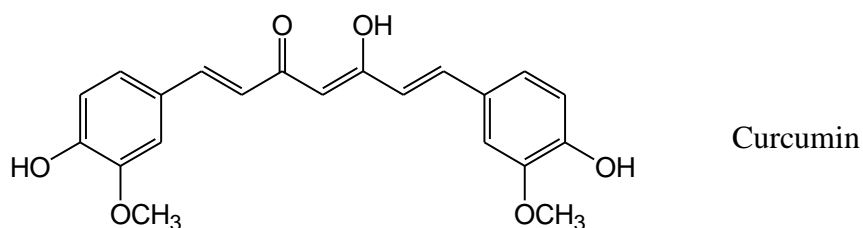
Cyanovirin A- It's a protein isolated from the cultured cyanobacterium *Nostoc ellipsosoprum* [111]. It irreversibly inactivates laboratory strains and primary isolates of HIV-1 and HIV-2 in low nanomolar concentrations. It also inhibits cell-to-cell fusion and transmission of HIV-1 infection [116]. Cyanovirin A interferes with viral interaction with target cell receptors by binding to viral glycoprotein. This interactions are essential for viral entry and cell to cell fusion [115]. At present it is under preclinical phase of clinical trial.

Several studies and reports on medicinal plants have proven the effectiveness and potential of natural/herbal medicines as anti-HIV agents. Although, present anti-HIV drugs have great contribution in treatment of HIV, still they are not completely devoid of undesirable side effects. There is need of continuous search of new lead molecule with new target. As discussed earlier HIV-1 RT-associated RNase H activity is an essential function for viral replication; it is an attractive target for HIV and is less explored. All RT inhibitors, currently in use or under clinical trial, inhibits polymerase activity and none of them inhibit RNase H function [87].

1.4 Human Rhinovirus (HRV)

Rhinoviruses (from a greek word "nose") are the most common viral infectious agents. HRVs are the major cause of common cold in human. HRV belongs to order "Picornavirales", family "Picornaviradae", and genus "Enterovirus". There are three known species at present; Rhinovirus A, B, and C. HRVs were first discovered in 1950s during the course of etiological study of common cold [117]. HRVs were thought to be a cause of upper respiratory tract infection; however studies have revealed that they are also linked to chronic obstructive pulmonary disease (COPD), asthma, bronchiolitis, pneumonia.

Earlier before 2009, HRVs were classified into two species, HRV- A and HRV-B, later a new species named HRV-C was identified. There are multiple HRVs in each species designated as "serotypes" or "strains". Hundred different types of strains were collected from the patients sample called prototype or reference set [118]. Partial sequencing of viral capsid-encoding regions, non coding regions, and a limited number of complete genomes led to a division of the original ninety-nine strains into two species: HRV-A (containing 74 serotypes) and HRV-B (containing 25 serotypes) [117,118]. Genome sequencing of the 99 serotype is completely examined by Palmenber *et.al.* [119] HRV-C has recently been recognized. International committee on taxonomy of viruses identify the novel species of rhinovirus named HRV-C [120]. Currently eleven types of HRV-C are known whose complete genomes are studied. Study reports on HRV suggest that HRV-C causes more severe respiratory illness and provocation of asthma leading to hospitalization than HRV-A or B.

HRV_S have been also classified into antiviral groups A and B according to their sensistivity toward a panel of antiviral compounds that reflect a different amino acid composition of the capsid proteins.

1.4.1 Structure of virion and viral replication

Rhinovirus is positive sense single stranded RNA virus of 7200bp [118,121]. Virions are about 8.5×10^6 daltons in mass, have an external diameter of 300 Å, and contain 60 promoters [122]. The genome has single gene, virally encoded protease cleaves the translated protein to yield 11 proteins [118]. The 5′UTR is typically ~650 bases, the open reading frame ~6500 bases (~2100

encoded amino acids) and the 3′UTR consists of ~50 bases. At the 5′-terminal U, all HRVs are covalently linked to a small viral protein (VPg), which serves as a primer for genome replication [118,123]. Capsid of HRV is composed of four viral proteins; VP1, VP2, VP3, and VP4. These viral proteins are arranged together to form a unit called protomer VP1, VP2, and VP3 form the major part of the capsid. VP4 is much smaller and it lies in between capsid and RNA genome. There are 60 copies of each of the 4 capsid protein which gives icosahedral structure to virion [117]. Fig. 8 shows organization of HRV genome.

Fig. 8: Organization of HRV genome [118].

Rhinoviruses replicate their genome and produce progeny in epithelial cells of upper and lower respiratory tract. Entry of major group of HRV into the host cell is mediated by cell surface receptor intercellular adhesion molecule-1 (ICAM-1), minor group attaches to the cell surface via low density lipoprotein receptor (LDLR) [117]. At least 78 of the 100 HRV serotypes recognize ICAM-1 as a cellular receptor [122]. Virus uptake occurs via clathrin dependent or independent endocytosis or via macropinocytosis [117]. Low pH in endosome or ICAM-1 initiates conformational changes in virion to release hydrophobic subviral particles. RNA genome crosses the endosome membrane into the cytosol through a pore formed by viral proteins or following membrane rupture. After the entry of RNA genome inside the cytosol; host cell ribosome translates the positive sense single stranded RNA into a polyprotein (structural and non

structural). Virion is then packed and assembled and undergoes to cellular export via cytolysis [117,118]. Fig. 9 shows the replication cycle of HRV.
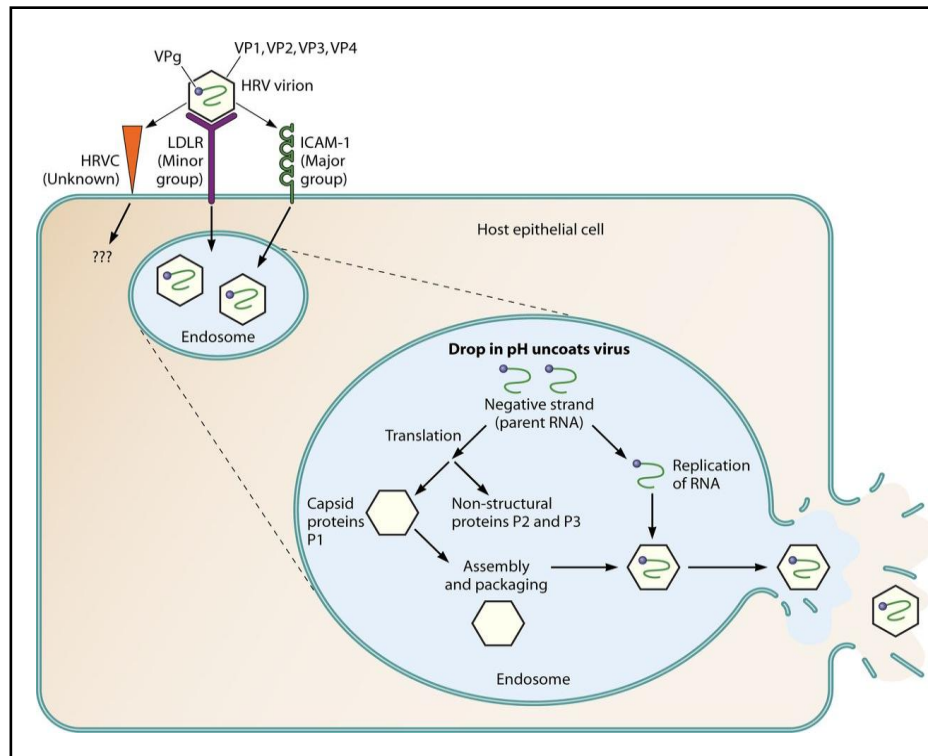

Fig.9: Replication cycle of rhinovirus

1.4.2 Rhinovirus cellular receptor

HRV-A and B serotypes are classified into two groups on the basis of cellular receptor specificity. Major group uses ICAM-1 and minor group utilizes LDLR. RV-C receptors are unknown until recently.

ICAM 1- Intracellular adhesion molecule is a cell surface transmembrane molecule, expressed at very low level. It is rapidly up-regulated by stimulation of cytokine, enhancing adhesion of leukocyte to endothelial cells at site of injury or infection [124]. ICAM-1 is a member of the immunoglobulin (Ig) superfamily of cell adhesion molecules expressed by several cell types including leukocytes, epithelial, and endothelial cells [125].

ICAM consists of five Ig (Immunoglobulin) domains (D1-D5), a transmembrane region and a small cytoplasmic domain [125,126]. The second, third and fourth Ig domains are heavily *N*-glycosylated with four potential sites in D2, two in D3 and two in D4 [127]. Major group of HRV (about 80%) utilizes human ICAM -1 as cell surface receptor [128]. Mutational & antigenic analyses and cryo-electron microscopy have shown that human RV attaches to the domain D1 of ICAM-1. This is primary step which triggers the entry of virus into host cell [129,130].
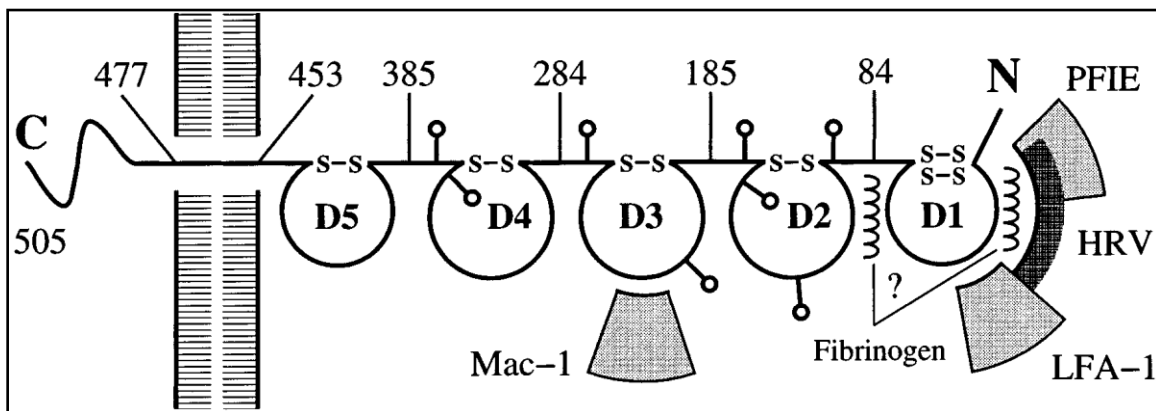
Fig.10: ICAM molecule

LDLR

LDLR is a type 1 transmembrane protein of 839 amino acids [131]. LDLR family of receptor has 3 members which can bind and allow RV to enter inside host cell [125]. They are,

- Low density lipoprotein receptor (LDLR),
- Very low density lipoprotein receptor (VLDLR), and
- Low density related receptor proteins (LRP)

Receptors in this family have presence of several structural modules in their extracellular regions and overall similar domain arrangements. These receptors can be recognized by the presence of ligand binding repeats, epidermal growth factor precursor, β-propeller modules, a single transmembrane domain, and a relatively short cytoplasmic tail [129,130]. Cholesterol carrying particles (CCP) are natural ligand of LDLR.

Circulating lipoprotein particles bind to LDL receptor at neutral pH. Receptor lipoprotein complexes enter cell by endocytosis via clathrin coated pits where the receptor molecule cluster on the cell surface [132]. This complex is then enters to endosome, low pH of the internal environment cause the release of the bound lipoprotein particle [133]. After delivery of receptors return back to cell surface by a process called receptor recycling.
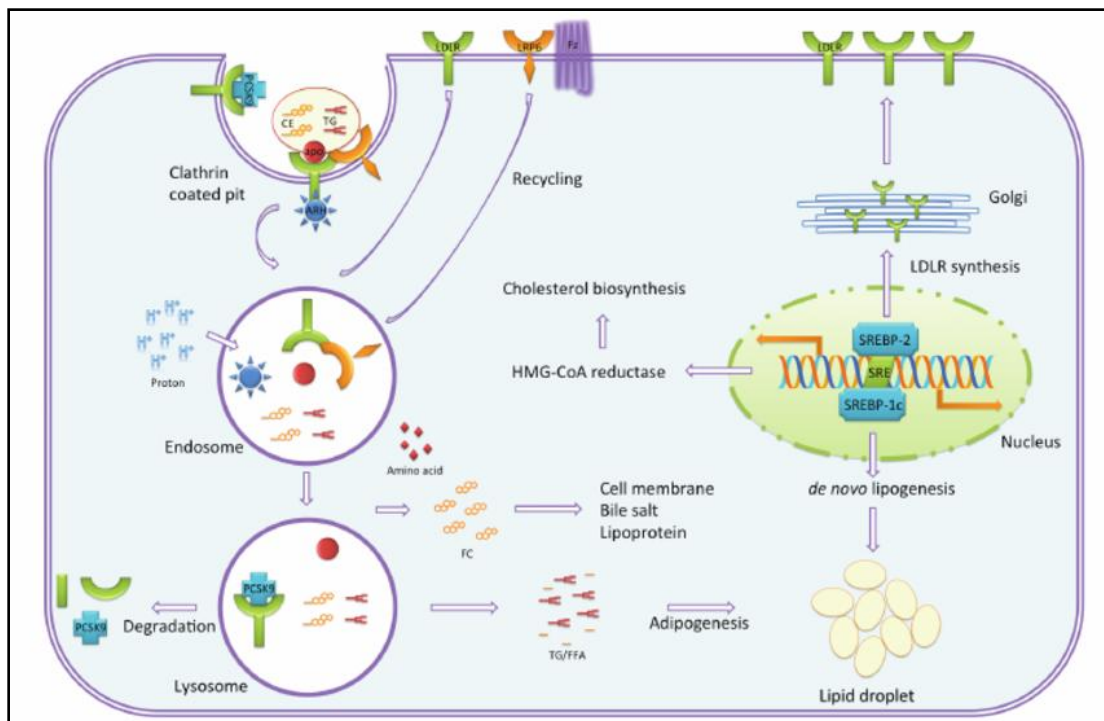
Fig.11: Uptake of lipoprotein particle by LDLR

1.4.3 Clinical syndromes of RV infection

Rhinoviruses are responsible for 30 to 50% of adult colds and 10 to 25% of colds in children [122,134]. Human Rhinoviruses are major cause of upper and lower respiratory tract infection. Some of its clinical syndromes are listed below.

- ➢ HRV causes problems of respiratory illness throughout the year and all over the world. Studies of molecular modeling and viral culture demonstrated that HRV is a cause of more than one half of cases of common cold [135]. Common symptoms of RV associated common cold include nasal congestion, rhinorhea, sore throat, cough, headache, fever, and malaise.

- ➢ HRV is linked to acute ottis media which increases severity of cold like illness in childhood [136].

- ➢ Sinus abnormalities (Rhino sinusitis) are frequently reported in patients with common cold. Maxillary and ethmoid sinuses are most commonly affected in patients with HRV infection [137]. Blowing nose is a potential mechanism which spread nasal fluids, containing viruses and pathogens, to sinuses in patients with cold symptoms.

- ➢ Croup- It is most commonly caused by parainfluenza viruses but also reported in children with HRV infection.

- ➢ Bronchiolitis is the most common clinical condition caused by HRV infection in children and accounts for 14% of HRV associated lower respiratory tract infection [138].

- ➢ Study reports of children hospitalized with community acquired pneumonia (CAP) concluded that HRV is common in viral CAP.

- ➢ HRV is increasingly being found as a significant cause of acute respiratory illness in patients with compromised immunity [139]. HRV causes both upper and lower respiratory tract infections in hematologic malignancy patients [139].

- ➢ Rhinoviruses are found to be associated with exacerbation of asthma. Asthamatic patients experience more frequent and severe lower respiratory tract infection. Two-thirds of asthma exacerbations, which are virus associated, are due to HRV [140,141]. Studies have revealed the correlation between HRV infection and exacerbation of chronic obstructive pulmonary disease (COPD).

1.4.4 Antiviral agents for treatment of RV infection

1] Capsid inhibiting compounds

Viral capsid, a type of viral protein, was the first target for the development of viral replication inhibitors. These agents bind to the hydrophobic pocket of the viral capsid, bring out conformational changes that increase the stability of the virion and interfere with its ability to interact with the cellular receptor [142]. Capsid-inhibiting compounds block viral uncoating and/or viral attachment to host cell receptors.

a) **Pleconaril -** {3-[3,5-dimethly-4-[(3-methyl-5-isoxazolyl)propyl]phenyl]-5-(trifluoromethyl)-1,2,4-oxadiazole}. It is the first of a new generation capsid inhibitor. It has shown broad spectrum and potent antiviral activity against EV and RV. Pleconaril has high oral bioavailability (70%), long half life, and better CNS penetration [143,144].
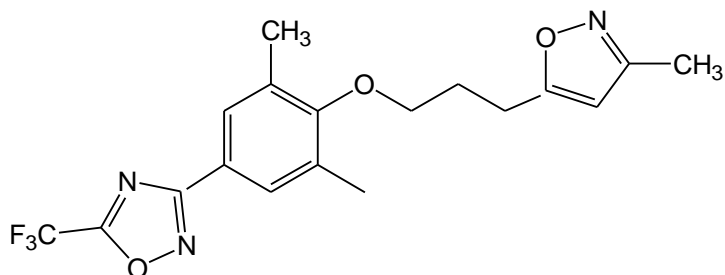
Pleconaril

b) **Vapendavir-** Is a type of capsid inhibitor, administered orally, that binds to HRV -VP1 capsid protein and thus prevents the release of viral RNA into the target cell. Vapendavir shows activity against HRV-A and HRV- B serotypes and some strains of EV.
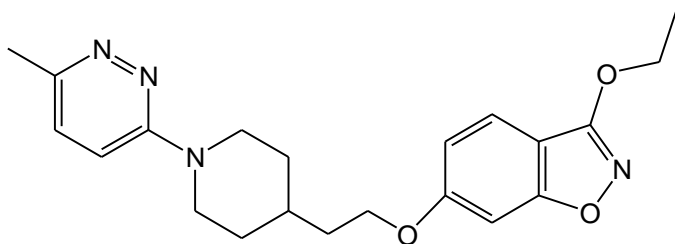

Vapendavir

c) **Pirodavir.** Intranasal capsid binding agent**;** it reached to phase 3 clinical trial but later on discontinued as it failed to show a significant reduction in severity of symptoms [145,146].
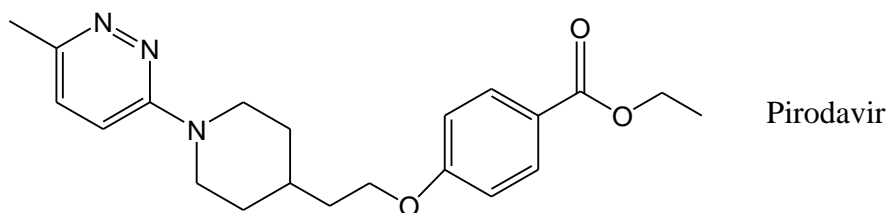
Pirodavir

2] Enviroxime related compounds

Enviroxime [2-amino-l-(isopropyisulphonyl)-6-benzimidazole phenyl ketone oxime] is a prototype compound, developed by Lilly Pharmaceuticals that lead to series of molecule with broad spectrum action against EV and RV [147]. Enviroxime inhibits the replication of RNA by targeting 3A protein coding region of the virus. It prevents formation of RNA replication intermediate and consequently formation of new plus strand RNA molecules [148]. Vinyl acetylene benzimidazoles derivatives of enviroxime provide improved bioavailability of the compounds; flouridation of these latter structures further enhances blood levels in animal models. Poor pharmacokinetics, undesirable toxicity, and side effects resulted in discontinuation of the Enviroxime program.
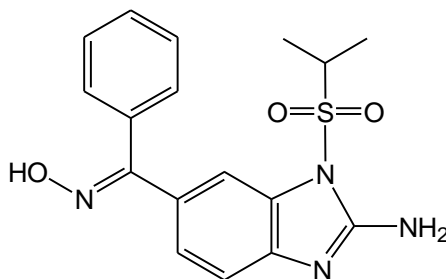
Enviroxime

3] 3C protease inhibitors

This class of compounds targets the 3C protease of picornavirus consequently inhibition of viral protein synthesis [149]. Rupintrivir was one of the most potent compounds to inhibit 3C protease *in vitro* and was active against a broad panel of HRVs and EVs [117,149]. In an HRV challenge trial, Rupintrivir was well tolerated and reduced viral loads and respiratory symptoms. However, in trials of natural infection, rupintrivir did not significantly affect viral loads and symptom severity [150,151]. Some researchers recently designed proline and azetidine based analogues of Rupintrivir that target the P2 pocket of the binding site, lead to compound with activity against HRV serotypes [152].
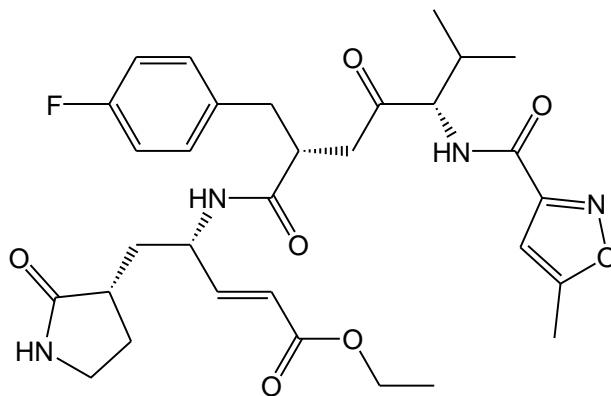
Rupintrivir

HRV infection and its associated clinical syndromes need more attention. At present very few antiviral drugs are available. Because of safety concern, undesirable side effects and lack of broad spectrum action many compounds failed to develop as a lead molecule.

1.5 GABA receptors

GABA (γ-amino butyric acid) is the major inhibitory neurotransmitter of mammalian Central Nervous System (CNS). GABA is essential for balance between neuronal excitation and inhibition which is consequently important for normal functioning of brain. Too much inhibition, or too little excitation, can lead to coma, depression, low blood pressure, sedation or sleep. Too much excitation, or too little inhibition, can result in a range of conditions including, convulsions, anxiety, high blood pressure, restlessness, and insomnia [153]. All neurons in the brain respond to GABA and 20% of them uses it as their primary transmitter [154].

Role of GABA receptor as inhibitory transmitter in CNS was experimentally demonstrated in late 1960s. GABA is produced in presynaptic neurons and stored in synaptic vesicle. Synthesis of GABA is modulated by an enzyme called L-glutamic acid decarboxylase [155]. After synthesis GABA is released into synapse where it acts on postsynaptic receptors or diffuses into extracellular space where it activates extra synaptic receptors [156,157]. GABA transporter then brings out the removal of GABA from extracellular space. This process of GABA release from presynaptic vesicle and uptake by GABA transporters balances the extracellular GABA level [157]. Figure 12 shows schematic representation of GABA synthesis and transport.
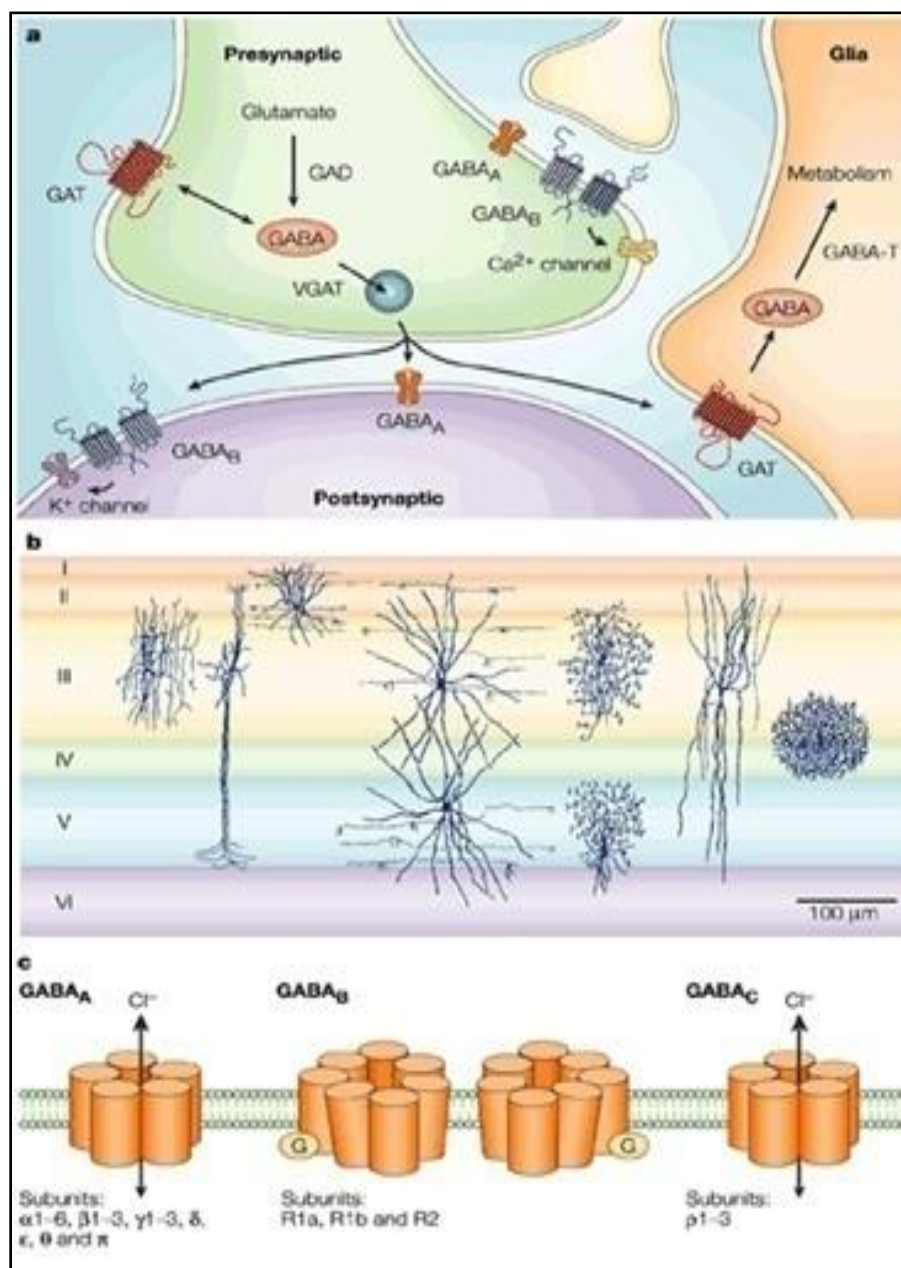
Fig.12: Schematic diagram of GABA synthesis and transport at synapse [158]

Inhibitory action of GABA is produced by a membrane bound receptors. These receptors are classified into two classes;

1] Ionotropic receptors (GABA$_A$ and GABA$_C$ receptor)

2] Metabotropic (GABA$_B$ receptor)

1.5.1 Ionotropic receptor (GABA$_A$ Receptor)

GABA$_A$ is a transmembrane hetero-oligomeric protein. They are expressed and widely distributed in peripheral and central nervous system [159]. These are ligand gated chloride ion channel receptors that means classical action of GABA$_A$ involves opening of chloride channel [160]. Upon activation receptor allows chloride ions to flow into the cell resulting in neuronal hyperpolarization. GABA$_A$ receptors are activated by GABA, muscimol and isoguvacine and inhibited by bicucullin, gabzin and B-hydrastin.

GABA$_A$ receptors belongs to the large "*Cys*-loop" super-family of evolutionarily related and structurally similar ligand-gated ion channels which also includes nicotinic acetylcholine receptors, glycine receptors, and the 5HT$_3$ receptor [159,161]. There are numerous subunit isoforms of GABA$_A$ receptor, which determine the receptor's agonist affinity, chance of opening, conductance, and other properties. GABA$_A$ receptors are construction of 19 different subunits, encoded by different genes and grouped into α, β, γ, δ, ε and ρ subunit. Various subunits of GABA receptors are α_1– α_6, β_1– β_3, γ_1– γ_3, δ, ε, and ρ_1 -ρ_3 [155-159,161-163]. The majority of GABA$_A$ receptors expressed in the CNS are $\alpha_1\beta_2\gamma_2$. Also $\alpha_3\beta_3\gamma_2$ and $\alpha_2\beta_3\gamma_2$ receptors are highly prevalent [163].
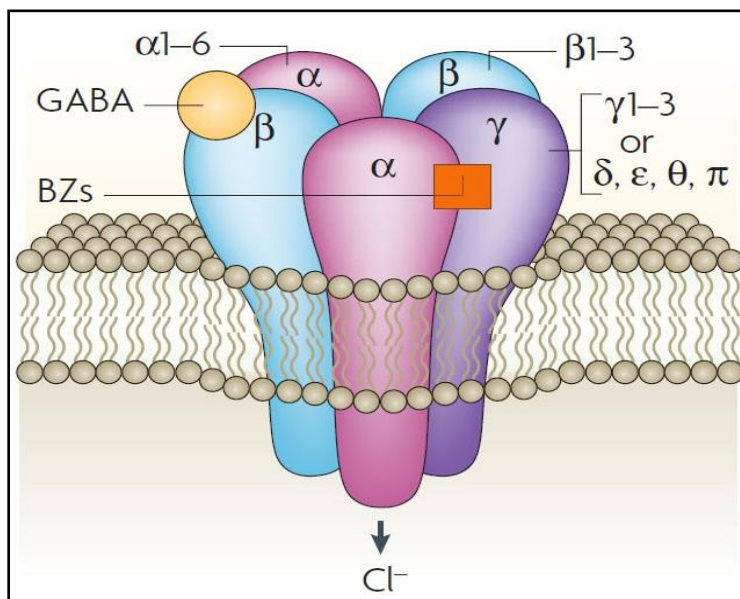
Fig.13: GABA$_A$ receptor and its subunit

After the discovery of GABA$_A$ and GABA$_B$ new class of receptors were discovered which was insensitive to bicuculline, barbiturates, benzodiazepines and baclofen. Johnston and colleagues in their studies found that *cis*-4-amino crotonic acid (CACA), an analog of GABA, selectively activates the class of receptor in mammalian CNS. These receptors were different from GABA$_A$ and GABA$_B$ and named as GABA$_C$ in 1984 [164]. These novel receptors were studied at molecular level and several studies revealed that GABA$_C$ receptors are composed of ρ subunit of GABA$_A$ receptor [164-166]. Recently, it has been proposed those receptor containing ρ subunits are special class of GABA$_A$ receptors as ρ subunits are structurally part of GABA$_A$ receptor subunit. International union of basic and clinical Pharmacology committee on receptor nomenclature and drug classification (IUPHAR) has recommended that the term GABAc be avoided and and classify this new class of receptor, GABAc, as a minor subspecies of GABA$_A$ receptor.

Ionotropic GABA receptors are considered to have five protein subunits which constitute a central pore to form actual ion channel. Each subunit has a large extracellular N-terminal domain, three membrane spanning domain, an intracellular loop of variable length, and a

membrane spanning domain with extracellular C-terminal. All subunits arrange themselves in a way that second membrane spanning domain forms the wall of channel pore and conduction of anions or cations through channel is depend on total charge of the domain. As discussed above $GABA_A$ receptors are heteromeric i.e. made up of different subunit (α, β, γ) and $GABA_C$ receptor are homomeric i.e. made of one type of subunit (ρ). As GABA is major inhibitory neurotransmitter, it is directly or indirectly involved in many brain disorders. Compounds acting on $GABA_A$ receptor has broad spectrum of therapeutic use as Anesthetics, Anticonvulsant, Anxiolytic, and Sedative -Hypnotics. These agents increase the GABA-mediated inhibition by direct activation of $GABA_A$ receptors or by enhancing the action of GABA on receptors. Figure 14 shows GABA receptor agonist and antagonist binding site.

$GABA_A$ agoinst includes Muscimol, GABA, Isoguvacin, Benzodiazepines (Diazepam, Clonazepam, Alprazolam, Lorazepam), Barbiturates (Phenobarbital and Pentobarbital), and Ethanol (partial agonist). Benzodiazepines (BZD) and Barbiturates are positive allosteric modulators of $GABA_A$ receptors. BZDs enhance presynaptic/postsynaptic inhibition through a specific BZD receptor which is an integral part of the $GABA_A$ receptor-Cl^-channel complex. The subunits of this complex form a pentameric transmembrane anion channel gated by the primary ligand (GABA), and modulated by secondary ligands which include BZDs. Only α and β subunits are required for GABA action, binding site for GABA is located on the β subunit, while α or γ subunit interface carry's the BZD binding site. The modulatory BZD receptor increases the frequency of Cl^- channel opening induced by submaximal concentrations of GABA. The BZDs also enhance binding of GABA to $GABA_A$ receptor. Barbiturates are positive allosteric modulator of $GABA_A$ and mediate its action through multiple homologous tramsmembrane pocket located at subunit surface. Binding site of barbiturates is distinct from that of GABA and benzodiazepines. Pentobarbital, an example of barbiturates class, mediates its response through $\alpha_4\,\beta_1\,\gamma_2$ and $\alpha_6\,\beta_1\,\gamma_2$ subunit $GABA_A$ receptor.

Bicucullin, Gabzin and B-hydrastin are the examples of $GABA_A$ antagonist. Bicucullin acts as a competitive $GABA_A$ receptor antagonist. It blocks inhibitory hyperpolarizing responses and reduces Cl^- conductance by modulating channel opening time and frequency.
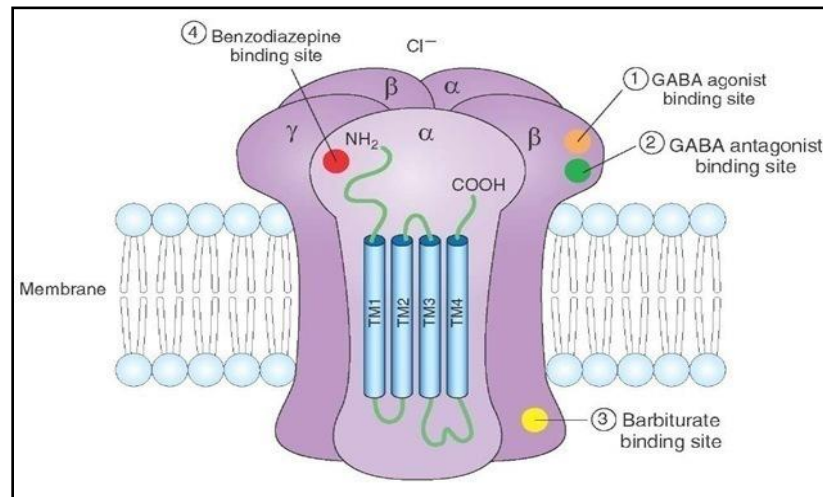
Fig. 14: GABA receptor agonist and antagonist binding site

1.5.2 GABA$_B$ receptors

These are metabotropic transmembrane receptors of GABA that are linked via G-proteins to potassium channels, change in potassium concentrations hyperpolarize the cell at the end of an action potential [167]. The GABA$_B$ receptors are distributed in the CNS and peripheral nervous system they are mainly localized to neurons, with their high density in the cerebral cortex, thalamic nuclei, cerebellum, and amygdale [168]. GABA$_B$ are similar in structure with metabotropic glutamate receptor. These receptors are pre and post synaptically present in brain; where they are coupled with Ca^{2+} and K^+ channels. Upon activation this receptor causes inhibition of transmitter release and neuronal hyperpolarization [169].

GABA$_B$ receptors have a central core domain which consists of seven transmembrane helices; this central core is responsible for G-protein coupling. GABA$_B$ is heterodimer formed by 2 subunits, GABA$_{B1}$ and GABA$_{B2}$ [169-171]. GABA$_B$ receptor predominantly couples to G protein and its primary effect is inhibitory [168]. This inhibitory effect is a consequence of inhibition of the presynaptic voltage-gated Ca^{+2} channel, activation of postsynaptic K^+ channels and inhibition of adenyl cyclase [170,171]. GABA$_B$ receptors have important modulatory effects in many circuits of the nervous system and their dysfunction may lead to epilepsy, cognitive

deficits, and behavioral abnormalities. Baclofen is the only compound in current clinical use mediates its effects by activation of GABA$_B$ receptors. Baclofen has well established beneficial effect in spasticity, dystonia, pain, cognitive deficits.
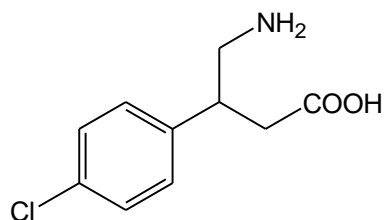
Baclofen

Chapter 2: Description of Plants

2.1 *Ocimum sanctum*

- Genus   : *Ocimum*
- Species   : *sanctum*
- Family   : Lamiaceae
- Habitat   : Throughout India, grown in houses, gardens, and temples.
- Synonyms   : In English - Holy basil, sacred basil. In Ayurveda - Tulasi, Surasaa, Surasa, Bhuutaghni, Suravalli, Sulabhaa, Manjarikaa, Bahumanjari, Devadundubhi, Apet-raakshasi, Shuulaghni, Graamya, Sulabhaa [172].

Fig.15: *Ocimum sanctum* (Tulsi) - Leaves and Inflorescence

Ocimum sanctum (Tulsi) is considered as "Elixir of life" as it offers innumerable health benefits. It is sacred and traditional medicinal plant. Whole plant (leaves, roots, seeds, stem inflorescence) has proved to have significant medicinal value and hence it is an essential element

in Ayurveda [173]. Ayurvedic pharmacopoeia recommends the use of leaf in rhinitis and influenza and the seeds in psychological disorder [172,174]. *O. sanctum* leaves are important component of many Ayurvedic cough syrups and expectorants [175]. Tulsi is branched shrub, about 30-60 cm in length. Stem is erect, hairy, branched, and woody with opposite leaves. Leaves are acute, simple, petiolate, ovate, and serrate and with aromatic smell. Color of leaves varies from light green to light purple. Flowers are small crimson to purplish in color arranged in group to form inflorescence. Fruit has group of 4 nutlets each with one seed. Seeds are rounded and oval brown in color.

2.1.1 Medicinal properties

Leaves of Tulsi are carminative, stomachic, antispasmodic, antihistaminic, expectorant, stimulant, hepatoprotective, and antipyretic. Juice of Tulsi leaves is usefeul in fever. Essential oil present in Tulsi has antibacterial and antifungal properties. Roots of tulsi have antimalarial activity. Also, boiled leaves with tea acts as preventive in malaria and dengue [176]. Plant extracts have exhibited antiulceregenic property against experimental ulcer. Tulsi leaves are effective against mouth ulcer and infections of mouth [172]. Tulsi leaves are important element of Ayurvedic cough syrups. Aqueous extracts of Tulsi leaves can be taken as drink to treat sore throat [177]. Chewing of leave reduces the level of blood cholesterol, strengthens the heart muscles and improves blood supply to the heart [178]. Juice of leaves effectively treats common paediatric problems like cough, cold, fever, diarrhoea, vomiting [177]. Consumption of Tulsi leaves regularly can help in kidney stone problem. Taking Tulsi leaves with honey and water for six months removes stones through urinary tract and also strengthens the kidney [179].

2.1.2 Chemical Composition

Aromatic odour of *O. sanctum* is due to the presence of essential oil. Other than essential oil the plant also contains saponins, alkaloids, glycosides, and tannins [173]. Volatile oil of Tulsi is mainly present in leaves; about 0.7% volatile oil is present in leaf of Tulsi. Major component of essential oil are eugenol, carvacrol, eugenolmethylethr, and nerol [172,180].

The alcoholic extract of leaf and other aerial parts contain ursolic acid, apigenin, luteolin, apigenin-7-*O*-glucuronide, luteolin-7-*O*-glucuronide, isorientin, orientin, molludistin, stigmasterol, circineol, gallic acid, gallic acid methyl ester, gallic acid ethyl ester, protocatechuic acid, vallinin, triacontanol ferulate, vicenin-2, vitexin, isovitexin, aesculectin, aesculin, chlorgrnic acid, galuteolin, 4-hydroxybenzoic acid, vallinin, caffeic acid, chlorogenic acid, β-stigmasterol and rosmarinic acid [181-184].
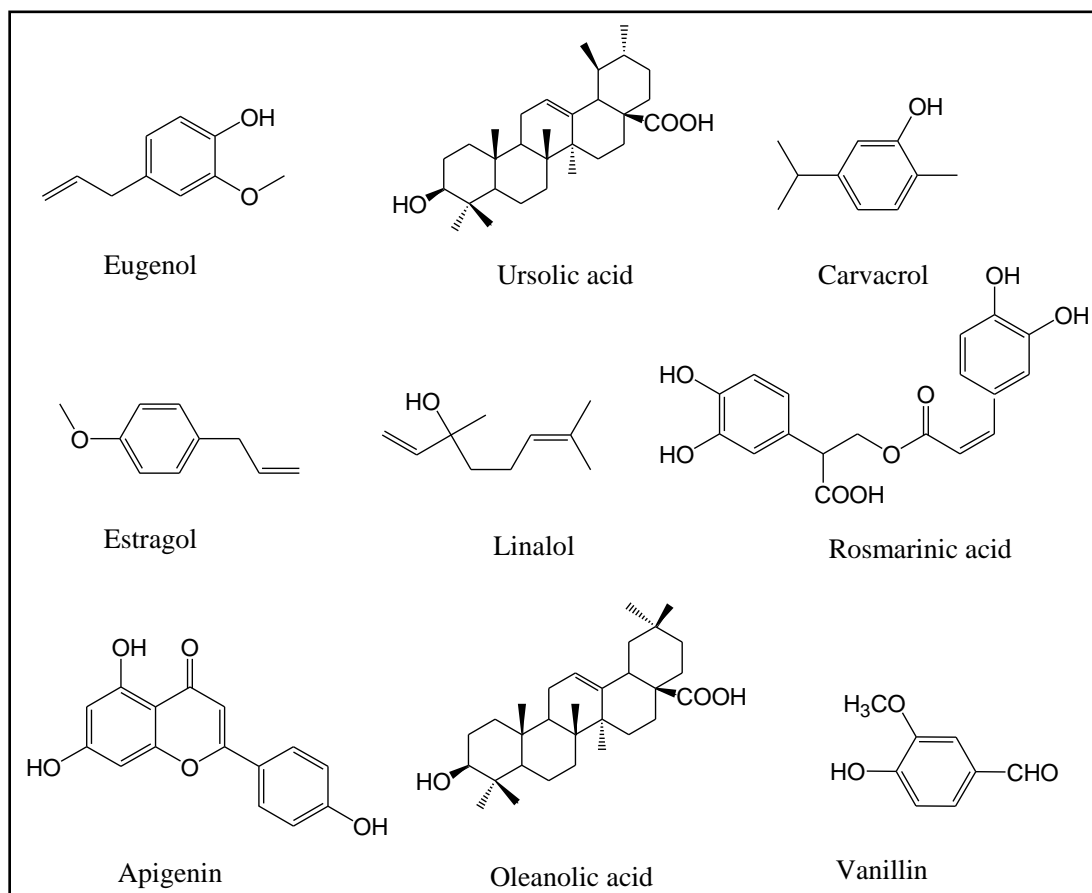
Fig.16: Structure of some important chemical constituents from *O. sanctum*

Major chemical constituents of the plants are eugenol, ursolic acid, carvacrol, linalool, limatrol, caryophyllene, estragol (methyl carvicol), oleanolic acid, linoleic acid. In addition to the above list phenolic compounds like rosmarinic acid, apigenin, cirsimaritin, isothymusin and isothymonin are also present. Volatile oil of seeds contains fatty acid and sitosterol.

2.1.3 Biological activities of *O. sanctum*

➢ Experimental studies using biological model have demonstrated that *O. sanctum* extract showed cytotoxic activity in fibrosarcoma cells [185]. Methanolic extract of *O. sanctum* have been shown to possess anticancer property through reduction of excess amount of nitric oxide.

➢ The fresh leaf of the *O. sanctum* has been shown to enhance the immunity and also exhibit anti-carcinogenic properties in experimental animals.

➢ *O. sanctum* has immuno stimulant capacity. It is found to be powerful adaptogenic or antistress agent. Studies have shown that leaves of *O. sanctum* significantly increase the levels of enzymatic and non enzymatic antioxidant suggesting its anti-stress potential [186].

➢ Leaves of *O. sanctum* have shown to have hypoglycemic effects in experimental animals. A study of leaves extract of the plant on rats suggested that constituents from the leaves has stimulatory effect on physiological pathway of insulin secretion [187].

➢ Aqueous decoction of Tulsi is helpful for patients suffering from gastric and hepatic disorder. Preparations containing Tulsi are suggested to shorten the clinical symptoms and biochemical parameters in patients with viral hepatitis.

➢ The phenolic compounds present in Tulsi e.g. irsilineol, cirsimaritin, isothymusin, apigenin and rosmarinic acid, and eugenol, a major component of the volatile oil have good antioxidant activity. *O. sanctum* extract has significant ability to scavange free radicals [188].

➢ Essential oil present in leaves and fixed oil present in seeds have been shown to exhibit humoral and cell mediated immune responses in non stressed and stressed animal.

➢ The flavanoids orientin and vicenin, isolated from the leaves of Tulsi showed better radio protective effect as compared with synthetic radio protectors. These flavanoids have shown significant protection to the human lymphocytes against the clastogenic effect of radiation at low, non toxic concentrations [189].

➢ *O.sanctum* has shown *in-vitro* anti-HIV activity. The inhibition involved two mechanisms; interference with gp 120/CD4 interaction and inhibition of reverse

transcriptase [108]. Ethanolic extract of *O. sanctum* revealed a probable anti HIV-protease action [109].

➢ Oleanolic acid and ursolic acid have shown anti-HIV activity. They are reported to inhibit HIV-1 replication in acutely infected H9 cells [190].

2.2 *Tinospora cordifolia*

- Genus   : *Tinospora*
- Species   : *cordifolia*
- Family   : Menispermaceae.
- Habitat   : Tropical areas of India, Myanmar, Sri Lanka and Andaman (an island of India)
- Synonyms : Gulvel, Guduuchi, Guduuchikaa, Guluuchi, Amrita, Amritaa, Amritalataa, Amritavalli, Chinnaruuhaa, Chinnodbhavaa, Madhuparni,Vatsaada-ni, Tantrikaa, Kundalini, Guduuchi sattva [172].

Fig. 17: *Tinospora Cordifolia* (stem bark and fruits)

Tinospora is large and extensively spreading climber type of shrub with several elongated twig branches. Leaves of the plants are simple alternate, ex-stipulate with long petiole and approximately 10-20 cm long and 15cm broad. Roots are aerial with tetra to penta arch primary structure. Stem of the plant is long, filiform, fleshy and climbing in nature. Bark is creamy whit to grey in colour. It is being used traditionally as medicinal plants since ages; Ayurvedic

Pharmacopoeia of India recommends the dried stems of this plant in treatment of jaundice, anaemia, polyuria and skin disease [172].

2.2.1 Medicinal properties

T. cordifolia finds a special place for its use in folk medicine. It is reported to have antipyretic, antiperiodic, anti-inflamatory, antirheumatic, spasmolytic, hypoglycaemic and hepatoprotective activity [172]. Stems juice is prescribed in high fever. Water extract of tinospora stem bark possess diuretic activity. Alkaloids present in stems and roots have anti-viral and anti-diabetic action, also they are immunomodulatory. In Sushurta Samhita, it is mentioned under "Tikta-Saka Varga" and claimed to be useful in treating *Kustha* (Leprosy), *Maha-jvara* (High fever), *Svasa* (Asthma) and *Aruchi* (anorexia).

2.2.2 Chemical Composition

Stems bark and roots are rich source of alkaloids. Berberine, choline, tembetarine, magnoflorine, tinosporin, palmetine, aporphine alkaloids, jatrorrhizine, tetrahydropalmatine are the alkaloids found in stems and roots (Fig. 18). Diterpenoid lactones, such as furanolactone, clerodane derivatives, tinosporon, tinosporides, isocolumbin and columbin, are found in whole plant (Fig. 18). 18-norclerodane glucoside, furanoid diterpene glucoside, tinocordiside, tinocordiofolioside, cordioside, cordiofolioside are the glycosides derivatives found in stem bark. It contains steroids like β–sitosterol, δ-sitosterol, 20 β-hydroxyecdysone, ecdysterone, makisterone a giloinsterol tinocordifolin is a sesquiterpenoid present in stems.
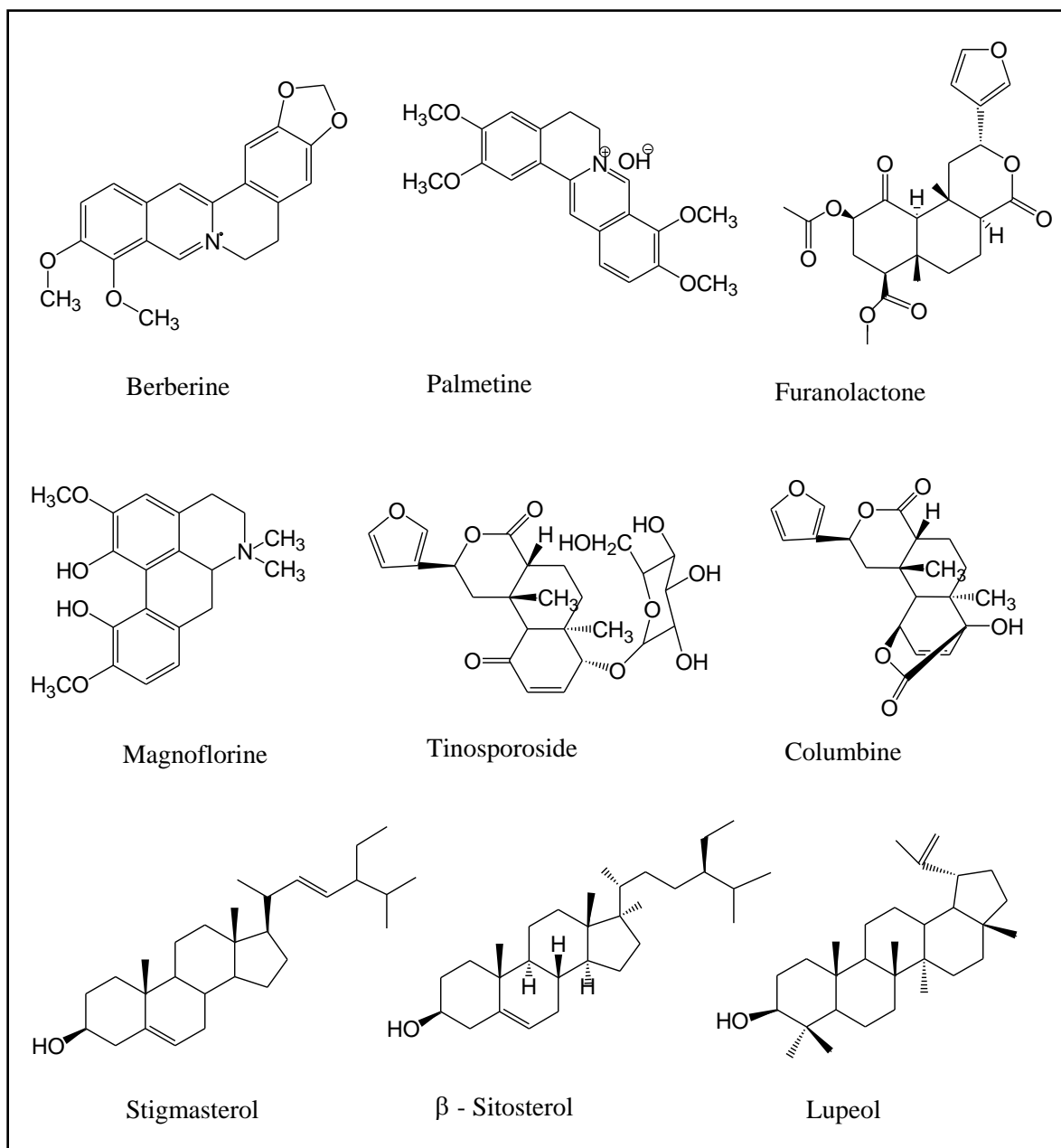
Fig. 18: Structure of some important constituents of *T. cordifolia.*

2.2.3 Biological activities of *T. cordifolia*

➤ *T. cordifolia* is reported to have one fifth of the analgesic effect of sodium salicylate [172]. An aqueous extract of *T. cordifolia* decreased bronchospasm in guinea pigs, decreased capillary permeability in mice and reduced the number of disrupted mast cells in rats [191].

➤ Stems of the plant are generally used for diabetes. Alcoholic extract of stem favours the endogenous secretion of insulin. Oral administration of alcoholic extract of the root significantly lowers the blood and urine glucose level [192]. Anti-diabetic properties of the plant are attributed to the presence of alkaloids (palmetine, jatrorrhizine), tannins, cardiac glycoside, flavanoid, saponins and steroids [193,194]. A new hypoglycaemic agent (1,2-substituted pyrrolidine) was isolated from the plant [172].

➤ A significant reduction in levels of SGOT, SGPT, ALP and bilirubin were observed following *T. cordifolia* treatment during CCl_4 intoxication in mature rats [195].

➤ *T. cordifolia* is well known for its immunomodulatory property. 11-hydroxymuskatone, N-methyle-2-pyrrolidone, N-formylannonain, cordifolioside A, magnoflorine, tinocordioside and syringin these are the compounds responsible for immunomodulatory action of *T. cordifolia*.

➤ Aqueous extracts of stem bark helps to resolve the problem of urinari calculi [196].

➤ Aqueous, methanolic and dichloromethane extract of *T. cordifolia* have shown dose dependent increase in lethality to HeLa cells [191].

➤ *T. cordifolia* also exhibits antioxidant potential. In vitro studies revealed that *T. cordifolia* extract reduces toxicity induced by free radicals, inhibits peroxidation of lipids. It also inhibits generation of superoxide and hydroxyl radical [191].

➤ Roots extract of *T. cordifolia* have shown decrease in regular resistance against HIV. Anti HIV effect is evidenced by reduction in eosinophil count, stimulation of B-lymphocyte, macrophages, and level of Hb count [197,198].

➤ Methanol extract of *T. cordifolia* stem bark have shown moderate activity against HIV-1 [107].

➤ Ethanolic extract of *T. cordifolia* have shown potent inhibitor activity *versus* HIV-protease; pepsin was used as substitute for HIV-protease [108].

2.3 *Bupleurum fruticosum* L.

- Genus   : *Bupleurum*
- Species   : *fruticosum*
- Family   : Apiaceae
- Habitat   : It is native of Mediterranean area In the Iberian Peninsula it is found in Barcelona, Castellon, Girona, Lleida, Tarragona and Valencia.
- Synonyms   : Adelfilla, Amarguera, baladre, batabuey, clujia fina, costibuey, Costilla de buey, cuchilleja, cuchilluela, custibuey, limoncillo, olivilla etc.

Fig. 19: *B. fruticosum* (Shrub, flowers and leaves).

The name of the genus *Bupleurum* originates from a latin word *Boupleuron* (*Bous- Ox* and *pleura/on-* rib/s), the word describes the shape of roots [199]. *B. fruticosum* is a large shrub of height up to 2 meter with compound umbels. The leaves are entire, glabrous, leathery, more or less linear oblong. Flowers are yellow, bisexual with five stamens and fruits occur mainly as cremocarps. Figure 19 shows leaves and flowers of the shrub.

2.3.1 Medicinal properties

Various species of the genus *Bupleurum* found their use as traditional medicine. *Bupleurum* species alone or in combination with other ingredients are used in treatment of common cold, hepatitis, inflammation, cancer, and fever. Over the counter herbal tea preparation and other preparations of *B. fruticosum* are available. *Bupleurum* species are officially listed in Japanese and Chinese Pharmacopoeia. *Bupleurum* is well known in Japan and Korea for the treatment of pain, fever, and inflammation associated with influenza and common cold [200]. Roots and stems of *B. fruticosum* are used in Sardinian folk medicine as an antirheumatic remedy [201].

2.3.2 Chemical constituents

A phytochemical investigation reports the presence of saponins, coumarins, and phenylpropanoids in *B. fruticosum.* Leaves and branches contain essential oil. Essential oil obtained from *Bupleurum* is rich in α pinene (21.7%), β phellandrene (21.3%) and β -pinene (13.2%) [202]. 22 constituents from the essential oil of the *Bupleurum* were identified. Tricycline, α-thujene, α-pinene, sabinene, β-pinene, β-myrcene, α-phellandrene, d-3- careen, α-terpinene, p-cymene, β-phellandrnene, β- (z)-ocimene, γ-terpinene, α-terpinolene, terpenen-4-ol, α-terpineol, methyl cavicol, geraniol, citronellyl acetate, geranyl acetate, α-copaene, β-cubebene, germacrene D, bicyclogermacrene, d-cadinene, (E)-nerolidol are the components of essential oil [203].
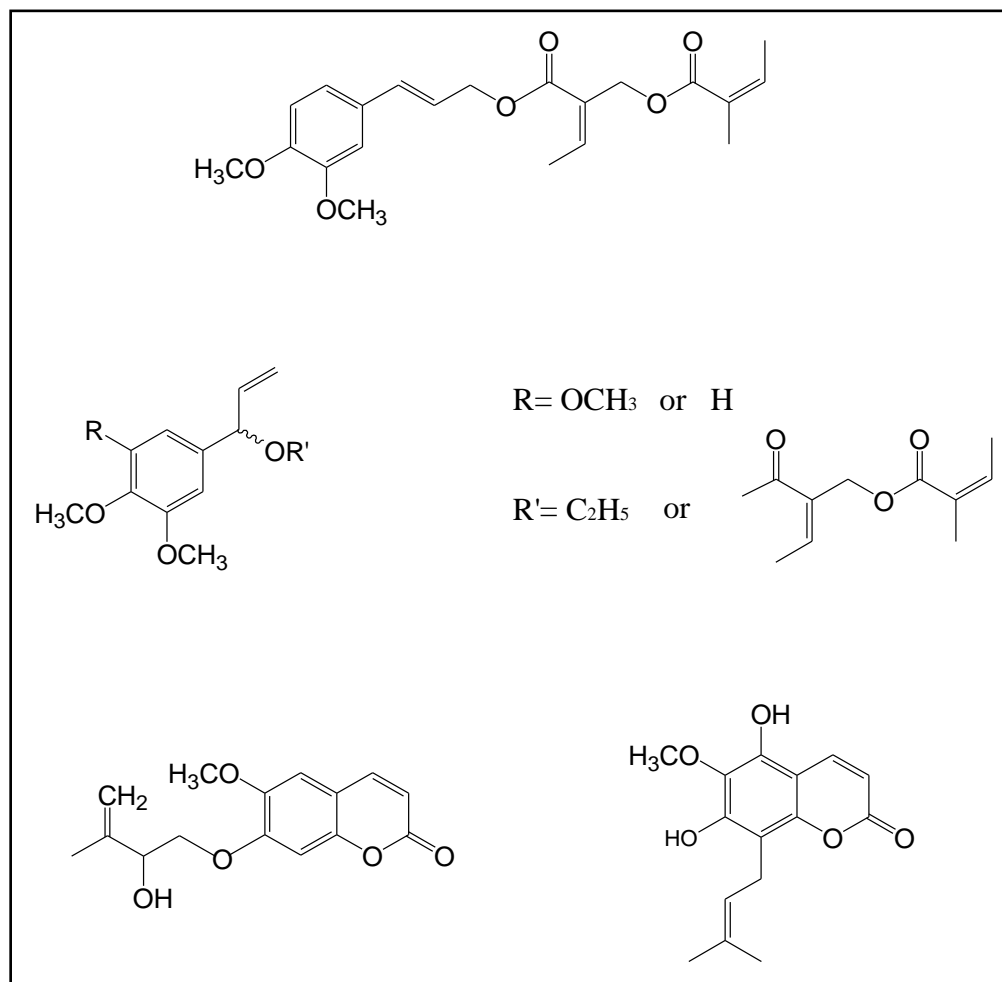
Fig. 20: Sturctures of phenylpropanoids and coumarins isolated from *B. fruticosum*

2.3.3 Biological activity of *B. fruticosum*

➢ *B. fruticosum* has been investigated for its immunomodulatory effect using several markers of the immune system. Petroleum ether extract of *Bupleurum* caused 80-100% release of IL-1β & IL-6 and synthesis of Prostaglandin (PG) E2 in human monocyte [199].

➢ Anti-inflamatory activity of essential oil of *B. fruticosum* was evaluated using carrageenan-induced edema model and chronic proliferative inflammation by evaluating the granuloma formation. Essential oil exhibited positive anti-inflammatory effect after oral and intra-peritoneal administration [204].

➢ Comparable antifungal and antibacterial activity was observed with the essential oil of *B. fruticosum* collected in Italy have shown comparable antibacterial and antifungal activity against the Gram positive pathogens *Streptococcus faecalis*, *Staphylococcus albus,* and *Staphylococcus aureus* [205].

2.4 *Withania somnifera*

- Genus   : *Withania*
- Species   : s*omnifera*
- Family   : Solanaceae
- Habitat   : Throughout the drier and subtropical part of India (Madhya Pradesh, Gujarat, Punjab, Sindha, Rajsthan)
- Synonyms- Winter cherry in English. In Ayurveda it is known by many names viz. Ashwagandhaa, Hayagandhaa, Ashwakanda, Gandharvagandhaa, Turaga, Turagagandhaa, Balyaa, Varadaa, Vaajigandhaa, Gokarnaa, Vrishaa, Varaahakarni, Vaajikari, Turangagandhaa.

Fig. 21: *W. somnifera* shrub, fruits and roots

    W. somnifera (L.) Dunal also known as, Ashwaganda or Indian ginseng is a green shrub belonging to the family of Solanaceae. This species is 35 to 75 centimeters tall and possesses tomentose branches extend radially from a central stem. The flowers are small and green. The ripe fruit is orange-red. Roots are 20-30 cm long and 6-12 mm in diameter, with a few (2 to 3)

lateral roots of slightly smaller size. Outer surface is buff to gray-yellow with longitudinal wrinkles and in the center soft, solid mass with scattered pores. The taste is bitter and acrid. The ripe fruit is orange-red (Fig. 21). The name Ashwaganda comes from the smell of horses, which the root emits, and the botanical suffix somnifera from the use of the plant as a sedative.

2.4.1 Medicinal properties

Ashwaganda holds a place in Ayurveda similar to that of *Ginseng* in Chinese medicine. It is reputed to be capable of imparting long life, youthful vigour and intellectual prowess and is an ingredient of many traditional preparations. The plant is used to treat various neurological disorders, geriatric debilities, arthritis, stress and behavior-related problems [206]. In the traditional system of medicine Ayurveda, this plant is claimed to have potent aphrodisiac, rejuvenative and life prolonging properties. It improves learning ability and memory capacity [207]. Ayurvedic Pharmacopoeia of India recommends use of Ashwagandha in impotency [172]. Roots of Ashwagandha are used as anti-inflammatory drug for swelling, tumor, and rheumatism. Roots also have sedative and hypnotic property. Leaves of Ashwagandha have anti-inflamatory, hepatoprotective, and antibacterial property.

2.4.2 Chemical constituents

The major constituents of the *W. somnifera* roots and leaves are a group of steroidal lactones called withanolides that have been considered exclusive of Solanaceae plants. Withanolides are a group of at least 300 naturally occurring chemical compounds and structurally, they consists of a C-28-steroidal skelelton in which C-22 and C-26 are appropriately oxidized to form a six-membered lactone ring . In the roots 17-hydroxy-27-deoxy withaferin A, withanolide A withaferin A, and withanolide B have been identified as the major withanolides while 27-hydroxy withanone, withanone, 17-hydroxy withaferin A, 27-hydroxy withanolide B and 27-deoxy withaferin A were detected as minor constituents.

In addition to withanolides, both leaves and roots contain relatively high amounts of alkaloids possessing a piperidine, pyrrolidine or pyrazole ring. Up to now ten alkaloids have

been isolated: D-L-isopelletierine, anaferine, hygrine, cuscohygrine, anahygrine, tropine, pseudotropine, 3alfa-tigloyloxytropane, withasomnine and coline [217,218].
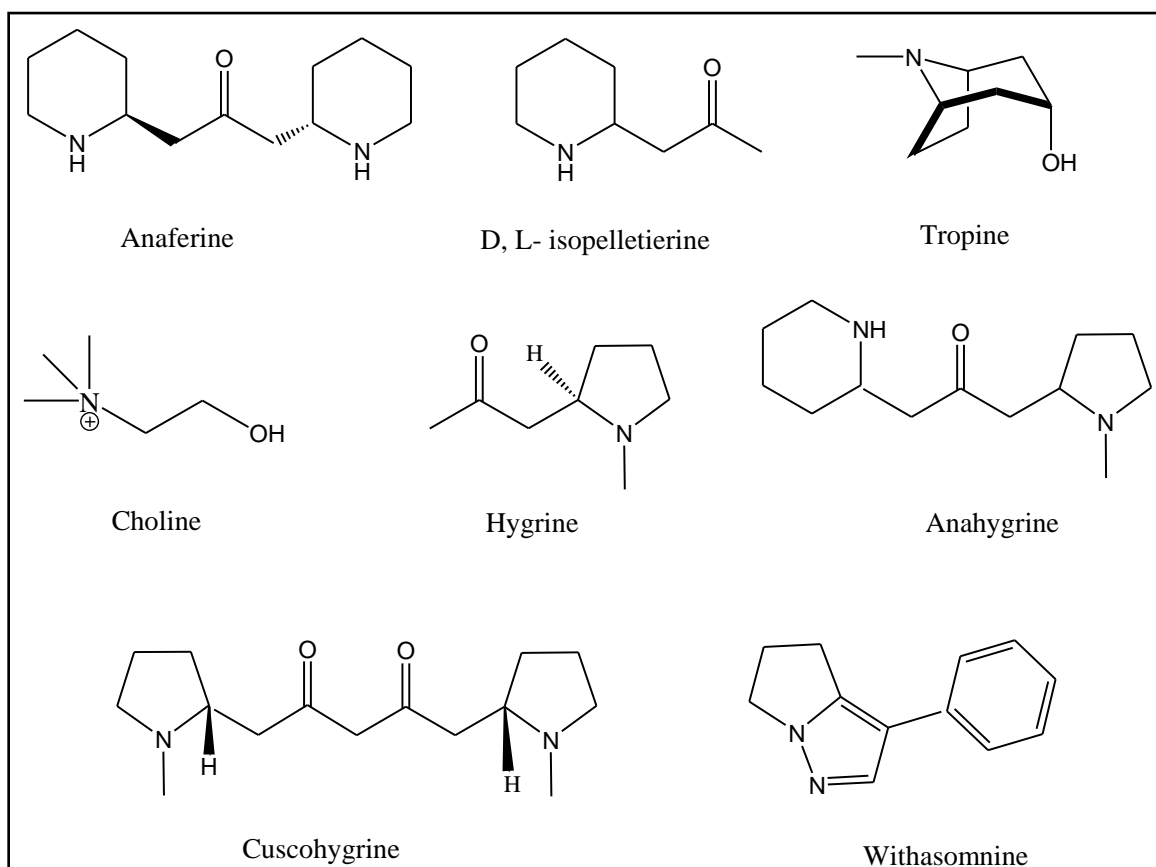
Fig. 22: Alkaloids from *W. somnifera*
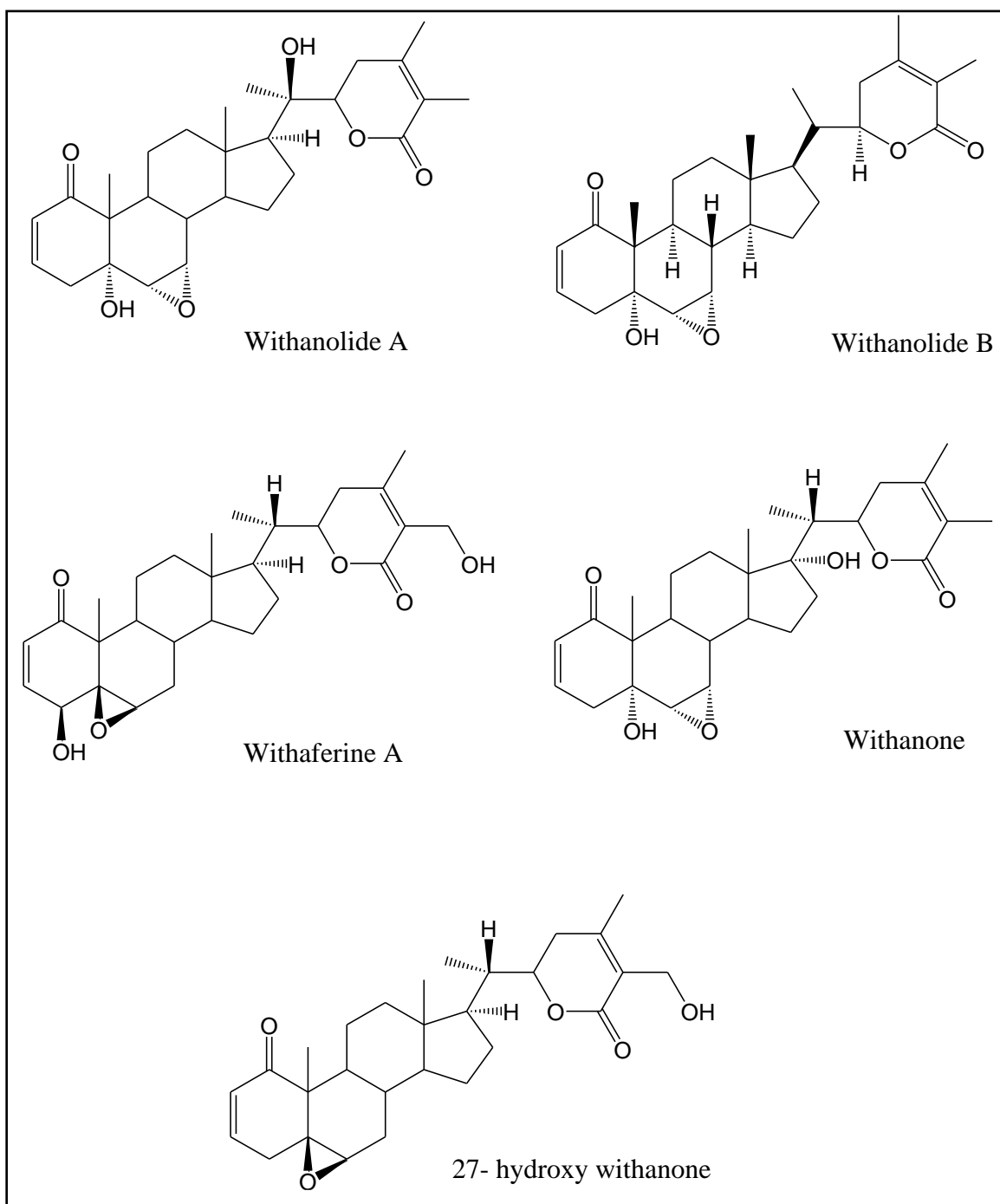
Fig. 23: Withanolides from *W. somnifera*

2.4.3 Biological activity of *W. somnifera*

➢ Several studies suggest that withaferin A is the most biologically active withanolide. It has antitumor, antiarthritic and antibacterial activities [208]. Anti-inflamatory activity is attributed to withanolides and withaferin A is the most active one [172].

➢ Withaferin A has been reported to inhibit angiogenesis and hence protective in certain cancer types [209]. The anti tumor activity of withaferin A is related, at least in part, to the binding with the intermediate filament protein vimentin [210].

➢ Withanolides are found to exert calcium antagonistic activity; also, they were found to inhibit acetylcholinesterase (AChE) and butyrylcholinesterase (BChE). These two activities suggests use of withanolide as a possible drug candidate in treatment of Alzheimer's disease [211].

➢ Recent studies reports that WS modulated the dopaminergic system in brain suggesting its antiparkinson's like activity [212].

➢ WS also exhibits CNS depressant action. In acute and chronic models of epilepsy WS have shown to posses' anticonvulsant activity. Root extracts of WS have shown antiepileptic activity against pentylenetetrazol (PTZ) induced kindling in mice. This antiepileptic property of WS is believed to be through GABAergic modulation [213].

➢ Our group of research demonstrated that the administration of *W. somnifera* methanol extract (WSE) prolongs the acute analgesic effect of morphine in the tail-flick test and prevents the development of hyperalgesia in a model of opioid-induced hyperalgesia [214].

➢ WS is extensively used for its stress relieving and antioxidant potential. In Ayurvedic practices, Ashwagandha has been traditionally used to reduce symptoms of anxiety and stress. WS have shown antistress activity in a mouse model of chronic fatigues syndrome [215].

Chapter 3 Aim and Objectives

As discussed in earlier chapter of this thesis, herbal/natural medicines could be a better alternative in treatment of various diseases. Also, chemical and biological studies of plants can give a lead which could be a starting point in drug discovery. In our research approach we worked with medicinal plants from India and Sardinia (an island of central south Italy). We tested various Indian and Sardinian plant extracts towards three different targets: HIV-1 RT, HRV replication and interaction with $GABA_A$ receptor. Selection of the plants was based on available literature report and traditional use of the plants for particular disease.

In a continuous search for secondary metabolites that can act as an anti-HIV-1, we screened the capability of eighteen different extracts obtained from seven Indian and ten Sardinian plants to inhibit the HIV-1 reverse transcriptase-associated RNase H function, an enzyme essential in viral replication. We found that some extracts, prepared by percolation, showed good inhibitory activity in the low micromolar range. In particular, the dichloromethane (DCM) and methanol extracts from *Ocimum sanctum* and *Tinospora cordifolia* have shown remarkable activity (Table 2) and therefore were selected for phytochemical investigation.

Table 2: Inhibition of RT RNase H function by plant extracts

Sr. no	Plant extract	IC_{50} (µg/ml)
1	*Ocimum sanctum* DCM	4.2 ± 0.9
2	*Ocimum sanctum* MeOH	1.1 ± 0.14
3	*Tinospora cordifolia* DCM	11.8 ± 2.2

Another target of interest was the Human Rhinovirus (HRV) and various Sardinian plant extracts were evaluated for their capability to inhibit the replication of two groups of HRV, HRV14 (group B) and HRV-39 (group A). In particular, We discovered that the DCM extract of

the Sardinian plant, *Bupleurum fruticosum,* was able to inhibit the replication of HRV A and HRV B at a relatively low concentration of 3.1 and 12.5 μg/ml, with low cytotoxicity against HeLa cells ($EC_{50} = 125$ μg/ml) and a selectively index (SI) of 40 and 10, respectively.

The third field of interest was aimed to search compounds able to interact with $GABA_A$ receptor. In the third screening we found that the methanol extract obtained from the roots of *Withania somnifera* was able to enhanced the amplitude of $GABA_A$-induced inhibitory postsynaptic currents ($IPSC_S$) by 38% $\pm$ 11 at the dose of 400 μg/ml.

Based on the results obtained from the biological screening we have selected active plant extracts for further study. The objectives of the study were as follow:

1) Bioassay guided fractionation of active extracts.
2) Isolation of secondary metabolites from the active fractions, by chromatographic techniques.
3) Identification of the isolated compounds by spectroscopic and spectrometric methods.
4) Test the biological activity of the isolated pure compounds

   ➢ Anti HIV testing- To assay the isolated pure compounds from *O. sanctum*, and *T. cordifolia,* against HIV-1 RT associated RNase-H and RNA dependent DNA polymerase function (RDDP).

   ➢ Synthesis of structural analogues of the compounds active against HIV-1 RT-associated RNase H activity.

   ➢ Test the synthetic analogues against RNase H and to establish structure-activity relationship.

   ➢ Study the cytotoxic profile of the active compounds.

   ➢ Test the inhibition of replication of HRV_S by the compounds isolated from *B. fruticosum*.

   ➢ Study the $GABA_A$ receptor modulatory activity of compounds from *W. somnifera*.

Chapter 4 Methods of Isolation and Structural Elucidation

4.1 Isolation methodology

Isolation of small natural molecules differs from the other more prevalent biological macromolecule. Plant or animal tissues always contain several classes of compounds with markedly different structures. Each class usually contains several or a lot of compounds closely related in the structure. Natural product chemistry usually begins from the separation and isolation of single pure compound from such many similarly related ingredients. The compounds which are essential for living organism (protein, enzymes, and nucleic acid) are termed as primary metabolites. The compounds which are present in relatively less amount and specific to each species of the plant are called as "secondary metabolites". The role of these compounds is obscure. Usually, target of the natural product chemistry is to isolate secondary metabolites present in plants.

Isolation of natural products can be divided in 3 main stages: extraction, fractionation, and purification

4.1.1 Extraction

Extraction is the first step for the isolation of secondary metabolites. Extraction is a way to separate a desired mixture of substances contained in in a solid body. The mixture is brought in contact with solvent in which the substances of interest are soluble while rests of the substances are insoluble. The method of choice and solvent for extraction is depends on nature of the source material and the compounds to be isolated. With the use of appropriate solvent, secondary metabolites separates out as through extraction can solublize them. Extraction helps in release of compounds from the cell mass and removal of bulk biomass, which is generally inert, insoluble and polymeric material. Extraction can be done by a single solvent or would be possible with successive use of different solvents. Successive extraction with increasing order of polarity is better approach to isolate compounds with different polarity [216]. Extraction is also possible with single solvent when the objective of the isolation is obtaining total extract. Polar solvents

like methanol dissolve most natural products. Maceration, decoction, percolation, soxhlet, supercritical fluid extraction, are only some of the extraction methods.

4.1.2 Fractionation

A crude natural product extract obtained by extraction is a mixture of compounds. If one has to isolate single and pure compounds it is difficult to apply a single separation technique. Hence, the crude extract is initially separated into various discrete fractions containing compounds with similar polarity or molecular size. It is advisable not to generate too many fractions of one extracts, because it may distribute the target compounds in different fractions. It is difficult to isolate pure compounds if they get spread in different fractions; secondary metabolites are already present in less amount. It is more logical to collect few larger fractions and go for further purification. Larger fractions can be obtained by vacuum liquid chromatography (VLC) and liquid-liquid extraction

4.1.3 Vacuum Liquid Chromatography (VLC)

VLC is a very convenient and simple chromatography method that is able to produce good resolution in short time. This technique involves the use of reduced pressure to increase the flow rate of the mobile phase through a short bed of stationary phase: most of the stationary phase could be used (silica gel, reversed phase material or aluminium oxide) and the technique is applicable to large scale separations. The advantage of this procedure includes its simplicity of equipment, low cost of operation and low solvent consumption, as well as the speed of separation. The disadvantage is that the resolution is only moderate. Larger fractions of an extract can be obtained using different solvents with increasing polarity.

4.1.4 Liquid-Liquid extraction

This is a method of purification by solvent extraction using partition coefficient. It involves the use of two immiscible solvents in a separating funnel. In this method compounds are distributed in two solvents according to their different partition coefficient. Before the inventions of modern chromatographic techniques solvent partitioning followed by crystallization were extensively used techniques. This techniques is very easy to perform and highly effective for preliminary separation of mixture of compounds into small fractions.
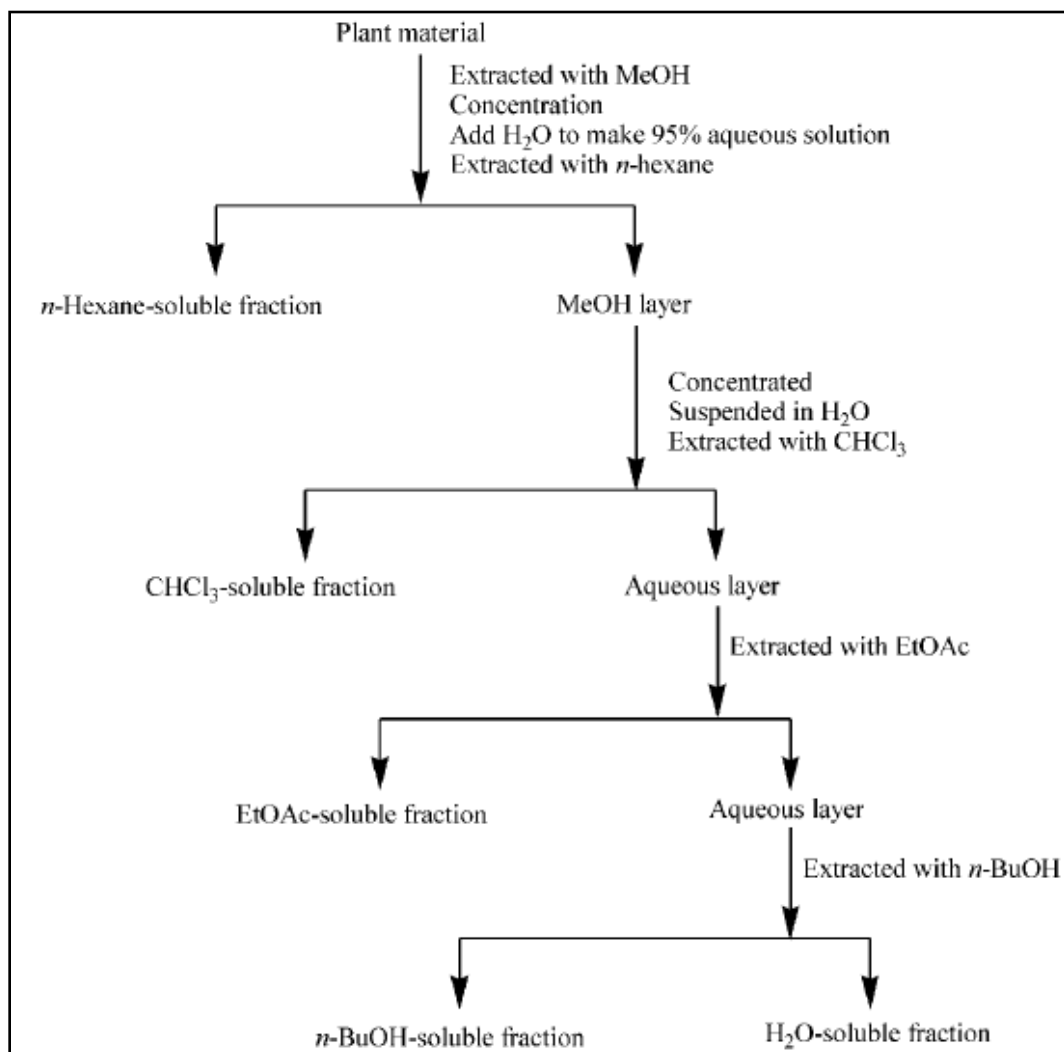
Fig. 24: A typical partitioning scheme using immiscible solvents

4.2. Purification

Purification is the final step of isolation which gives single pure compounds. High resolution separation techniques are use for final purification. This includes chromatographic techniques of separation like open column chromatography and High Performance Liquid Chromatography (HPLC).

4.2.1 Open column chromatography

The gravity-driven open column chromatography method is still widely used in natural product chemistry, as it represents rapid and efficient techniques to obtain pure compounds. The separation is based on differential partitioning between the mobile and stationary phases. Subtle differences in a compound's partition coefficient result in differential retention on the stationary phase and thus changing the separation. The main advantage of column chromatography is the relatively low cost and disposability of the stationary phase used in the process. The most used stationary phase is silica gel. The chemical nature of the surface of silica gel consists of exposed silanol groups. These hydroxyl groups are the active centers and potentially can form strong hydrogen bonds with compounds being chromatographed. Thus, in general, the stronger the hydrogen-bonding potential of a compound, the stronger it will be retained by silica gel, so that polar compounds are strongly adsorbed, while non-polar molecules are poorly or non-retained on silica gel. Other stationary phases are aluminium oxide, reversed phase (RP) and Sephadex. Coloumn chromatography using sephadex as stationary phase is size exclusion chromatography. Separation in this method is based on molecular size, larger compounds elute first followed by smaller ones.

4.2.2 HPLC

Preparative or semipreparative HPLC is a versatile and widely used technique for the final purification of natural compound. The main difference between HPLC and other models of column chromatography is that the diameter of the stationary phase particles is comparatively low (3-10 μm) [216,217] and these particles are tightly packed to give a very uniform column bed structure. The low particle diameter means that a high pressure is needed to drive the eluent

through the bed. However, because of the very high total surface area available for interactions with solutes, the resolving power of HPLC is very high. Purification of natural products by preparative HPLC employs one of the four chromatographic modes: normal phase, reversed phase, gel permeation chromatography, and ion exchange chromatography. Selection of type of column and solvent is key factor of HPLC operations. Solvents used in HPLC must be high purity to maintain integrity of the instrument and sample. Also, solvent must be compatible with the detector and should not interfere with the compound signals.

4.3 Structural elucidation

Structural elucidation or conclusive identification of compounds isolated from plants is a bottleneck of natural products research. There are many spectroscopic methods available to get structural information and interpretation of spectra requires detailed knowledge of spectroscopy and wide experience in chemistry of natural products. It becomes easy when the compound of interest is known; comparing the spectroscopic data with literature reports or with reference standard gives conclusive structure. However, if the target compound is unknown then a systematic approach using various physical, chemical, and spectroscopic techniques is required.

Following are some spectroscopic techniques used in structural elucidation;

I] Ultraviolet- Visible (*Uvi-vis*) spectroscopy- Gives information about chromospheres present in the molecule. Absorption spectrum of the plant constituents is measured in dilute solution against solvent blank. Wavelength of the maxima and minima of the absorption and also the intensity of the absorption at particular maxima and minima is recorded [217]. Some of the natural products like Flavanoids, isoquinoline alkaloids, coumarins etc are primarily characterize by absorption peaks.

II] Infrared (IR) spectroscopy – IR spectroscopy exploits the fact that the molecule absorbs particular frequencies which is characteristic of structure of molecule. IR data gives information about type of functional group and type of bonds present in molecule. IR spectrum is simplest and most reliable method of assigning of the class of compound because functional groups can be identified by their characteristic vibrational frequencies [217].

III] Nuclear Magnetic Resonance spectroscopy (NMR) - Amongst all modern methods of structure elucidation; NMR Spectroscopy provides the most complete information, with or without prior structural knowledge. When a single radiofrequency pulse of a few microsecond duration is applied to atoms that in nature possess a non zero spin quantum number as ^1H or ^{13}C, their nuclei excites and results in the emission of a signal knows as free induction decays (FID). Fourier transformation of this decay yields the NMR spectrum.

In the **^1H NMR** spectrum we observe different resonance lines that represent the chemical shift interaction for the protons in different position in a molecule. Thus it is a convenient method for the determination of the chemical shift of each resonance calculated from their integrated intensities. Where the multiplicity and the coupling pattern of a signal is interpretable, the number and the stereo chemical orientation of adjacent protons can be proposed as well.

The **^{13}C NMR** spectrum provides important structural information, since it arises directly from the nuclei that form the framework of the organic molecules. The normal ^{13}C spectrum is acquired with full proton decoupling: in the absence of coupling to ^1H nuclei, all of the ^{13}C signals in the spectrum appear as single lines, allowing the number of carbons in the molecule to be readily determined. The ^{13}C spectrum also confirms the presence of quaternary carbons but multiplicity cannot be established. The number of hydrogen bonded to each carbon can be detected by **DEPT** experiment: **DEPT 135** shows all protonated carbon signals, with CH_3 and CH resonance being positive, while CH_2 signals are negative. To distinguish CH_3 from CH, DEPT 90 is used: in this experiment only CH gives a signal, while carbons with all other substitution patterns are not detected.

The Attenuation Polarization Transfer (**APT**) experiment is another way to assign C-H multiplicities in ^{13}C NMR spectra. It provides the information on all sorts of carbons within one experiment. Depending on the number of hydrogens bound to a carbon atom, n, CHn spin vectors evolve differently after the initial pulse: CH and CH_3 vectors have opposite phases compared to quaternary carbons and CH_2.Two dimensional NMR spectra are obtained by recording a series of 1D spectra differing only by a time increment. They could be divided into two groups: homonuclear and heteronuclear methods. Within the homonuclear experiments,

DQF-COSY (Double Quantum Filtered COrrelation Spectroscopy) shows vicinal and geminal protons correlated via scalar coupling.

The Nuclear Overhauser Effect (NOE) allows the identification of those nuclei within a molecule that are close in space. A 2D NOE experiment (**NOESY** or **ROESY**) therefore provides information on the three dimensional molecular structure, hence the relative sterochemistry of the molecule.

Heteronuclear experiments are used in the form of **HSQC** (Heteronuclear Single Quantum Coherence) to assign the protons to their attached carbons. **HMBC** (Heteronuclear Multiple Bond Correlations) provides a wealth of structural information by the ability to identify ^{1}H-^{13}C correlations across carbon-carbon or carbon-heteroatom linkages.

IV] Mass Spectrometry (MS)

Mass spectrometry (MS) is an analytical technique that produces spectra of the masses of the atoms or molecules comprising a sample of material. Mass spectrometry works by ionizing chemical compounds to generate charged molecules or molecule fragments and measuring their mass-to-charge ratios.

The ions are detected by a mechanism capable of detecting charged particles. Signal processing results are displayed as spectra of the relative abundance of ions as a function of the mass-to-charge ratio. The atoms or molecules can be identified by correlating known masses to the identified masses or through a characteristic fragmentation pattern. A standard method is Electrospray Ionization Mass Spectrometry (**ESI MS**) that is typically used to determine the molecular weights of a wide range of molecules. Soft ionization is a useful technique when considering biological molecules of large molecular mass, such as the aformetioned, because this process does not fragment the macromolecules into smaller charged particles, rather it turns the macromolecule being ionized into small droplets. These droplets will then be further desolvated into even smaller droplets, which creates molecules with attached protons. These protonated and desolvated molecular ions will then be passed through the mass analyzer to the detector, and the mass of the sample can be determined.

The High Resolution Electrospray Ionization Mass Spectrometry (**HR ESI MS**) allowed the determination of the exact molecular mass.

Chapter 5 Results and Discussion

5.1 *Ocimum sanctum*

5.1.1 Isolation and structural elucidation of compounds from DCM extract of *O. sanctum*

5.1.1.1 Extraction procedure

Air-dried and powdered leaves of *O. sanctum* (500 g) were subjected to extraction using DCM by percolation (during the day) and maceration (during the night) to give 8.22 g dried extract. The remaining plant material was then extracted with MeOH giving 22.81 g dried extract.

5.1.1.2 Isolation of secondary metabolites from DCM extract

DCM extract have shown significant inhibitory activity ($IC_{50}= 4.2 \pm 0.9$ µg/ml) against HIV-1 RT-associated RNase H function. Therefore, DCM extract was subjected to fractionation by silica gel vacuum liquid chromatography (VLC) to afford seven major fractions (F1-F7). All fractions were evaluated for their anti-RNase H activity (Table 3).

Table 3: Effect of *O. sanctum* fractions on the HIV-1 RT-associated RNase H function

Fractions	RNase H [a]IC_{50} (µg/ml)
DCM extract	4.2 ± 0.9
F1	96 ± 5
F2	36 ± 6
F3	21 ± 0.1
F4	3.2 ± 0.1
F5	2.3 ± 0.3
F6	4 ± 1.5
F7	2.4 ± 0.3

[a] Extract concentration required to reduce the HIV-1 RT-associated RNase H activity by 50%.

Since F4-F7 showed significantly low IC$_{50}$ values (2.4 - 4.0 µg/ml), they were subjected to purification by column chromatography (silica gel and Sephadex LH-20) and semi-preparative HPLC to afford four triterpenoids namely oleanolic acid (**1**), ursolic acid (**2**), pomolic acid (**3**), and betulinic acid (**4**). Other compounds isolated were stigmasterol (**5**), vanillin (**6**), and two ferulic acid derivatives namely ferulaldehyde (**7**) and tetradecyl ferulate (**8**).
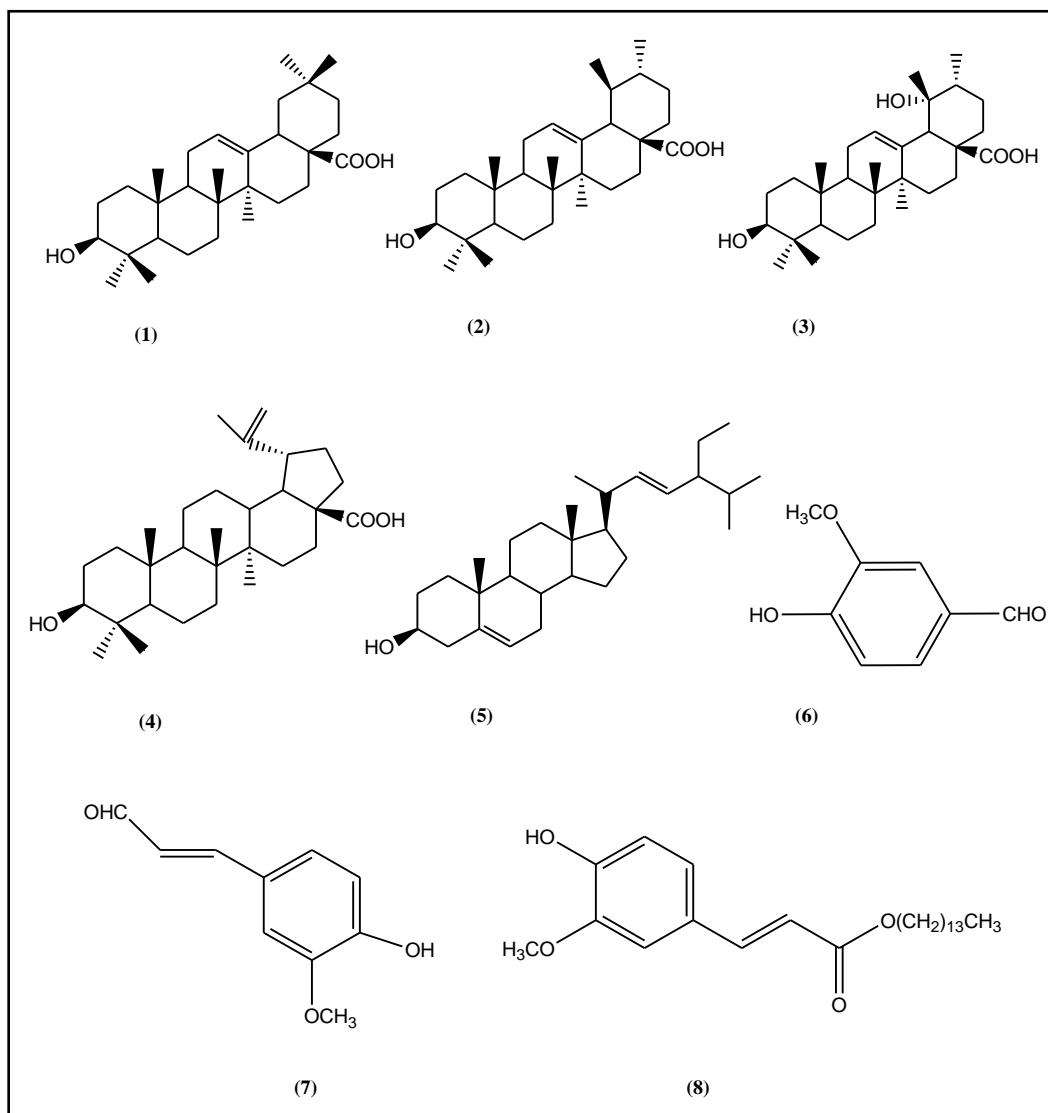
Fig. 25: .Structures of the isolated compounds from *O. sanctum*

5.1.1.3 Structural elucidation of compounds from the DCM extract of *O. sanctum*

Compound 1

Compound **1** was identified as oleanolic acid by 1D (¹H and ¹³C NMR), and 2D NMR (DQF-COSY, HSQC, HMBC, and ROESY) spectroscopy and mass spectrometry and comparison with literature data [218].¹³C NMR spectrum of compound **1** is reported in experimental section (Fig. 110).
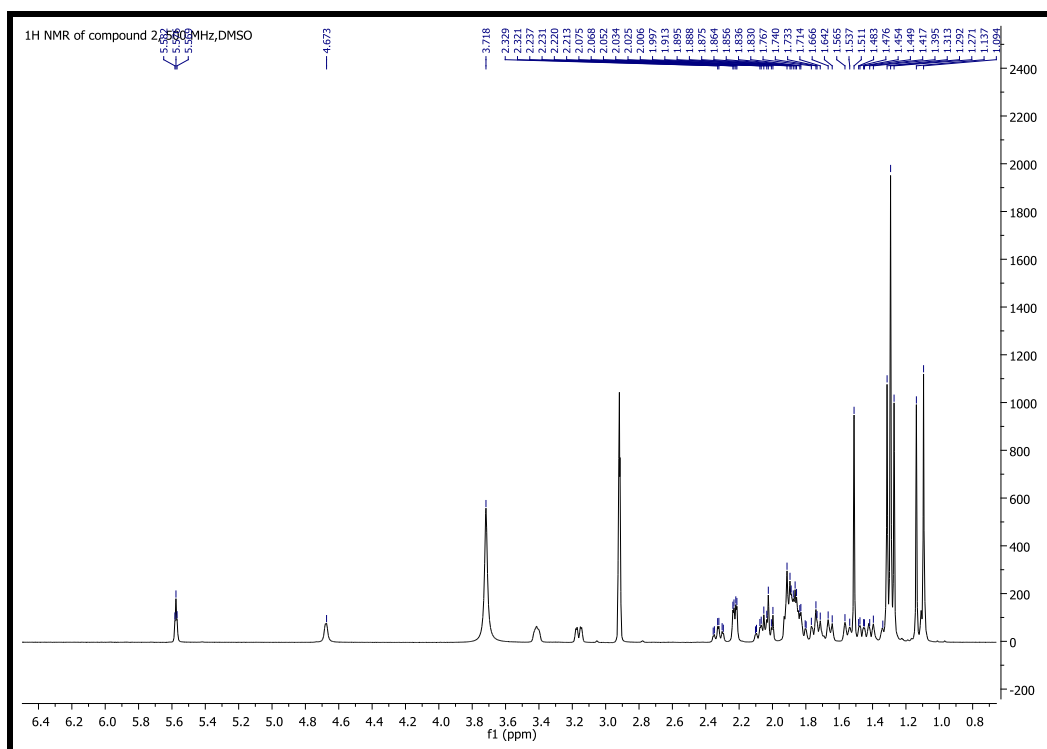
Fig.26: ¹H NMR spectrum of compound **1** (oleanolic acid), 500MHz, DMSO
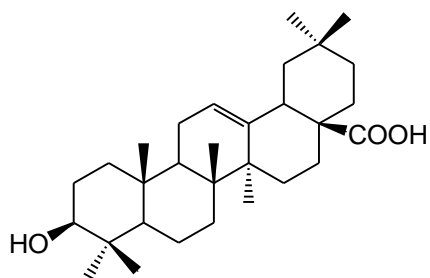
Compound **1** (Oleanolic acid)

Compound 2

Compound **2** was identified as ursolic acid by 1D (^{1}H and ^{13}C NMR), and 2D NMR (DQF-COSY, HSQC, HMBC, and ROESY) spectroscopy and mass spectrometry and by comparison with literature data [218]. 2D NMR spectra of compound **2** are reported in experimental section (Fig.111).
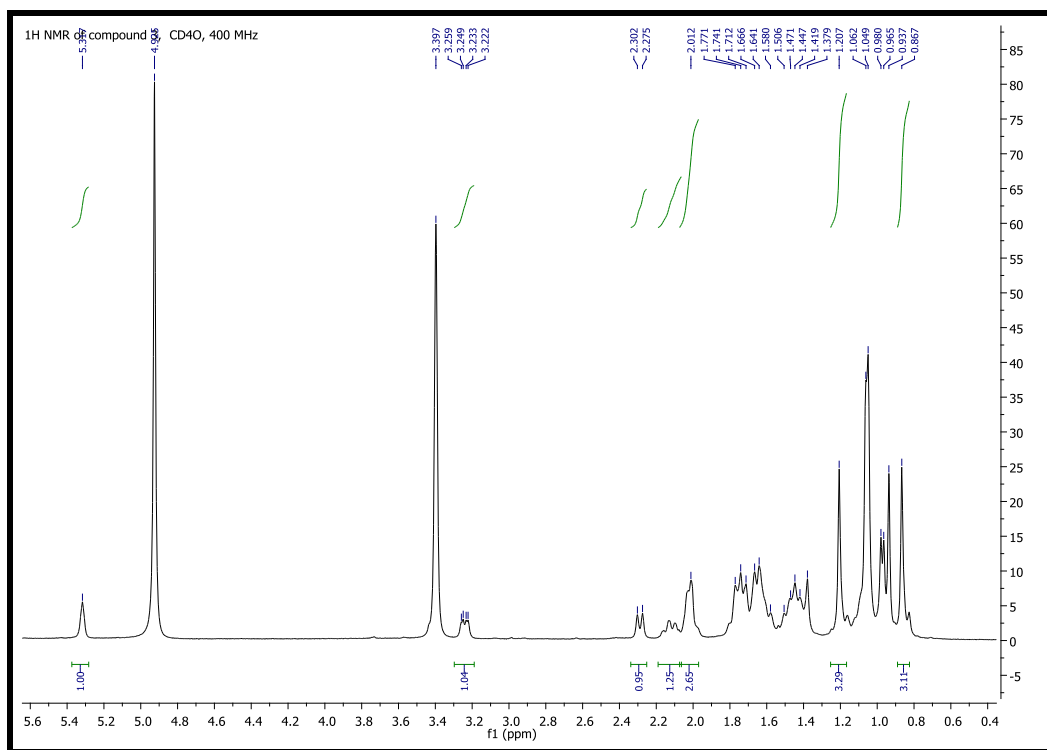
Fig.27: ^{1}H NMR spectrum of compound **2** (ursolic acid), 400MHz, CD$_4$O
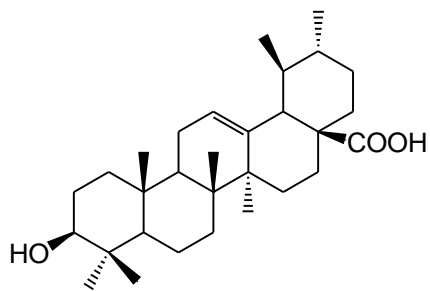
Compound **2** (Ursolic acid)

Compound 3

Compound **3** was identified as pomolic acid by 1D (^{1}H and ^{13}C NMR), and 2D NMR (DQF-COSY, HSQC, HMBC, and ROESY) spectroscopy and mass spectrometry and comparison with literature data [219]. 2D NMR spectra of compound **3** are reported in experimental section (Fig. 112-114)
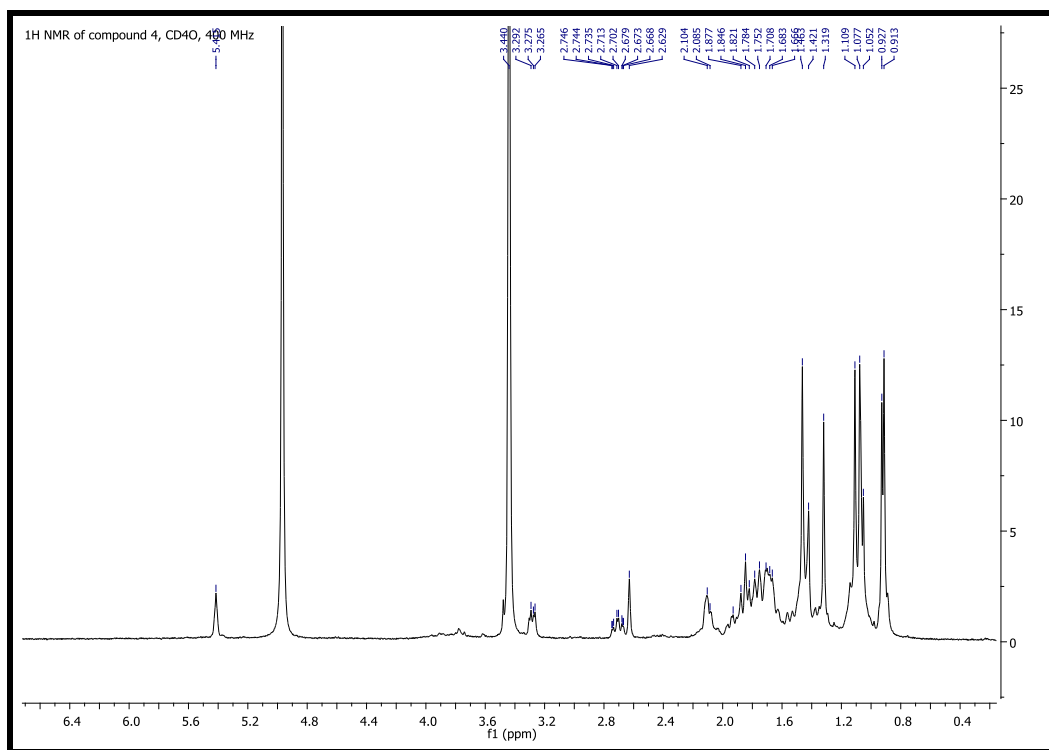
Fig.28: ^{1}H NMR spectrum of compound **3** (pomolic acid), 400MHz, CD_4O
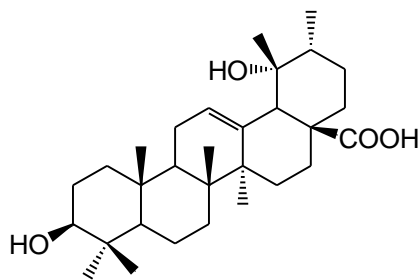
Compound **3** (Pomolic acid)

Compound 4

Compound **4** was identified as betulinic acid by 1D (^{1}H and ^{13}C NMR), and 2D NMR (DQF-COSY, HSQC, HMBC, and ROESY) spectroscopy and mass spectrometry and comparison with literature data [220]. 1D and 2D NMR spectra of compound **4** are reported in experimental section (Fig. 115-117).
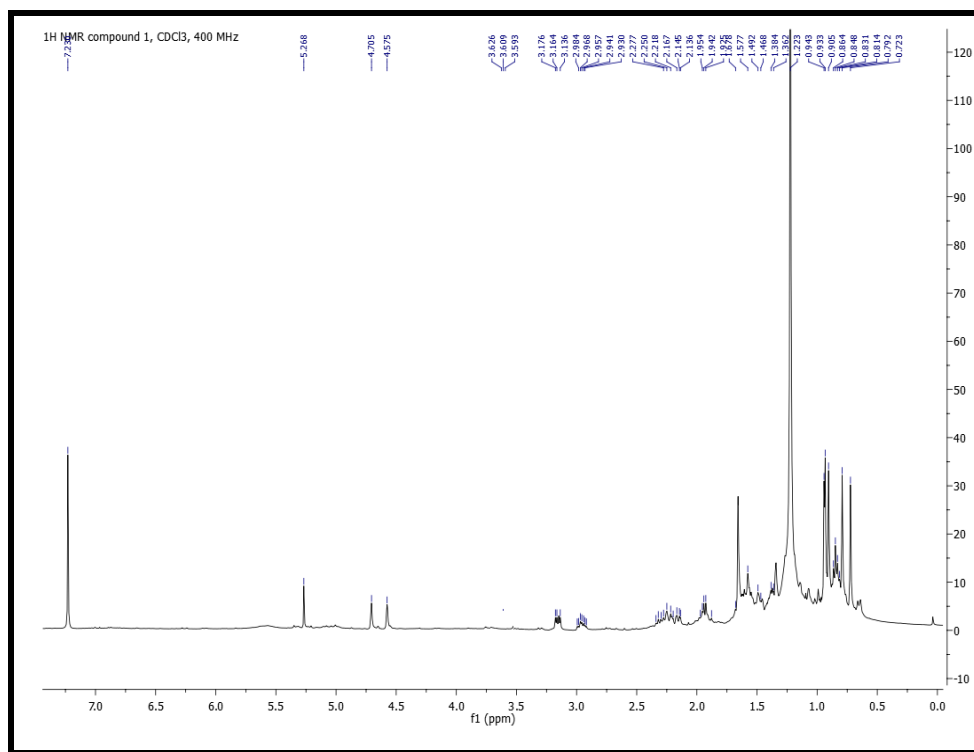
Fig.29: ^{1}H NMR spectrum of compound **4** (betulinic acid), 400MHz, CDCl$_3$
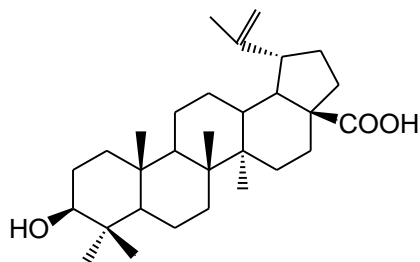
Compound **4** (Betulinic acid)

Compound 5

Compound **5** was identified as stigmasterol by 1D (^{1}H and ^{13}C NMR), and 2D NMR (DQF-COSY, HSQC, HMBC, and ROESY) spectroscopy and mass spectrometry and comparison with literature data [221]. 2D NMR spectra of compound 5 are reported in experimental section (Fig. 118-120).
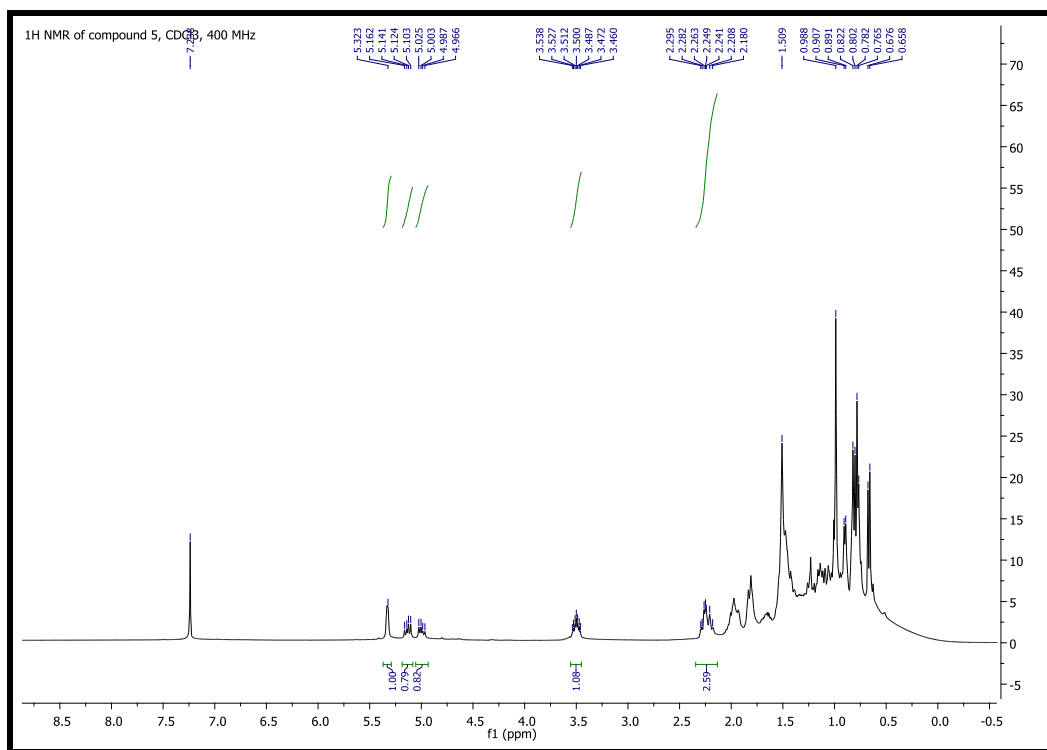
Fig.30: ^{1}H NMR spectrum of compound **5** (stigmasterol), 400 MHz, CDCl$_3$
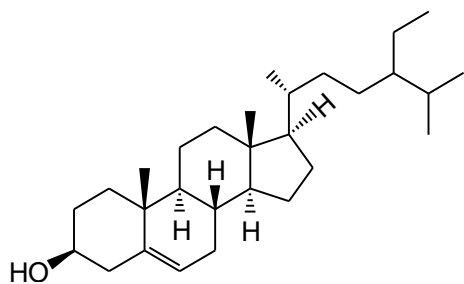
Compound **5** (Stigmasterol)

Compound 6

Compound **6** was identified as vanillin by 1D (^{1}H and ^{13}C NMR), and 2D NMR (DQF-COSY, HSQC, HMBC, and ROESY) spectroscopy and mass spectrometry and comparison with literature data [222]. ^{13}C NMR spectrum of compound **6** is reported in experimental section (Fig. 121).
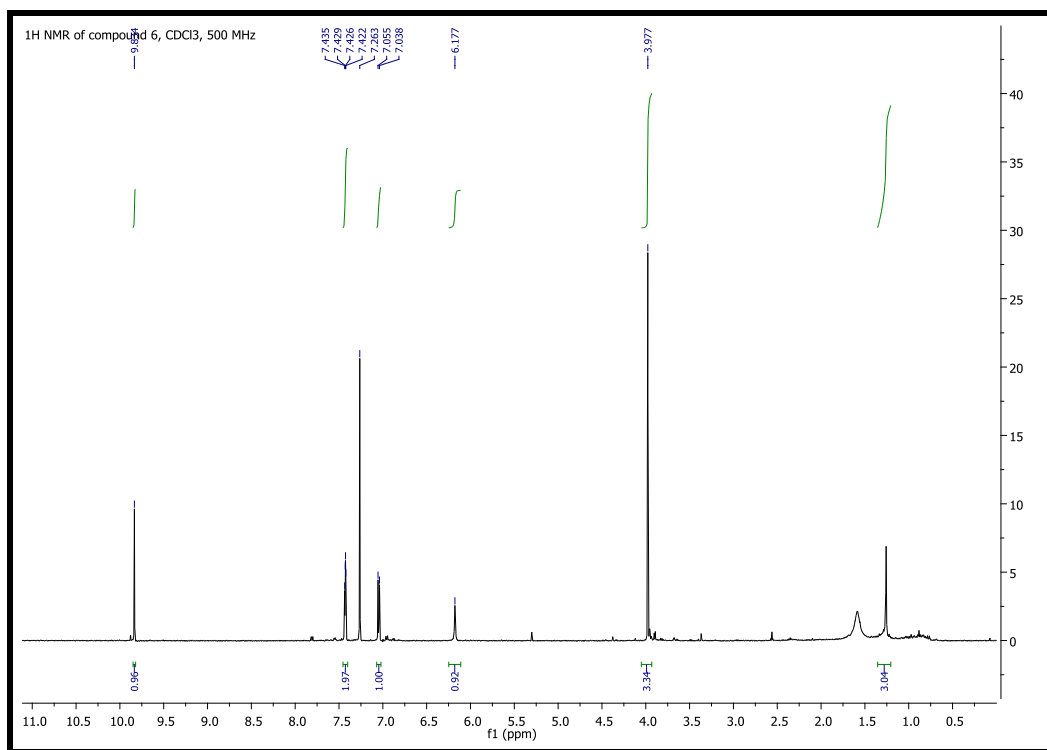
Fig.31: ^{1}H NMR spectrum of compound **6** (vanillin), 500MHz, CDCl$_3$
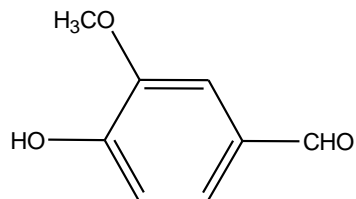
Compound **6** (Vanillin)

Compound 7

Compound **7** was identified as ferulaldehyde by 1D (^{1}H and ^{13}C NMR), and 2D NMR (DQF-COSY, HSQC, HMBC, and ROESY) spectroscopy and mass spectrometry and comparison with literature data [223].
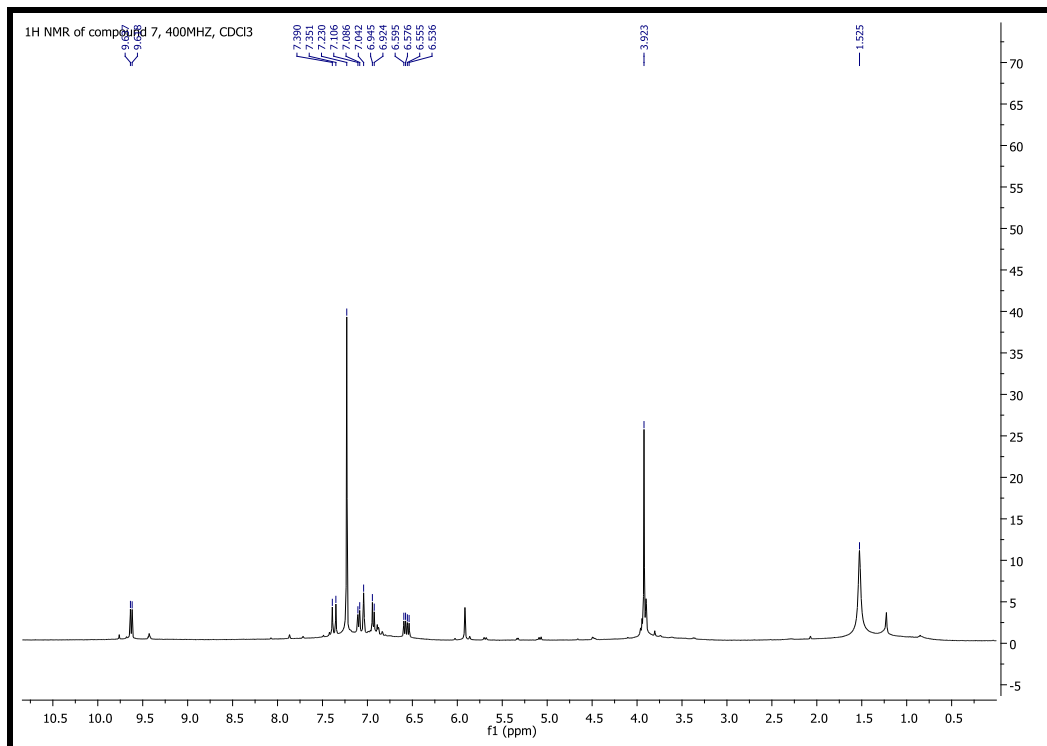
Fig.32:.^{1}H NMR spectrum of compound **7** (ferulaldehyde), 400MHz, CDCl$_3$
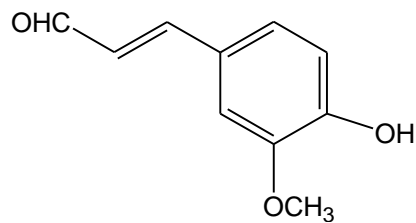
Compound **7** (Ferulaldehyde)

Compound 8

The ^{1}H NMR spectrum of compound **8** showed a group of proton signals at 7.61 (d, J = 16.0 Hz, 1H), 7.07 (dd, J = 1.5, 8.0, 1H), 7.04 (d, br, 1H), 6.77 (d, J = 8.0 Hz, 1H), 6.29 (d, J = 16.0 Hz, 1H) and 3.93 (s, 3H) ppm, assignable to a feruloyl moiety.
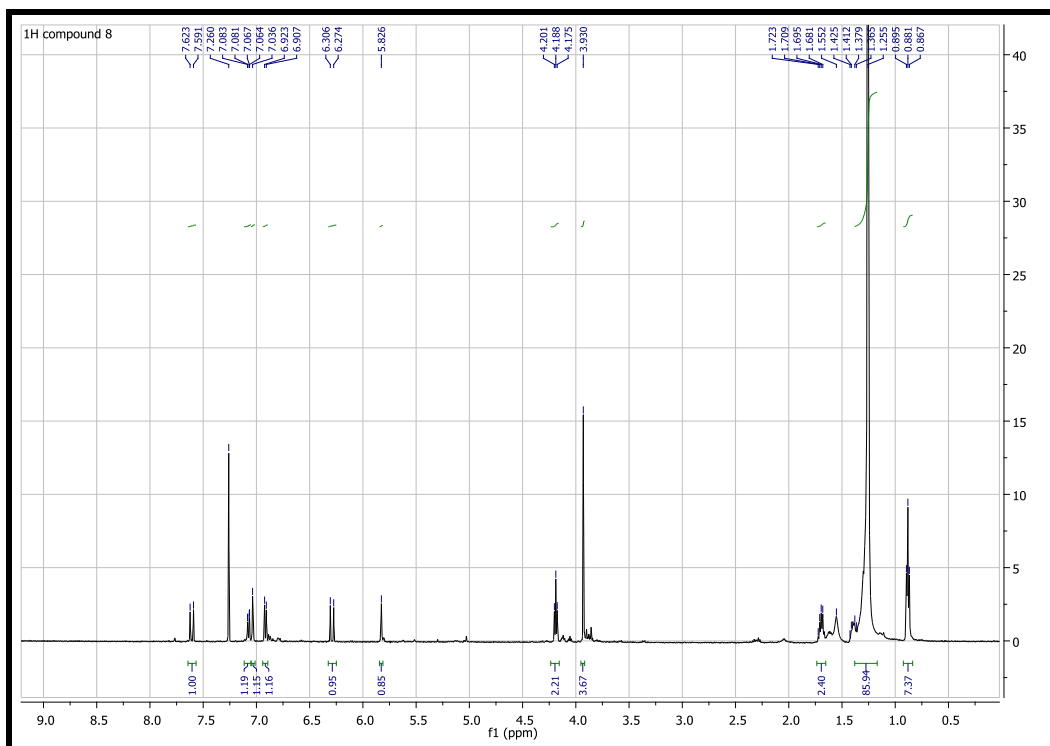
Fig.33: ^{1}H NMR spectrum of compound **8**, 500MHz, CDCl$_3$

The cross-peak between the oxymethylene protons at 4.19 (t, J = 6.5 Hz, 2H) ppm and the carbonyl group at δ 167.7 observed in the HMBC spectrum, together with a cluster of aliphatic methylene groups (δ_H 1.26) and a terminal methyl (δ_H 0.88, t, J = 7.0 Hz 3H), indicated a ferulic acid long-chain alkyl ester.
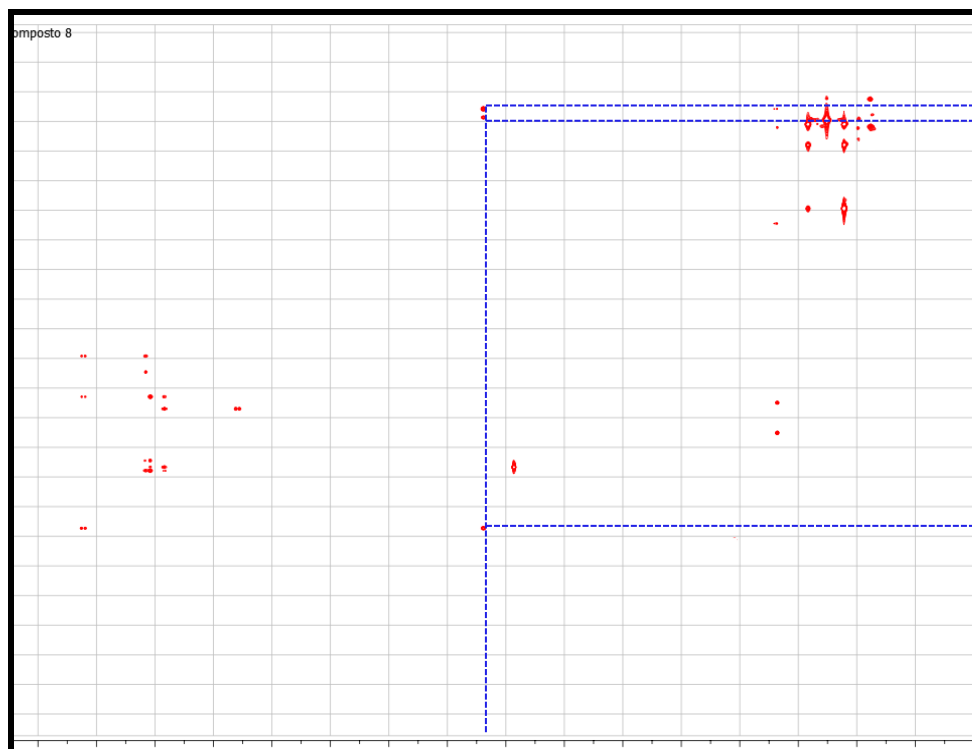
Fig.34:.HMBC spectrum of compound **8**, 500MHz, CDCl₃

The length of the alkyl chain was unambiguously determined by ESI MS showing a molecular ion at 391 [M+H]$^+$. DQF-COSY, HSQC and HMBC experiments allowed the complete assignments of all signals and the identification of compound **8** as tetradecyl ferulate [224].
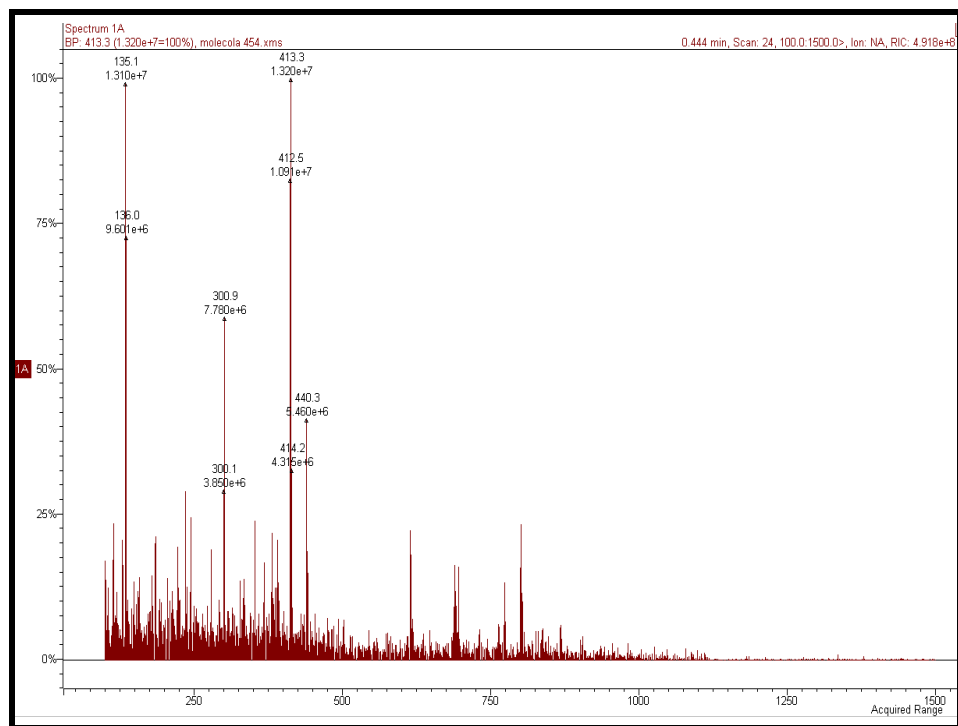
Fig.35: Mass spectrum of compound **8** (ESI MS in positive mode)
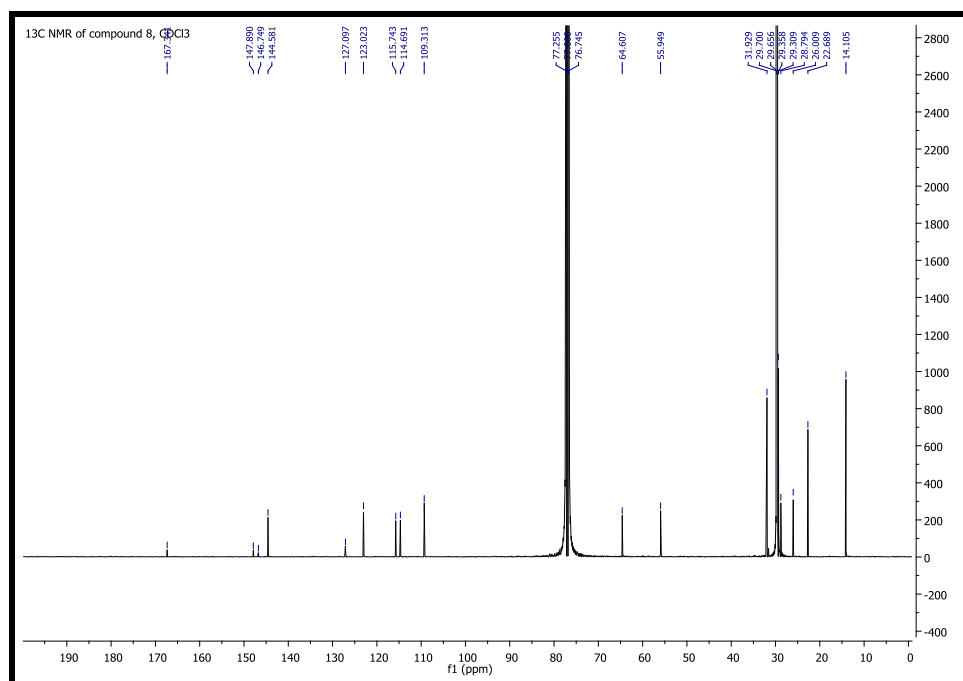
Fig.36: ^{13}C NMR spectrum of compound **8**, 100 MHz, CDCl$_3$
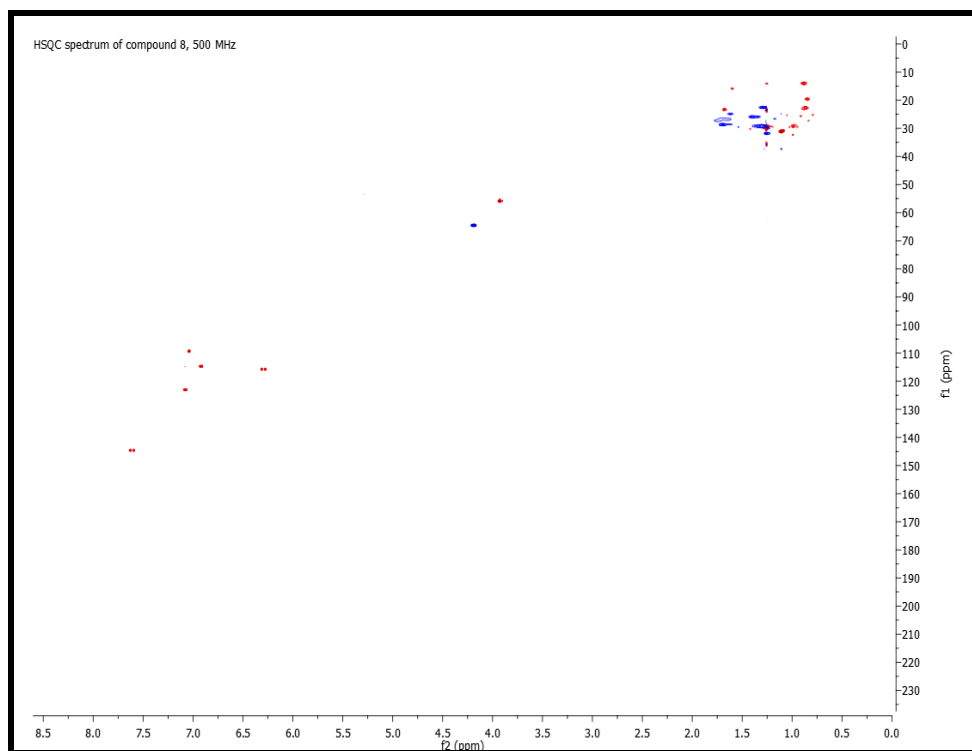
Fig.37: HSQC of compound **8**, 500 MHz, CDCl$_3$
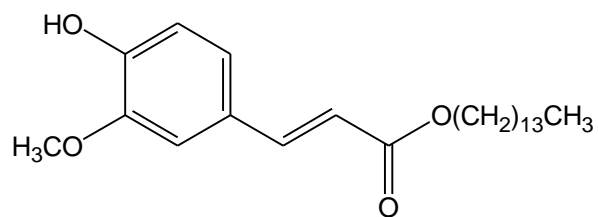
Compound **8** (tetradecyl ferulate)

5.1.2 Biological results

HIV-1 RT associated RNase H function inhibitory activity of compounds 1-8

The compounds isolated from the active fractions of *O. sanctum* extract were evaluated for their anti-RNase H activity (Table 4) using RDS1759 as positive control, a diketoacid inhibitor of the RNase H function that binds the catalytic site [225]. Among triterpenes, ursolic acid (**2**) was the most potent inhibitor with a IC$_{50}$ value of 5.5 µM but also oleanolic acid (**1**) and pomolic acid (**3**) showed high potency with 7.5 and 9.3 µM, respectively. The substitution of the cyclohexane E ring with a cyclopentane, as in betulinic acid (**4**), reduced the potency and indicates the importance of the cyclohexane ring for the activity. Stigmasterol (**5**), containing a sterol skeleton, did not show any remarkable inhibitory activity with a IC$_{50}$ of 153.3 µM. Among the 3-methoxy-4-hydroxy phenyl derivatives (**6-8**), tetradecyl ferulate (**8**) demonstrated an interesting anti-RNase H effect (IC$_{50}$ 12.1 µM) whereas compounds **6** and **7**, possessing the same aromatic scaffold, did not showed any RT inhibitory activity.

Table 4: Effect of the compounds isolated from *O. sanctum* on HIV-1 RT-associated RNase H

Compound	RNase-H IC$_{50}$ (µM)
Oleanolic acid (**1**)	7.5 ± 0.9
Ursolic acid (**2**)	5.5 ± 0.3
Pomolic acid (**3**)	9.3 ± 0.2
Betulinic acid (**4**)	13.2 ± 1.9
Stigmasterol (**5**)	158.3 ± 7.8
Vanillin (**6**)	>100
Ferulaldehyde (**7**)	>100
Tetradecyl ferulate (**8**)	12.1 ± 1.1
RDS 1759	10.1 ± 2.2

5.1.3 Synthesis of Ferulic acid esters and amide

Although we reported for the first time the RNase H inhibitory activity of triterpenes **1-3**, they have been already demonstrated to possess anti HIV-1 RT effect [226] and various semi-synthetic triterpene derivatives are known as anti HIV maturation/fusion agents [227]. For this reason, we focused our attention on compound **8** for which, as far as we know, no biological studies have been reported. In addition, the synthetic accessibility of ferulic acid derivatives increased their appeal as lead compounds for potential anti HIV-1 agents development. Thus, we firstly asked whether tetradecyl ferulate might inhibit also the HIV-1 RT-associated RDDP function using efavirenz as positive control (Table 5) but the assay revealed that compound **8** did not inhibit the RDDP activity ($IC_{50} > 100$ μM).

In order to find a structure-activity relationship, we decided to test the inhibitory activities of the commercially available ferulic acid (**9**) and ethyl ferulate (**12a**) against both RNase H and RDDP functions. Both compounds did not display any activity *versus* the two RT-associated functions (Table 5). All these data led to the conclusion that the esterification of ferulic acid with a long alkyl chain is essential for the inhibition of RNase H function. Therefore, using saturated and unsaturated aliphatic alcohols, we decided to synthesize a series of ferulic acid esters **(12b-g)** (Scheme 1) and to evaluate their inhibition potency towards the two RT associated functions.

5.1.3.1 Synthesis of esters (12b-l) and amide (13f) of ferulic acid

The synthesis of ferulic acid esters **12b-l** was performed according to a previously described procedure [228] with some slight modifications, as illustrated in scheme 1. Briefly, the reaction involved the synthesis of a mixed anhydride obtained by reaction of ferulic acid (**9**) and ethyl chloroformate in presence of TEA, at -15 °C. This step led to a simultaneous protection/activation of ferulic acid. The protected ferulic acid anhydride (**10**) was not isolated and the appropriate alcohol, in presence of catalytic amount of DMAP, was added to afford the protected esters (**11b-l**). The deprotection was easily achieved using excessive amounts of nucleophilic base (piperidine) at 0 °C, to give the expected esters (**12b-l**) in good yields. The amide **13f** was obtained adding excessive amounts of oleyl amine to the DCM solution of **10**

giving, at once, amidation and deprotection (Scheme 1). ^{1}H- and ^{13}C NMR spectra and data of synthesized compounds (**12b-l, 13f,**) are reported in experimental section (Fig.125-148).

5.1.3.2 Synthesis of esters (17f,g) and amide (18f) of caffeic acid

The synthesis of esters (**17f, g**) and amide (**18f**) of caffeic acid was carried out using the same procedure of the ferulic acid esters but the protected caffeic acid mixed anhydride was obtained by reaction of caffeic acid with 4.4 equivalents of ethylchloroformate instead of 2.2 equivalents (Scheme 2). ^{1}H- and ^{13}C NMR spectra and data of synthesized compounds (**17f-g,** and **18f**) are reported in experimental section (Fig. 149-154).

Scheme 1
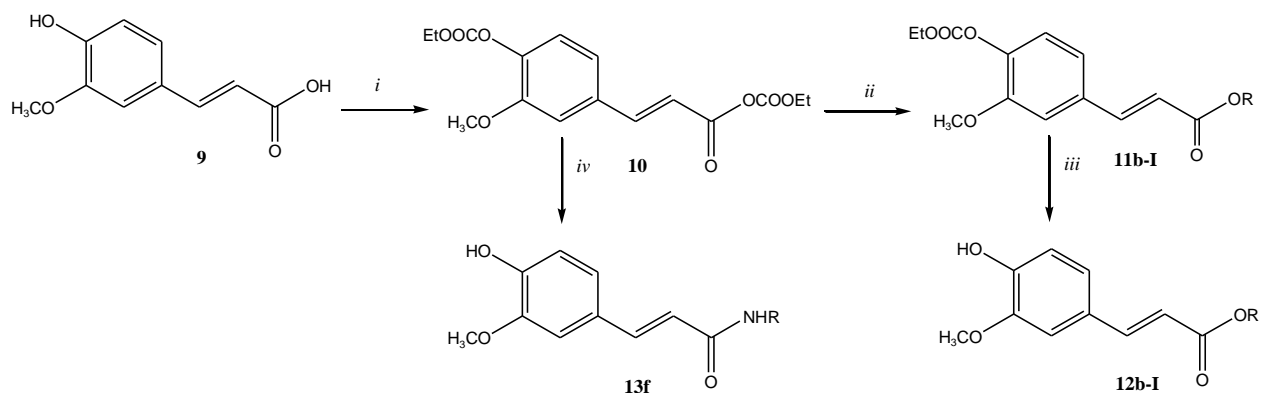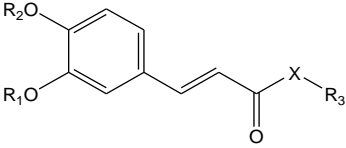
Scheme 2
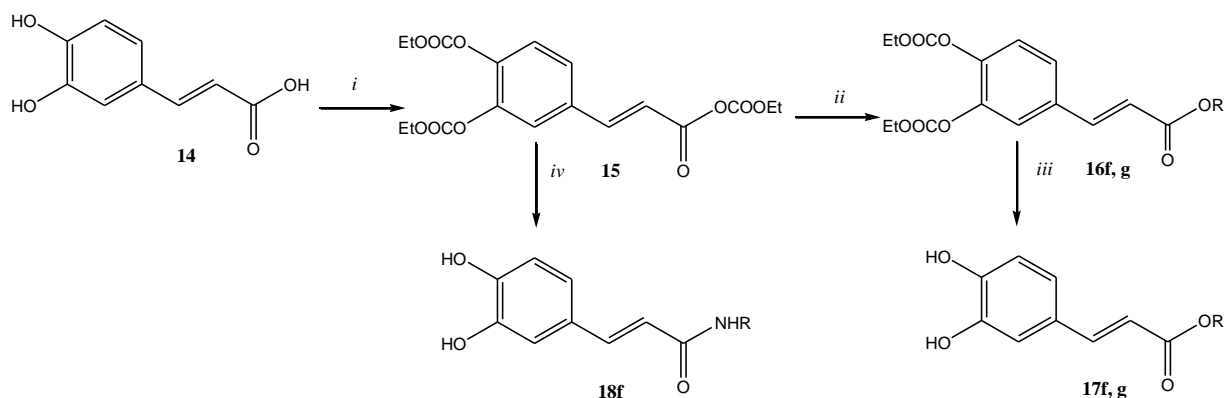
i:ClCOOEt, TEA, DCM, -15ºC, 1h; *ii*:ROH, DMAP, r.t.; *iii*: piperidine, 0ºC, 1h; *iv*: NH$_2$R,

Table 5: Effect of the synthesized compounds on the HIV-1 RT-associated RNase H and RDDP functions

1-9, 12a-l, 13f, 16f-g, 17f-g, 18f

Compounds	R1	R2	R3	X	RNaseH [a]IC_{50} (µM)	RDDP [b]IC_{50} (µM)
Oleanolic acid (1)	-	-	-	-	7.5 ± 0.9	[c]ND
Ursolic acid (2)	-	-	-	-	5.5 ± 0.3	ND
Pomolic acid (3)	-	-	-	-	9.3 ± 0.2	ND
Betulinic acid (4)	-	-	-	-	13.2 ± 1.9	ND
Stigmasterol (5)	-	-	-	-	158.3 ± 7.8	ND
Vanillin (6)	-	-	-	-	>100	>100
7	CH_3	H	-	H	>100	>100
8	CH_3	H	*n*-tetradecyl	O	12.1 ± 1.1	>100
9	CH_3	H	H	O	>100	>100
12a	CH_3	H	ethyl	O	>100	>100
12b	CH_3	H	*n*-decyl	O	22.8 ± 1.7	25.1 ± 0.5
12c	CH_3	H	*n*-dodecyl	O	17.0 ± 1.7	18.2 ± 1.4
12d	CH_3	H	*n*-hexadecyl	O	23.9 ± 0.2	>100
12e	CH_3	H	*n*-octadecyl	O	26.9 ± 0.7	>100
12f	CH_3	H	oleyl	O	10.6 ± 0.3	23.6 ± 3.2
12g	CH_3	H	geranylgeranyl	O	8.4 ± 0.2	9.8 ± 0.5
12h	CH_3	H	2-phenylethyl	O	>100	>100
12i	CH_3	H	2-(p-methylphenyl)ethyl	O	84.0 ± 1	50.0 ± 2
12j	CH_3	H	2-(o-methylphenyl)ethyl	O	75.0 ± 1	78.0 ± 2
12k	CH_3	H	2-(p-chlorophenyl)ethyl	O	57.3 ± 3	70.0 ± 3
12l	CH_3	H	2-(1-naphthyl)ethyl	O	37.3 ± 6	27.0 ± 1
13f	CH_3	H	oleyl	NH	25.3 ± 3.7	11.3 ± 2.1
16f	$COOC_2H_5$	$COOC_2H_5$	oleyl	O	15.6 ± 0.8	18.2 ± 3.0
16g	$COOC_2H_5$	$COOC_2H_5$	geranylgeranyl	O	11.7 ± 1.9	12.2 ± 1.4
17f	H	H	oleyl	O	1.06 ± 0.17	1.6 ± 0.08
17g	H	H	geranylgeranyl	O	1.04 ± 0.12	1.5 ± 0.02
18f	H	H	oleyl	NH	0.68 ± 0.15	2.3 ± 0.07
Oleyl alcohol	-	-	-	-	40.0 ± 5	53.0 ± 8
Geranylgeraniol	-	-	-	-	39.0 ± 7	22.2 ± 8
EFV	-	-		-	ND	0.012 ± 0.03
RDS1759	-	-	-	-	10.1 ± 2.2	ND

[a]Compound concentration required to reduce the HIV-1 RT-associated RNase H activity by 50%., [b]Compound concentration required to reduce the HIV-1 RT-associated RNAdependent DNA polymerase activity by 50%, [c]ND, not done.

5.1.4 HIV-1 RT associated RNase H and RDDP functions inhibitory activity of the synthesized compounds

The inhibitory activity of the RNase H function of the saturated 10C-18C alkyl ferulates changed only slightly, with the natural tetradecyl ferulate (**8**) being still the most active (Table 5). As regards the anti RDDP activity, a relatively short chain of 10C-12C allowed the double inhibition of RT-associated activities, whereas a chain longer than 12C annulled the anti RDDP function of ferulates. The introduction of double bonds in long alkyl chain ferulates (**12f,g**), by reaction with oleyl alcohol or geranylgeraniol, permitted to regain the anti RDDP activity and to increase potency towards RNase H function. Considering the increase of activity achieved by substitution of unsaturated alkyl chain, we decided to modify the aromatic portion synthesizing esters of caffeic acid (**17f,g**) in which geranylgeranyl or oleyl chain was held constant. It was found that the replacement of methyl ether in oleyl ferulate (**12f**) and geranylgeranyl ferulate (**12g**) with a hydroxyl group resulted in a strong enhancement of potency towards both RNase H (10-fold in **17f** and 8-fold in **17g**) and RDDP (15-fold in **17f** and 7-fold in **17g**) functions. The importance of *o*-hydroxyl substitution was determined analyzing the anti-RNase and anti RDDP activities of the oleyl- and geranylgeranyl 3,4-diethoxycarbonyloxy caffeate (**16f,g**). With respect to oleyl and geranylgeranyl caffeate, compounds **16f,g** showed a substantial loss of potency from 8 to 15 folds, suggesting the importance of free hydroxyl groups for the interactions with both RT functions.

Furthermore, to exclude the possibility that the inhibitory activity was only due to the fatty alcohols, oleyl alcohol and geranylgeraniol were assayed for their inhibiting capability towards the two RT-associated functions. The two fatty alcohols showed very low inhibiting activity underling the requirement of their esterification with ferulic or caffeic acid. Bioisosteric replacement of ester functionality in compounds **12f** and **17f** with an amide moiety resulted either in an increase or reduction of potency, depending on the amides. In fact, among all tested compounds, N-oleylcaffeamide (**18f**) showed the higher inhibitory activity towards RNase H function with a IC$_{50}$ of 0.68 μM maintaining a potency *versus* RDDP function very close to that of oleyl caffeate **17f**. On the contrary, N-oleylferulamide (**13f**) resulted in substantial loss of

potency toward the RT-associated RNase function (2.5-fold) when compared to oleyl ferulate (**12f**) while the RDDP inhibition increased of 2-fold.

To explore whether the substitution of the alkyl chain with a lipophilic aromatic moiety might increase the potency of ferulates, a series of ferulic acid phenethyl esters (**12h-l**) were synthesized. Ferulic acid phenylethyl ester (**12h**) did not show any efficacy against the two RT functions up to 100 μM and its analogues substituted at the phenyl ring either with electron-withdrawing (**12k**) or with electron-releasing (**12i,j**) groups were only slightly active (Table 5). The replacement of the phenyl ring by a naphthyl group (**12l**) further enhanced the inhibitory activity towards both RT-associated function but the IC$_{50}$ values were only moderate.

5.1.5 In-silico molecular modeling study

In order to gain a deeper understanding of the RT–ligand interactions docking experiments were carried out. To overcome the exponential problem inherent to flexible ligand docking methods, 7 clustered conformations of the target were selected [229-231]. Furthermore, due to the high flexibility of the ligands we have taken into account the conformations within 5 kcal/mol from the global minimum conformation and among them the most diverse conformations (with different values of RMSD compared with the global minimum) were selected and subjected to ligand flexible docking experiments. In fact several studies highlighted the different possible conformation adopted by compounds with a large number of rotatable bonds [232,233]. In addition, different evaluation of docking studies analysed the influence of starting 3D ligand conformation and the number of those initial conformations on final docking results. Generally using more structures results in better conformational space searching. This assumption has been shown to be more accurate in several comparative experiments [234]. Performing docking studies with different starting conformations when the ligand has a low number of rotatable bonds is not necessary but, with high flexible ligands, this can be an important issue. Indeed, the size of the conformational space to be sampled increases exponentially with ligand flexibility and the thoroughness of the sampling is important for the correct prediction of binding mode [235]. QM-Polarized Ligand (QMPL) [235] docking experiments were carried out. The same docking protocol was applied successfully in previous studies [230,236]. Two favourable

binding pockets were retrieved. One close to the polymerase catalytic site; the other below the RNAse H catalytic site between the two subunit P66 and P51 [230,236].

The docking mode of the synthesized N-oleylcaffeamide (**18f**) compared to the natural compound tetradecyl ferulate (**8**) show immediately that the complex **18f-RT** is more stable than **8-RT** especially if we compared the Emodel energy. While for the synthesized compound both pockets are energetically favourable, for the natural one the second pocket is the best. Best docking complexes were subjected to post-docking procedure based on energy minimization (Figures **38** and **39**) [230,236].

In figure **38** it is clearly depicted how compound **18f** has the ability to harpoon the site discovered by Himmel as RNase allosteric site as well as the NNRTI [91]. This could lead to the inhibition of both RT HIV-1 catalytic activities. In fact, as hypothesized by Himmel, the compounds could be able to deviate the dsDNA-RNA preventing it binding to the RNAse H catalytic site and, at the same time, they are able to interact with the NNRTI binding pocket locking the enzyme in a conformation that inhibits also its polymerase activity. Furthermore, docking experiments highlighted the possibility to bind also in another site below the RNase H catalytic site between the two subunits P66 and P51. The poses show the importance of the length of the chain and the possibility to be accommodated; thanks to presence of the *cis* configured double bond. The geometry of the compound allows entering the RNAse H allosteric cavity which is narrow and long and with its optimal length is able to enter into the NNRTI binding pocket. The ligand enzyme complex is stabilized by hydrogen bond with Lys223, Tyr188, Leu 228 and hydrophobic interactions (green residues). The binding in the second site appears slightly less favored but could contribute to the inhibition of the RNAse H activity by deviating the trajectory of the nucleic acid. Similarly, in this case the complex is stabilized by hydrogen bond interactions (arrows) and hydrophobic interactions (green residues).

Natural compound instead is better stabilized in pocket 2 by hydrogen bonds and pi-cation interaction with Lys431 (Fig. **39**). However, the long hydrophobic chain is exposed to the solvent in some points and this is probably responsible for the higher energy. Furthermore, the bulkier methoxy group is not able to donate hydrogen bond and this could contribute to its weaker activity.
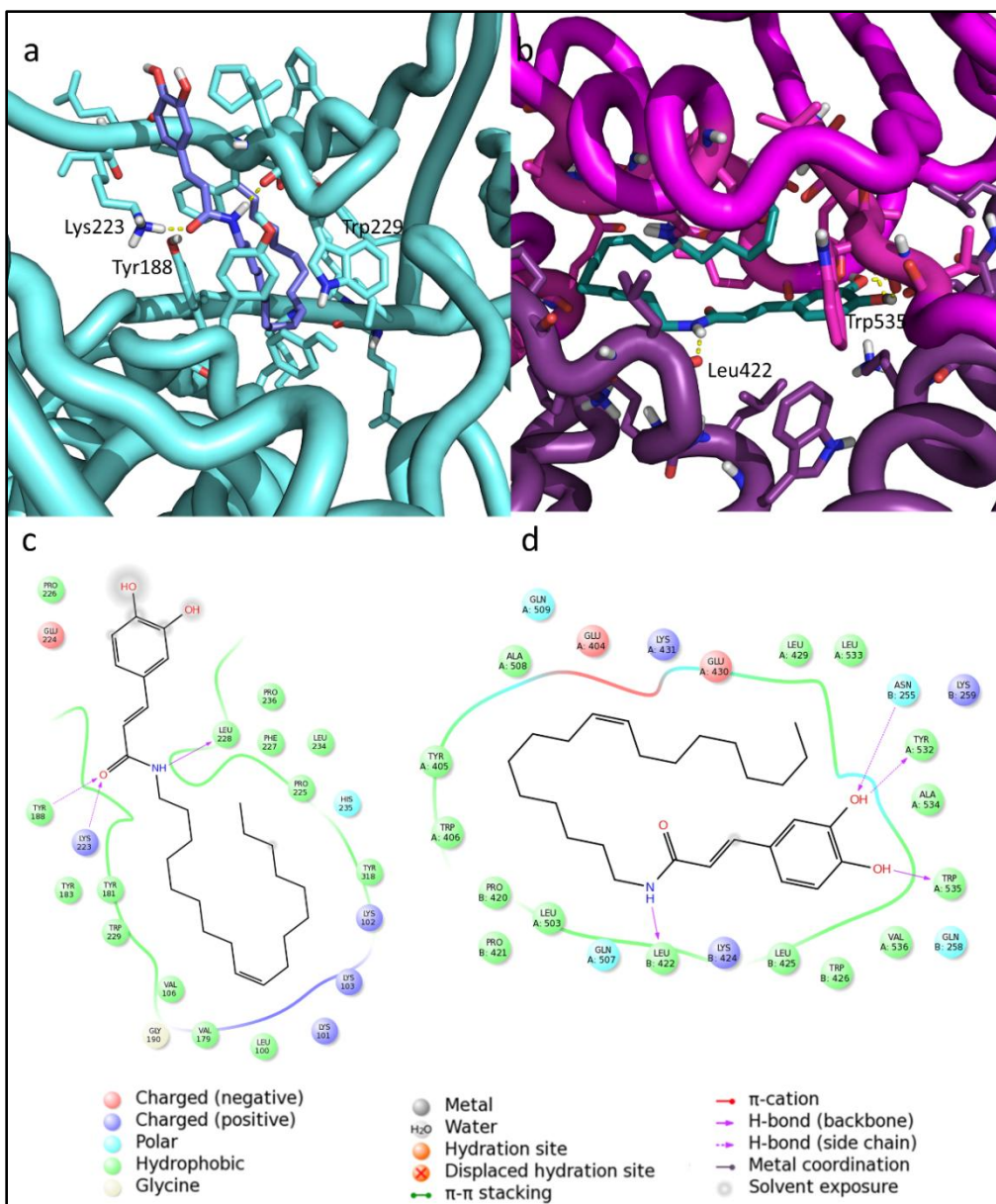
Fig. 38: Putative binding mode of **18f**-Enzyme a) in pocket 1; b) in pocket 2; c-d) respective 2D representation of compound and binding pocket interacting residues
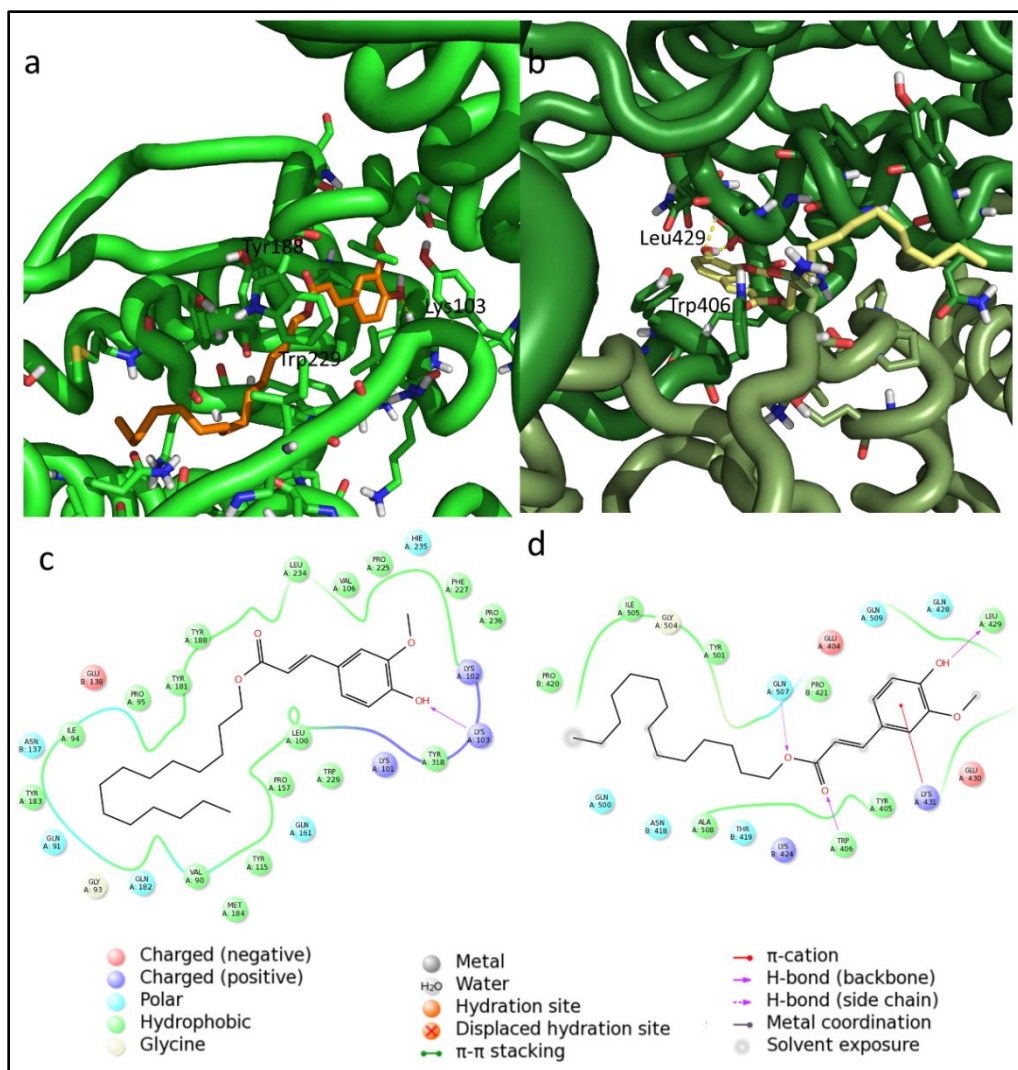
Fig. 39: Putative binding mode of **8**-Enzyme a) in pocket 1; b) in pocket 2; c-d) respective 2D representation of compound and binding pocket interacting residues

5.1.6 Yonetani–Theorell analysis

Hence, the molecular modelling studies indicated that amide **18f** inhibited the RNase H activity binding an allosteric site, despite its catechol moiety, potentially able to coordinate the Mg^{++} ions within the RNase H catalytic site. In order to validate the docking poses, we firstly decided to verify the chelating potential of compound **18f** by measuring its UV spectrum of absorbance in the absence and in presence of $MgCl_2$, using the diketo acid derivative RDS1759 as positive control (Fig. 40).
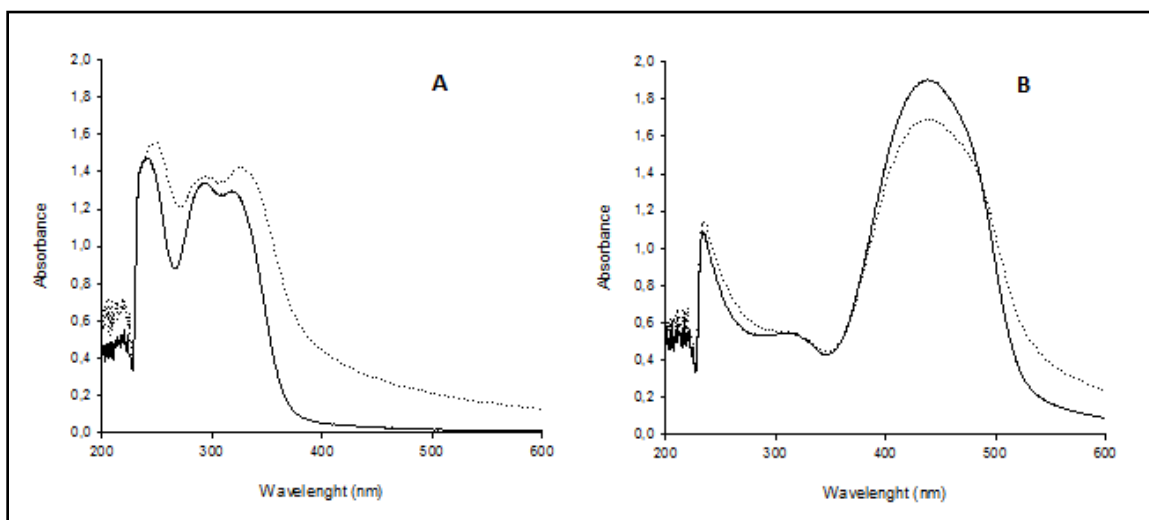
Fig. 40: Effect of $MgCl_2$ on the spectrum of absorbance of N-oleylcaffeamide. Chelation of Mg^{2+} by N-oleylcaffeamide (panel A) and RDS1759 (panel B). UV–vis spectrum was measured with compound alone (unbroken line) or in the presence of 6 mM $MgCl_2$ (dotted line).

Results showed that **18f** maximum of absorbance shifted from 239 nm to 248 nm, in the presence of $MgCl_2$ suggesting the theoretical capability to chelate magnesium ions in the catalytic site of the RNase H function; however, the chelating capability is a necessary but not sufficient condition to bind the catalytic site. Hence, we further investigated the mode of action of compound **18f** with respect to RDS1759 by a revised Yonetani-Theorell analysis [237] on the combined effects of **18f** and RDS1759 on RNase H function. This model allows to discriminate between inhibitors that are kinetically mutually exclusive (potentially competing for a single binding site) and inhibitors that are kinetically not mutually exclusive (potentially binding to

non-overlapping sites). Results showed that the binding of compound **18f** is not kinetically mutually exclusive with RDS1759 for binding the catalytic site of the RNase H function, since in figure 5 we observed a series of intersected lines due to the binding of the two inhibitors to different enzyme sites (Fig. 41, panel A). Furthermore, isobologram analysis (Fig. 41, panel B) displayed a clear additive effect of the two compounds on the inhibition of HIV-1 RT-associated RNase H function.
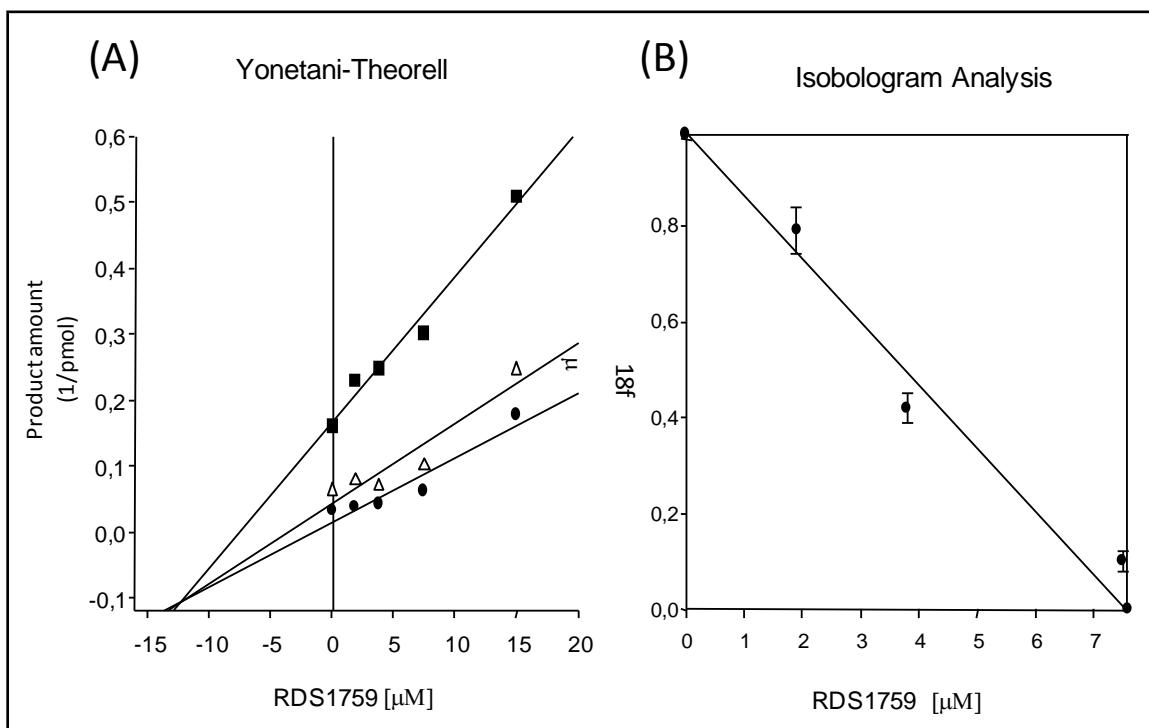
Fig.41: Panel A. Yonetani–Theorell analysis. Combination of N-Oleylcaffeamide and RDS1759 on the HIV-1 RT RNase H activity. HIVRT was incubated in the presence of RDS1759 alone (●) or combined with increasing concentrations of N-Oleylcaffeamide 1μM (Δ), 2μM(■). Panel B. Isobologram analysis combination of compound N-Oleylcaffeamide and RDS1759 on the HIV-1 RT RNase H activity.

5.1.7 Isolation of secondary metabolites from the MeOH extract of *O. sanctum*

5.1.7.1 Extraction procedure

The MeOH extract of *O. sanctum* have shown inhibition of HIV-1 RT-associated RNase H function with IC_{50} value of 1.1 ± 0.14 µg/ml (Table 6) and therefore was subjected to fractionation by RP-18 vacuum liquid chromatography (VLC) to afford five major fractions (F1-F5). All fractions were evaluated for their anti-RNase H activity (Table 6).

Table 6: Effect of *O. sanctum* MeOH fractions on the HIV-1 RT-associated RNase H function

Fractions	RNase-H [a]IC_{50} (µg/ml)
MeOH extract	1.1 ± 0.14
F1	2.40 ± 0.15
F2	2.86 ± 0.34
F3	1.67 ± 0.10
F4	2.65 ± 0.09
F5	2.67 ± 0.13

[a]Extract concentration required to reduce the HIV-1 RT-associated RNase H activity by 50%.

Since the entire tested fraction showed comparable low IC_{50} values ($1.67 - 2.86$ µg/ml), they were injected in HPLC in order to verify the chemical profile of each fraction. We used an RP-18 analytical column and as eluents MeOH: H_2O: Trifluoroacetic acid (70:30:0.5), flow: 2.5 ml/min. The wavelengths were 250 and 360 nm. HPLC analysis revealed that all the fractions contained the same compounds, but in different ratio (data not shown), we decided to isolate the two major compounds by different chromatographic techniques such as column chromatography (silica gel and Sephadex LH-20) and semi-preparative HPLC. Rabdosiin (**19**) and rosmarinic acid (**20**) were the two compounds isolated from MeOH extract. Structures of the compounds were confirmed by 1D and 2D NMR.

5.1.7.2 Structural elucidation of secondary metabolites from *O. sanctum*

Compound 19

Compound **19** was identified as rabdosiin by ^{1}H NMR, and 2D NMR (DQF-COSY, HSQC, HMBC) spectroscopy, mass spectrometry, optical rotation and by comparison with literature data [238]. 2D NMR spectra of compound **19** are reported in experimental section (Fig.122-124).

Since the NMR data accorded for both rabdosiin and it's enantiomer, the assignment of compound **19** was achieved by measuring the optical rotation ($[\alpha]^{25}_{D}$) that was - 58.5°. This value is in accord with the literature value of rabdosiin whereas the optical rotation for its enantiomer is +140° [238].
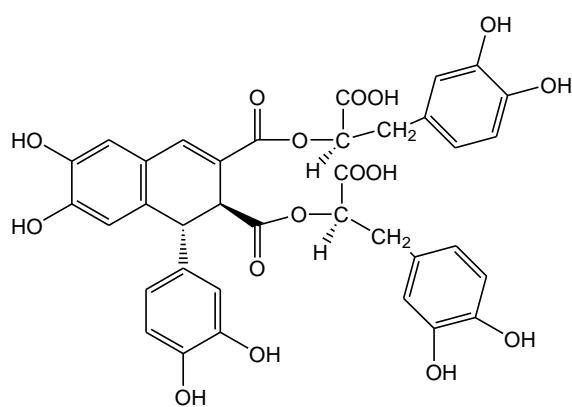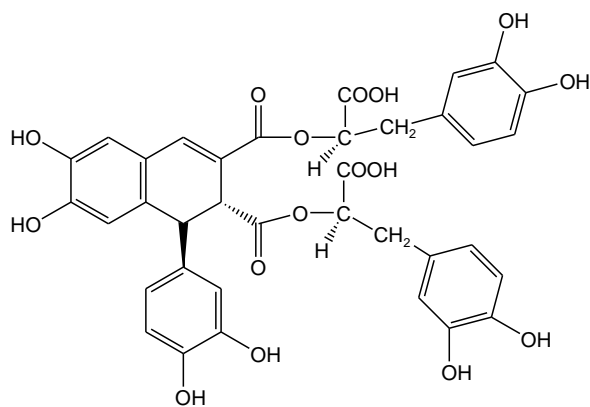
Rabdosiin (**19**)   Rabdosiin enantiomer
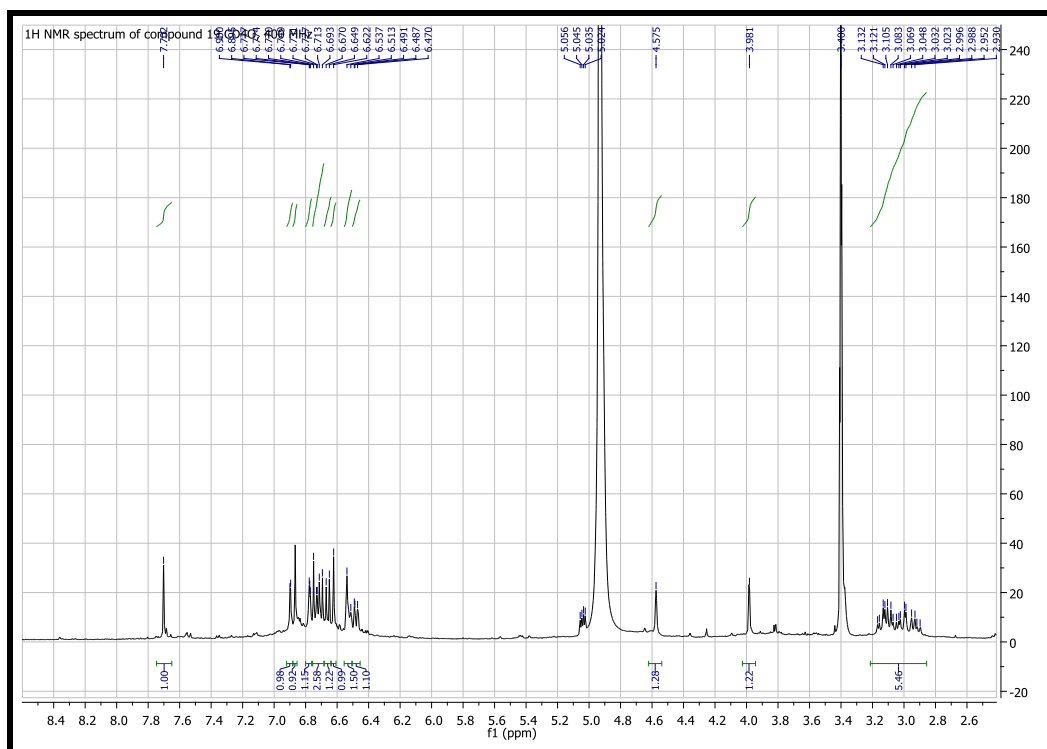
Fig. 42: ^{1}H NMR spectrum of compound **19** (rabdosiin), 400 MHz, CD$_4$O

Compound 20

Compound 20 was identified as rosmarinic acid by ^{1}H- and ^{13}C NMR, and by comparison with literature data [239].
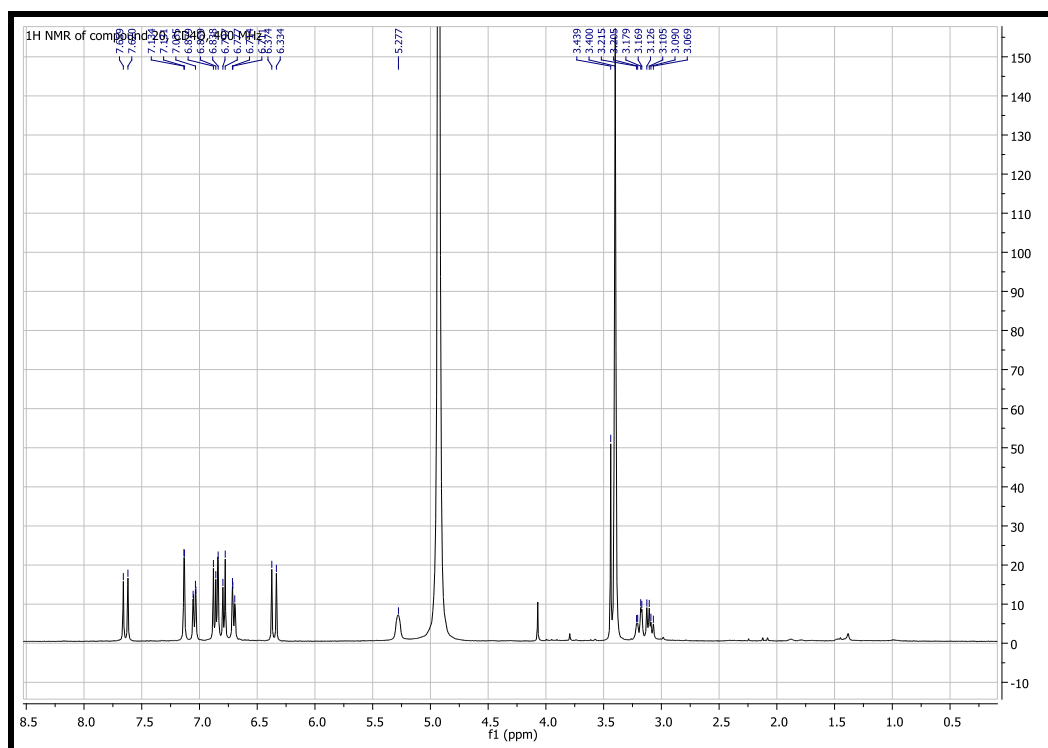
Fig.43: ^{1}H NMR spectrum of compound **20** (Rosmarinic acid), 400 MHz, CD$_4$O
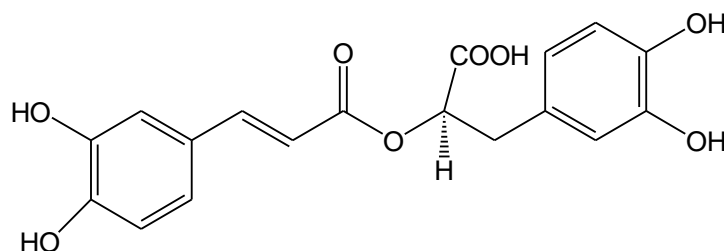
Compound **20** Rosmarinic acid

5.1.7.3 Biological results

Compounds isolated from MeOH extract were testedd agaisnt HIV-1 RT associated Rnase H and RDDP function (Table 7). Rabdosiin (**19**) was found as dual inhibitor of reverse transcriptase. It was able to inhibit RNase H with IC_{50} value 2.16 ± 0.11 µM and RDDP with IC_{50} value 4.0 ± 0.8 µM. This is the most potent natural compound against both RT functions that we have found in this work. Rosmarinic acid (**20**) was moderatley active against RNase H ($IC_{50}= 20.7 \pm 0.7$ µM) and RDDP (32.3 ± 8.5 µM).

Table 7:.Effect of the compounds isolated from *O. sanctum* on the HIV-1 RT-associated RNase H and RDDP activities

Compound	RNase-H IC_{50} (µM)	RDDP IC_{50} (µM)
Rosmarinic acid (**20**)	20.7 ± 0.7	32.3 ± 8.5
Rabdosiin (**19**)	2.16 ± 0.11	4.0 ± 0.8
RDS1759	10.1 ± 2.2	-
Efavirenz	-	0.012 ± 0.03

5.2 *Tinospora cordifolia*

5.2.1 Extraction and isolation of secondary metabolites

Air-dried and powdered stem bark of *T. cordifolia* (300 g) was subjected to extraction using DCM by percolation (during the day) and maceration (during the night) to give 5.4 g of dried extract.

DCM extract have shown significant inhibitory activity (IC$_{50}$= 11.8 ± 2.2 µg/ml) against HIV-1 RT-associated RNase H function. Therefore, DCM extract was subjected to fractionation by silica gel vacuum liquid chromatography (VLC), coloumn chromatography (silica gel and sephadex LH 20) and semi preparative normal phase (NP) or reverse phase (RP) HPLC. Five triterpenoids namely lupenone (**21**), lupeol (**22**), 11-oxo-β amyrin (**23**), stigmasterol (**24**), β-sitosterol (**25**) were isolated. Besides triterpenes, columbin (**26**), vanillin (**27**), β-asarone (**28**), N-*trans*-feruloyltyramine (**29**), and (+)-balanophonin (**30**) were isolated.

The structure of the compounds were deduced from the 1D and 2D NMR spectra as well ESI mass spectra and confirmed with the literature values.
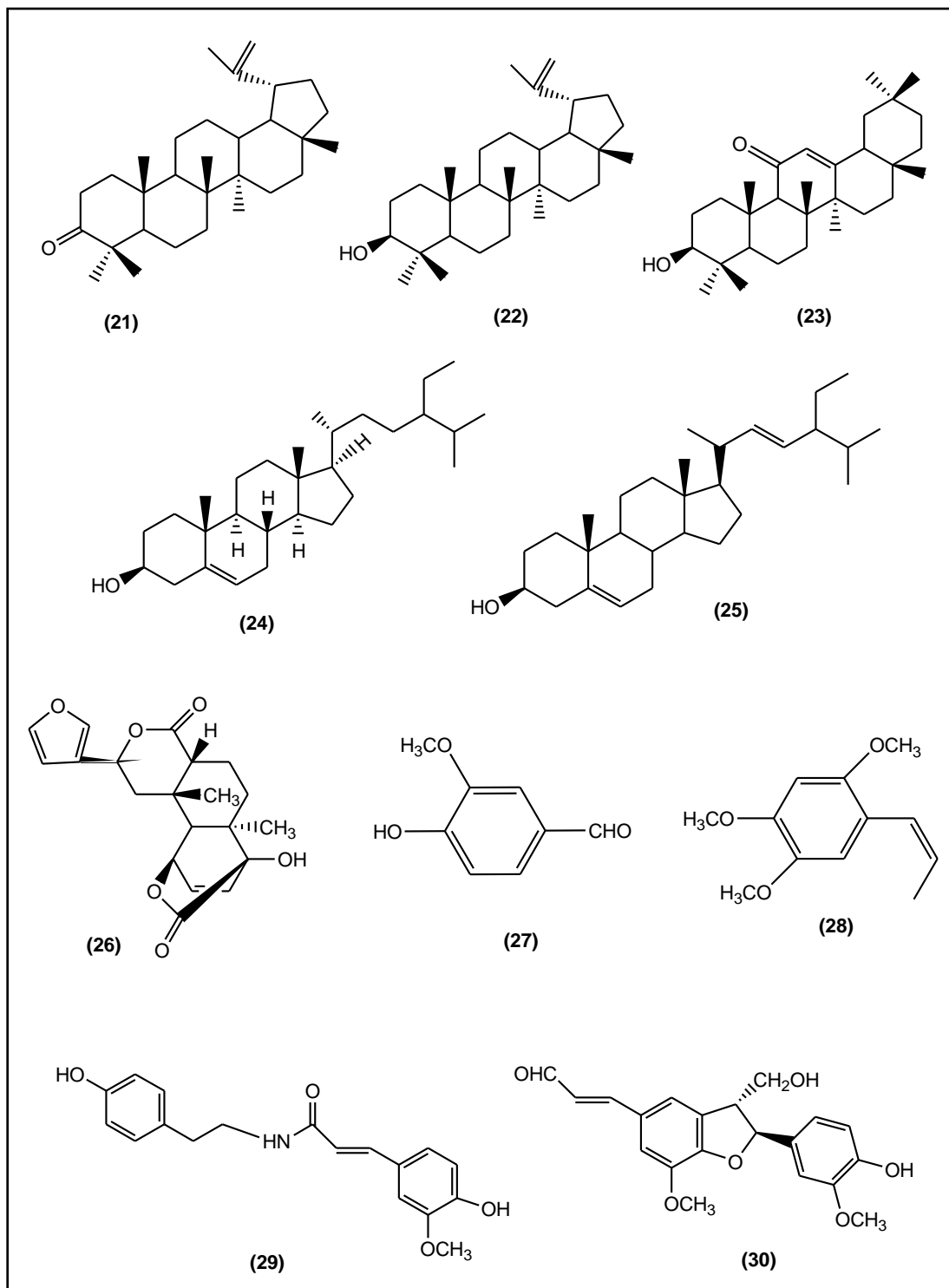
Fig. 44: Structure of the isolated compounds from the DCM extract of *T. cordifolia*

5.2.2 Structural elucidation of secondary metabolites from *T.cordifolia*

Compound 21

Compound **21** was identified as lupenone by 1D (^{1}H and ^{13}C NMR), and 2D NMR (DQF-COSY, HSQC, HMBC, and ROESY) spectroscopy and mass spectrometry (ESI MS) and by comparison with literature data [218]. ESI-MS and 2D MNR spectra of compound **21** are reported in experimental section (Fig.156-158).
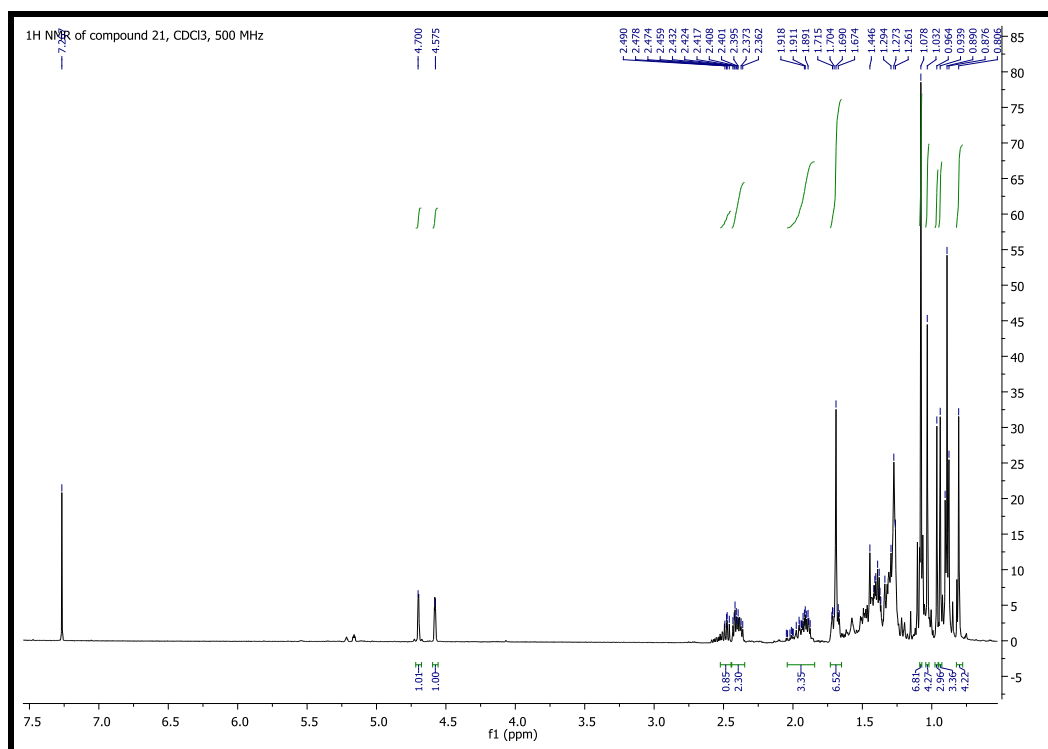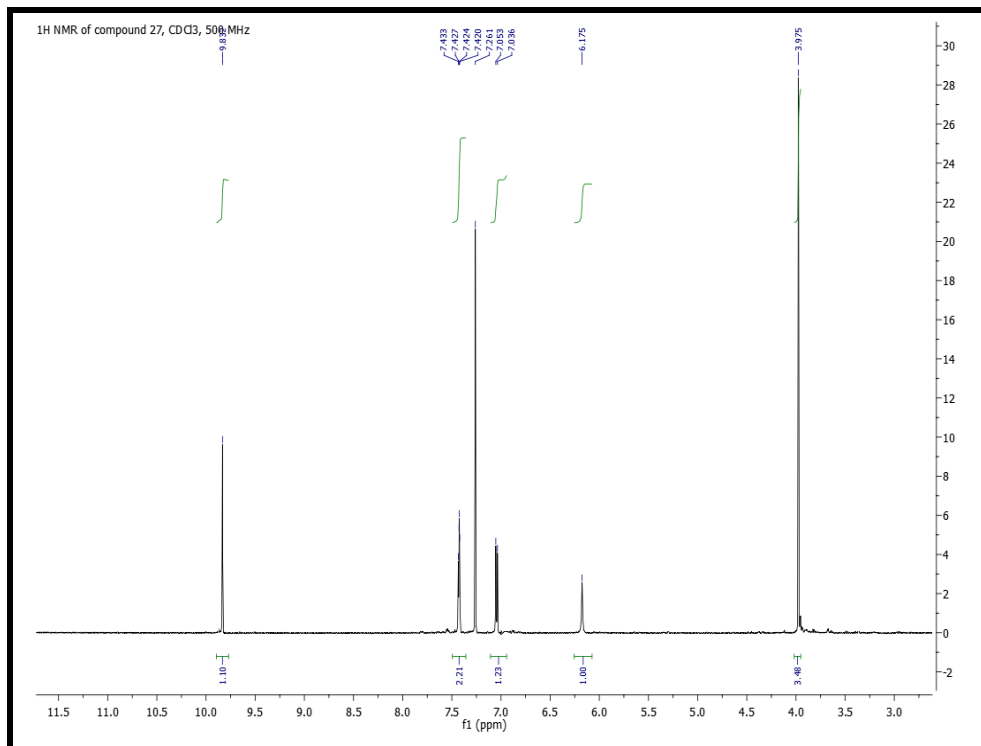

Fig. 45: ^{1}H NMR spectrum of compound **21** (lupenone), 500 MHz, CDCl$_3$
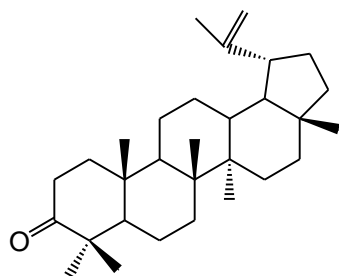
Compound **21** (Lupenone)

Compound 22

Compound **22** was identified as lupeol by 1D (^{1}H and ^{13}C NMR), and 2D NMR (DQF-COSY, HSQC, HMBC, and ROESY) spectroscopy and mass spectrometry (ESI MS) and by comparison with literature data [218]. 1D and 2D NMR spectra of compound **22** are reported in experimental section (Fig. 159-161).
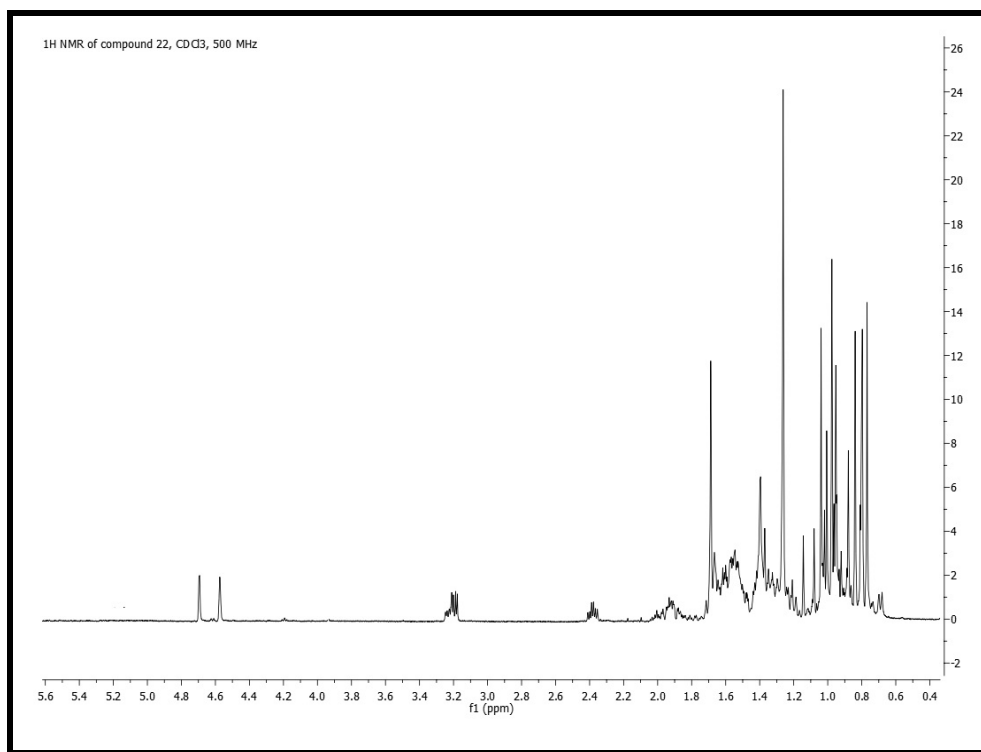
Fig. 46: ^{1}H NMR spectrum of compound **22** (lupeol) 500 MHz, CDCl$_3$
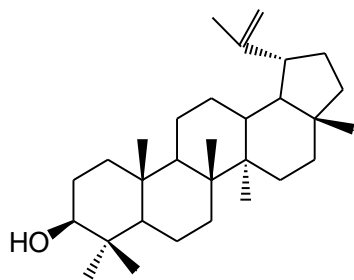
Compound **22** (Lupeol)

Compound 23

Compound **23** was identified as 11-oxo-β-amyrin by 1D (^{1}H and ^{13}C NMR), and 2D NMR (DQF-COSY, HSQC, HMBC, and ROESY) spectroscopy and mass spectrometry (ESI MS) and by comparison with literature data [218]. 2D MNR spectra of compound **23** are reported in experimental section (Fig.162-165).
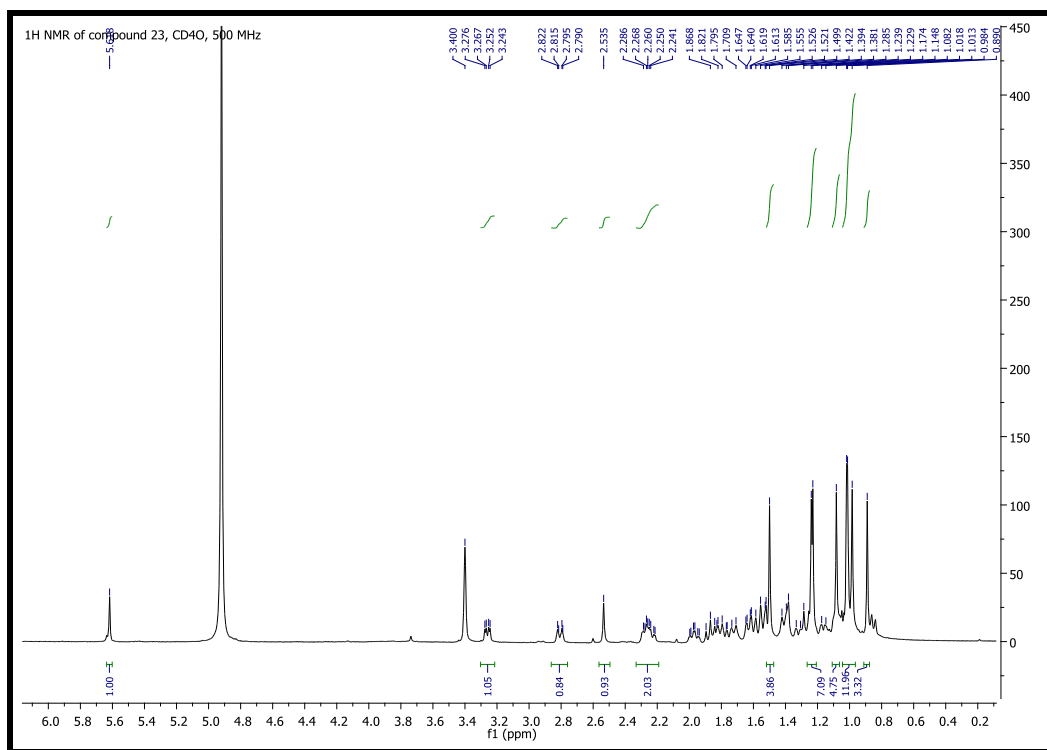
Fig. 47: ^{1}H NMR spectrum of compound **23** (11-oxo-β-amyrin), 500 MHz, CD$_4$O
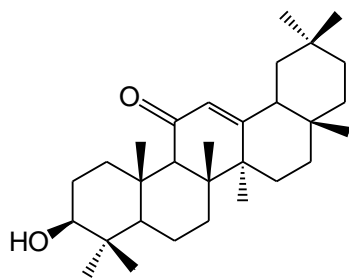
Compound **23** (11-oxo- β-amyrin)

Compound 24

Compound **24** was identified as stigmasterol by 1D (^{1}H and ^{13}C NMR), and 2D NMR (DQF-COSY, HSQC, HMBC, and ROESY) spectroscopy and mass spectrometry (ESI MS) and by comparison with literature data [221]. 2D NMR spectra of compound **24** are reported in experimental section (Fig. 166-167).
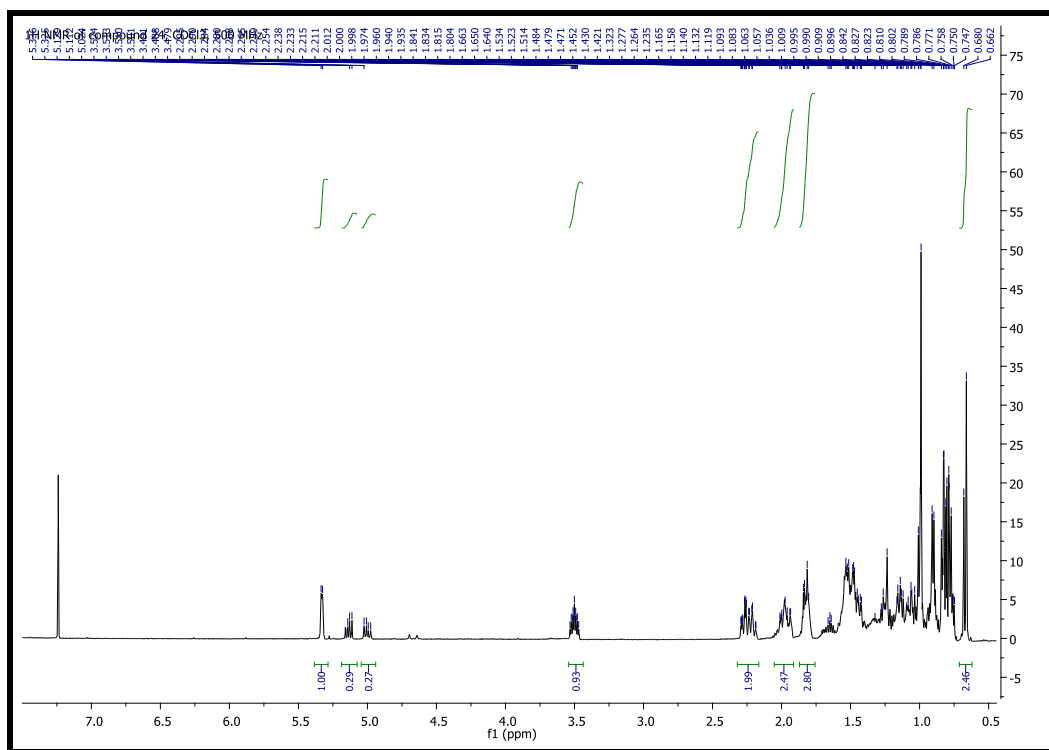

Fig. 48: ^{1}H NMR spectrum of compound **24** (stigmasterol), 500 MHz, CDCl$_3$
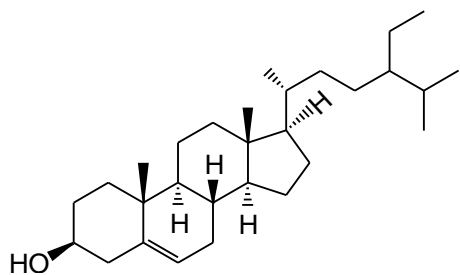
Compound **24** (Stigmasterol)

Compound 25

Compound **25** was identified as β-sitosterol by ^{1}H and ^{13}C NMR spectroscopy and mass spectrometry (ESI MS) and by comparison with literature data [218].^{13}C NMR spectrum of compound **25** is reported in experimental section (Fig. 168)
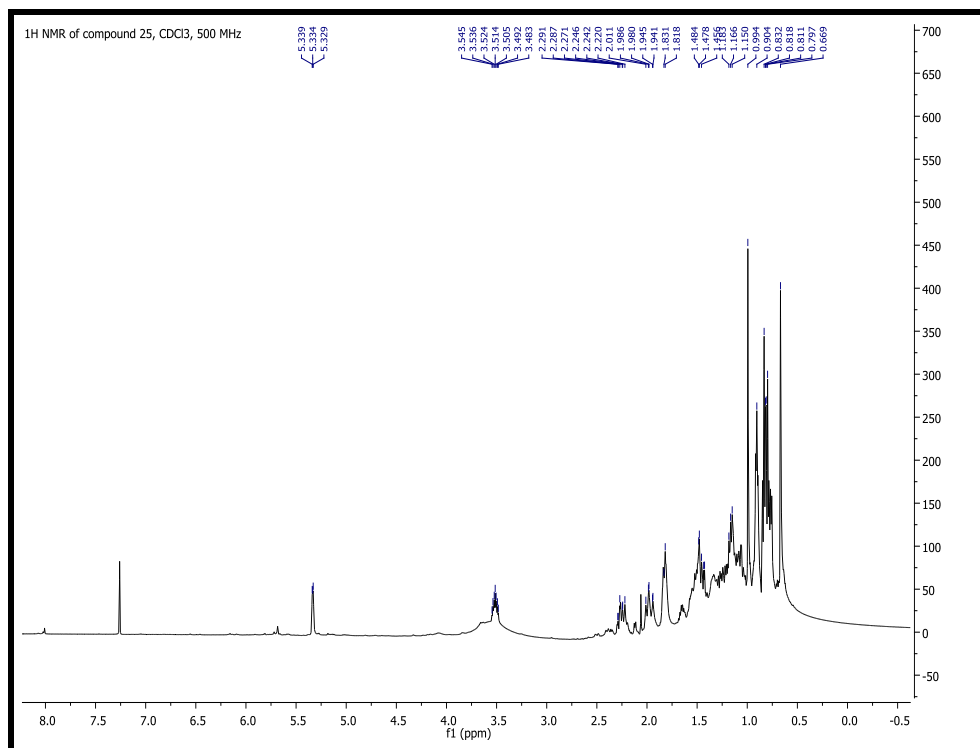
Fig. 49: ^{1}H NMR spectrum of compound **25** (β-sitosterol), 500 MHz, CDCl$_3$
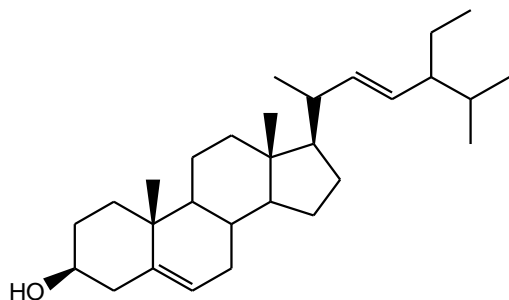
Compound **25** (β- sitosterol)

Compound 26

Compound **26** was identified as columbin by 1D (^{1}H and ^{13}C NMR), and 2D NMR (DQF-COSY, HSQC, HMBC, and ROESY) spectroscopy and mass spectrometry (ESI MS) and by comparison with literature data [240]. ESI-MS, 1D and 2D NMR spectra of compound **26** are reported in experimental section (Fig. 169-173).
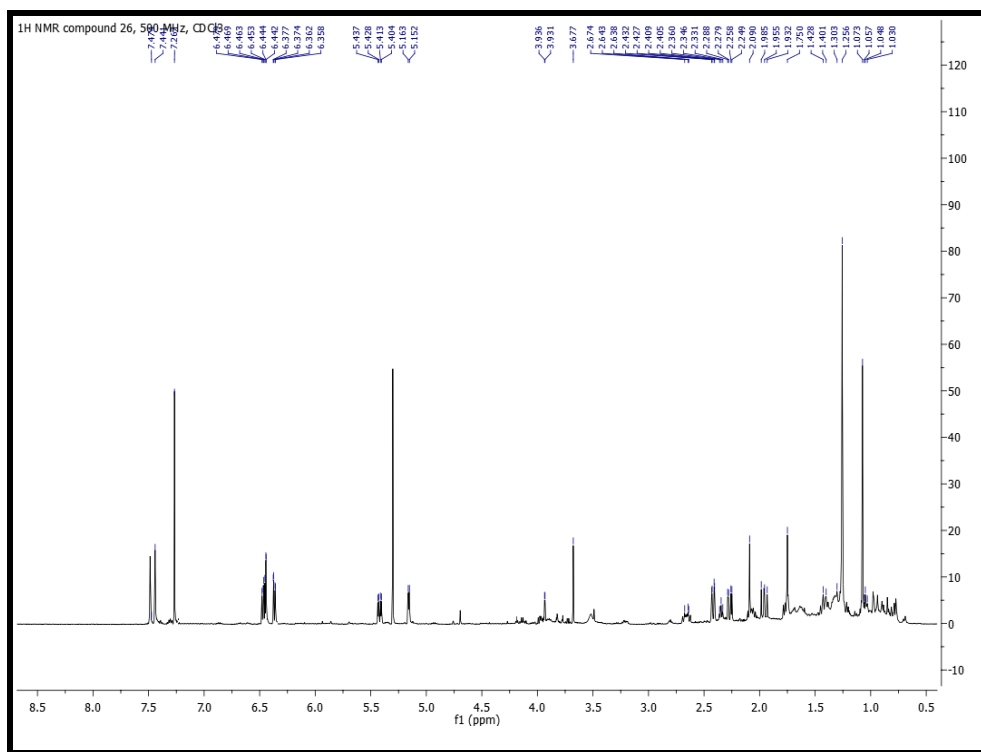
Fig. 50: ^{1}H NMR spectrum of compound **26** (columbin), 500 MHz, CDCl$_3$
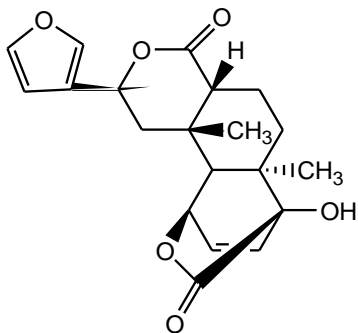
Compound **26** (Columbin)

Compound 27

Compound **27** was identified as vanillin by 1D (^{1}H and ^{13}C NMR) spectroscopy and mass spectrometry (ESI MS) and by comparison with literature data [222]. ^{13}C NMR spectrum of compound **27** is reported in experimental section (Fig.174).

Fig. 51: ^{1}H NMR spectrum of compound **27** (vanillin), 500 MHz, CDCl$_3$
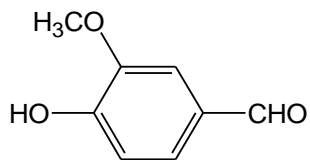
Compound **27** (Vanillin)

Compound 28

Compound **28** was identified as β-asarone (*cis*-asarone) by 1D (^{1}H and ^{13}C NMR), and 2D NMR (DQF-COSY, HSQC, HMBC, and ROESY) spectroscopy and mass spectrometry (ESI MS) and by comparison with literature data [241]. ESI-MS, and 2D NMR spectra of compound **28** are reported in experimental section (Fig. 175-178).
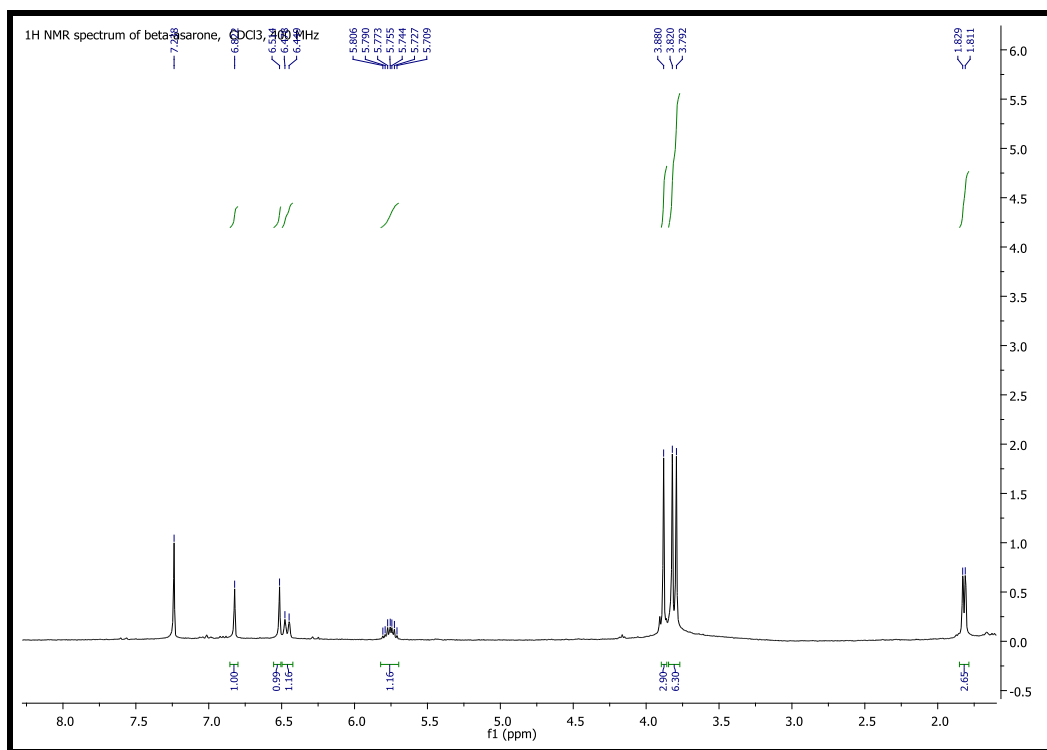
Fig. 52: ^{1}H NMR spectrum of compound **28** (β-asarone), 500MHz, CDCl$_3$
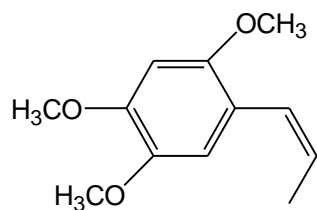
Compound **28** (β-asarone)

Compound 29

Compound **29** was identified as N-*trans*-feruloyltyramine by 1D (^{1}H and ^{13}C NMR), and 2D NMR (DQF-COSY,) spectroscopy and mass spectrometry (ESI MS) and by comparison with literature data [242]. 2D NMR spectra of compound **29** are reported in experimental section (Fig. 179).
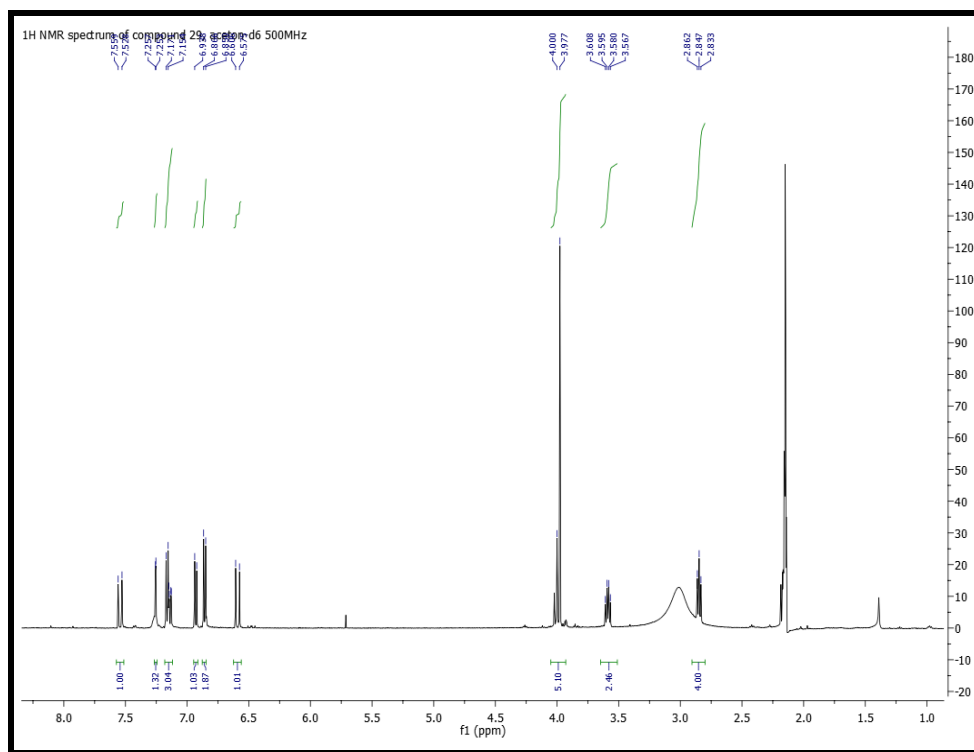
Fig. 53: ^{1}H NMR spectrum of compound **29** (N-*trans*-feruloyltyramine), 500MHz, d_6-acetone
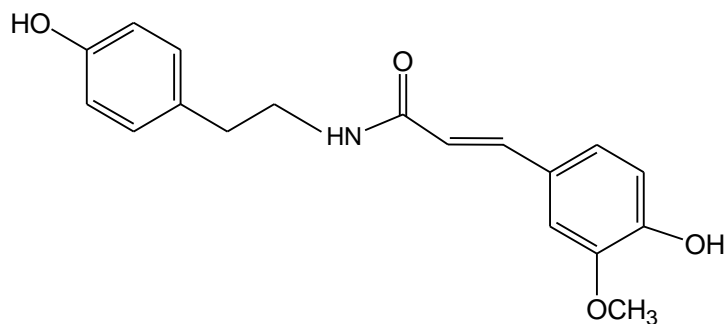
Compound **29** (N-*trans*-feruloyltyramine)

Compound 30

Compound **30** was identified as (+)-balanophonin by 1D (^{1}H and ^{13}C NMR), and 2D NMR (DQF-COSY, HSQC, HMBC, ROESY) spectroscopy and mass spectrometry (ESI MS) and by comparison with literature data [243]. 2D NMR spectra of compound **30** are reported in experimental section (Fig. 180-183).
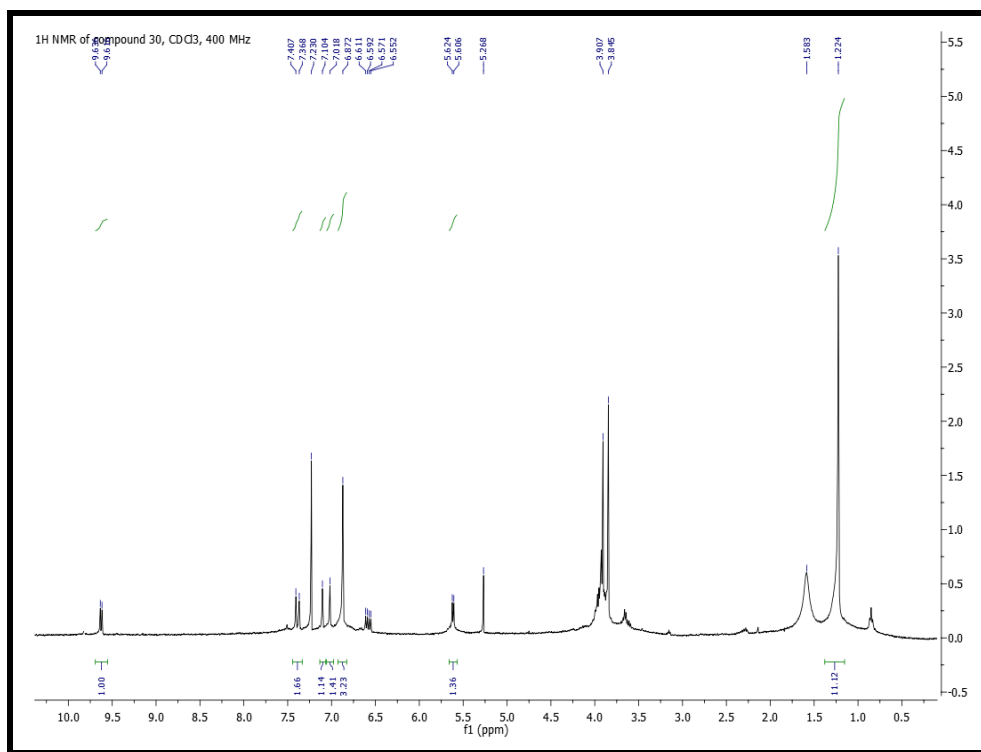
Fig. 54: ^{1}H NMR spectrum of compound **30** (+)-balanophonin), 400MHz, CDCl$_3$
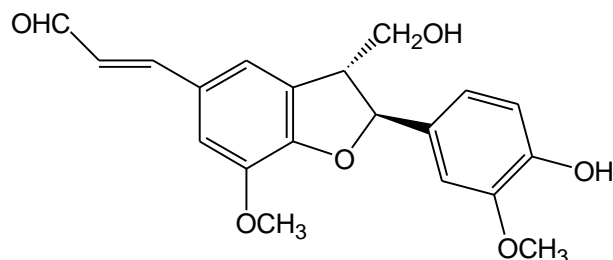
Compound **30** (Balanophonin)

5.2.3 Biological results

Table 8: Effect of the isolated compounds on the HIV-1 RT-associated RNase H

Compound	RNase-H IC$_{50}$ (µM)
DCM extract	11.8 ± 2.2 µg/ml*
Lupenone (**21**)	>58.9
Lupeol (**22**)	5.9±0.24
11-oxo-β-amyrin (**23**)	13.61 ± 0.5
Stigmasterol (**24**)	158.3 ± 7.8
β-sitosterol (**25**)	>241
Columbin (**26**)	46.43±3.58
Vanillin (**27**)	> 100
β-asarone (**28**)	99.8 ± 0.40
N-trans-feruloyltyramine (**29**)	232 ± 7.01
Balanophonin (**30**)	56.77 ± 7.5
RDS1759	10.1 ± 2.2

*IC$_{50}$ value of DCM extract of *T. cordifoila* is reported in µg/ml

The isolated compounds were tested against HIV-1 RT associated RNase H function. RDS1759, a diketoacid inhibitor of the RNase H function that binds the catalytic site, was used as positive control. Among the triterpenes lupeol was the most potent inhibitor with IC$_{50}$ value of 5.9 ± 0.24µM. Also, 11-oxo-β-amyrine showed good potency with IC$_{50}$ of 13.61 ± 0.5 µM. A structure-activity relationship (SAR) revealed that the substitution of C-OH group at 3β position of triterpene scaffold by a keto group, as in lupenone (IC$_{50}$ >58.9 µM), reduced the potency to a

greater extent. This explains the importance of OH group at 3β position for the interaction with the RNase activity.

As regards the other compounds only columbine and (+)-balanophonin showed appreciable inhibitory activity with a IC_{50} of 46.43 ± 3.58 and 56.77 ± 7.5 µM, respectively. Therefore it appears that the inhibitory activity of the extract is mainly due to lupeol and 11-oxo-β-amyrine.

5.3 *Bupleurum fruticosum* **L.**

A series of Sardinian and Indian plant extracts were *in vitro* tested in order to evaluate the capability to inhibit the replication of two human Rhinovirus, HRV 39 and HRV 14, belonging to group A and B, respectively (data not shown). Among all, the DCM extract of *B. fruticosum* was able to inhibit the replication of HRV 39 and HRV 14 with a EC_{50} values of 3.1 ± 1.5 and 12.5 ± 6.1 µg/ml, respectively with low cytotoxicity against HeLa cells (CC_{50} 125 ± 31 µg/ml) (Table 9). Pirodavir was used as reference compound. Therefore, the Selective Index (SI: CC_{50}/EC_{50}) of the extract was good for the group B Rhinovirus (SI=10) and very good for the group A (SI=40) and, as a result the DCM extract was subjected to phytochemical investigation in order to find the bioactive compound(s).

5.3.1 Extraction and isolation of secondary metabolites

460 g of dried powder of *Bupleurum fruticosum* leaves were percolated with DCM. Repetitive cycles of percolation (during the day) and maceration (during the night) were carried out. 23.5 g of DCM extract were obtained.

5.3.2 Isolation of secondary metabolites from DCM extract

With the aim to carry out bioguided isolation, the DCM extract was subjected to fractionation by silica gel VLC obtaining six major fractions (F1-F6). The single fractions were then tested against HRV 39 and HRV 14 and only F3 was able to inhibit the replication of both rhinovirus with an EC_{50} of 6.2 ± 3.1 µg/ml and with low cytotoxicity towards HeLa cells (CC_{50} 125 ± 31 µg/ml) and a SI of 10 (Table 9).

Table 9: Cytotoxic and anti-Rhinovirus activity of DCM fractions from *B. fruticosum*

Extract/fractions	CC_{50} $(\mu g/ml)^a$	EC_{50} HRV 14[b] $(\mu g/ml)^a$	EC_{50} HRV 39[b] $(\mu g/ml)^a$
DCM extract	125 ± 31	12.5 ± 6.1 (SI=10)[c]	3.1 ± 1.5 (SI=40)[c]
F1	62±15	>62	>62
F2	62±15	>62	>62
F3	62±15	6.2±3.1 (SI=10)	6.2±3.1 (SI=10)
F4	62±15	>62	>62
F5	62±15	>62	>62
F6	62±15	>62	>62
Pirodavir	3.1±0.1	0.02±0.005	0.006±0.0001

[a]CC_{50}: cytotoxic concentration 50%; EC_{50}: Effective concentration 50%,

[b]Viruses HRV14: group B; HRV39: group A,

[c]SI: Selective index = CC_{50}/EC_{50}

Compounds were isolated by means of different chromatographic techniques, such as coloumn chromatography (silica gel and sephadex LH 20) and semi preparative normal phase (NP) or reverse phase (RP) HPLC. From the active fraction F3, we have isolated one polyacetylene (**32**), two phenylpropanoid (**34** and **38**), and one monoterpene (**40**). In order to find a structure-activity relationship, also, F1, F2, and F4 were purified yielding one polyacetylene (**31**), and further five phenylpropanoids (**33, 35, 36, 37,** and **39**).

Among all the isolated compounds, **31** and **40** are new in the literature while six (**32, 35-39**) have been isolated from this plant for the first time. Polyacetylenes are very common compounds in *Bupleurum* species [244], but, surprisingly, although various works on the phytochemical study of *Bupleurum fruticosum* have been reported [245,246], even from Sardinian samples [247,248], nobody detected this type of compounds in *B. fruticosum* .
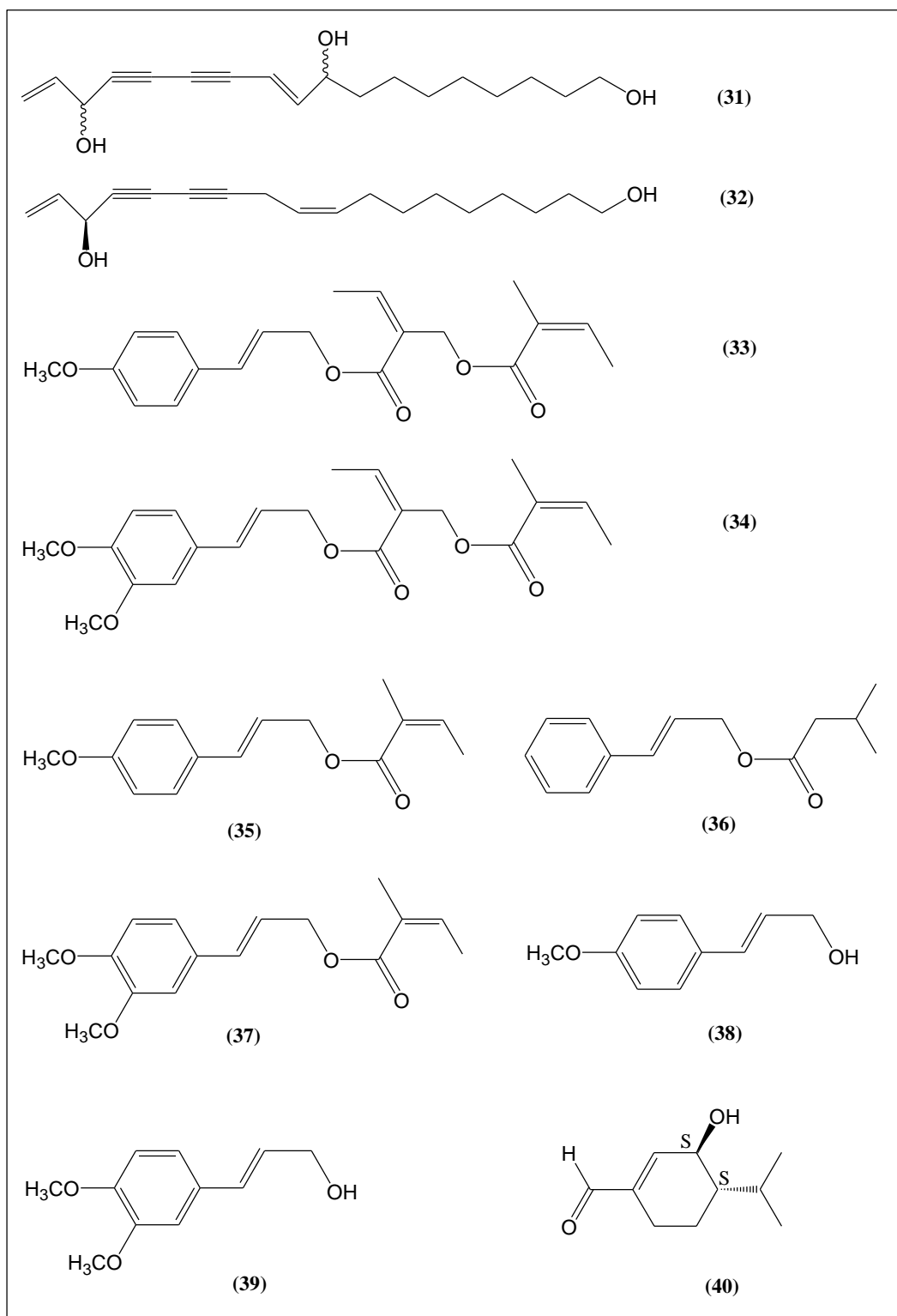
Fig. 55: Structures of the compounds isolated from the DCM extract of *B. fruticosum*

5.3.3 Structural elucidation of secondary metabolites from *B. fruticosum* L.

Compound 31

Compound **31** showed a pseudomolecular ion peak at *m/z* 289.1802 [M-H]⁻ (calc. 289.1803) in HR-TOF-ESI mass spectrum, accounting for the elemental composition of $C_{18}H_{26}O_3$ (Fig. 56).
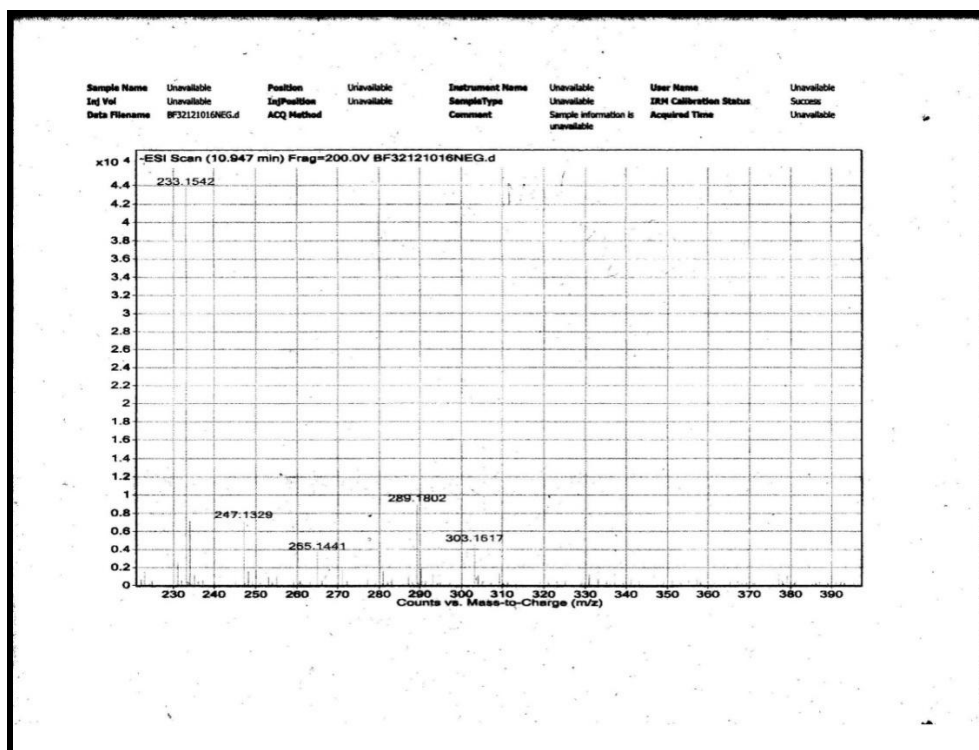
Fig. 56: HR ESI MS spectrum of compound **31** (negative mode)

The ^{1}H NMR spectrum of compound **31** revealed five olefinic proton signals at δ 6.33 (1H, dd, *J* = 5.5, 16 Hz), 5.96 (1H, ddd, J = 17.5, 10.0, 5.0 Hz), 5.78 (1H, d, J = 16 Hz), 5.48 (1H, d, J = 17.5 Hz) and 5.26 (1H, d, J = 10.0 Hz), two oxygenated methine proton signals at δ 4.97 (1H, d, J = 5.0 Hz) and 4.19 (1H,dt, J = 6.5), one oxymethylene group at δ 3.64 (2H, t, J = 7.0 Hz) and two cluster of methylene proton signals at δ 1.54 (m) and 1.30 (m) (Fig. 57, 58).

Fig.57: ^{1}H NMR spectrum of compound **31** measured in CDCl$_3$, 500 MHz
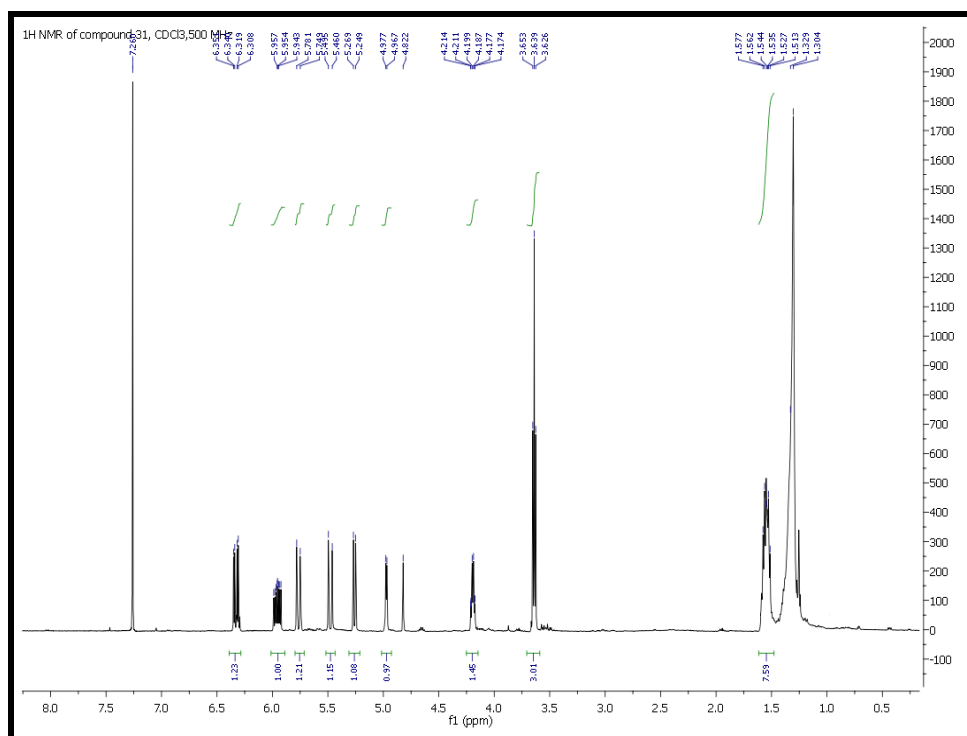
Fig. 58: ^{1}H NMR partial spectrum of compound **31** measured in CDCl$_3$, 500 MHz
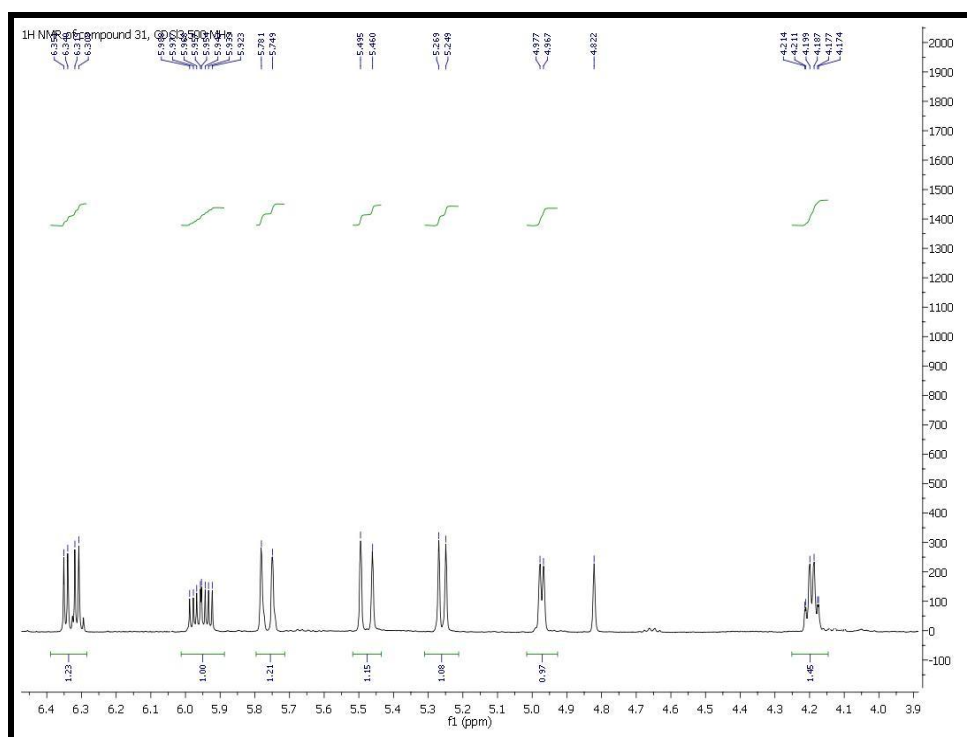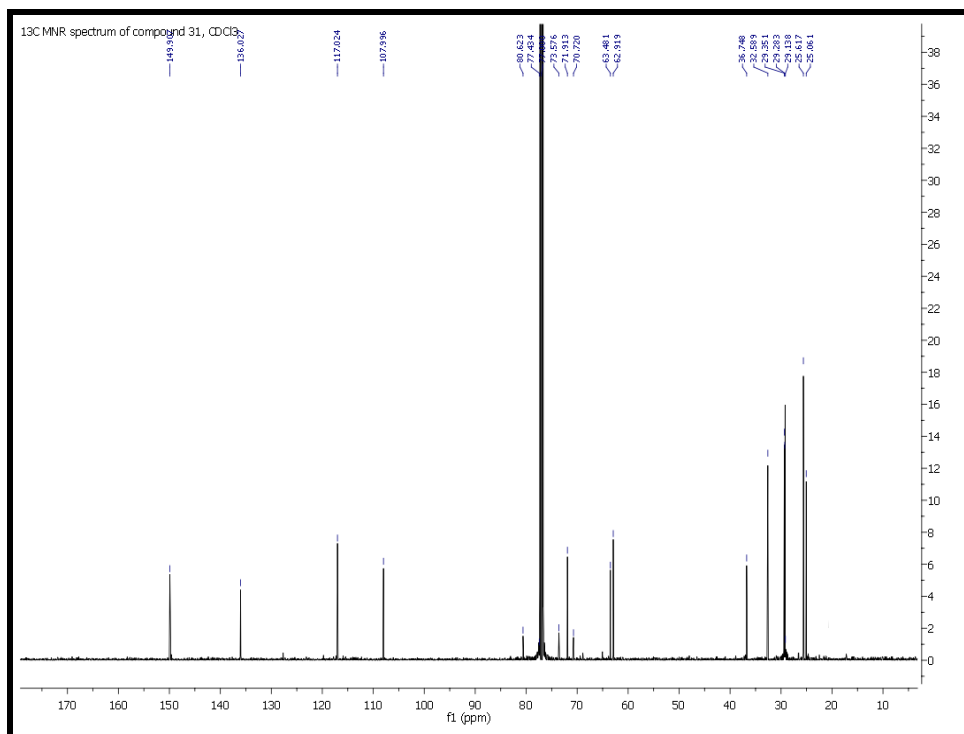
Fig. 59: ^{13}C NMR spectrum of compound **31** measured in CDCl$_3$, 100 MHz
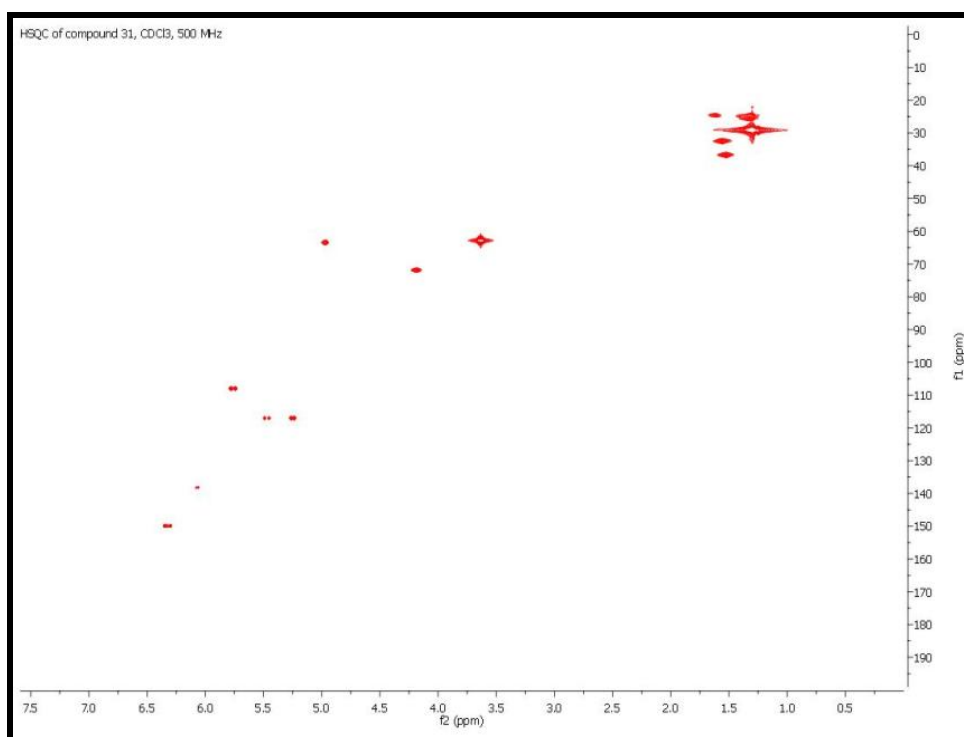
Fig. 60: HSQC spectrum of compound **31** measured in CDCl$_3$, 500 MHz

Analysis of the ^{13}C NMR spectrum showed eighteen signals, of which four quaternary carbons at δ 80.6, 77.4, 73.6 and 70. 7 were characteristic of a diyne (Fig. 59). The HSQC experiment permitted to assign each proton to the corresponding carbon (Fig. 60)

^{1}H-^{1}H COSY spectrum (Fig.61) showed correlations between the vinyl proton at 5.96 ppm and the oxymethine at 4.97 ppm and the terminal methylene protons at 5.48 and 5.26 ppm that, besides the cross-peaks observed in the HMBC spectrum between the methylene protons at δ 5.48 and 5.26 and the carbons at 136.0 and 63.48 ppm and between the oxymethine at 4.97 ppm and the carbons at 136.0, 117.0, 80.6, 70.7 and 73.6 ppm, permitted to establish the partial structure of CH_2=CH-CH(OH)-C≡C-C≡C- (Fig.62). Further HMBC correlations observed from the proton at δ 5.78 to 77.4, 73.6, 149.9 and 71.9 ppm, and from the oxymethine at δ 4.19 to 149.9, 108.0, 36.7 and 25.1 ppm, located the olefinic protons at 6.33 and 5.78 ppm at C-10 and C-11, respectively and the secondary alcoholic group at 4.19 ppm, at C-9.
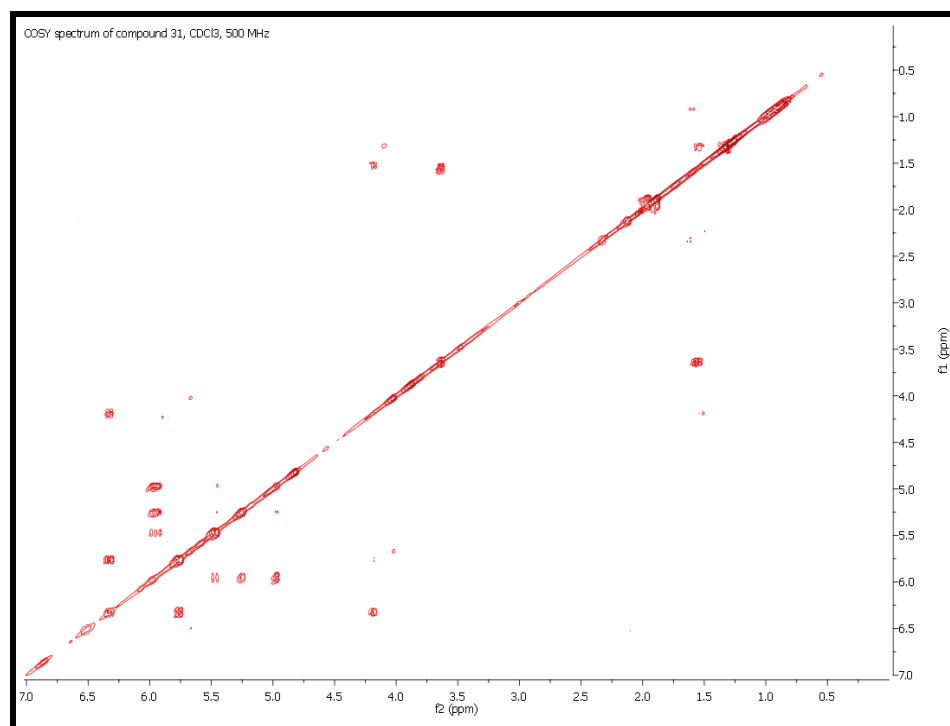
Fig. 61: COSY spectrum of compound **31** measured in CDCl₃, 500 MHz
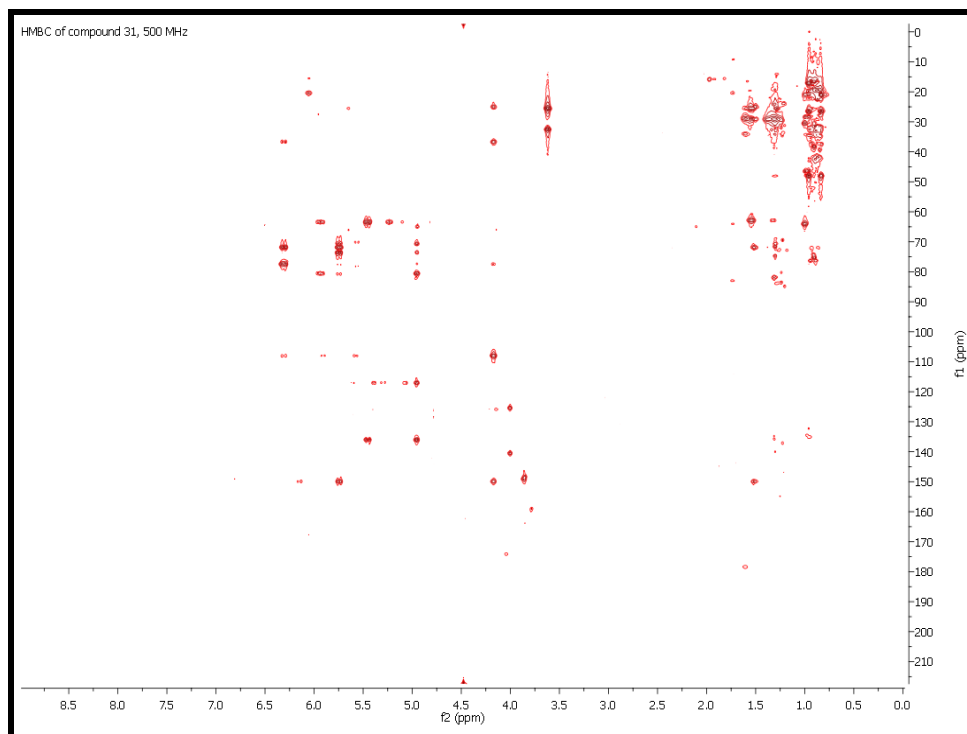
Fig. 62: HMBC spectrum of compound **31** measured in, CDCl₃, 500 MHz

The geometry at the double bond at C-10 was clearly *trans* according with the coupling constant between H-10 and H-11 ($J_{10,11}$ = 16 Hz). In the ¹H NMR spectrum of compound **31** the absence of a methyl group and the cross-peaks observed in the HMBC spectrum between the oxymethylene protons at δ 3.64 (δ_C 62.9) and C-2 (δ_C 32.6) and C-3 (δ_C 25.6) fixed the primary alcohol at C-1 (Fig. 62). The absolute configuration of compound **31** could not be determined by NMR experiments. An attempt to assign the configuration at C-9 and C-16 by Mosher's method failed because the instability of the molecule. DQF-COSY and HMBC experiments allowed the complete assignment of all signals and the identification of compound **31** as *trans*-10,17-octadecadien-12,14-diyne-1,9,16-triol. Compound **31** is a new molecule, and it was named as fruticotriol.

Table 10. ^1H and ^{13}C NMR data of compound **31**

Position	δ_C, Multiplicity	δ_H, Multiplicity [a]
	Compound 31	
1	62.9 (t)	3.64 t (7.0)
2	32.6 (t)	1.55, m
3	25.6b (t)	1.29, m
4	29.4b (t)	1.29, m
5	29.3b (t)	1.29, m
6	29.1 (t)	1.29, m
7	25.1 (t)	1.29, m
8	36.7 (t)	1.54, m
9	71.9 (d)	4.19, dt (6.5)
10	149.9 (d)	6.33, dd, (5.5, 16)
11	108.0 (d)	5.78, d, (16)
12	77.4 (s)	
13	73.6 (s)	
14	70.7 (s)	
15	80.6 (s)	
16	63.5 (d)	4.97, d, (5.0)
17	136.0 (d)	5.96, ddd, (17.5, 10.0, 5.0)
18	117.0 (t)	Ha : 5.48, d,(17.5) Hb : 5.26, d, (10.0)

[a]Value of *J* (Hz) in bracket; [b]These values may be interchangeable

Compound **31** (fruticotriol)
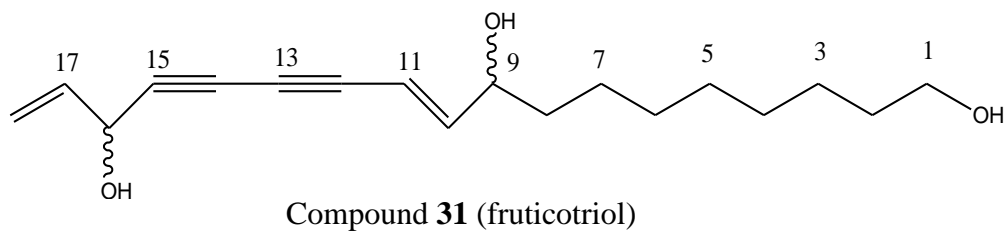
Compound 32

Compound **32** was identified as *cis*-9,17-octadecadiene-12,14-diyne-1,16-diol by 1D (^{1}H and ^{13}C NMR), and 2D NMR (DQF-COSY, HSQC, HMBC) spectroscopy, mass spectrometry (ESI MS) and optical rotation and by comparison with literature data [249].
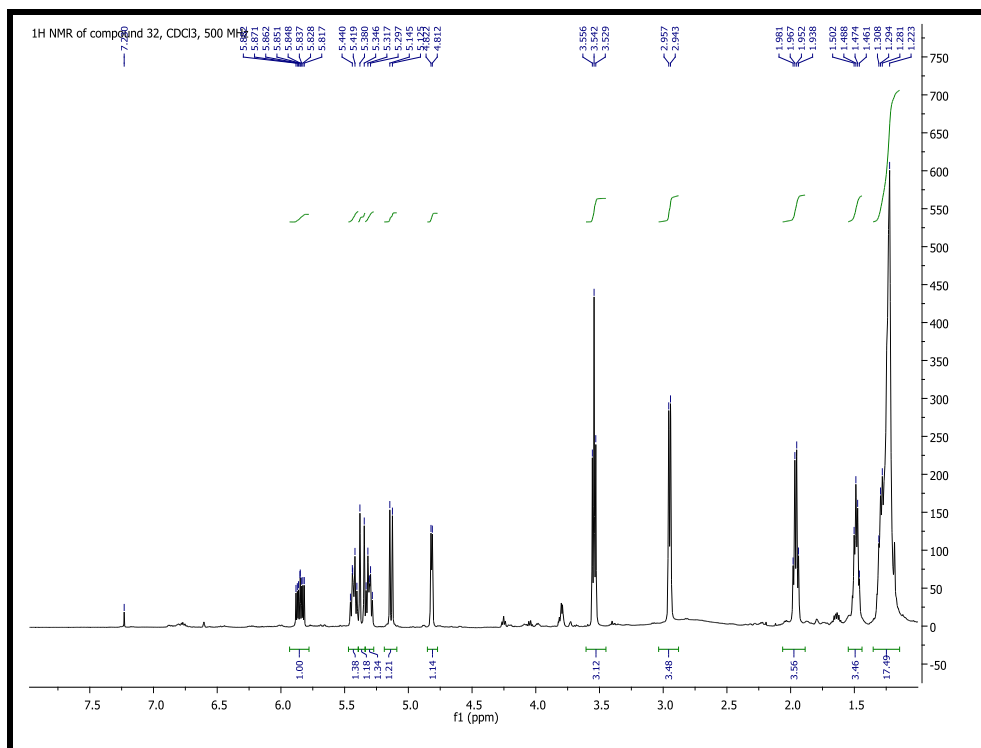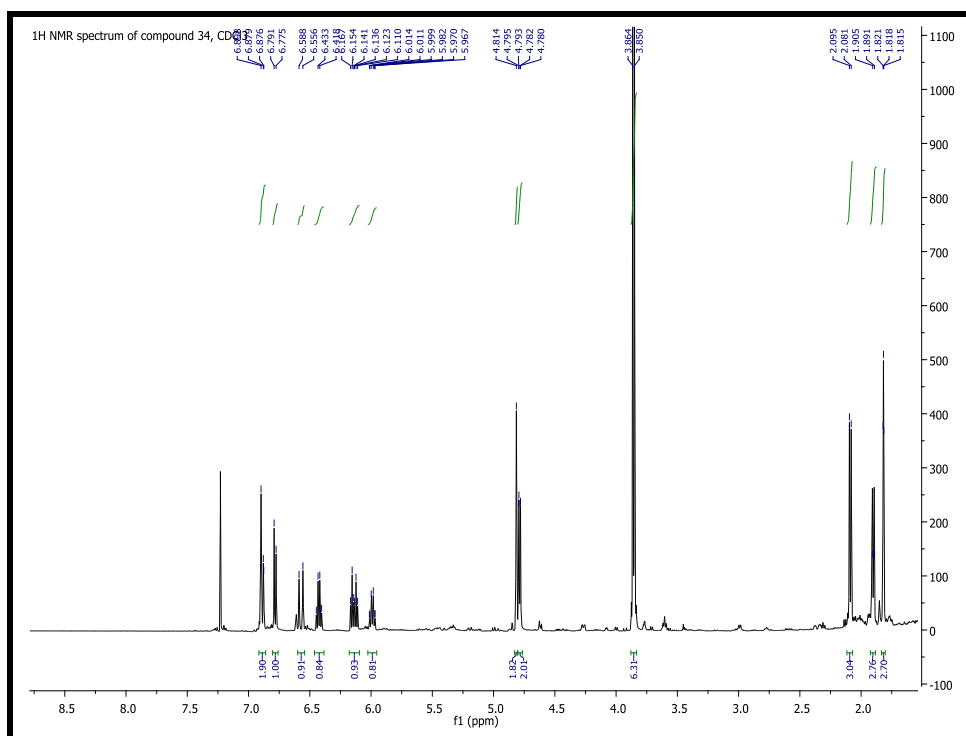

**Fig. 63:** ^{1}H NMR spectrum of compound **32** measured in CDCl$_3$, 500 MHz
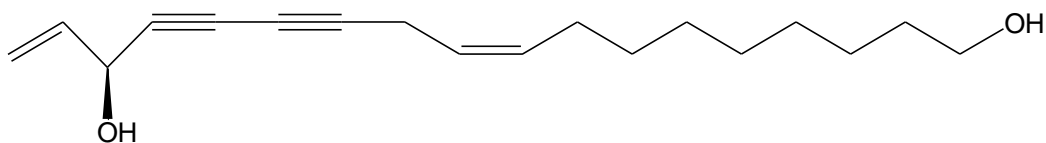
Compound **32**

Compound 33

Compound **33** was identified as (E)-3-(4-methoxyphenyl)-2-propen-1-yl (Z)-2-[(Z)-2-methyl-2-butenoyloxymethyl) butenoate by 1D (^{1}H and ^{13}C NMR), and 2D NMR (DQF-COSY, HSQC, HMBC) spectroscopy, mass spectrometry (ESI MS) and by comparison with literature data [247].^{13}C NMR spectrum of compound **33** is reported in experimental section (fFig. 185).
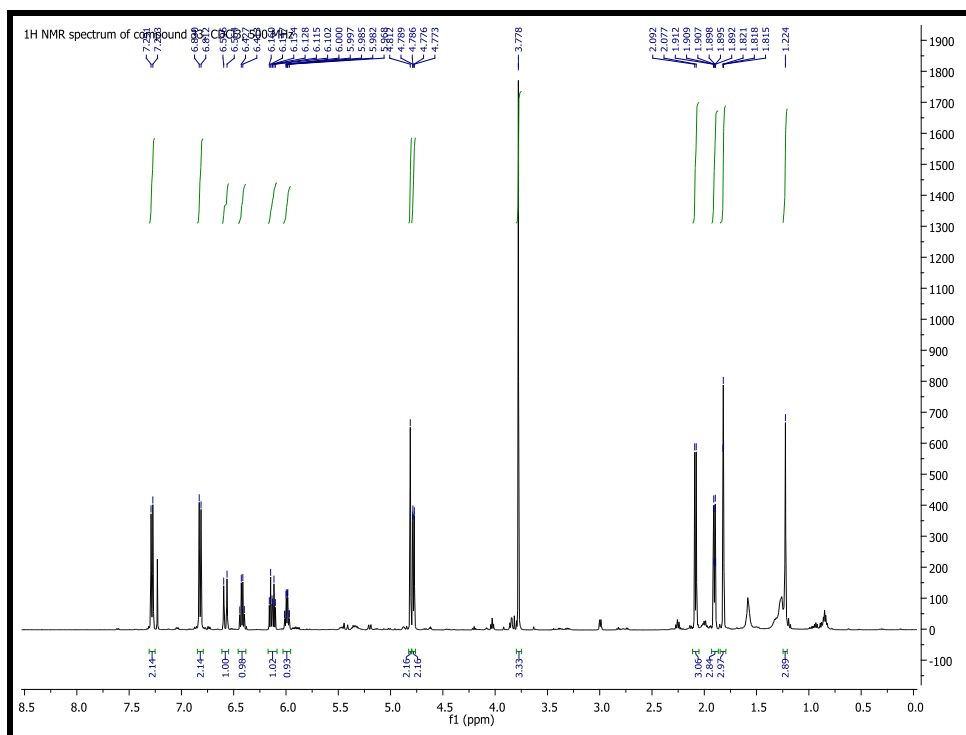
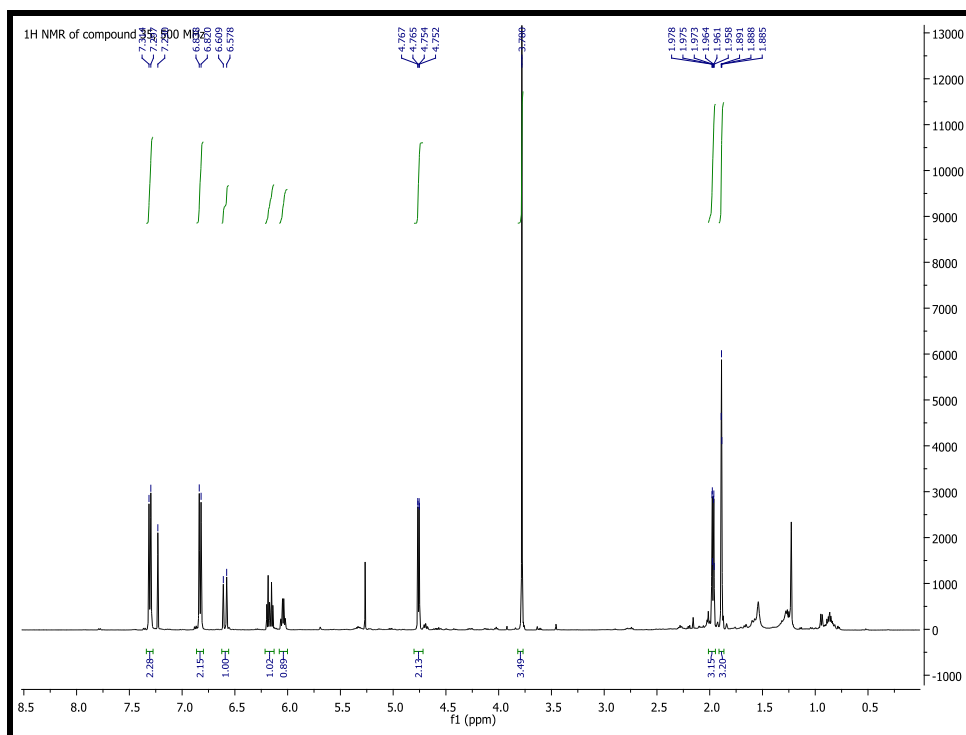**Fig. 64:** ^{1}H NMR spectrum of compound **33** measured in CDCl$_3$, 500 MHz
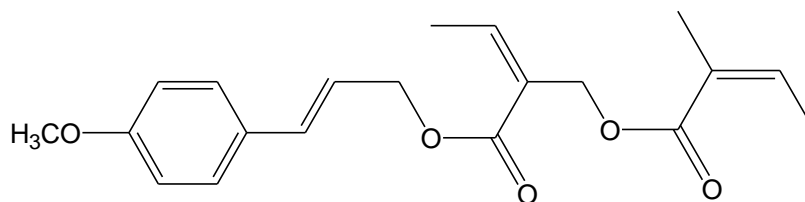
Compound **33**

Compound 34

Compound **34** was identified as (E)-3-(3,4-dimethoxyphenyl)-2-propen-1-yl (Z)-2-[(Z)-2-methyl-2-butenoyloxymethyl)butenoate by 1D (^{1}H and ^{13}C NMR), and 2D NMR (DQF-COSY, HSQC, HMBC) spectroscopy, mass spectrometry (ESI MS) and by comparison with literature data [247]. 1D and 2D NMR spectra of compound **34** are reported in experimental section (Fig. 186-187).
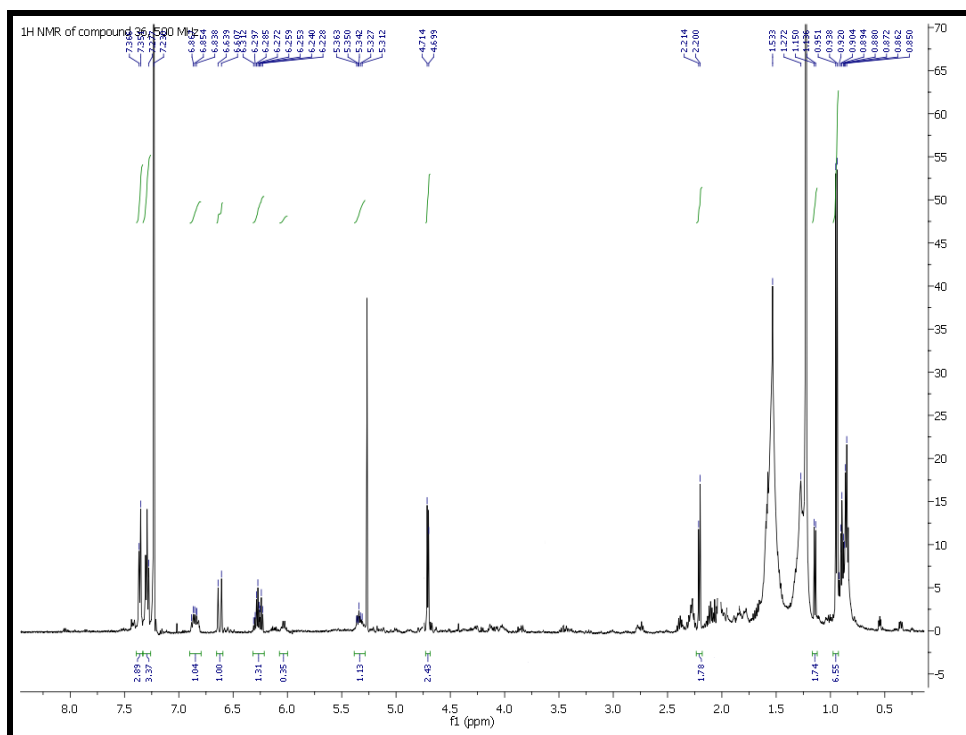

Fig. 65: ^{1}H NMR spectrum of compound **34** measured in, CDCl$_3$, 500 MHz
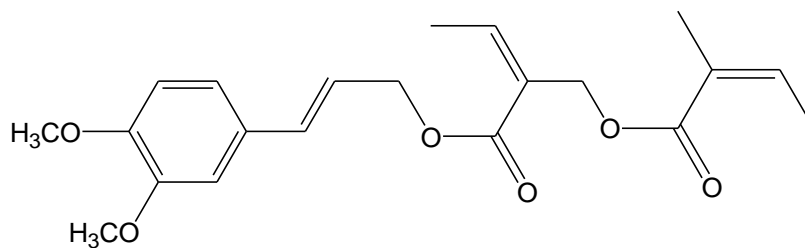
Compound **34**

Compound 35

Compound **35** was identified as 4-*O*-methylcinnamyl angelic acid ester by 1D (^{1}H and ^{13}C NMR), and 2D NMR (DQF-COSY, HSQC, HMBC) spectroscopy, mass spectrometry (ESI MS) and by comparison with literature data [250]. 1D and 2D NMR spectra of compound **35** are reported in experimental section (Fig. 188-190).

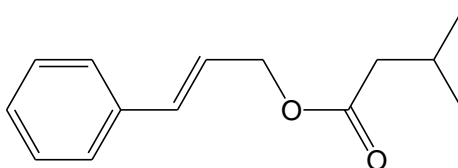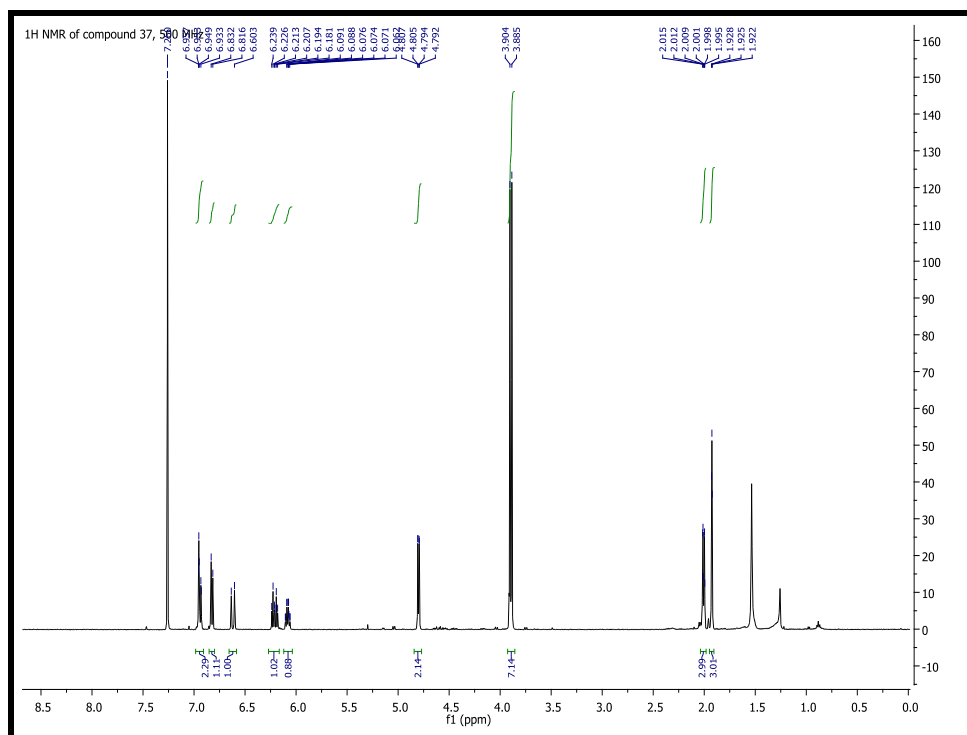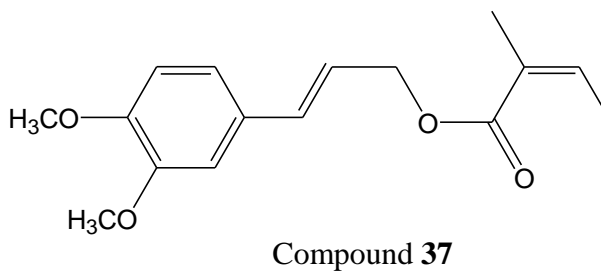**Fig. 66:** ^{1}H NMR spectrum of compound **35** measured in CDCl$_3$, 500 MHz
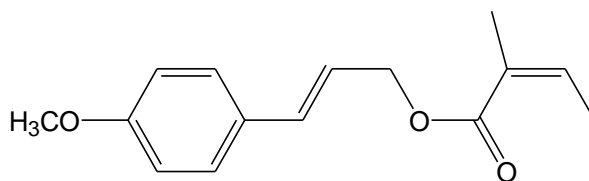
Compound **35**

Compound 36

Compound **36** was identified as cinnamyl isovalerate by 1D (^{1}H and ^{13}C NMR), and 2D NMR (DQF-COSY, HSQC, HMBC) spectroscopy, mass spectrometry (ESI MS) and by comparison with literature data [245]. 2D NMR spectra of compound **36** are reported in experimental section (Fig. 191-193).

Fig. 67: ^{1}H NMR spectrum of compound **36** measured in CDCl$_3$, 500 MHz

Compound **36**

Compound 37

Compound **37** was identified as 4-*O*-methyl-(*E*)-coniferyl angelic acid ester by 1D (¹H and ¹³C NMR), and 2D NMR (DQF-COSY, HSQC, HMBC) spectroscopy, mass spectrometry (ESI MS) and by comparison with literature data [250]. ¹³C NMR spectrum of compound **37** is reported in experimetal section (Fig.194).
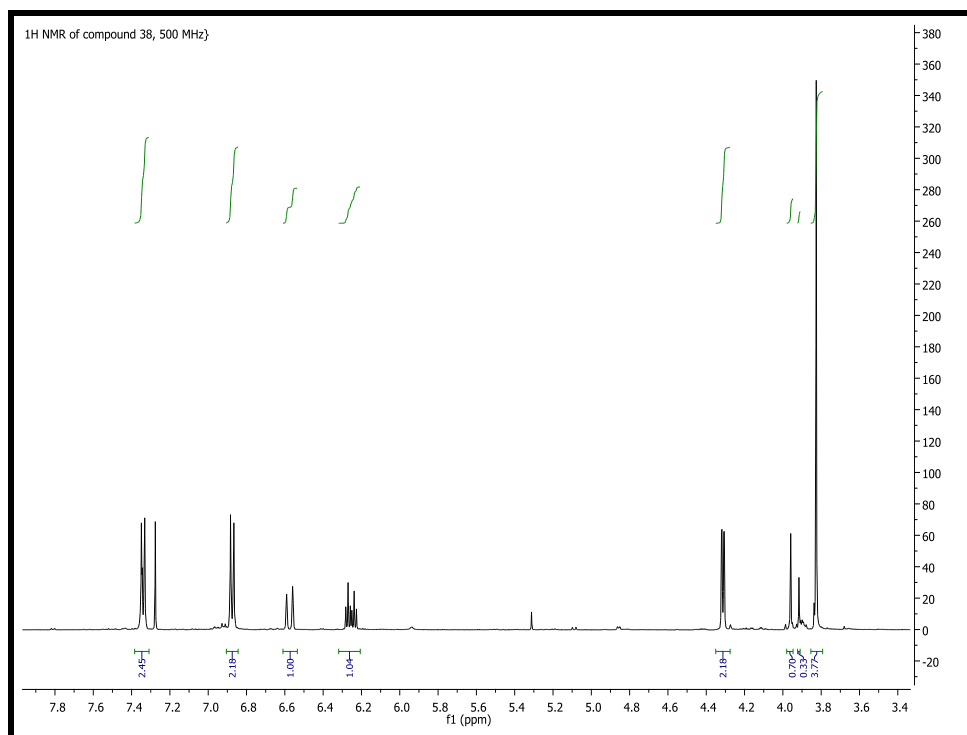

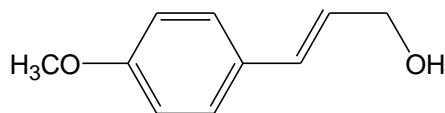**Fig. 68:** ¹H NMR spectrum of compound **37** measured in CDCl₃, 500 MHz

Compound **37**

Compound 38

Compound **38** was identified as 4-methoxycinnamyl alcohol by 1D (^{1}H and ^{13}C NMR), and 2D NMR (DQF-COSY, HSQC, HMBC) spectroscopy, mass spectrometry (ESI MS) and by comparison with literature data [251]. 1D and 2D NMR spectra of compound **38** are reported in experimental section (Fig. 195-197).
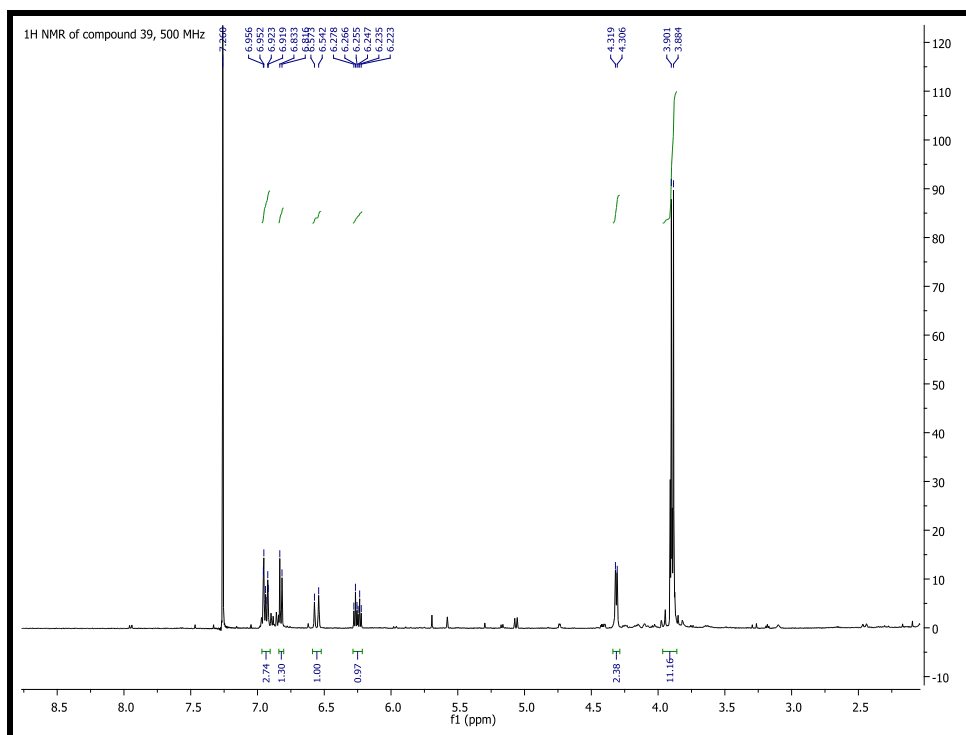

Fig. 69: ^{1}H NMR spectrum of compound **38** measured in CDCl$_3$, 500 MHz

Compound **38**
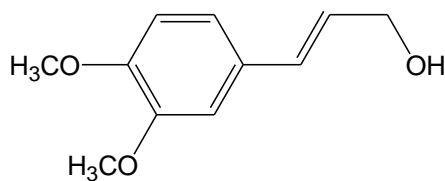
Compound 39

Compound **39** was identified as 3, 4-dimethoxycinnamyl alcohol by 1D (^{1}H and ^{13}C NMR), and 2D NMR (DQF-COSY, HSQC, HMBC) spectroscopy, mass spectrometry (ESI MS) and by comparison with literature data [252].^{13}C NMR spectrum of compound **39** is reported in experimental section (Fig. 198).
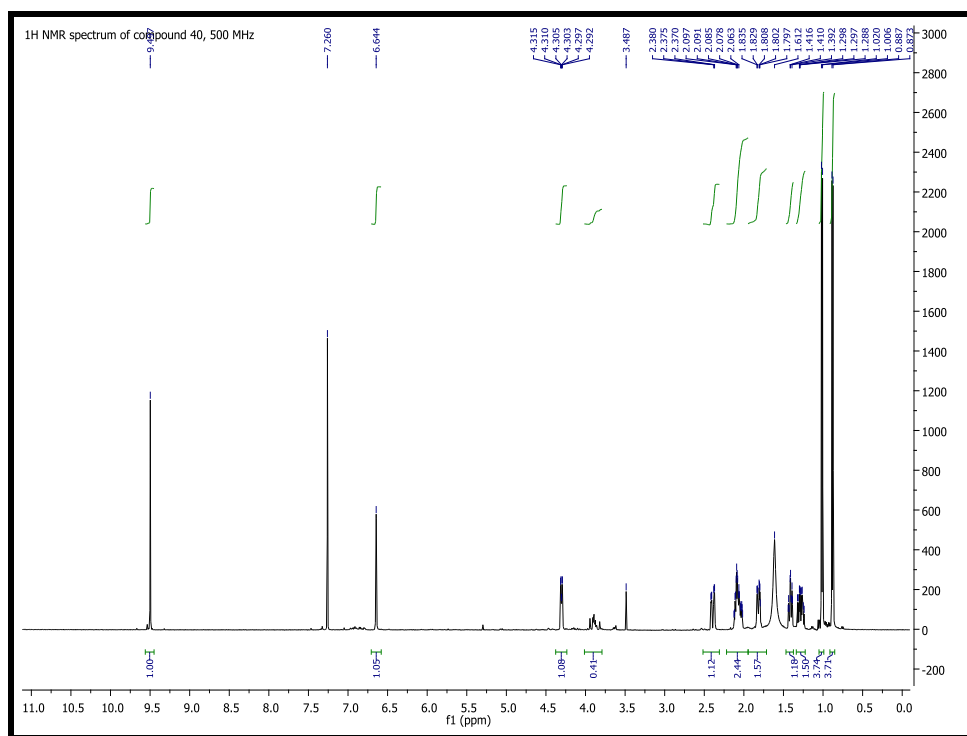

Fig. 70: ^{1}H NMR spectrum of compound **39** measured in CDCl$_3$, 500 MHz

Compound **39**
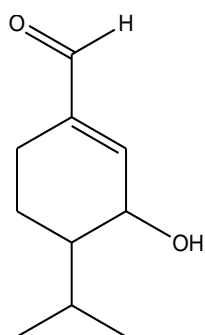
Compound 40

The ^{1}H- and ^{13}C NMR data as well as the 2D NMR experiments (^{1}H-^{1}H COSY, HSQC and HMBC) are in agreement with the structure of eucamalol [253].

Fig. 71: ^{1}H NMR spectrum of compound **40** measured in CDCl$_3$, 500 MHz,

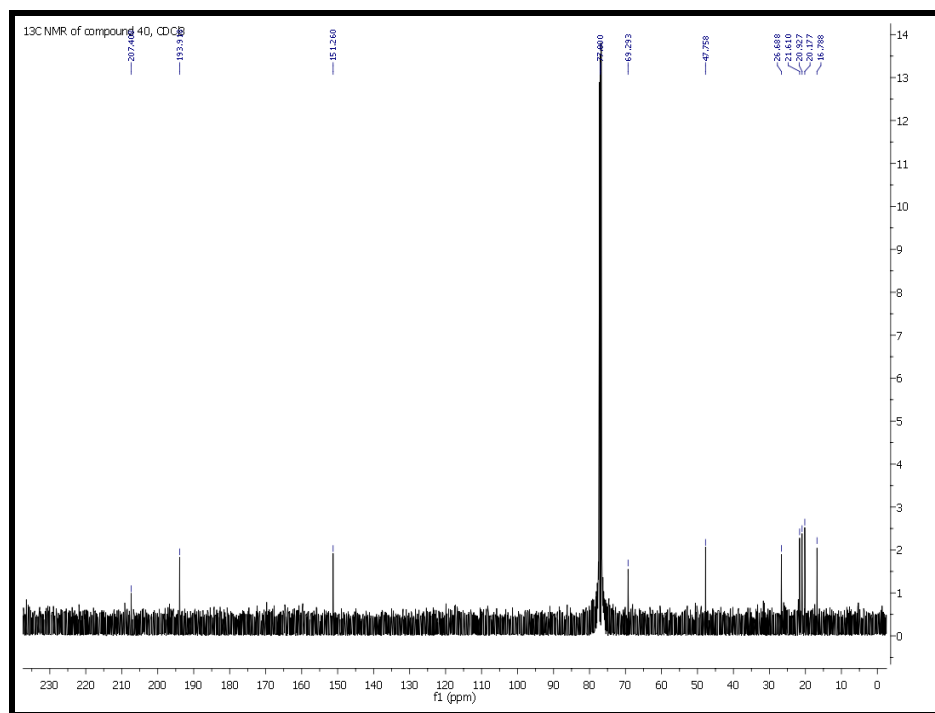Structure of Eucamalol

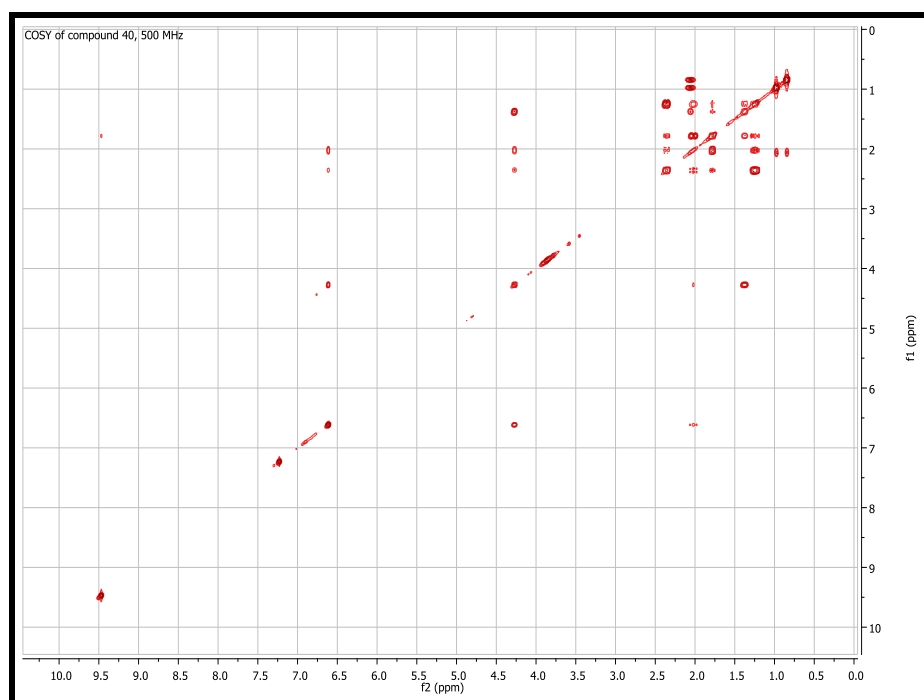**Fig. 72:** ^{13}C NMR spectrum of compound **40** measured in, CDCl$_3$, 100 MHz

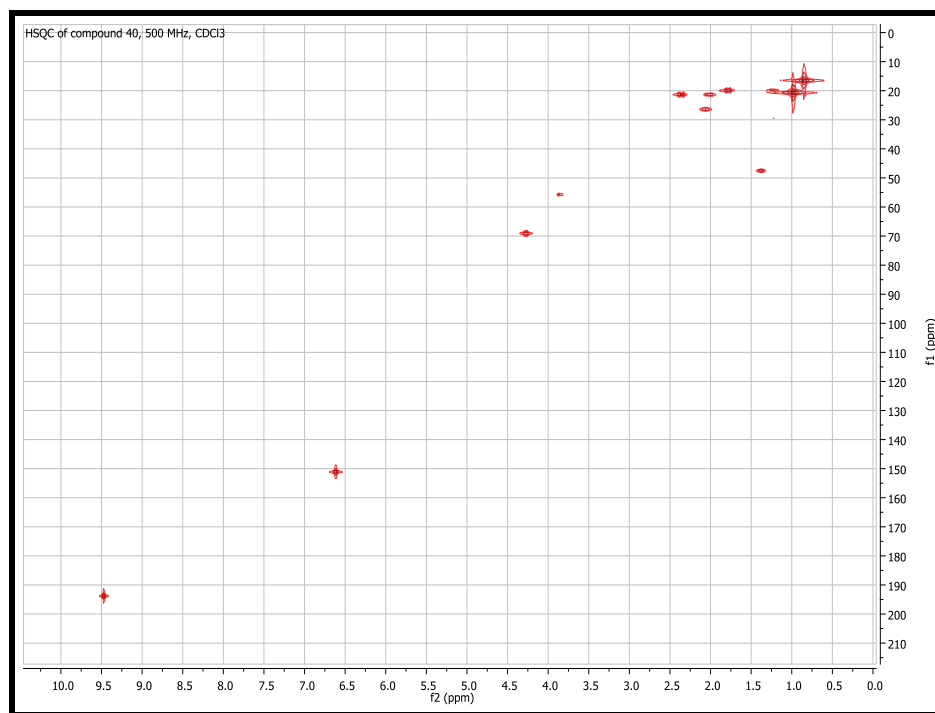**Fig. 73:** COSY spectrum of compound **40** measured in, CDCl$_3$, 500 MHz

Fig. 74: HSQC spectrum of compound **40** measured in CDCl$_3$, 500 MHz
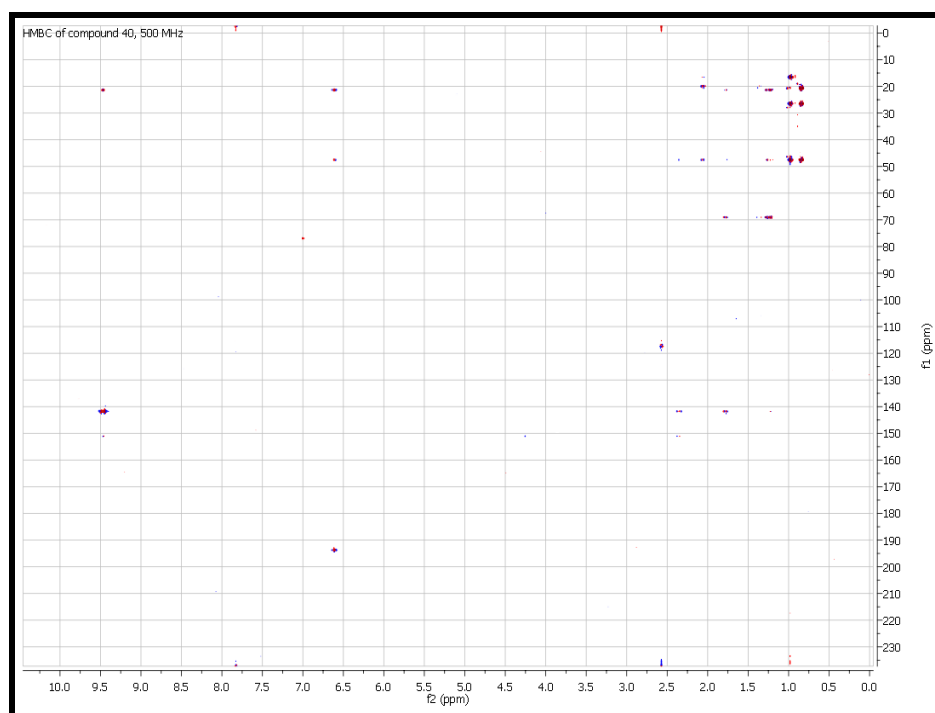
Fig. 75: HMBC spectrum of compound **40,** measured in CDCl$_3$, 500 MHz

The $J_{1,6}$ value (9 Hz) between the proton at δ 4.27 (H-1) and the proton at δ 1.38 (H-6) showed an axial-axial coupling suggesting a *trans* disposition of the hydroxyl and isopropyl groups. The relative stereochemistry at C-1 and C-6 was also confirmed by ROESY experiments showing a very weak cross-peak between these two protons (Fig.76A).
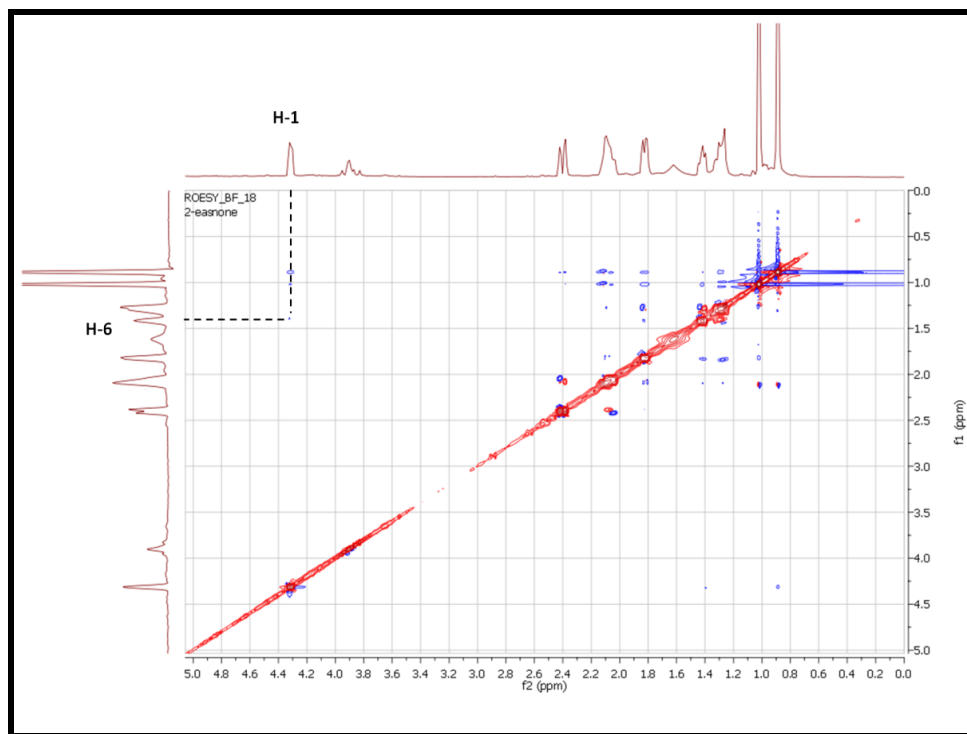
Fig. 76A: ROESY spectrum of compound **40**, measured in CDCl$_3$, 500 MHz

As consequence, two stereoisomers (A and B) are congruent with the experimental data.
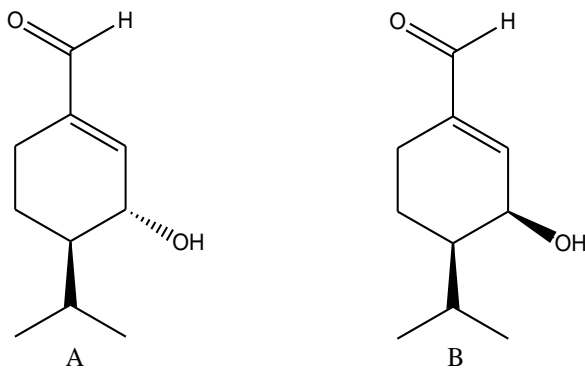
Compound **40** showed a molecular ion peak at *m/z* 168.2, recorded on GC coupled with mass detector (GC-MS), confirming the molecular weight accounting for elemental composition of $C_{10}H_{16}O_2$ (Fig. 76 B).
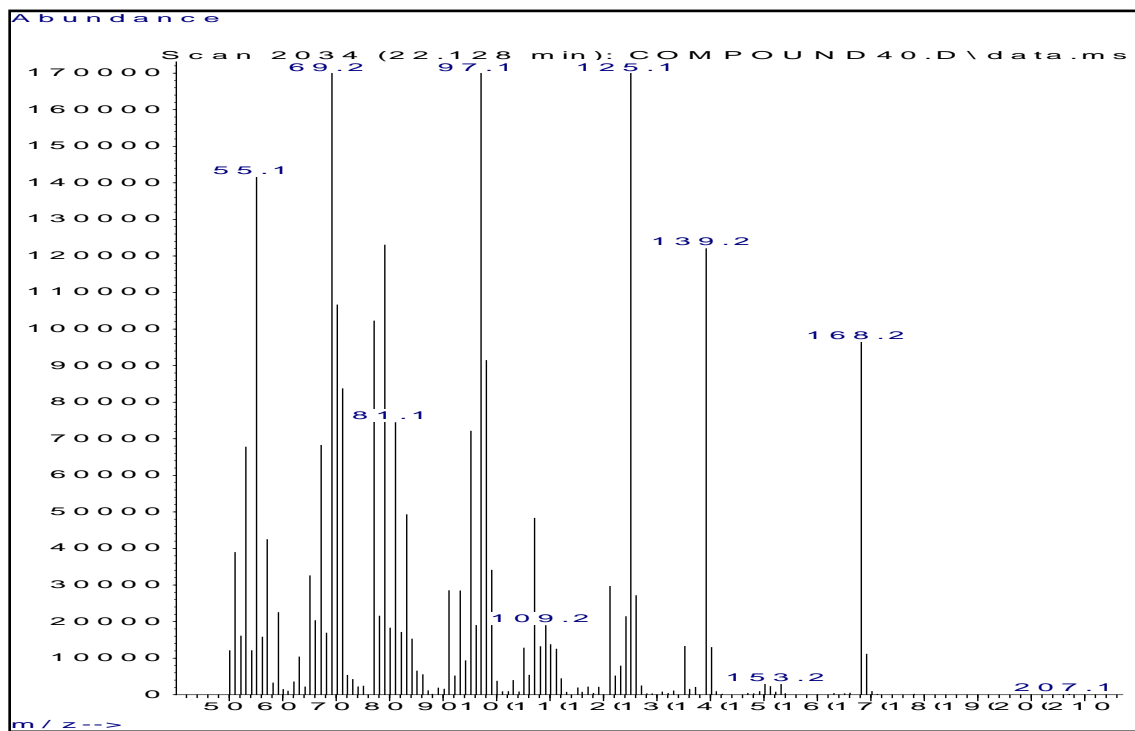
Fig. 76 B: Mass spectrum of compound **40**

Satoh *et al*. [253] reported for the synthesized (+)-eucamalol, possessing a *trans* disposition, an absolute configuration 1*R*, 6*R* with a specific optical rotation $[\alpha]^{25}_D$ + 14.1° whereas its epimer, (-)-1-*epi*-Eucamalol, showed a specific rotation of -234.6°.

1R,6R (+)-Eucamalol
[alfa] = + 14.1°

(-)-1-epi-Eucamalol
[alfa] = - 234.6°
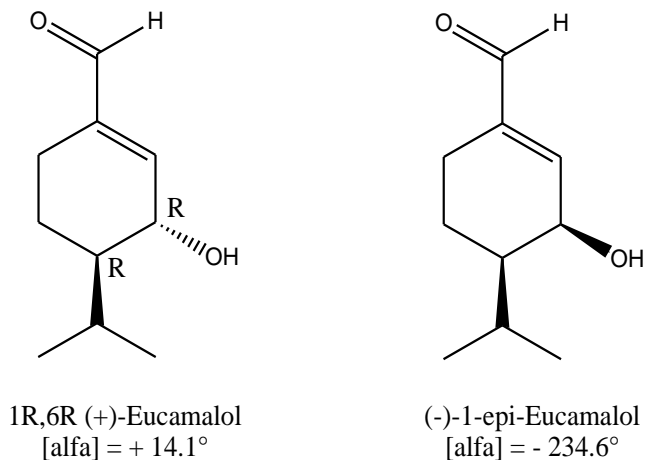
Since for compound **40** we have found a *trans* disposition for H-1 and H-6 and an optical rotation of -17.0°, compared with (+)-eucamalol, it must have an absolute configuration 1*S*, 6*S* and thus compound **40** is 1*S*,6*S*-(-)-3-formyl-6-isopropyl-2-cyclohexen-1-ol. Compound **40** is a new natural compound and we named (-)-eucamanol.
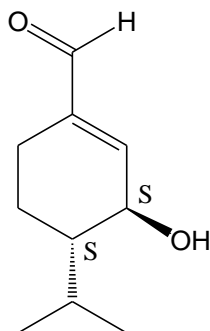
Compound (**40**) [(-)-eucamanol (1*S*,6*S*-(-)-3-formyl-6-isopropyl-2-cyclohexen-1-ol)]

5.3.4 Anti-Rhinovirus activity

The cytotoxicity against the HeLA cells and the anti-Rhinovirus (HRV 39 and HRV 14) activity of all the isolated compounds are reported in Table 11.

Among the phenylpropanoids, the most active was compound **34** with a EC_{50} of 0.9 µg/ml against HRV 39 and moderate cytotoxicity versus HeLa cells (7.6 µg/ml). The SI was 8.4.

In compound **34** the substitution of the methoxy group at C-3 position of the phenyl ring with a hydrogen, as in compound **33**, annulled the activity ($EC_{50} > 7.6$ µg/ml) and increased the cytotoxicity.

The replacement at the same time of the angeloyl and 3-methoxy groups led to a reduced activity (~ 10 fold). The ester functionality seemed essential for the antiviral activity as compounds **38** and **39** are completely inactive.

A 3,4-dimethoxyphenyl ring and an ester function were necessary but not sufficent since **37**, containing a shorter alkyl chain respect to **34**, was not able to inhibit the replication of HRV_S.

The polyacetylene **32** was the most active inhibitor of HRV-39 replication with a EC_{50} of 0.5 µg/ml but the cytotoxicity was more high (4 µg/ml) with respect to **34**, although the SI was comparable.

The new polyacetylene **31** was not able to inhibit the replication of both HRV serotypes probably due to a more hydrophilicity and/or to the different double bond geometry when compared to compound **32**.

Interestingly, the compounds are able to inhibit only HRV-39 indicating a probable selective capsid-binding towards the group A strain.

Table 11: Cytotoxic and anti-Rhinovirus activity of compounds **31**-**40**

| Compound	[a]CC$_{50}$ μg/ml	[a]EC$_{50}$ μg/ml	[a]EC$_{50}$ μg/ml (SI[c])
		HRV14[b]	HRV39[b]
31	31±7.5	>31	>31
32	4±0.7	>4	0.5 ±0.02 (**SI=8**)
33	12.5±2.1	>12.5	>12.5
34	7.6±1.8	>7.6	0.9±0.04 (**SI=8.4**)
35	61±1.5	>61	7.6±0.9 (**SI=8.0**)
36	31± 2.2	>31	>31
37	125±31	>125	>125
38	31±1.5	>31	>31
39	31±2.5	>31	>31
40	8±0.7	>8	>8
Pirodavir	3.1±0.1	0.02±0.005	0.006±0.0001

[a]CC$_{50}$: cytotoxic concentration 50%; EC$_{50}$: Effective concentration 50%

[b]Viruses HRV14: group B; HRV39: group A; [c]SI: Selective index= CC$_{50}$/ EC$_{50}$

In very recent works [254,255] it has been reported a series of structure-based guided synthesized compound able to inhibit the replication of HRV-14 (group B) but not HRV-2

(group A). Molecular modeling studies also demonstrated that these compounds were able to bind into the pocket the canyon of the HRV-14 VP1 protein.

Compound **34** showed remarkable similarities with the synthesized compounds but, interestingly, our 3,4-dimethoxybenzene derivative was not active towards group B but specific to group A serotypes. These differences could be explained by a diverse aminoacid composition and shape of the two Rhinovirus groups. On the basis of these findings, we can assume that also compounds **34** and **35** could be HRV capsid inhibitors.
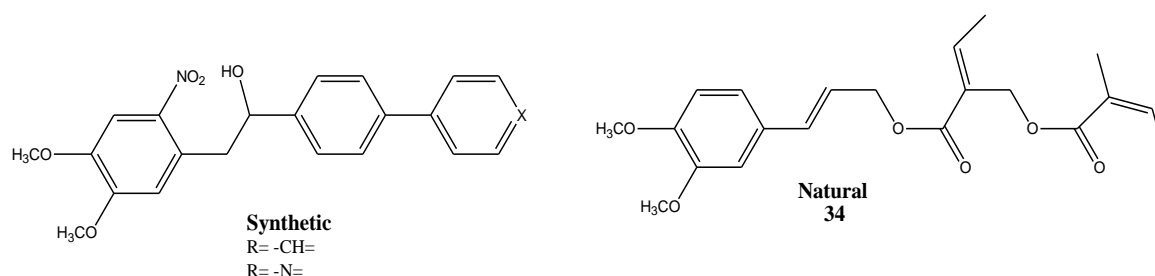

Structural comparison between the compounds isolated from *B. fruticosum* and synthetic derivatives.

5.3.5 Mechanism of Action of compound 34

In order to elucidate the mechanism of action of the most active and stable compound, its antiviral activity on the inhibition of HRV 39 replication under one-step growth conditions was evaluated. Compound **32**, even active, was not tested due to its chemical instability. Fig.77 shows the effect of varying the time of addition of compound **34** (5 µg/ml) on the inhibition of HRV 39 replication under one-step growth conditions. Pirodavir (5 µg/ml) was used as reference molecule. Virus yield was determined by plaque assay after 24-36 h of incubation at 33°C. The treatment of cells with compound **34** prior to infection reduced by 100% of the virus yield, suggesting an ability of **34** to adsorb to the cell surface in a suitable position to prevent infection. Almost the same level of inhibition (90%) was observed when compound **34** was added to cells together with the virus and maintained until the end of HRV 39 multiplication. This behaviour is quite similar to that expressed by Pirodavir, and means that **34** is an antiviral molecule which

exerts its activity in the early phases of viral replication and behaves as a capsid binder towards HRV 39. In contrast with Pirodavir, addition of **34** to the infected HeLa cells after 1h post binding still resulted in a strong reduction in virus yield (78%). Addition of **34** to the infected culture medium after 2-3 h post binding resulted less effective (65% and 50% reduction, respectively) but still significant. The remarkable inhibitory effect of compound **34** when added after virus binding (1-3 h) strongly suggested the capability for compound **34** to enter the host cells and to act with a further mode of action probably based on the uncoating of viral genome.
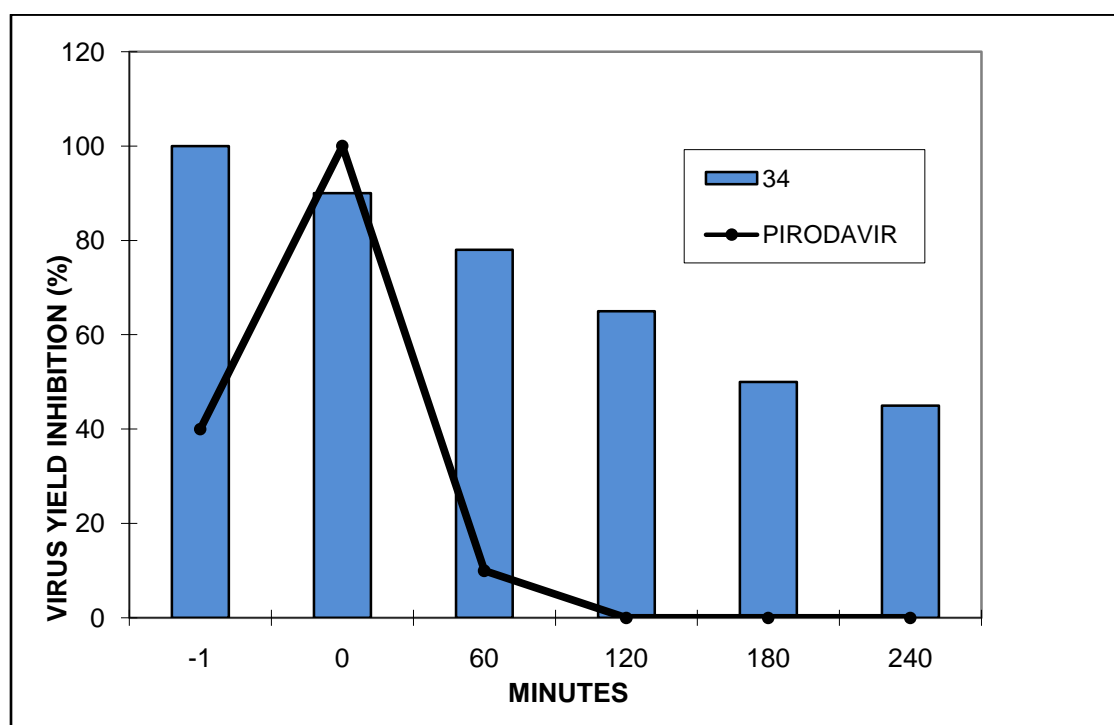
Fig.77:. Effect of addition of **34** and pirodavir at different times during HRV 39 one-step growth cycle in HeLa cells. Compound **34** and Pirodavir were used at a concentration of 5 µg/ml. Compounds were added prior to (-1h), at the time of (0h), or after viral infection (1-4h) at indicated time points and virus yield inhibition (%) was determined by plaque assay.

5.4 *Withania somnifera*

5.4.1 Extraction and isolation of secondary metabolites

20 g of of *W. somnifera* roots MeOH extract were dissolved in DCM. The DCM extract (1.2 g), rich in withanolides, was purified by coloumn chromatography (silica gel and sephadex LH 20) and semi-preparative HPLC (normal phase (NP) or reverse phase (RP).

Two new withanolides, Withasomniferolide A (**41**) and Withasomniferolide B (**42**), besides the known Withanolide B (**47**), Withanolide A (**48**), and Withaferin A (**49**) were isolated. A dimer of ferulic acid (**43**) as well as a mixture of three ferulic acid esters (**44-46**) were also obtained (Fig. 78). .

As far as we know this is the first report from *W. somnnifera* of withanolides with a A/B ring system represented by a 8,9-dihydronapthalene-1-one moiety (withasomniferolides A and B).

A series of ferulic acid esters **(43-46)** was isolated. Although compound **43** has been reported by synthesis [256], this is the first report from natural sources and the esters of ferulic acid **(44-46)** have been isolated for the first time from *W. somnifera*.

Withanolide B (**47**), Withanolide A (**48**), and Withaferin A (**49**) are the most abundant witanolides in *W. somnifera* roots.
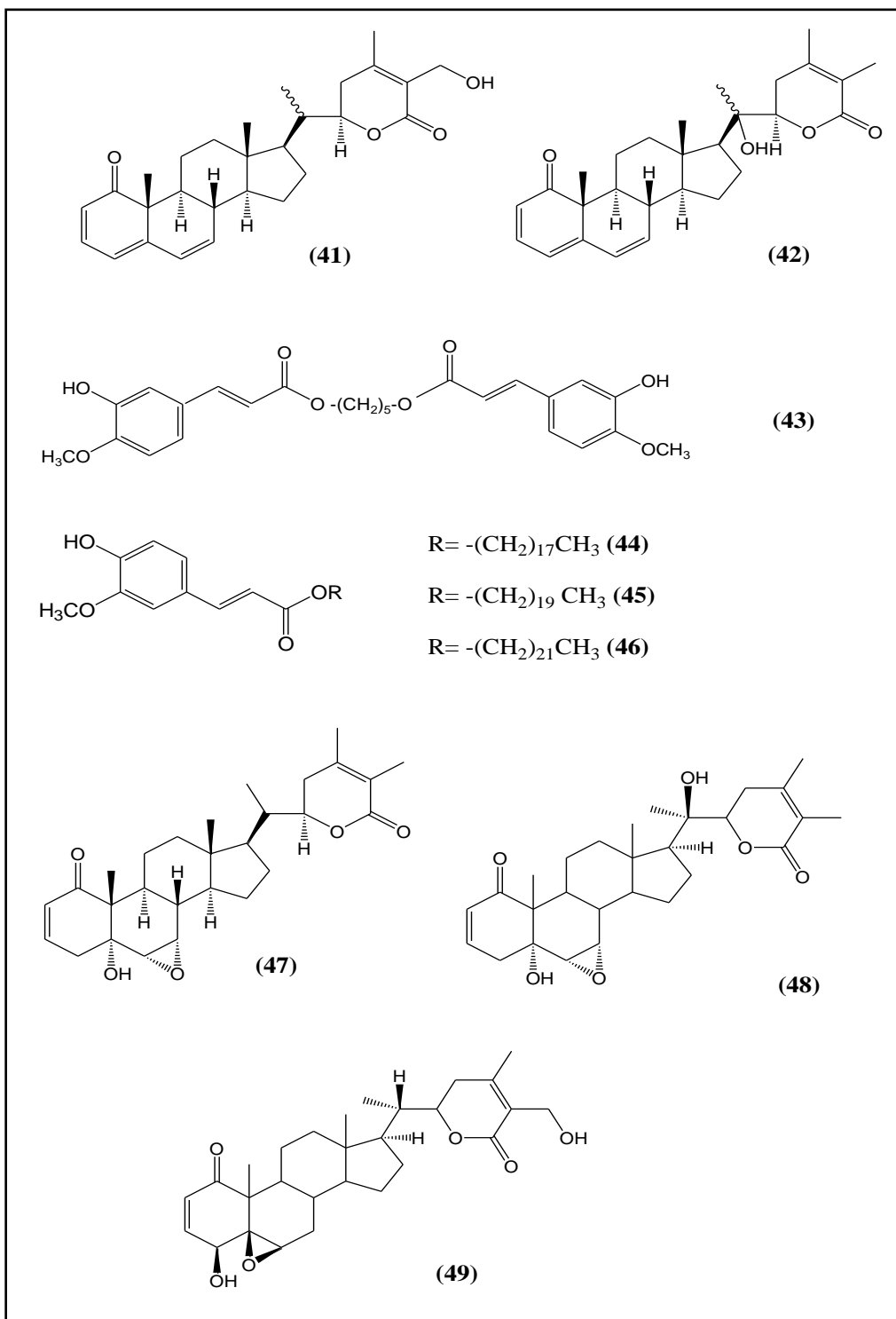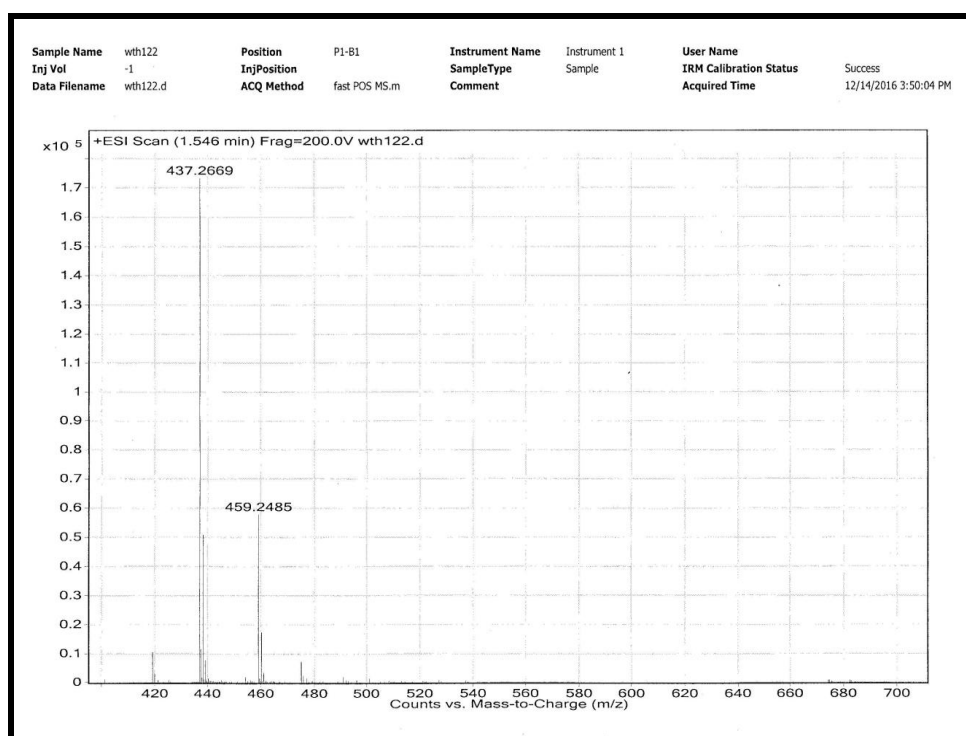
Fig.78: Structures of the isolated compounds from of *W. somnifera*

**5.4.2 Structural elucidation of secondary metabolites from *W. somnifera***

Compound 41

The HR MS of compound **41** showed a molecular ion at *m/z* 437.2669 (calcd. 437.2684) (Fig.79). This molecular mass in combination with ^{1}H and ^{13}C NMR data allowed establishing the molecular formula as $C_{28}H_{36}O_4$. Because of the large number of the overlapped saturated CH_2 and CH signals showed in the ^{1}H NMR spectrum, the structure elucidation of compound **41** resulted rather complicated.

Sample Name	wth122	Position	P1-B1	Instrument Name	Instrument 1	User Name	
Inj Vol	-1	InjPosition		SampleType	Sample	IRM Calibration Status	Success
Data Filename	wth122.d	ACQ Method	fast POS MS.m	Comment		Acquired Time	12/14/2016 3:50:04 PM

Fig.79: HR ESIMS spectrum of compound **41** measured in positive mode

In particular, in this spectrum four methyl groups at 0.786 (3H, s), 1.0 (3H, d, J= 6.5 Hz), 1.231 (3H, s) and 2.009 (3H, s) ppm could be detected besides a group of CH_2 and CH signals between 1 and 2 ppm. In the same spectrum five olefinic protons at 6.930 (1H, dd, J = 10, 2 Hz), 6.111 (1H, dd, J = 10, 2.5 Hz), 5.91 (1H, d, J = 5.5 Hz), 5.89 (1H, d, J = 9.5 Hz) and 5.971 (1H, dd, J = 10, 2 Hz) with an oxymethylene group at δ_H 4.32 (1H, d, J = 12.5 Hz) and 4.35 (1H, d, J = 12.5 Hz) and a oxymethine proton at 4.41 (1H, m) were also present.
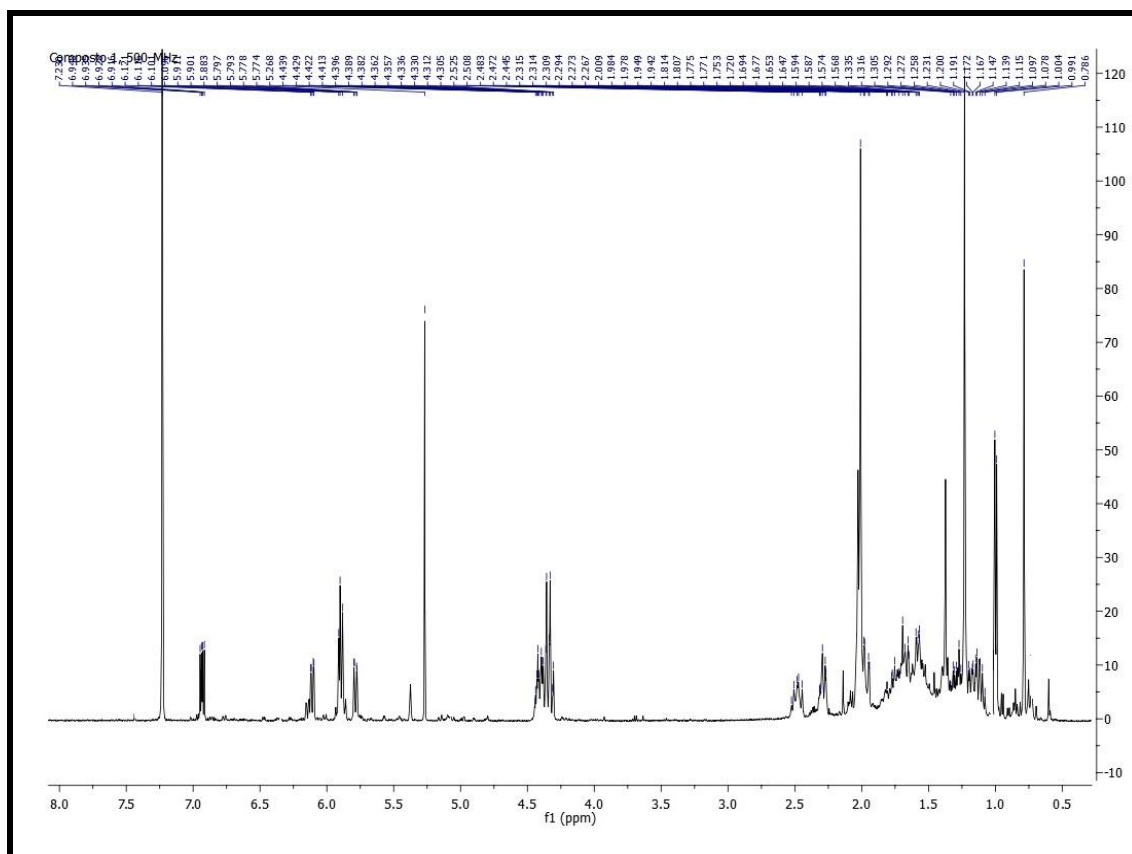
Fig. 80: ^{1}H NMR spectrum of compound **41**, 500 MHz, CDCl$_3$
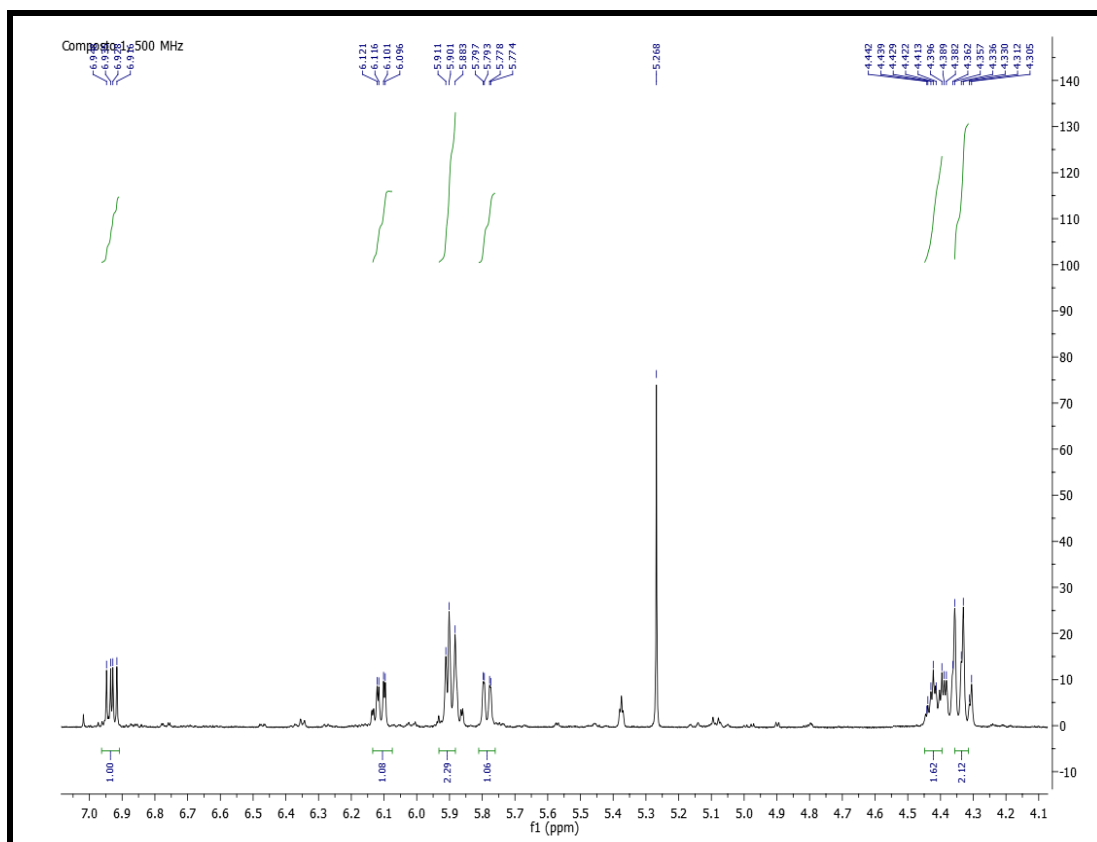
Fig. 81: ^{1}H NMR spectrum (partial) of compound **41**, 500 MHz, CDCl$_3$
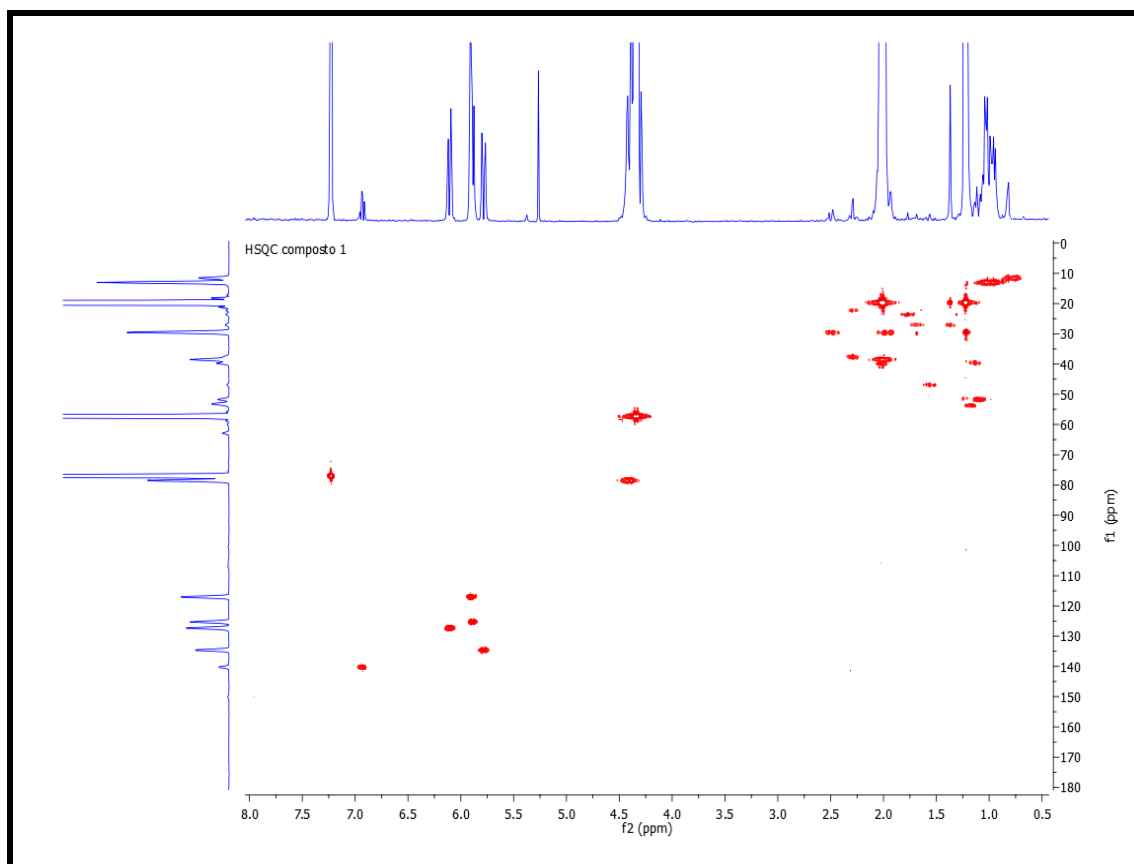
Fig. 82: HSQC spectrum of compound **41**, 500MHz, CDCl$_3$

With the help of HSQC experiment all the above reported protons were assigned to the respective carbons (Fig.82).

In the ^{1}H-^{1}H COSY spectrum (Fig. 83) the proton at 5.91 ppm correlated with the proton at 6.93 ppm which in turn correlated with the proton at 5.89 ppm, while the methyl at 1 ppm showed a cross-peak with the CH at 1.91 ppm.
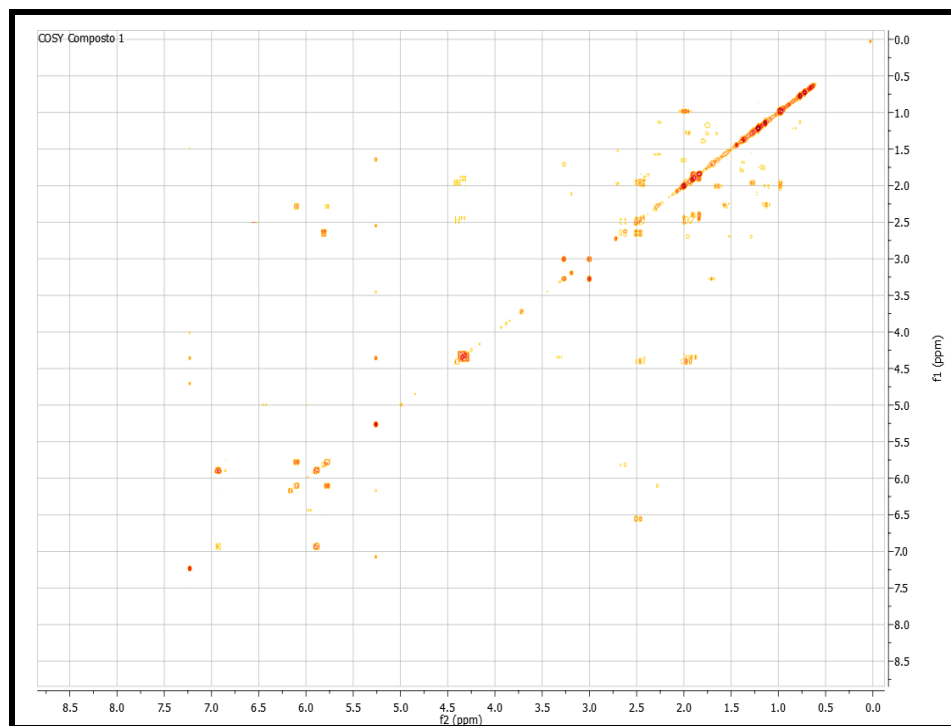
Fig.83: COSY spectrum of compound **41**, 500MHz, CDCl$_3$
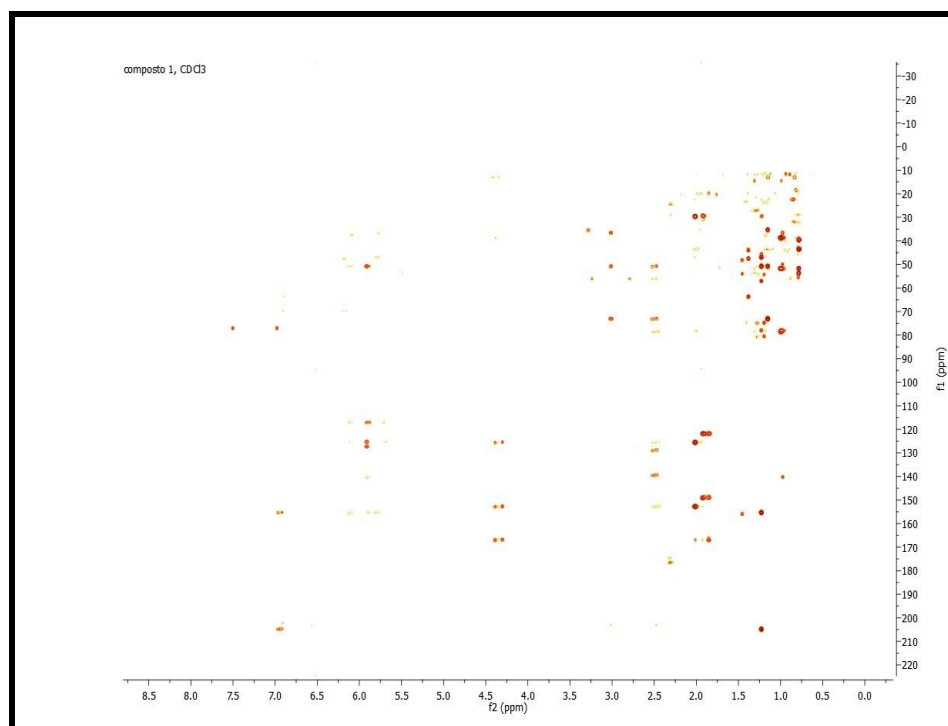
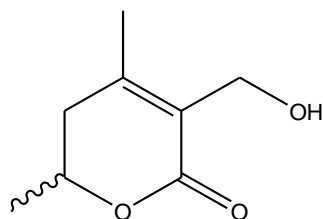**Fig.84:** HMBC spectrum of compound **41**, 500MHz, CDCl$_3$

In the HMBC spectrum (Fig. 84) the long-range correlations between the oxymethylene protons at 4.32 (δ_C: 57.3) and the carbons at δ 166.8, 152.6 and 125.4 ppm and those of the methyl at 2.009 ppm (δ_C: 19.8) with the carbons at δ 166.8, 152.6, 125.4 and 29.6 ppm suggested the presence of a lactone ring characteristic of a withanolide.


Lactone ring identified in compound **41**

In the same experiment it may be noted that the lactone ring is linked to the cyclopentane ring of the withanolide through a **methine** group as shown by the cross-peaks between the methyl at δ 1.0 (d, J = 6.5 Hz) and the carbons at 38.7 (C-20), 51.7 (C-17) and 78.5 (C-22) ppm. Additional correlations between the olefinic proton at 6.93 (δc 140.4) and the carbons at 204.8 (C-1), 155.4 (C-5) and 117.0 (C-4), between the olefinic proton at 6.1 (δc 127.3) and the carbons at 155.4 (C-5), 117.0 (C-4), 50.8 (C-10) and 37.6 (C-8) and between the methyl at δ 0.786 (δc 19.7) and the C-1 (δc 204.8), C-10 (δc 50.8) and C-9 (δc 47.0) permitted to define a 8,9-dihydronapthalene-1-one nucleus of the A and B fused rings.

ROESY experiments (Fig 85) and analyzing scalar ($^3J_{H-H}$) coupling of the protons were used to determine the stereochemistry for most of the molecule. Strong ROESY cross-peaks from H-8 (δ_H 2.80) to H-18 (δ_H 1.231) and H-19 (δ_H 0.786) and absent cross-peak from H-18 to H-17, implying that H-17 was on the other side of the molecule with respect to H-8, H-18 and H-19. The stereochemistry at C-22 was determined as *R*, as the literature indicated that an α-oriented H at C-22 gives rise to $J_{22,23}$ values of between 0.5-7 and 9-13.8 Hz, whereas the β-oriented form exhibited values between 2.5-7 and 2-5 Hz. The observed coupling constants for the proton at C-22 in A (*J* = 3.5 and 13 Hz) fell under the former limits [257]. It was not possible to establish the stereochemistry of C-20 with ROESY experiments because of the free rotation of C-17-C-20 bond.

The detailed study of DQF-COSY, HSQC and HMBC experiments allowed the complete assignment of all signals and the identification of compound **41** as (22R)-1-oxo-27-hydroxywitha-2,4,6-trienolide. Compound **41** is a new molecule and was named withasomniferolide A.
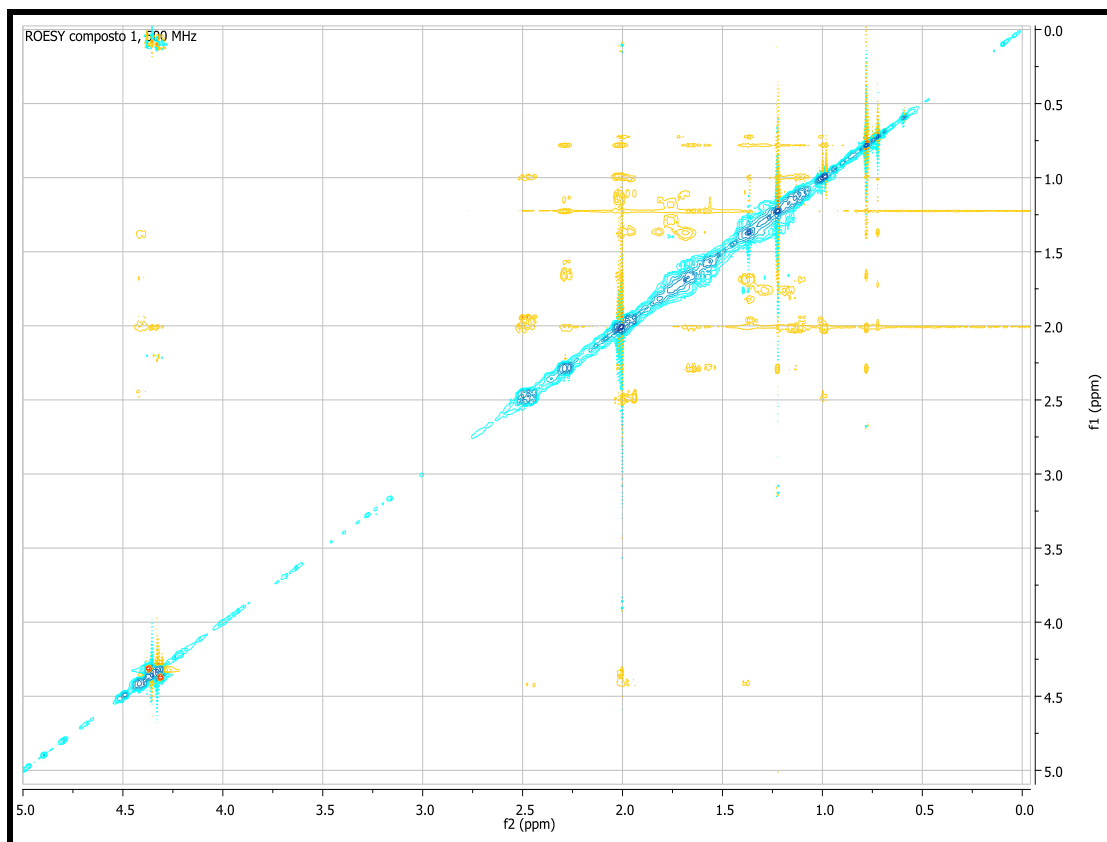
Fig.85: ROESY spectrum of compound **41**, 500MHz, CDCl₃
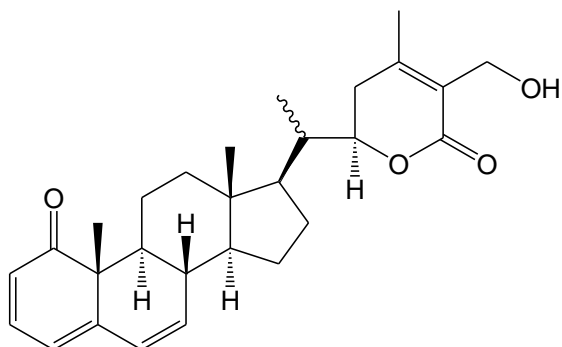
Compound **41** (withasomniferolide A)

Compound 42

Compound **42** showed a pseudomolecular ion peak at *m/z* 437.2683 (calcd. 437.2684) in the HR ESI MS accounting for the elemental composition of $C_{28}H_{36}O_4$.
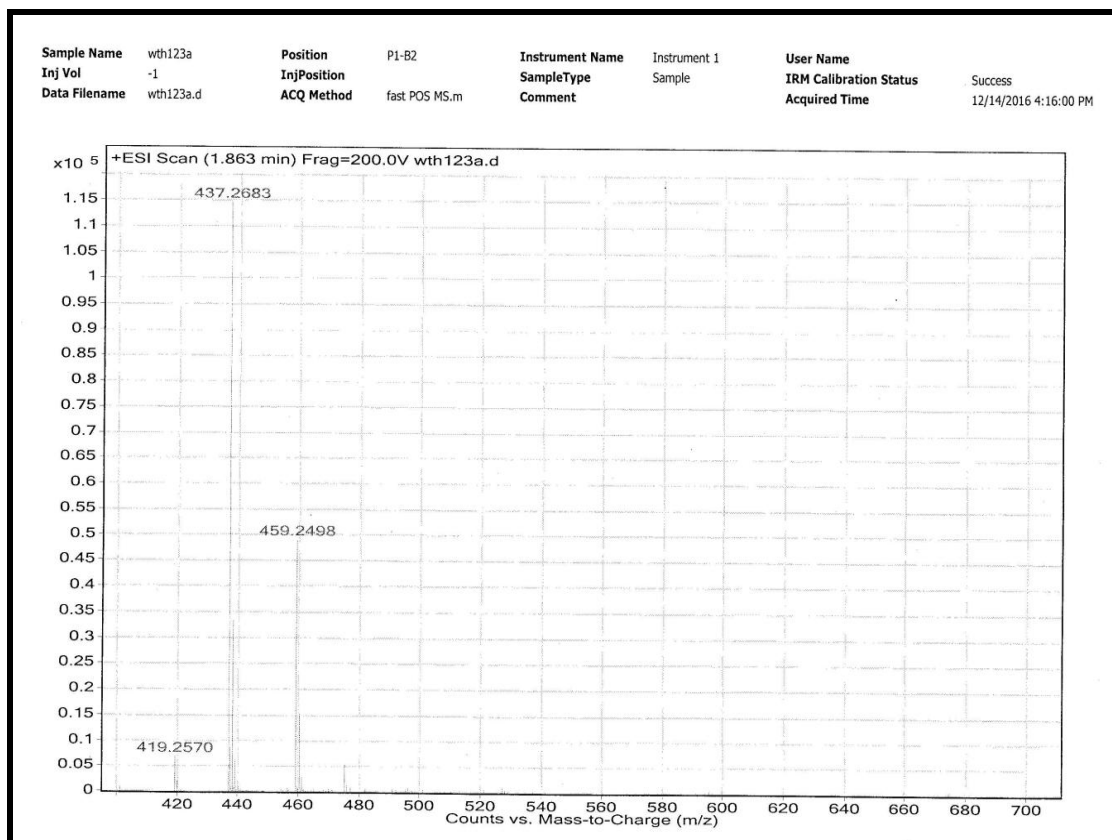
Fig. 86: HR ESIMS spectrum of compound **42** measured in positive mode

The downfield region (5.7< δ_H <7) of the ^{1}H NMR spectrum of compound **42** was superimposable to those of **41**, suggesting the presence of a 8,9-dihydronapthalene-1-one moiety (Fig.87). The major significant differences between the spectrum of **42** with that of **41** was the upfield shift of the oxygenated methine at 4.20 (1H, dd, J = 3.2, 13.2 Hz) ppm and the disappearance of the oxymetylene protons at C-27 (δ_H 4.32 and 4.35 in the spectrum of **41**. Another difference between the two ^{1}H NMR spectra is the number of methyl groups that in those of compound **41** were four and in compound **42** are five.

Fig. 87: ^{1}H NMR spectrum of compound **42**, 500 MHz, CDCl$_3$
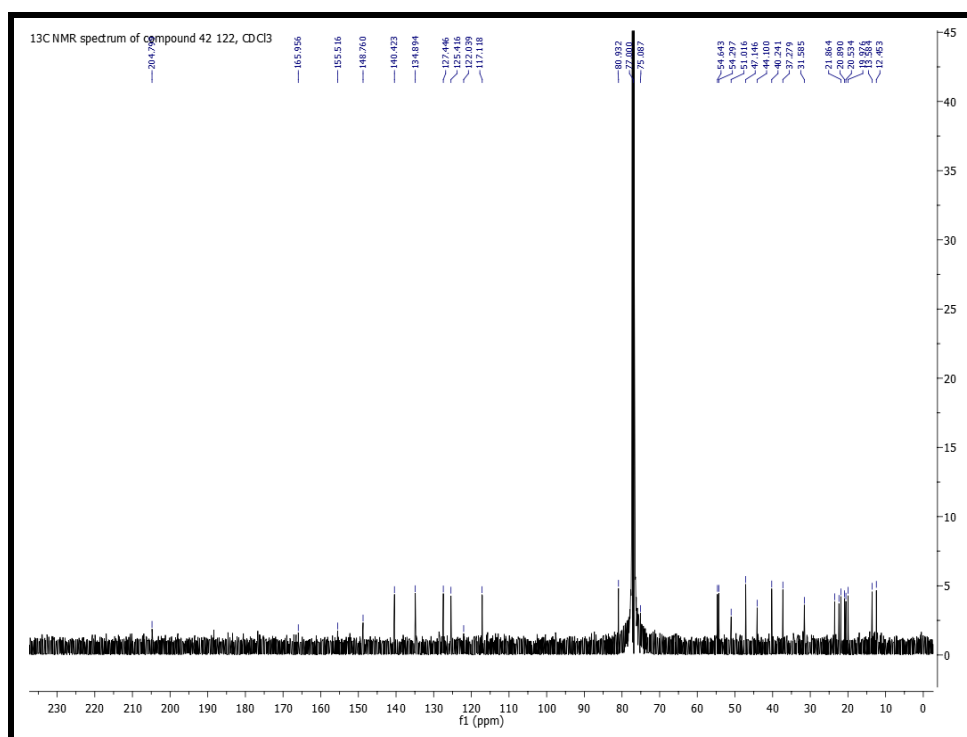
Fig. 88: ^{13}C NMR spectrum of compound **42**, 500 MHz, CDCl$_3$

DQF-COSY, HSQC and HMBC experiments revealed that rings A-D of compound **42** were consistent with those of withasomniferolide A.
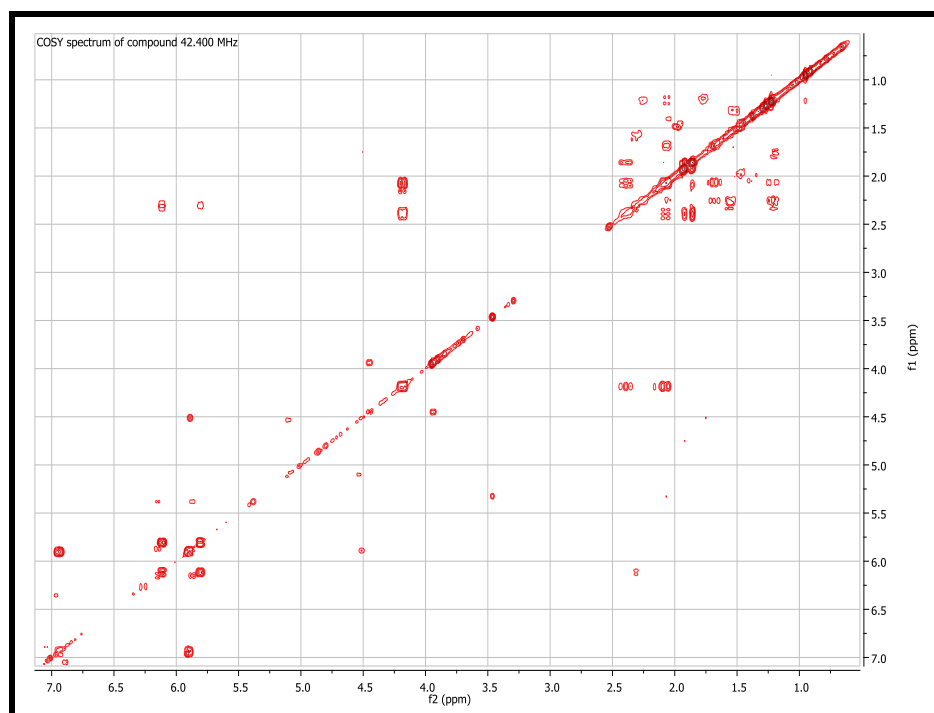
Fig.89: COSY spectrum of compound **42**, 400MHz, CDCl$_3$
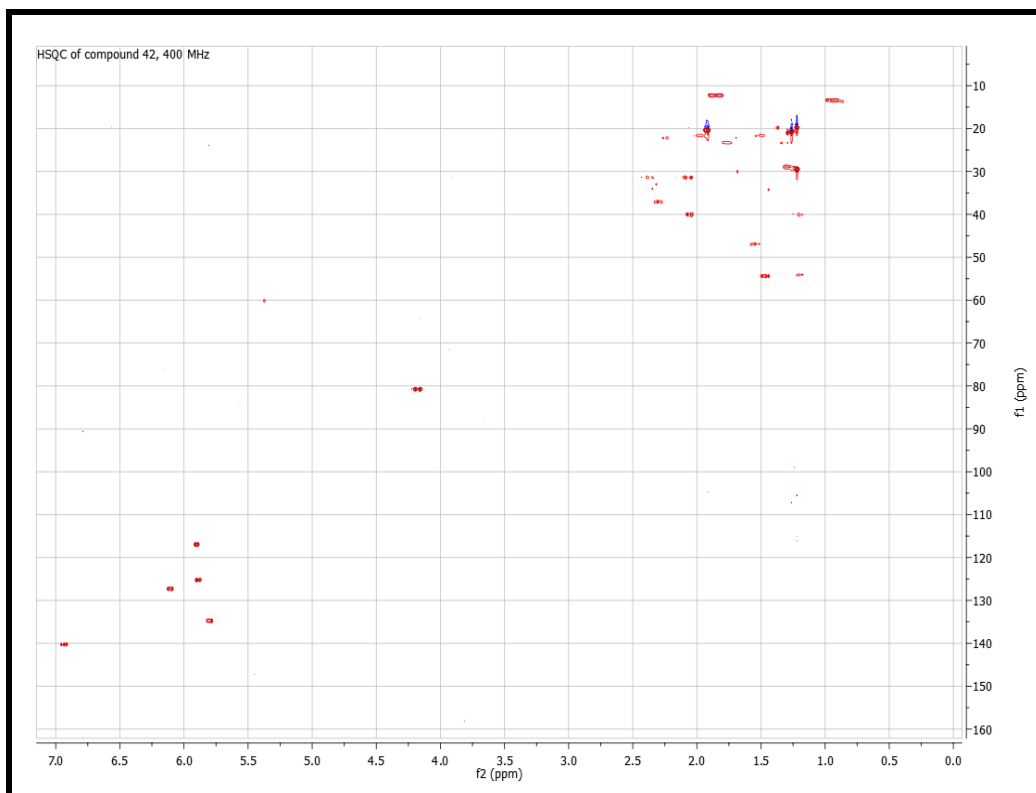
Fig.90: HSQC spectrum of compound **42**, 400MHz, CDCl$_3$

The HMBC spectrum showed correlations from the methyl protons at 1.30 ppm (δ_c 20.9) to the quaternary carbon at 75.1 and to the methine carbons at 54.6 and 80.9 ppm (Fig.91) as well as from methyl protons at 1.95 (δc 20.5) to carbons at 31.6, 148.8 and 122.0 and from the CH$_3$ at 1.88 (δc 12.5) to carbons at 148.8, 122.0 and 166.0 ppm. These connectivities lead to the conclusion that a methyl group is present at the C-27 position in compound **42**. Further HMBC crosspeaks between H-22 (δ_H 4.20) and C-23 (δ_C 31.6), C-20 (δ_C 75.1) and C-17 (δ_C 54.6) and between H-21 (δ_H 1.30) and C-22 (δ_C 80.9), C-20 and C-17 revealed that C-20 is a quaternary oxygenated carbon and thus compound **42** is an isomer of withasomniferolide A and differs from the latter only for the displacement of the OH group from position 27 to 20. Furthermore, ROESY cross-peaks confirmed the same stereochemistry reported for withasomniferolide A.

Therefore, the structure of compound **42** was determined as (22R)-1-oxo-20-hydroxywitha-2,4,6-trienolide, and this compound was named withasomniferolide B.
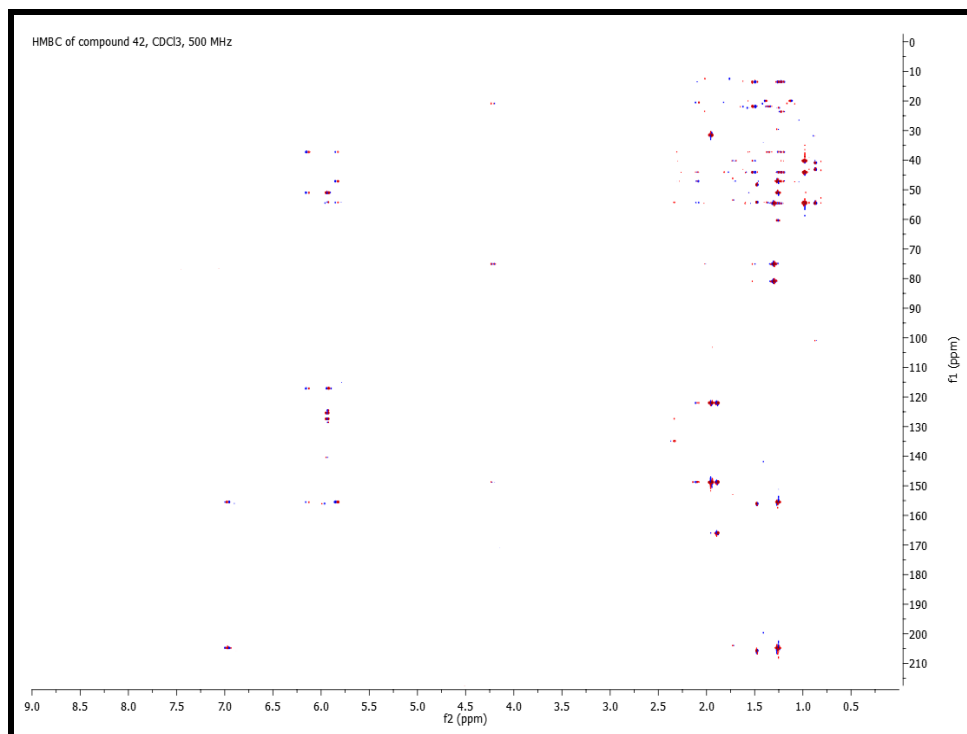
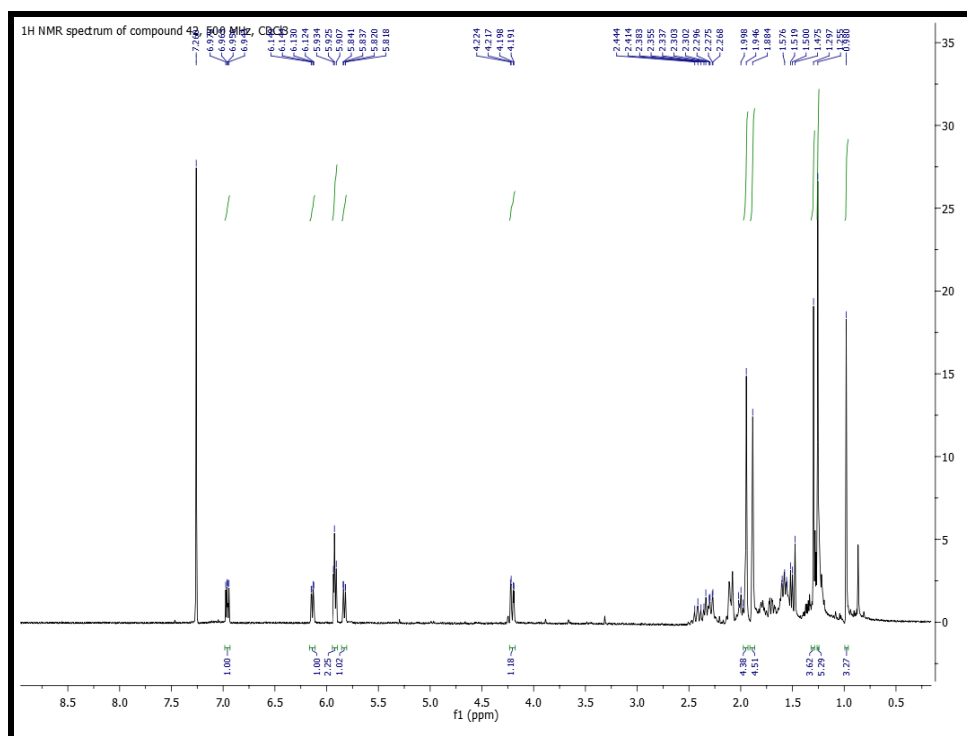**Fig. 91:** HMBC spectrum of compound **42**, 500MHz, CDCl$_3$
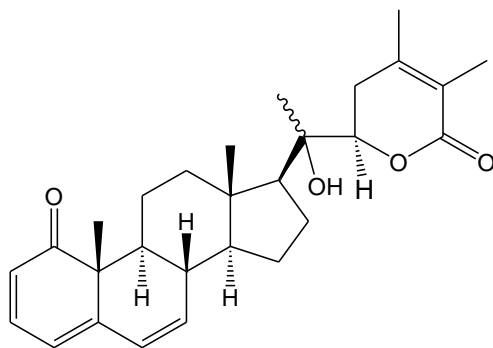
Compound **42** (withasomniferolide B)

Table 12. ^1H and ^{13}C NMR data of compounds **41** and **42**

| Position	Compound 41		Compound 42	
	δ_C, Multiplicity	δ_H, Multiplicity a	δ_C, Multiplicity	δ_H, Multiplicity a
1	204.8 (s)		204.8 (s)	
2	125.2 (d)	5.890, d (9.5)	125.4 (d)	5.91, d (9.5)
3	140.4 (d)	6.930, dd (9.5, 5.5)	140.4 (d)	6.96, dd (9.5, 5.5)
4	117.0 (d)	5.910, d (5.5)	117.1 (d)	5.93, d (5.5)
5	155.4 (s)		155.5 (s)	
6	127.3 (d)	6.110, dd (10, 2.5)	127.4 (d)	6.14, dd (10, 2.5)
7	134.5 (d)	5.791, dd (10, 2)	134.9 (d)	5.83, dd (10, 2)
8	37.6 (d)	2.291, m	37.3 (d)	2.31, m
9	47.0 (d)	1.565, m	47.1 (d)	1.55, m
10	50.8 (s)		51.0 (s)	
11	27.0 (t)	1.655, m 1H; 1.318, m 1H	23.5 (t)	1.76, m
12	39.7 (t)	2.015, m 1H; 1.130, m 1H	40.2 (t)	2.06, m 1H; 1.19 m, 1H
13	43.6 (s)		44.1 (s)	
14	53.7 (d)	1.18, m	54.3 (d)	1.23, m
15	23.8 (t)	1.767, m	22.4 (t)	2.23, m
16	29.4 (t)	1.219, m	21.9 (t)	1.98, m
17	51.7 (d)	1.130, m	54.6 (d)	1.492, m
18	11.7 (q)	0.783, s	13.6 (q)	0.98, s
19	19.7 (q)	1.229, s	20.0 (q)	1.26, s
20	38.7 (d)	2.002, m	75.1 (s)	
21	13.1 (q)	1.000, d (6.5)	20.9 (q)	1.30, s
22	78.5 (d)	4.441, m	80.9 (d)	4.20, dd (3.2, 13.2)
23	29.6 (t)	1.957, m 1H; 2.457, m 1H	31.6 (t)	2.05, m 1H; 2.39, m 1H
24	152.6 (s)		148.8 (s)	
25	125.4 (s)		122.0 (s)	
26	166.8 (s)		166.0 (s)	
27	19.8 (q)	2.008, s	12.5 (q)	1.88, s
28	57.3 (t)	4.320, d (12.5) 1H; 4.350, d (12.5) 1H	20.5 (q)	1.95, s

^{a}Value of *J* (Hz) in bracket

168

Compound 43

The ^{1}H NMR spectrum of compound **43** (Fig. 92) showed typical signals of a ferulic acid derivative at 7.57 (d, $J = 16$ Hz, 1H), 7.04 (dd, $J = 1.5$, 8 Hz, 1H), 7.0 (d, $J = 1.5$ Hz, 1H), 6.88 (d, $J = 8.0$ Hz, 1H), 6.26 (d, $J = 16$ Hz, 1H) and 3.90 (s, 3H) ppm. The chemical shift values at δ_C 167.4 and 64.6 displayed in the ^{13}C NMR spectrum (Fig.93) of compound **43**, besides the long range correlations of the methylene protons at δ_C 64.6, with the carbons at δ_C 167.4 28.8, and 26.0 observed in the HMBC spectrum (Fig.94), suggested the presence of a ferulic acid alkyl ester. However, in the ^{1}H NMR spectrum a terminal methyl group or a further oxymethylene moiety could not be detected suggesting the presence of a ferulate dimeric derivative.
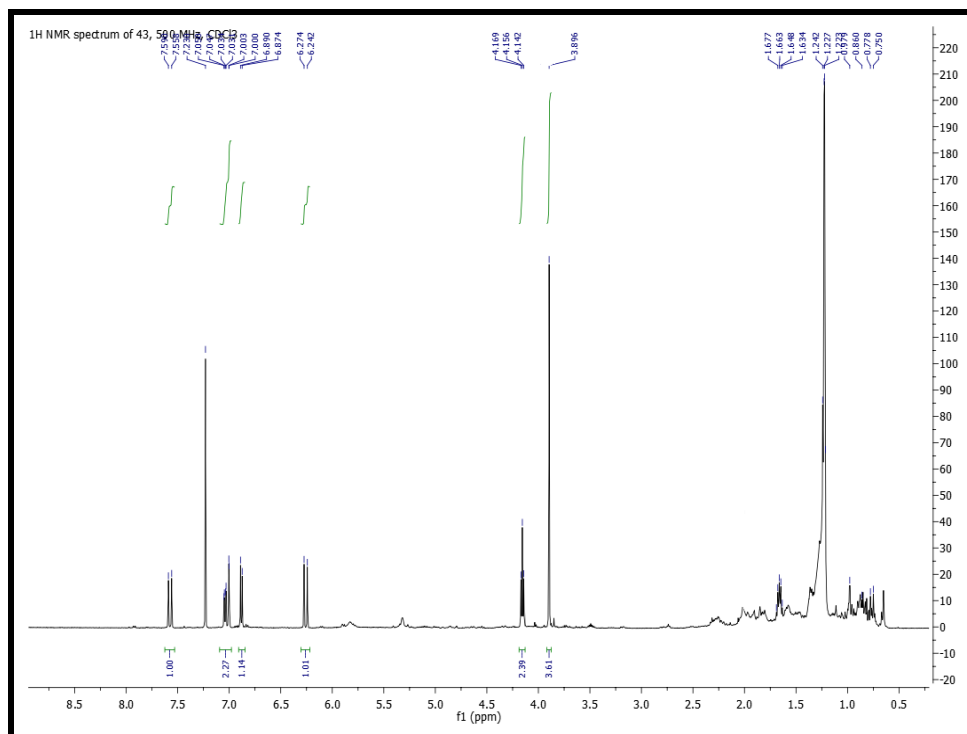
Fig. 92: ^{1}H NMR spectrum of compound **43**, 500MHz, CDCl$_3$
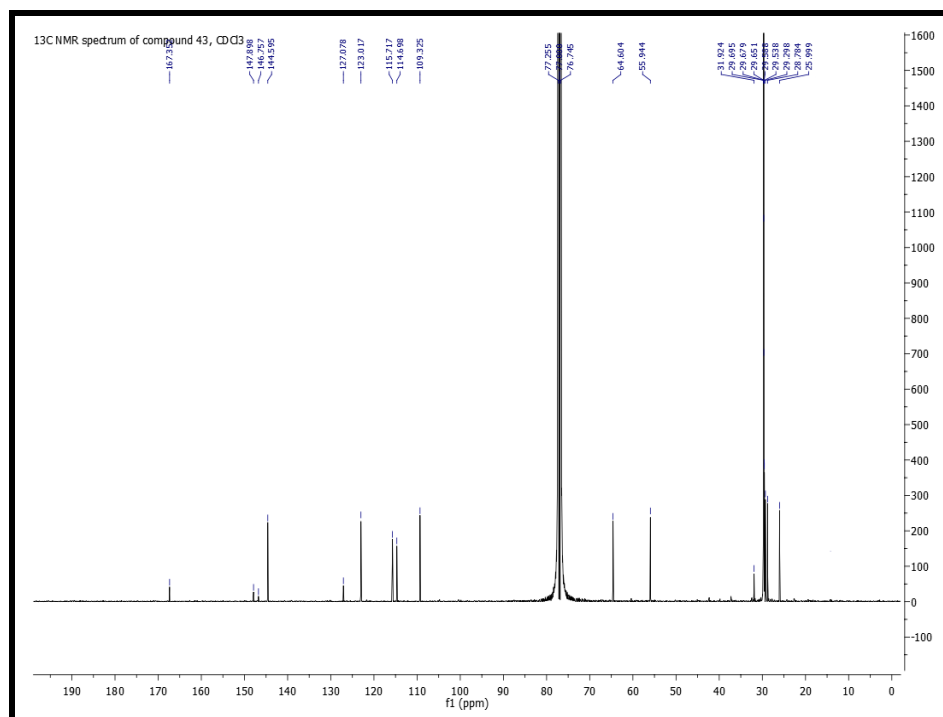
Fig. 93: ^{13}C NMR spectrum of compound **43**, 100MHz, CDCl$_3$
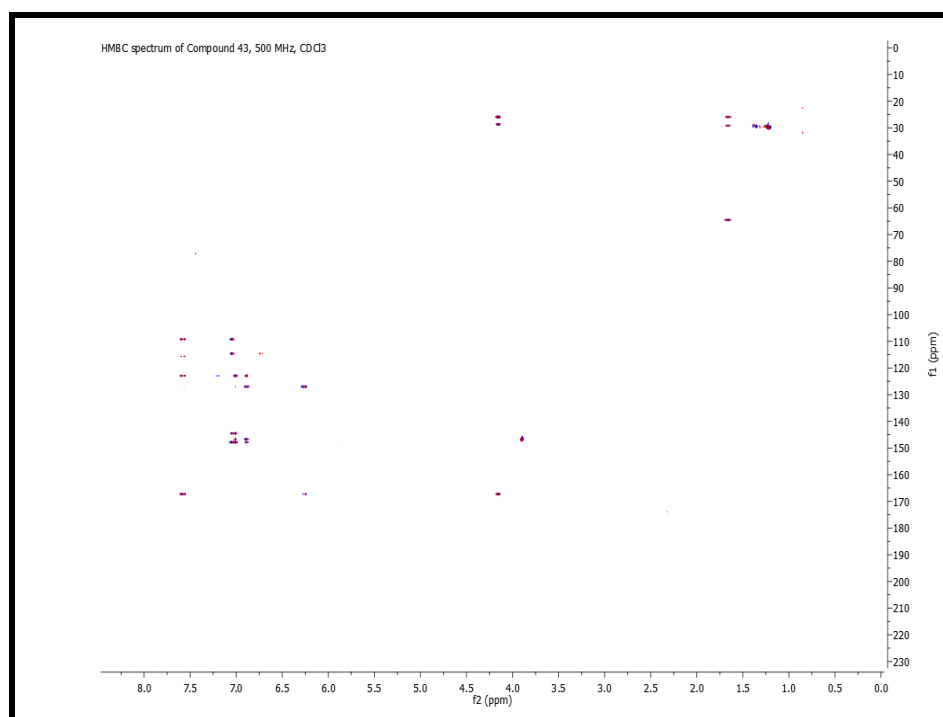
Fig.94: HMBC spectrum of compound **43**, 500MHz, CDCl$_3$

The ESI MS spectrum showed a molecular ion peak at *m/z* 455 [M-H]⁻ and a fragmentation ion at *m/z* 279 [M-$C_{10}H_9O_3$]⁻ (Fig. 95). This is in accord with the molecular formula $C_{25}H_{28}O_8$ reported in figure and therefore compound **43** is 1,5-di-O-feruloylpentanediol.The ^1H and ^{13}C NMR as well as the MS data are congruent with literature data [256]. In order to confirm the structure and to obtain more compounds for the biological screenings, compound **43** was also synthesized (see the next paragraph).
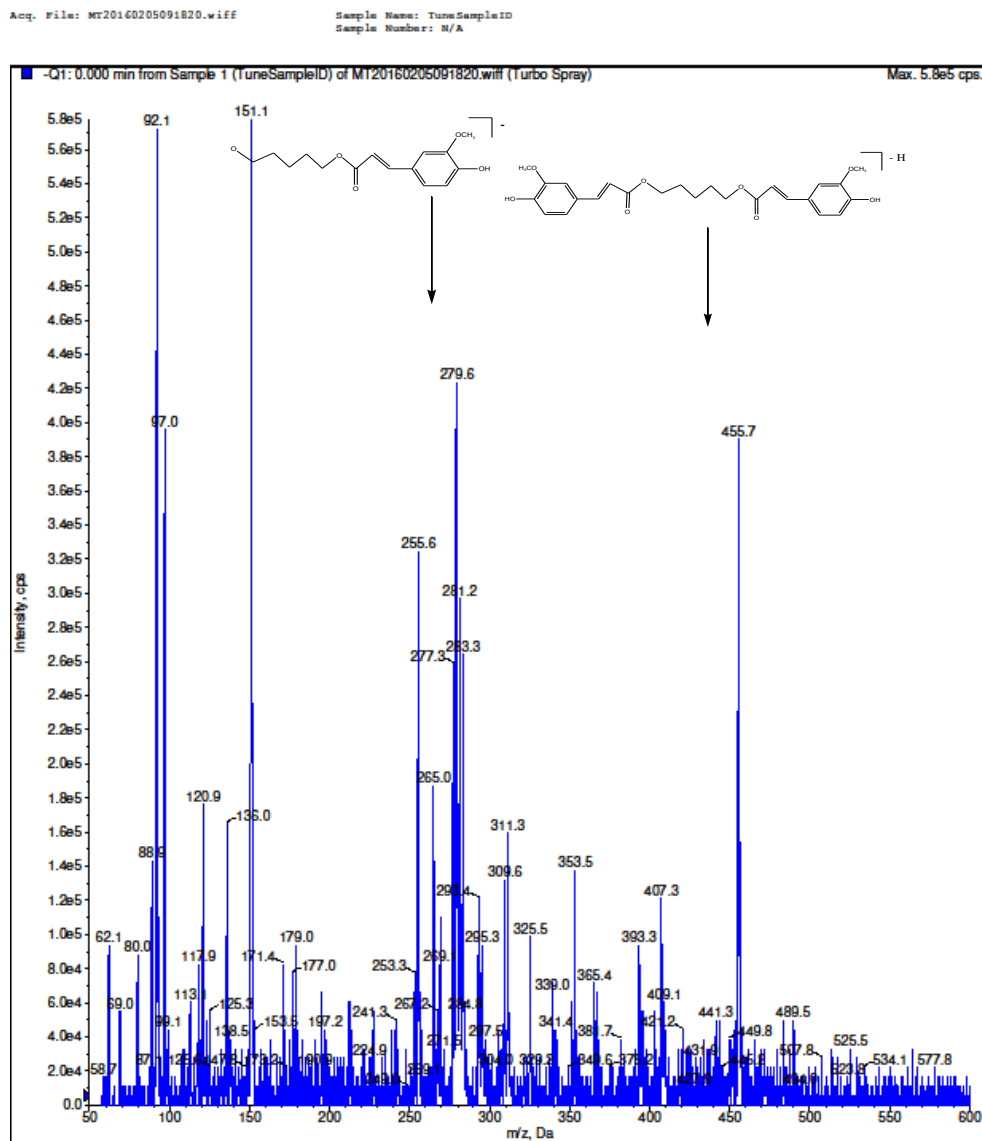
Fig.95: ESI MS spectrum of compound **43** (negative mode)
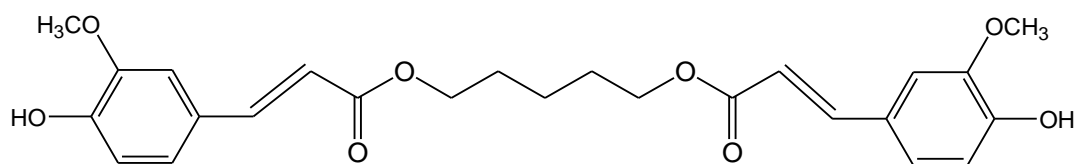
Compound **43** (1,5-di-*O*-feruloylpentanediol)

Compounds 44-46

The ^{1}H NMR spectrum (Fig. 96) of the isolated compound perfectly matched with a long alkyl chain ferulate, already identified in the DCM extract of *Ocimum sanctum*.
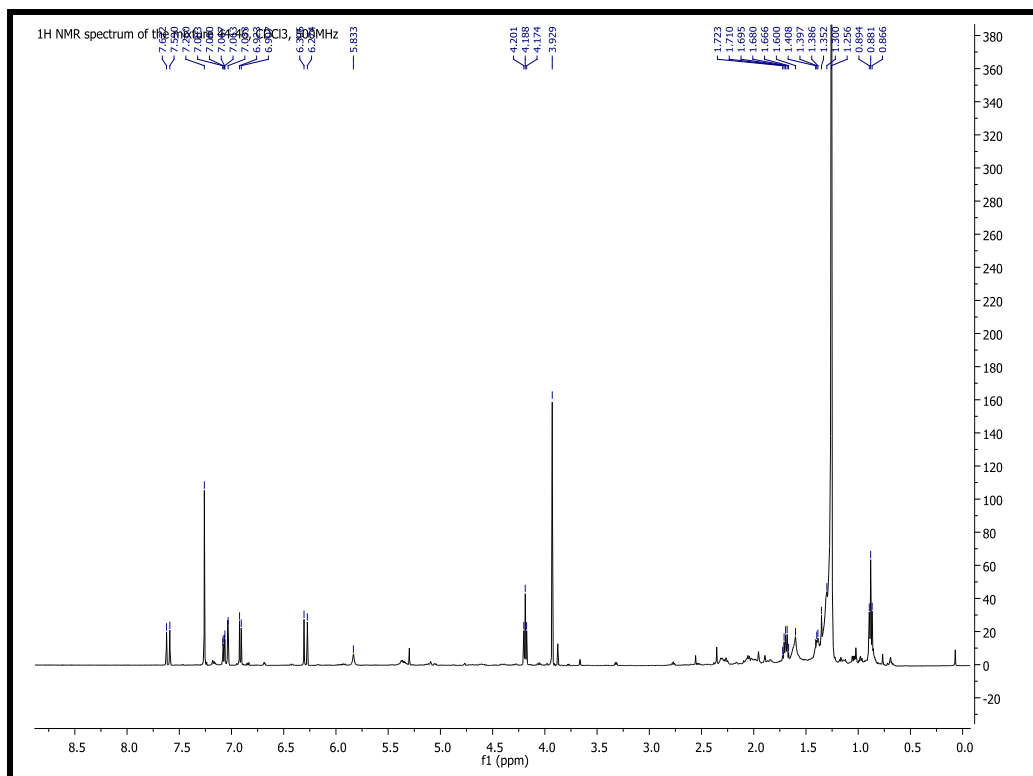
Fig.96: ^{1}H NMR spectrum of the mixture **44-46**, 500MHz, CDCl$_3$

The ESI MS spectrum (negative mode) revealed three ion peaks at *m/z* 501, 473 and 445 (Fig. 97). MS/MS spectra of the three ion peaks, each showing a loss of a methyl group, (Fig. 98: A, B, and C), clearly demonstrated that peaks at *m/z* 473 and 445 did not originate from that at *m/z* 501. Therefore, the compound was a mixture of three long chain alkyl ferulates differing each other only by the number of the methylene groups and was identified as mixture of octadecyl ferulate (**44**), eicosanyl ferulate (**45**) and docosanyl ferulate (**46**). Their structures were confirmed by comparison of their spectral data [258] and by synthesis (see scheme 4).
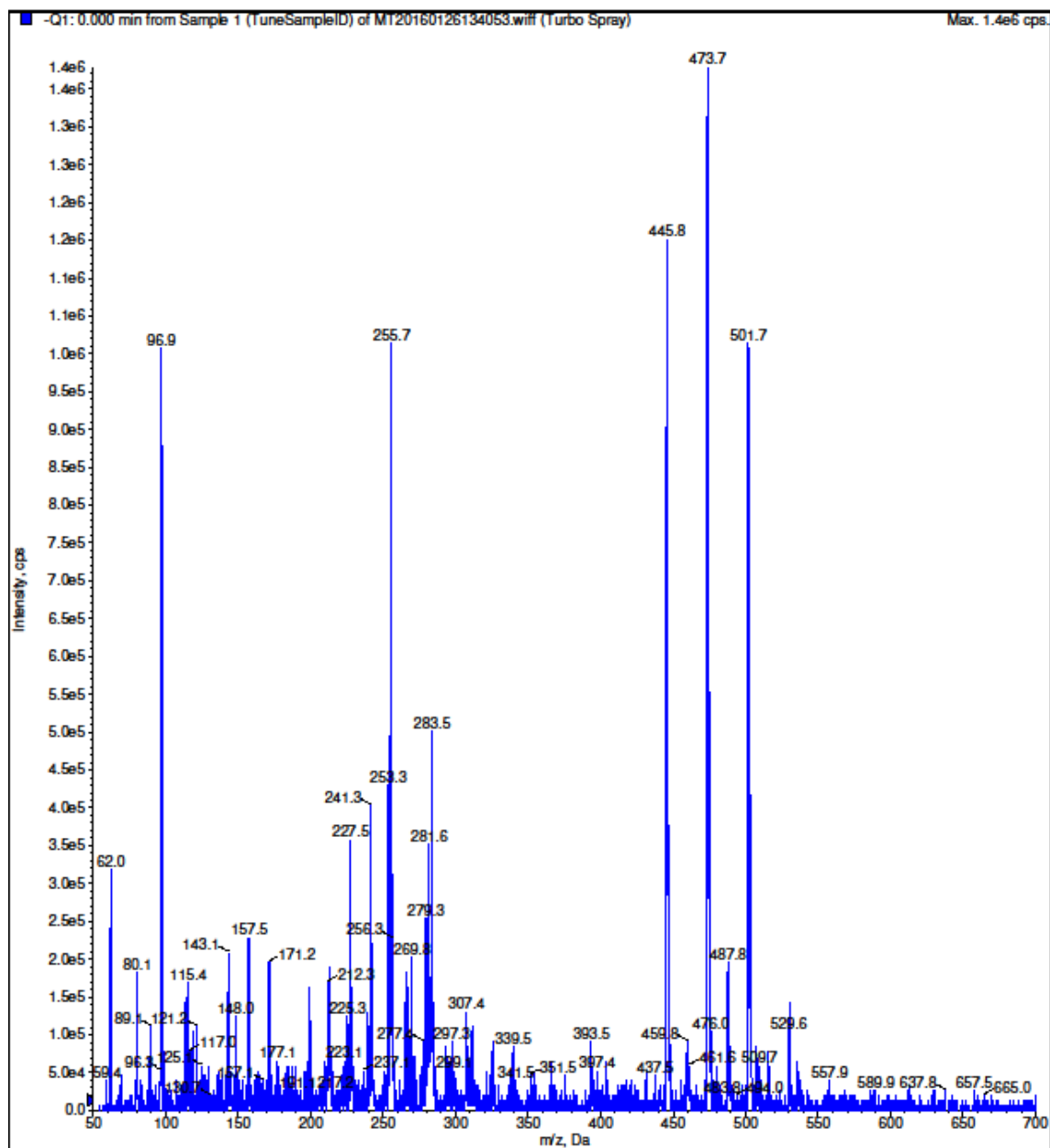
Fig.97: ESI MS spectrum (negative mode) of the mixture **44**-**46**
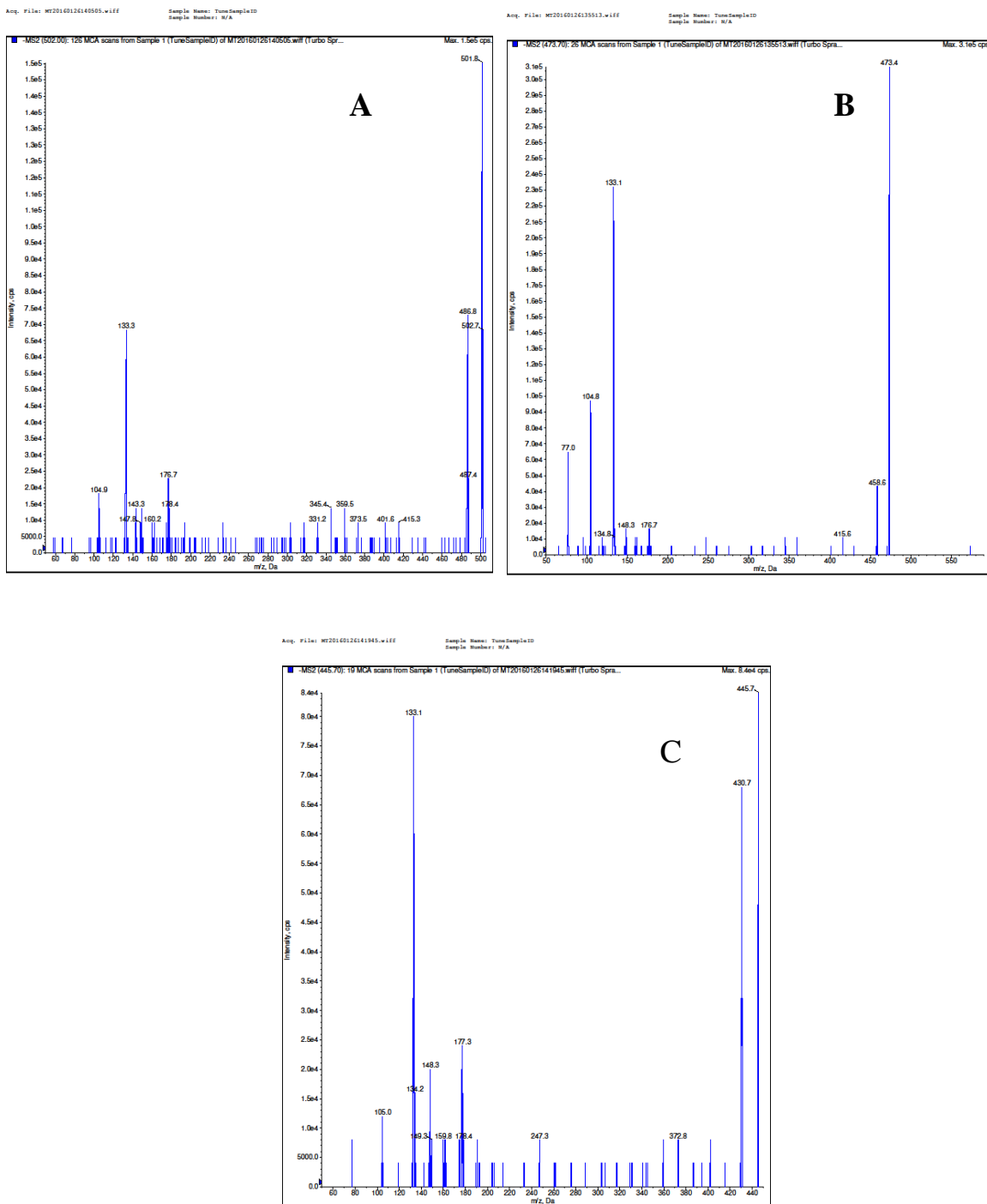
Fig.98: MS/MS spectrum of the ion peak at *m/z* 501 (A), 473(B) and 445 (C)

Compound 47

Compound **47** was identified as withanolide B. The structure is confirmed by 1D (^{1}H-, ^{13}C NMR) and 2D NMR experiments and by comparison with literature data [259].
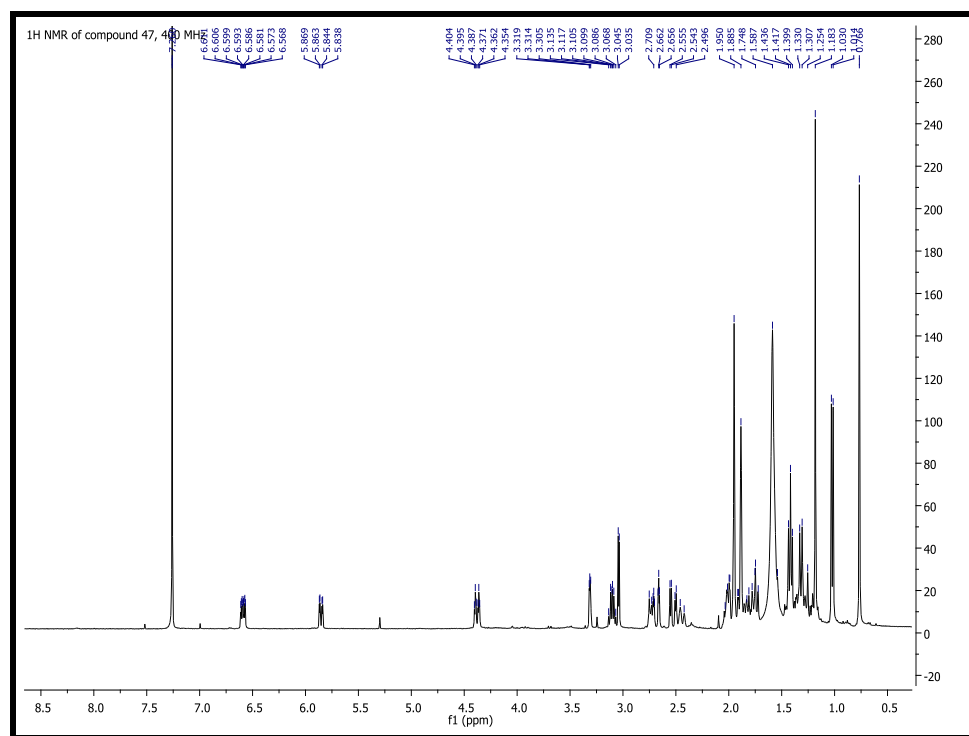
Fig. 99: ^{1}H NMR spectrum of withanolide B (**47**), 500MHz, CDCl$_3$
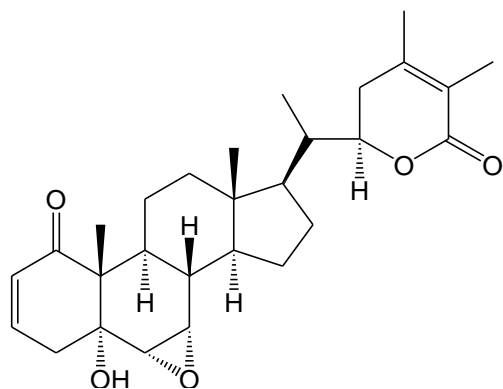
Compound **47** (withanolide B)

Compound 48

Compound **48** was identified as withanolide A. The structure is confirmed by 1D (^{1}H-, ^{13}C NMR) and 2D NMR experiments and by comparison with literature data [259].
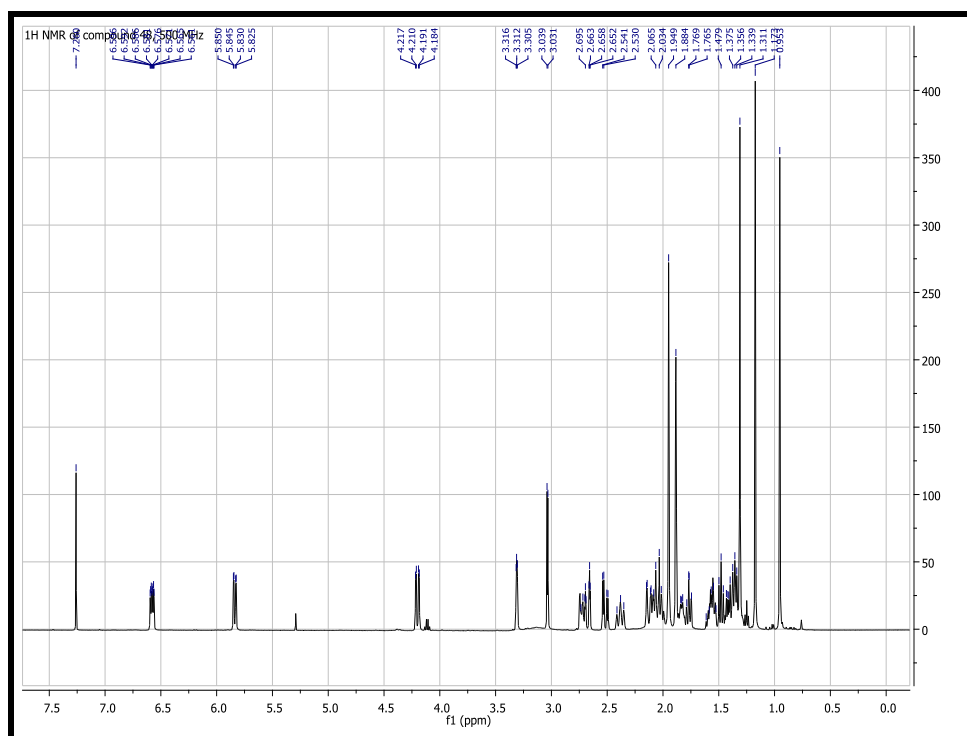
Fig.100: ^{1}H NMR spectrum of withanolide A (**48**), 500MHz, CDCl$_3$
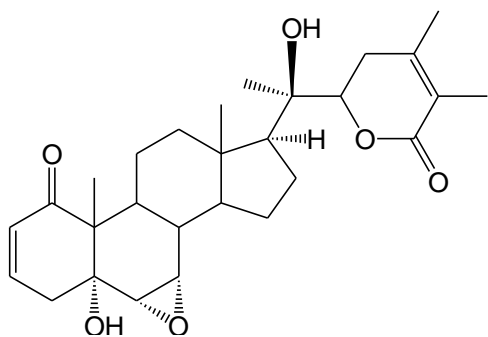
Compound **48** (withanolide A)

Compound 49

Compound **49** was identified as withaferin A. The structure is confirmed by 1D (^{1}H-, ^{13}C NMR) and 2D NMR experiments and by comparison with literature data [259].
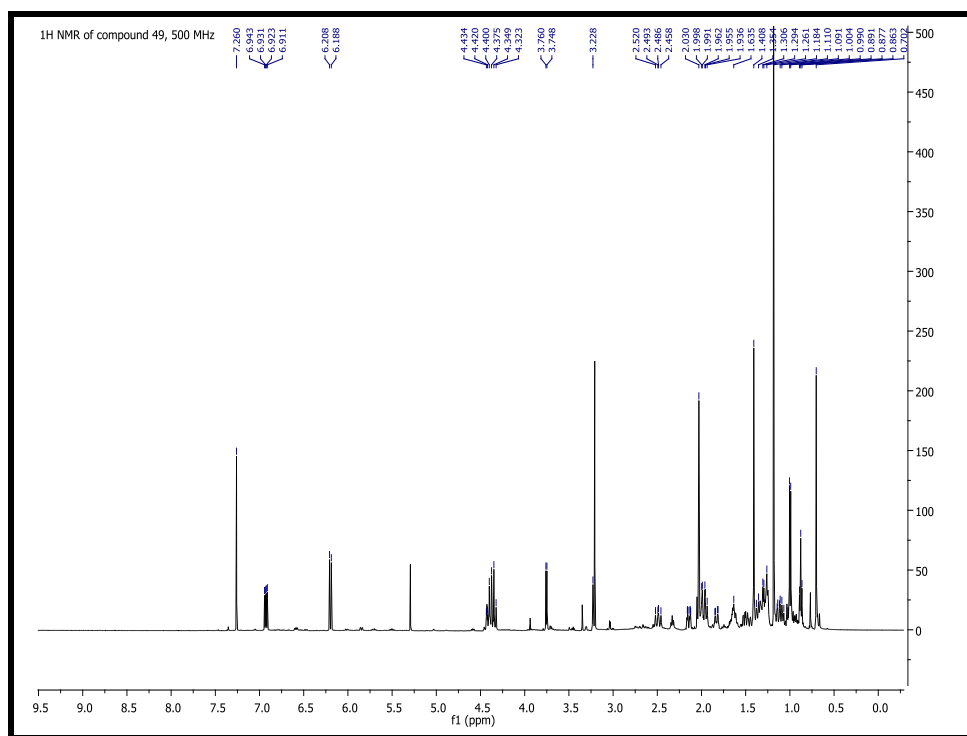
Fig. 101: ^{1}H NMR spectrum of withaferin A (**49**), 500MHz, CDCl$_3$
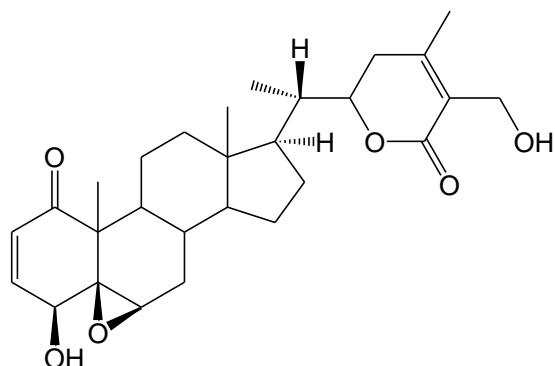
Compound **49** (Withaferin A)

5.4.3 Synthesis of 1,5-di-*O*-feruloylpentanediol (43)

The synthesis of 1,5-di-*O*-feruloylpentanediol (**43**) was performed according to a previously described procedure [228] with some slight modifications, as illustrated in scheme 3. Briefly, the reaction involved the synthesis of a mixed anhydride obtained by reaction of ferulic acid and ethyl chloroformate in presence of TEA, at -15 °C. This step led to a simultaneous protection/activation of ferulic acid. The protected ferulic acid anhydride was not isolated and 1,5-pentanediol, in presence of catalytic amount of DMAP, was added to afford the protected ester. The deprotection was easily achieved using excessive amounts of nucleophilic base (piperidine) at 0 °C, to give the expected 1,5-di-*O*-feruloylpentanediol (**43**) in good yields.
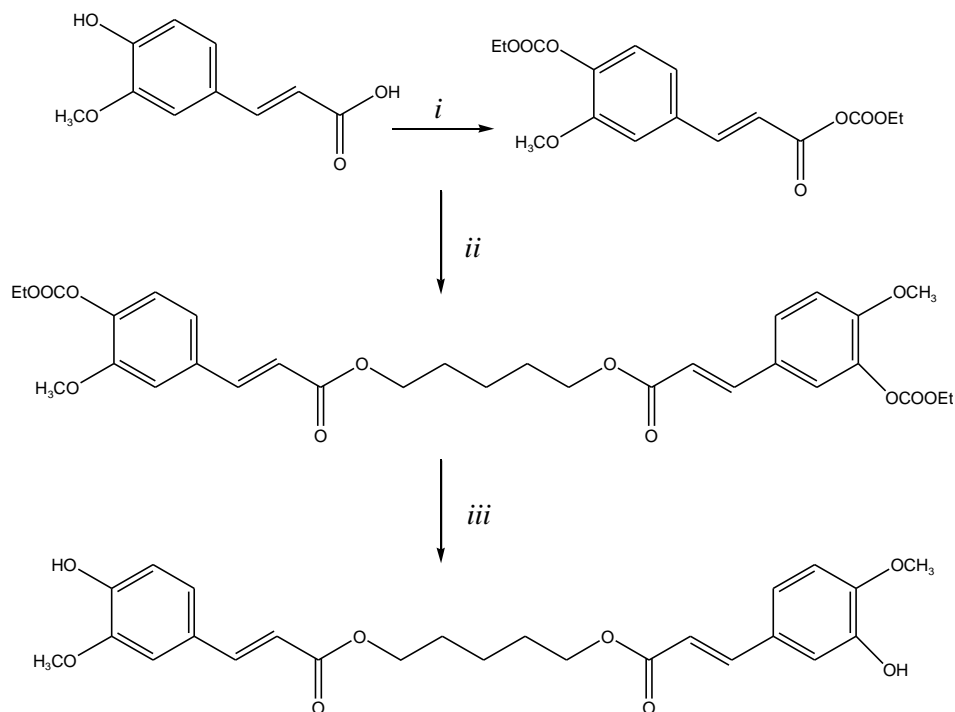
i:ClCOOEt, TEA, DCM, -15ºC, 1h; *ii*: 1,5-pentanediol, DMAP, r.t.; *iii*: piperidine, 0ºC, 1h

Scheme 3: Synthetic pathway to 1,5-di-*O*-feruloylpentanediol (**43**)
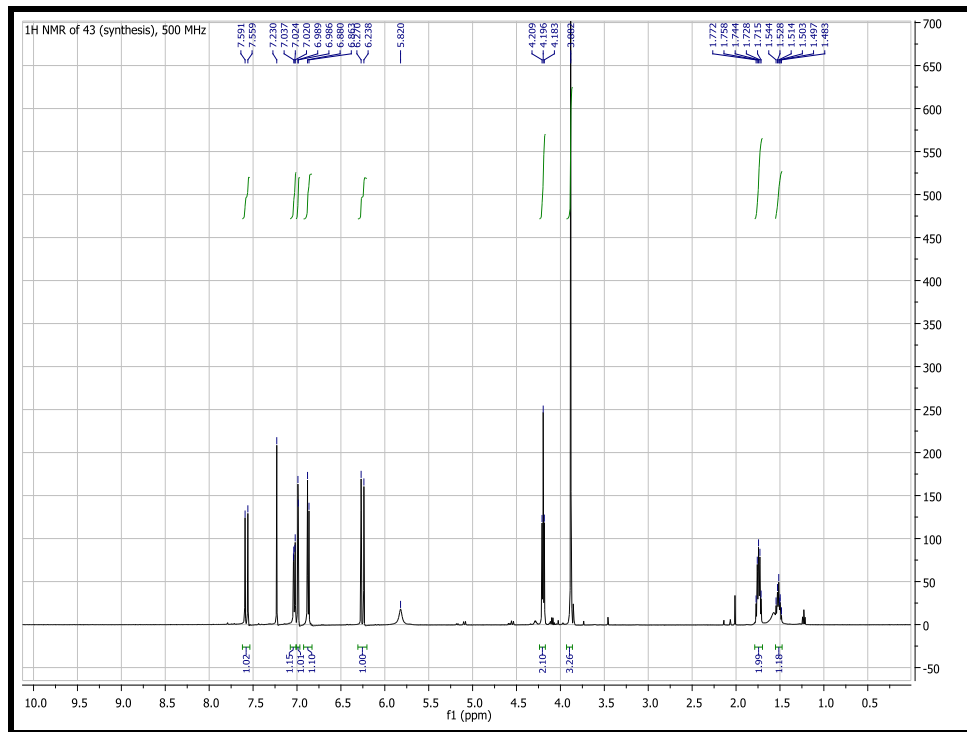
Fig.102: ^{1}H NMR spectrum of the synthesized 1,5-di-*O*-feruloylpentanediol (**43**), 500MHz, CDCl$_3$

5.4.4 Synthesis of compounds 44-46

The synthesis of octadecyl ferulate (**44**), eicosanyl ferulate (**45**) and docosanyl ferulate (**46**) was carried out with the same procedure of compound **43** but using different molar ratio between alcohols and mixed anhydride (see experimental part).

44: R= $(CH_2)_{17}CH_3$
45: R= $(CH_2)_{19}CH_3$
46: R= $(CH_2)_{21}CH_3$
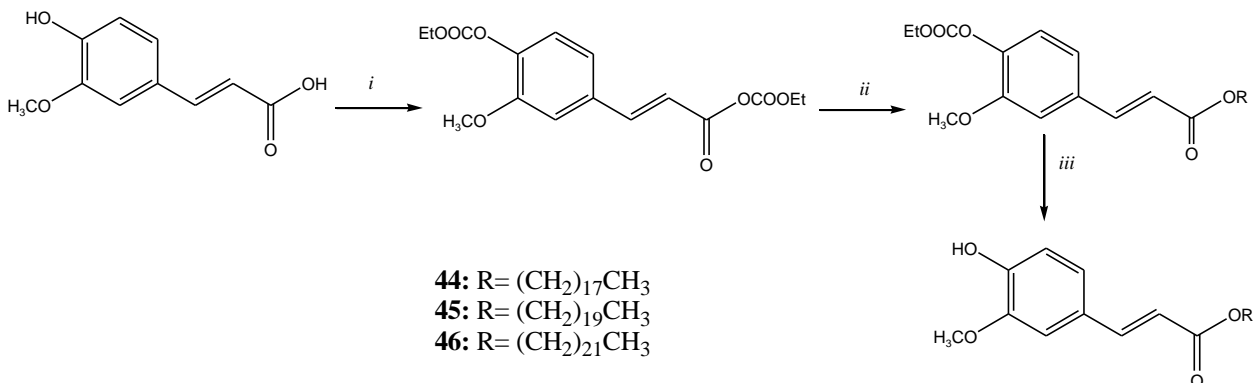
*i:*ClCOOEt, TEA, DCM, -15ºC, 1h; *ii:*ROH, DMAP, r.t.; *iii*: piperidine, 0ºC, 1h

Scheme 4: Synthetic pathway to esters of ferulic acid **44-46**
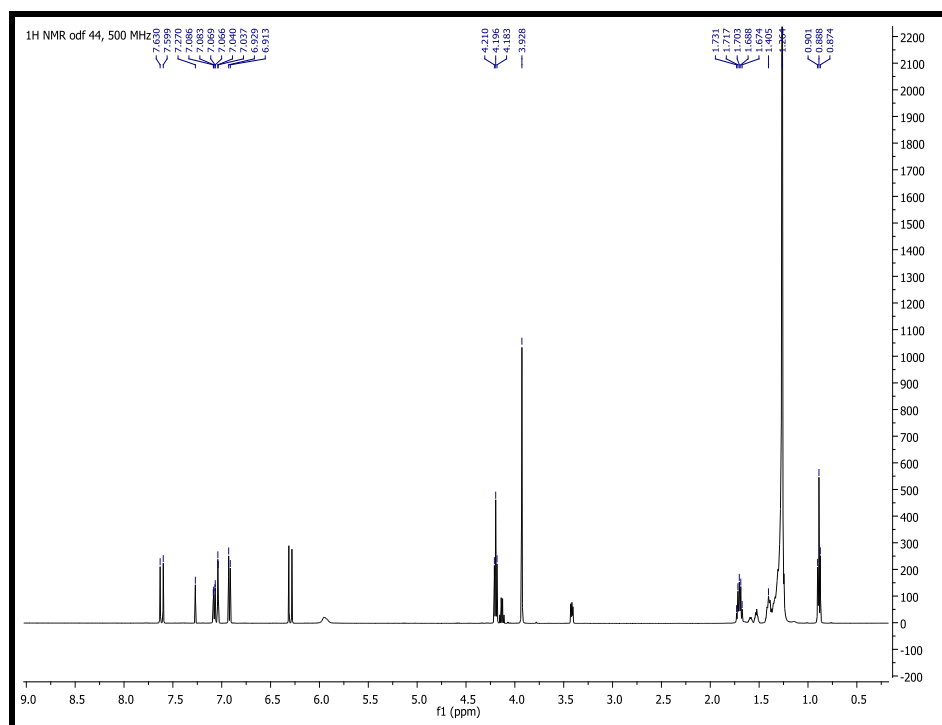
Fig.103: ^{1}H NMR spectrum of compound **44** (octadecyl ferulate), 500 MHz, CDCl$_3$
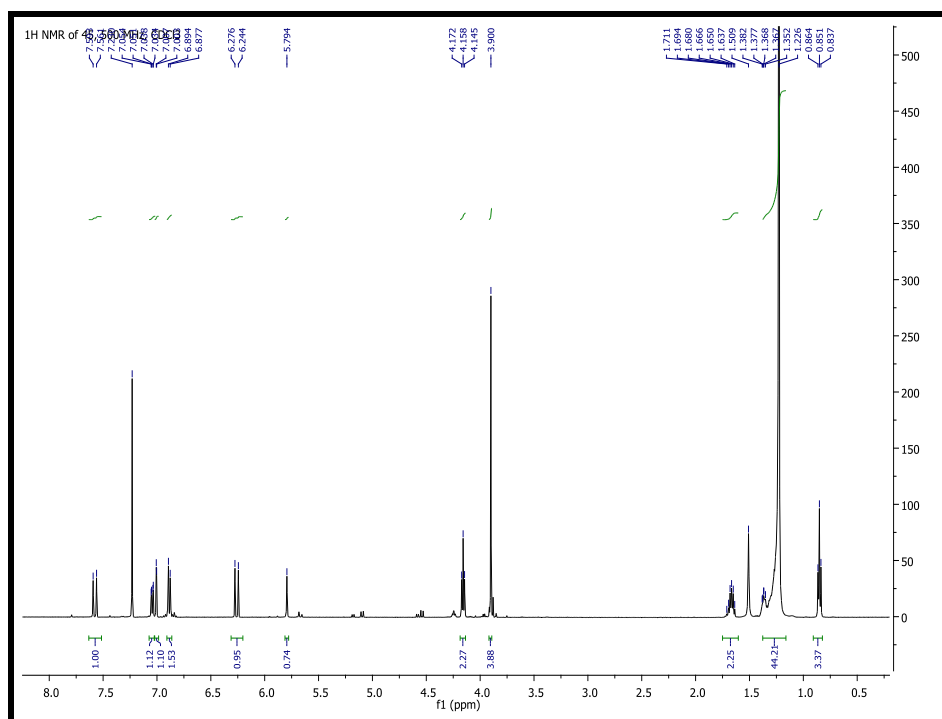
Fig.104: ^{1}H NMR spectrum of compound **45** (eicosanyl ferulate), 500 MHz, CDCl$_3$
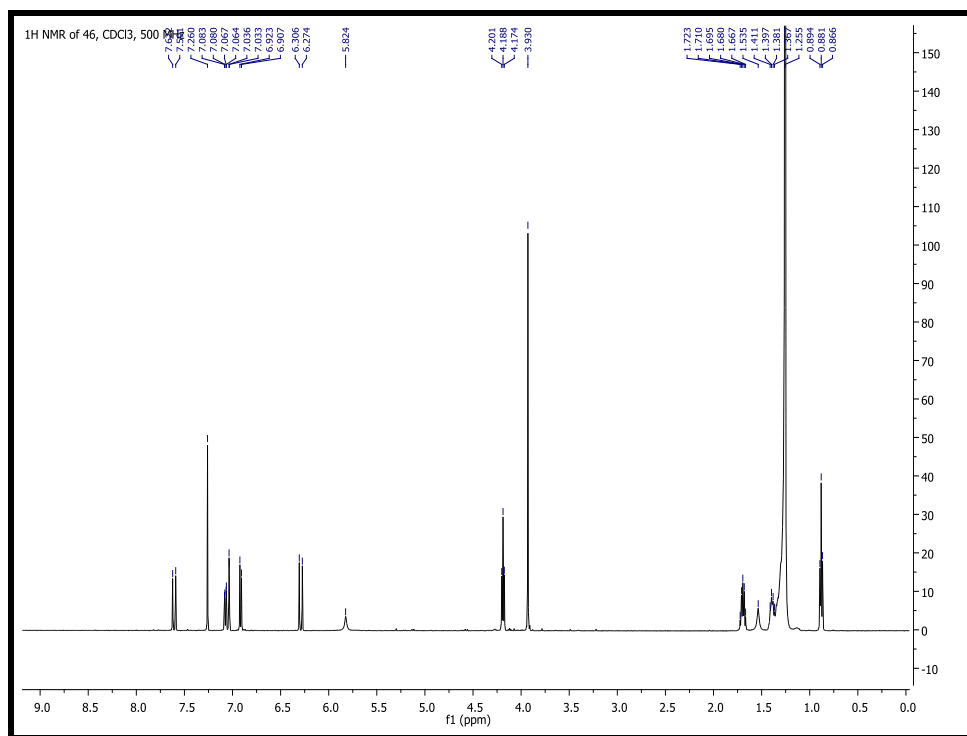
Fig.105: ^{1}H NMR spectrum of compound **46** (docosanyl ferulate), 500 MHz, CDCl$_3$

5.4.5 Biological results

Modulatory effects of compounds 41-49 at GABA$_A$ receptor

In order to evaluate the potential modulatory activity of compounds **41-49** as well as the methanol extract of *W. somnifera* (WSe) on the function of GABA$_A$ receptors, GABA-induced inhibitory postsynaptic currents (IPSCs) were recorded in voltage-clamped (-65 mV) dentate gyrus (DG) granule cells that were present in rat hippocampal slices. To this end, GABAergic afferents, coming from surrounding inhibitory interneurons and projecting to granule cell dendrites, were electrically stimulated and the resulting release of GABA activates transient IPSCs due to the activation of postsynaptic GABA$_A$ receptors (Fig.106).

In different DG granule cells, IPSCs were recorded before and after perfusion of either 400µg/ml Wse or 10µM of each of the nine compounds. Representative electrophysiological tracings are shown in figure 106. The bar graph in panel C shows the averaged data relative to the effects of the different compounds obtained in different neurons. The results show that WSe significantly ($p < 0.05$) enhanced the amplitude of GABA-induced IPSCs by 38% ± 11 compared to the value of the control response (Fig.106). Similarly, docosanyl ferulate (**46**) potentiated IPSC amplitude by 37% ± 14 ($p < 0.05$) above control. On the contrary, octadecyl ferulate (**44**) and withasomniferolide B (**42**), significantly ($p < 0.05$) reduced IPSC amplitude by 36% ± 9 and 30% ± 7, respectively. 1,5-di-*O*-feruloylpentanediol (**43**), eicosanyl ferulate (**45**), withasomniferolide A (**41**), and withanolide B (**47**) produced no significant alteration of IPSC amplitude (Fig. 106). Also compounds **48** (withanolide A) and **49** (withaferin A) were not able to produce significant alteration of IPSC amplitude (data not shown).
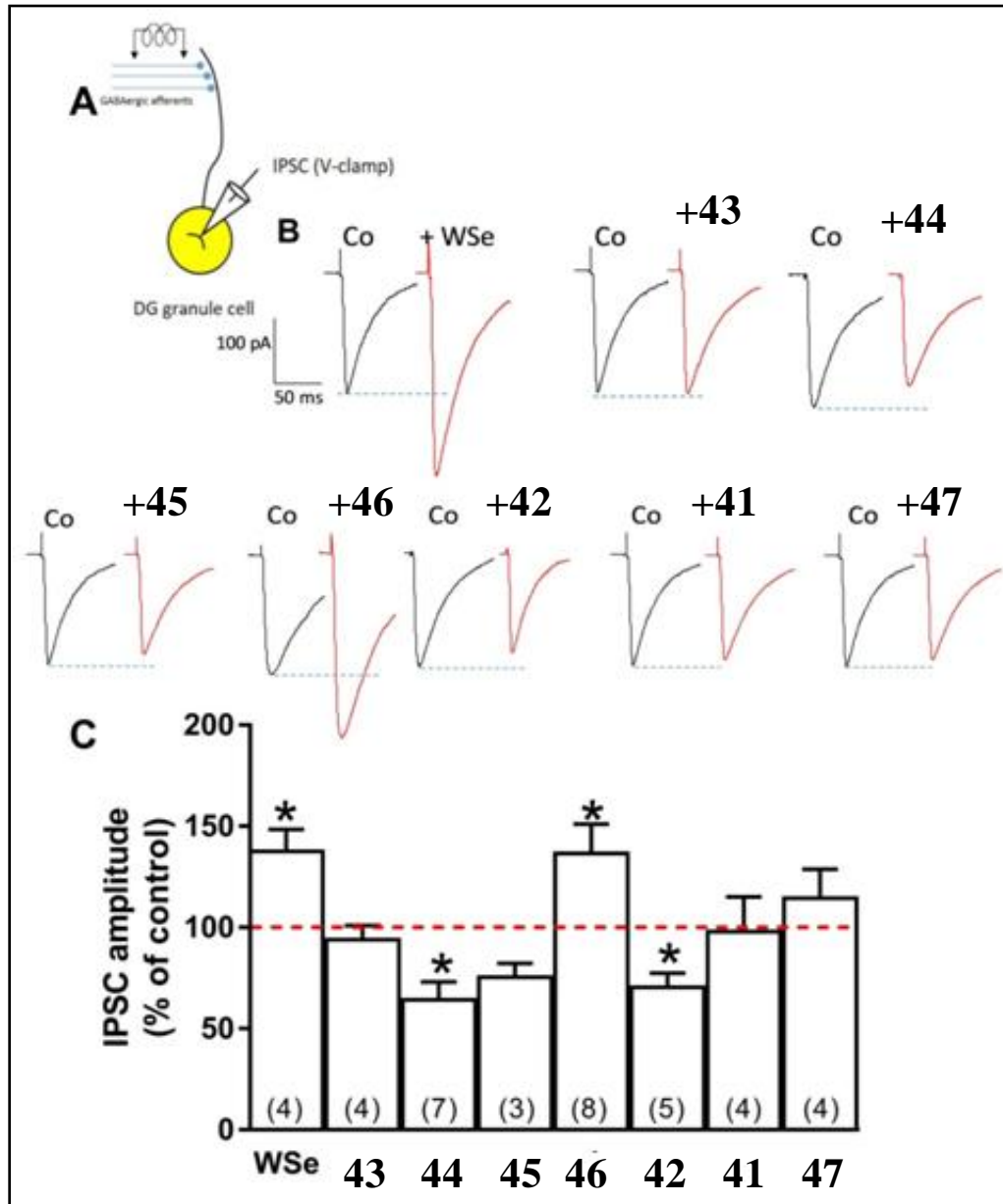
Fig.106: Modulatory activity of WSe and compounds **41-47** on GABA$_A$ receptor-mediated IPSCs recorded in DG granule cells. (A) Schematic representation of the recording protocol, involving the electrical stimulation of GABAergic afferents and the recording of IPSC generated postsynaptically by the release of GABA. (B) Representative tracings obtained by single granule cells in control conditions (black trace) and in the presence of the given compound (red trace). (C) Bar graph summarizing the changes in IPSC amplitude produced by the tested compounds. Data are expressed as the averaged percent of the control response ± standard error. Numbers inside the columns indicate the number of cells tested. ($p < 0.05$ vs control response)

This is the first report of a modulatory effect of esters of ferulic acid at GABA$_A$ receptor. Interestingly, withasomniferolide B was able to negatively modulate GABA$_A$ receptor while all the other withanolides produced no significant alteration of IPSC amplitude. This different interaction with GABA$_A$ receptor may be due to a more unsaturated A and B ring system in withasomniferolides A and B compared to the known withanolides that causes a partial planar system (Fig. 107). Consequently, withasomniferolide B could offer a better binding with GABA$_A$ receptor.

The absence of alteration of IPSC amplitude of withasomniferolide A could be ascribed to its instability in aqueous solution.

3D- structure of Withasomniferolide B

3D- structure of Withanolide B
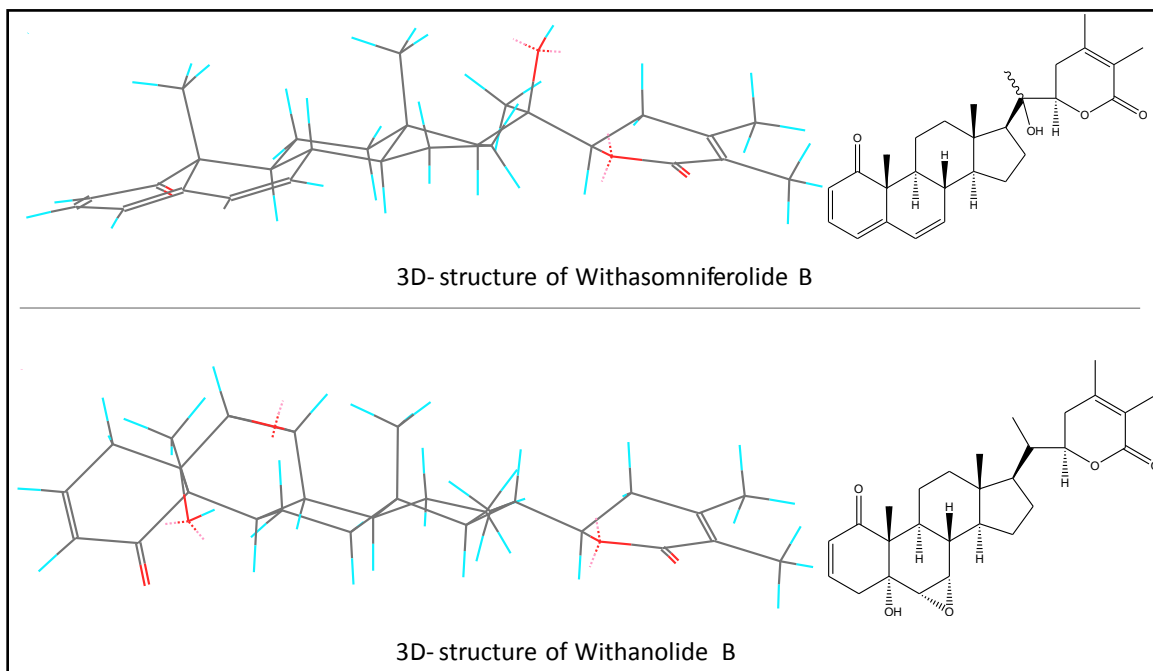
Fig.107: 3D structures of withasomniferolide B and withanolide B

5.5 Antioxidant assay of plant extracts

MeOH extract of *O. sanctum, T. cordifolia,* and *B. fruticosum* and DCM extract of *O. sanctum* and *B. fruticosum* were tested for their antioxidant capacity. Antioxidant potential of the plant extracts were measured by four different methods. Free radical scavenging activity of the extracts was measured by DPPH, ABTS and Galvinoxyl antiradical acivity test, Caffeic acid and Trolox were used as reference standard (Table 13). Chelation potential was measured by Iron chelation method using EDTA as reference standard (Table 14). There are many different methodologies for determination of the antioxidant activities of the plant extracts reported in the literature Therefore, use of different assays lead to scattered results, with no possibility for their comparison. These four methods were selected because of their simplicity, sensitivity, and reproducibility.

MeOH extract of *O. sanctum* was found most active by all three methods of antiradical activity. The extract was able to reduce Galvinoxyl free radical ($IC_{50} = 11.9 \pm 1.8$ µg/ml), DPPH radical ($IC_{50} = 34 \pm 0.45$ µg/ml), and ABTS radical ($IC_{50} = 38 \pm 0.245$ µg/ml). Also, it was able to chelate 93.91% of the Fe^{+3} ions at concentration of 19.2 µg/ml. DCM extract of *O. sanctum* was found less active compared to MeOH extract. It was able to reduce Galvinoxyl free radical ($IC_{50} = 86 \pm 4.7$ µg/ml), DPPH radical ($IC_{50} = 94 \pm 15$ µg/ml), and ABTS radical ($IC_{50} = 40 \pm 0.82$ µg/ml). Chelation of Fe^{+3} by DCM extract at concentration of 19.2 µg/ml was 66.11%.

MeOH extract of *T. cordifolia* was able to reduce Galvinoxyl free radical ($IC_{50} = 57 \pm 7.5$ µg/ml) and ABTS radical ($IC_{50} = 61 \pm 1$ µg/ml). Chelation of Fe^{+3} by MeOH extract at concentration of 19.2 µg/ml was 93.24%. DPPH radical reducing potential of this extract was found less ($IC_{50} = 179 \pm 3.2$ µg/ml).

MeOH extract of *B. fruticosum* was found active by all three methods of antiradical activity. The extract was able to reduce Galvinoxyl free radical ($IC_{50} = 57 \pm 1.8$ µg/ml), DPPH radical ($IC_{50} = 85.7 \pm 3$ µg/ml), and ABTS radical ($IC_{50} = 70 \pm 2$ µg/ml). Also, it was able to chelate 89.84% of the Fe^{+3} ions at concentration of 19.2 µg/ml. DCM extract of *B. fruticosum* was found not active when measured for their antiradical activity by GO ($IC_{50} = 358 \pm 32.3$

µg/ml), DPPH (IC_{50} >1000 µg/ml), and ABTS method (IC_{50} = 359 ± 57 µg/ml). Surprisingly DCM extract was able to chelate 76.96% of the Fe^{+3} ions at concentration of 19.2 µg/ml.

Table 13: Antioxidant activity of plant extract (GO, DPPH, ABTS)

Sample	Antiradical activity IC_{50} µg/ml		
	GO	DPPH	ABTS
O. sanctum (MeOH)	11.9± 1.8	34± 0.45	38± 0.2
O. sanctum (DCM)	86±4.7	94±15	40±0.82
T.cordifolia (MeOH)	57± 7.5	179± 3.2	61± 1
B. fruticosum (MeOH)	57±1.8	85. 7±3	70±2
B. fruticosum (DCM)	358 ±32.3	>1000	359± 57
Caffeic acid	2.32± 0.02	3.83± 0.03	2.91± 0.036
Trolox	4.56± 0.036	5.93± 0.02	5.36± 0.020

Table 14: Antioxidant activity of plant extracts (Iron Chelation method)

Sample	% chelation at 19.2 µg/ml
O. sanctum (MeOH)	93.91
O. sanctum (DCM)	66.11
T.cordifolia (MeOH)	93.24
B. fruticosum (MeOH)	89.84
B. fruticosum (DCM)	76.96
EDTA	73.68

Chapter 6 Conclusions

Using an HIV-1 Reverse Transcriptase-associated RNase H inhibition assay as lead, the phytochemical investigation of the DCM and MeOH extracts from *O. sanctum* as well of the DCM extract from the stems of *T. cordifolia*, yielded twenty secondary metabolites. Among all, the most potent inhibitors of RT-asscociated RNase H function were the triterpenoids ursolic acid (IC_{50}= 5.5 ± 0.3 µM), lupeol (IC_{50}= 5.9 ± 0.24 µM) and oleanolic acid (IC_{50}= 7.5 ± 0.3 µM) and the dimer of rosmarinic acid, rabdosiin. The later not only was the most potent isolated compound towards RNA H activity (IC_{50}= 2.16 ± 0.11 µM) but also showed a very good inhibition of RDDP function (IC_{50}= 4.0 ± 0.8 µM) and therefore is a RT dual inhibitor.

As ursolic, oleanolic and pomolic acids represented the 0.5 % of the total DCM extract of *O. sanctum*, we can assume that the anti RNase H activity of the extract is due to this three compounds and to a lesser extent to another metabolite, tetradecyl ferulate (IC_{50}= 12.1 ± 1.1). We decided to focus our attention on tetradecyl ferulate for which, as far as we know, no biological studies have been reported. In addition, the synthetic accessibility of ferulic acid derivatives increased their appeal as lead compounds for potential anti HIV-1 agents development. Thus, a series of ferulic and caffeic acid esters and amides were synthesized. Among the synthesized compounds, *n*-oleyl caffeate (RNase H IC_{50} = 1.06 µM, RDDP IC_{50} = 1.6 µM), N-oleylcaffeamide (RNase H IC_{50}= 0.68 µM, RDDP IC_{50} = 2.3 µM), and geranylgeranyl caffeate (RNase H IC_{50} = 1.04 µM, RDDP IC_{50}= 1.5 µM) were the most active. Also, these compounds were able to inhibit both the RT-associated functions. Molecular modelling studies, together with Yonetani-Theorell analysis, demonstrated that N-oleylcaffeamide is able to bind both RNase allosteric site and NNRTI binding pocket. Thus, N-oleylcaffeamide and analogues may offer a new class of interesting HIV-1 RT inhibitor as lead compounds for the further optimization.

As regards *T. cordifolia*, its RNase H inhibitory potential is mainly due to a triterpenoid, lupeol (**22**) and to a lesser extent to 11-oxo-β- amyrin (**23**).

The RNase H inhibitory activity of all the isolated triterpenoids, except for betulinic acid [260], have been reported for the first time.

Another target of interest was the Human Rhinovirus (HRV). We have found that the DCM extract of the Sardinian plant, *Bupleurum fruticosum,* was able to inhibit the replication of the serotypes HRV-14 and HRV-39 at a relatively low concentration of 12.5 and 3.1 µg/ml, with low cytotoxicity against HeLa cells (EC_{50} = 125 µg/ml). The selective index (SI) of the extract was 10 for the group B Rhinovirus (HRV-14) and 40 for the group A (HRV-39). Bioguided isolation yielded ten compounds of which fruticotriol (**31**) and (-)-eucamanol (**40**) are new to the literature. The polyacetylene *cis*-9,17-octadecadiene-12,14-diyne-1,16-diol was the most potent inhibitor of HRV-39 replication with a EC_{50} of 0.5 µg/ml but the cytotoxicity was relatively high (4 µg/ml).

Among the phenylpropanoids, the most active was compound **34** with a EC_{50} of 0.9 µg/ml against HRV 39 and moderate cytotoxicity (7.6 µg/ml). SAR of compounds **33**-**39** revealed that inhibition of replication strictly depending on the methoxylation of phenyl ring and on the nature of ester alkyl chain. Interestingly, the compounds are able to inhibit only HRV-39 replication, indicating a probable selective capsid-binding towards the group A strain. Plaque inhibition assay using compound **34** suggests that it behave as capsid binder towards HRV39 and also acts by another mode of action, probably uncoating of viral genome.

The third field of interest was aimed to search compounds able to interact with $GABA_A$ receptor. We found that the methanol extract obtained from the roots of *W. somnifera* was able to enhance the amplitude of $GABA_A$-induced inhibitory postsynaptic currents ($IPSC_S$) by 38% ± 11 at the dose of 400 µg/ml. Nine compounds were isolated from MeOH extract of *W. somnifera*. The steroidal lactones withasomniferolide A (**41**) and withasomniferolide B (**42**) are new molecules and 1,5-di-*O*-feruloylpentanediol (**43**) is reported from a natural source for the first time. Since compounds **44**-**46** have been obtained as not separable mixture, with the aim to test them individually, they were synthesized. Due to the low amount in the extract, also compound **43** was synthesized.

Docosanyl ferulate (**46)** enhanced the amplitude of IPSCs by 37% ± 14. In contrast octadecyl ferulate (**44)** and withasomniferolide B (**42**) decreased the amplitude of IPSCs by 36% ± 9 and 30% ± 7. From these results seems that the observed $GABA_A$ modulation of MeOH

extract was due to docosanyl ferulate (**46**). Small change in structure may alter the binding to GABA$_A$ receptor as observed with compounds **46** and **44**, both are similar in structure but had opposite activity. This is also evidenced from the fact that other compounds form the plant (**41, 48,** and **49**) which shares similar structure with withasomniferolide B (**42**) had no significant effect over IPSCs. Absence of GABA$_A$ modulatory activity of withasomniferolide A (**41**) could be due to its instability in aqueous solution. Further studies are needed to evaluate the binding site, GABA$_A$ receptor or allosteric site, as well the intrinsic activity of compounds **42**, **44**, and **46**.

Chapter 7 Materials and Methods

7.1 Instruments

NMR Experiments- NMR spectra were recorded at 25 °C on Unity Inova 500NB high-resolution spectrometer (Agilent Technologies, CA, USA) operating at 500 MHz for ^{1}H and 100 MHz for ^{13}C, respectively. Compounds were measured in $CDCl_3$ or CD_3OD and the spectra referenced against residual non-deuterated solvents.

Mass Experiment-HR-ESIMS were measured on a Agilent 6520 Time of Flight (TOF) MS instrument while ESIMS experiments were performed on a Varian 1200 L triple quadrupole. ESIMS were measured on a AB Sciex 3200 QTrap LC-MS/MS triple quadrupole instrument. Also, mass spectra was recorded on Agilent 6850 GC coupled with mass detector 5973 and 7683B series injector autosampler (Agilent technologies).

Methods of Chromatography- Coloumn chromatography was carried out under TLC monitoring using silica gel (40-63 μm, Merck), and Sephadex LH-20 (25-100 μm, Pharmacia). For vacuum-liquid chromatography (VLC), silica gel (40-63 μm) (Merck) was used. TLC was performed on silica gel 60 F_{254} or RP-18 F_{254} (Merck).

Semi-preparative HPLC was conducted by means of a Varian 920 LH instrument fitted with an autosampler module with a 1000 μl loop. The columns were a 250 x 10 mm Spherisorb 223 silica, particle size 5 μm (Waters) and a 250 x 10 mm Polaris C-18-A, particle size 5 μm (Varian).

All melting points were determined on a Köfler apparatus and are uncorrected

Optical rotations were measured in $CHCl_3$ or MeOH at 25 °C using a Perkin-Elmer 241 polarimeter.

UV spectra were recorded on a GBC Cintra 5 spectrophotometer.

Antioxidant assay- Multimode plate reader: Biotek Synergy HT.

7.2 Methodology of isolation for *Ocimum sanctum*

7.2.1 Plant material

Dried leaves of *O. sanctum* were procured in August, 2014 from Vedshree Ayurvedic Medical, Nashik (India). Plant material was identified by Dr. N V Malpure (Dept. of Botany, SSGM College of Science, Kopargaon, India). The voucher specimen was deposited in the Herbarium of the Department of Life and Environmental Science, Drug Sciences Section, University of Cagliari.

7.2.2 Extraction method

500 g of completely dried and powdered leaves were subjected to extraction. Extraction was successively carried out using DCM and Methanol at room temperature. Repetitive cycles of percolation (during the day) and maceration (during the night) were implemented. Solvents were evaporated under reduced pressure using rotatory evaporator. 8.22 g of DCM extract and 22.81 g of MeOH extract were obtained at the end of percolation.

7.2.3 Isolation of secondary metabolites from DCM extract

The CH_2Cl_2 extract (8.22 g) was subjected to vacuum-liquid chromatography (VLC) (silica gel, 100 g, 40 - 63 μm) using a step gradient of *n*-hexane/CH_2Cl_2/EtOAc/MeOH (7.5: 2.5: 0 : 0 to 0: 0: 7.5: 2.5, 300 ml each) to yield 7 main fractions (F1-F7).

An aliquot of fraction F4 (2.50 g, eluted with CH_2Cl_2, 300 ml) was separated by column chromatography (CC) over silica gel using CH_2Cl_2/EtOAc (9.5: 0.5) as eluent to obtain eight subfractions (F4.1-F4.8). F4.5 (35 mg) was chromatographed by RP-HPLC using acetonitrile/H_2O (8.5:1.5, flow 2 ml/min) to give **vanillin (6),** (3.4 mg, t_R 7.1 min). F4.6 (32 mg) was treated with ACN and the insoluble portion resulted **tetradecyl ferulate** (**8**), (8.5 mg). The ACN soluble portion was purified by RP-HPLC using acetonitrile/H_2O (8.5:1.5, flow 2 ml/min) to yield **vanillin,** (2.3 mg, t_R 7.1 min). F4.7 (160 mg) was separated by CC on Sephadex LH-20 with MeOH as eluent to give two subfractions (F4.7.1-F4.7.2). F4.7.1 yielded **stigmasterol (5),** (28 mg) while F4.8.2 (9.0 mg) was further chromatographed by RP-HPLC using *n*-hexan/EtOAc

(7:3, flow 2.3 ml/min) to give **ferulaldehyde (7),** (2.0 mg, t_R 13.0 min). An aliquot (20 mg) of F4.8 (1.20 g) was purified by RP-HPLC using MeOH/H_2O/trifluoroacetic acid (TFAA) (9.7:0.3:0.1, flow 2 ml/min) to yield **oleanolic acid (1),** (3.0 mg, t_R 11.5 min) and **ursolic acid (2),** (2.3 mg, t_R 12.5 min).

F5 (840 mg), eluted with CH_2Cl_2/EtOAc (7.5: 2.5, 300 ml), was subjected to column chromatography over silica gel to give six subfractions (F5.1-F5.6). F5.1 (80 mg) was purified by Sephadex LH-20 (MeOH) to give **betulinic acid (4),** (6.5 mg). An aliquot (50 mg) of F5.3 (210 mg) was subjected to RP-HPLC using MeOH/H_2O/trifluoroacetic acid (TFAA) (9.7:0.3:0.1, flow 2 ml/min) to yield **pomolic acid (3),** (7.6 mg, t_R 8.5 min) and ursolic acid (4.6 mg, t_R 12.5 min). An aliquot (45 mg) of F5.6 (170 mg) was purified by RP-HPLC using MeOH/H_2O/trifluoroacetic acid (TFAA) (9.7:0.3:0.1, flow 2 ml/min) to yield **oleanolic acid,** (7.8 mg, t_R 11.5 min) and **ursolic acid,** (9.9 mg, t_R 12.5 min). Using the same condition described above, RP-HPLC analysis indicated that F6 (1.06 g) and F7 (1.58g) contained a mixture of **2** and **3** in a ratio of about 3:1.
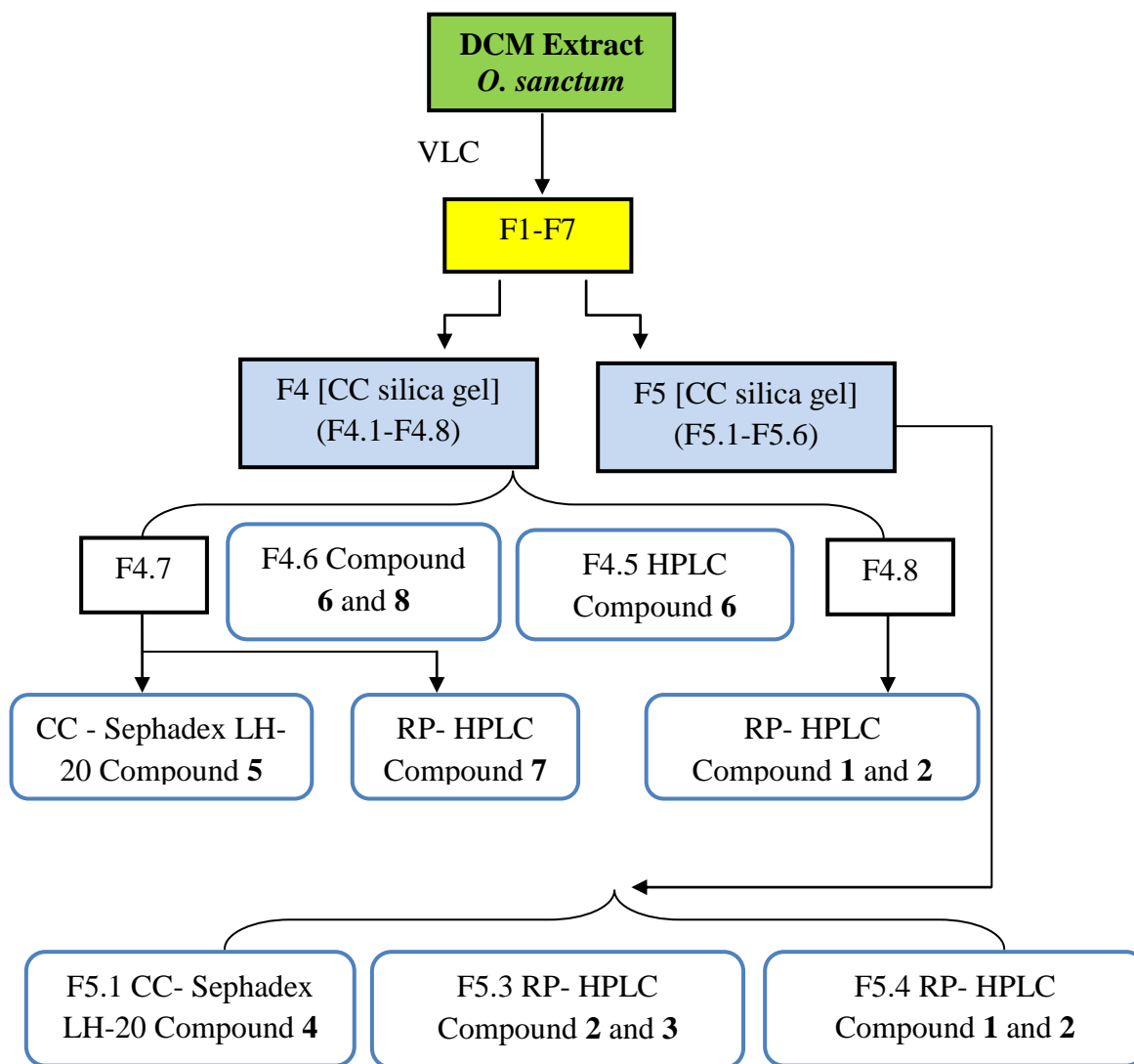
Fig.108: Scheme of isolation of secondary metabolites from DCM extract of *O. sanctum*

7.2.4 Isolation of secondary metabolites from MeOH extract of *O. sanctum*

MeOH extract was subjected to VLC (Reverse Phase silica gel, 100 g) using a step gradient of H_2O/MeOH/ACN (5: 7.5: 10 to 7.5: 5: 2.5: 0, 250 ml each) to yield 5 main fractions (F1-F5). Since the entire tested fraction showed comparable low IC_{50} values (1.67 − 2.86 µg/ml), they were injected in HPLC in order to verify the chemical profile of each fraction. We used an RP-18 analytical column and as eluents MeOH: H_2O: Trifluoroacetic acid (70: 30: 0.5), flow: 2.5 ml/min. The wavelengths were 250 and 360 nm.

HPLC analysis revealed that all the fractions contained the same compounds, but in different ratio (data not shown), we decided to isolated the two major compounds by different chromatographic techniques such as column chromatography (silica gel and Sephadex LH-20) and semi-preparative HPLC. Rabdosin **(19)** and rosmarinic acid **(20)** were the 2 compounds isolated from MeOH extract. Structures of the compounds were confirmed by1D and 2D NMR.
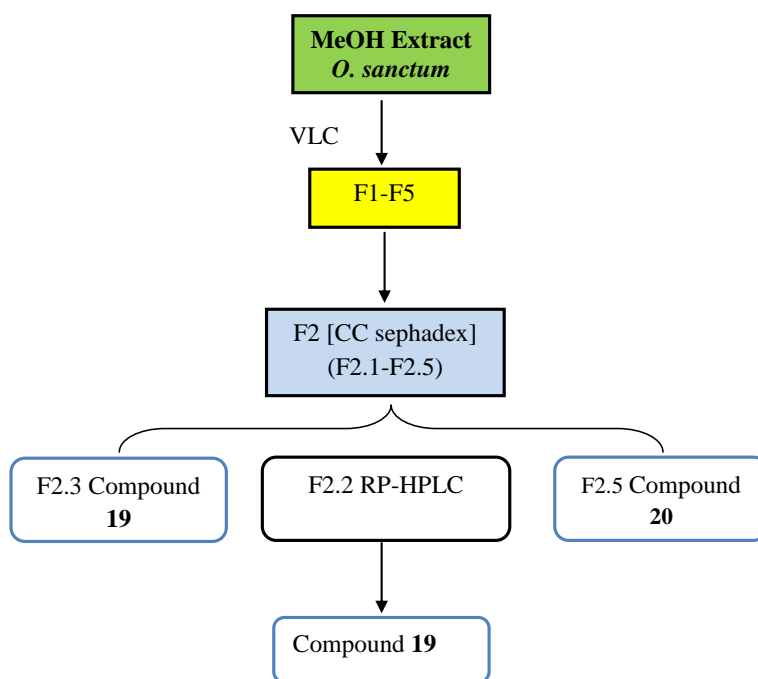
Fig.109: Scheme of isolation of secondary metabolites from MeOH extract of *O. sanctum*

7.2.5 NMR spectra of compounds Isolated from *O. sanctu*m

Compound 1
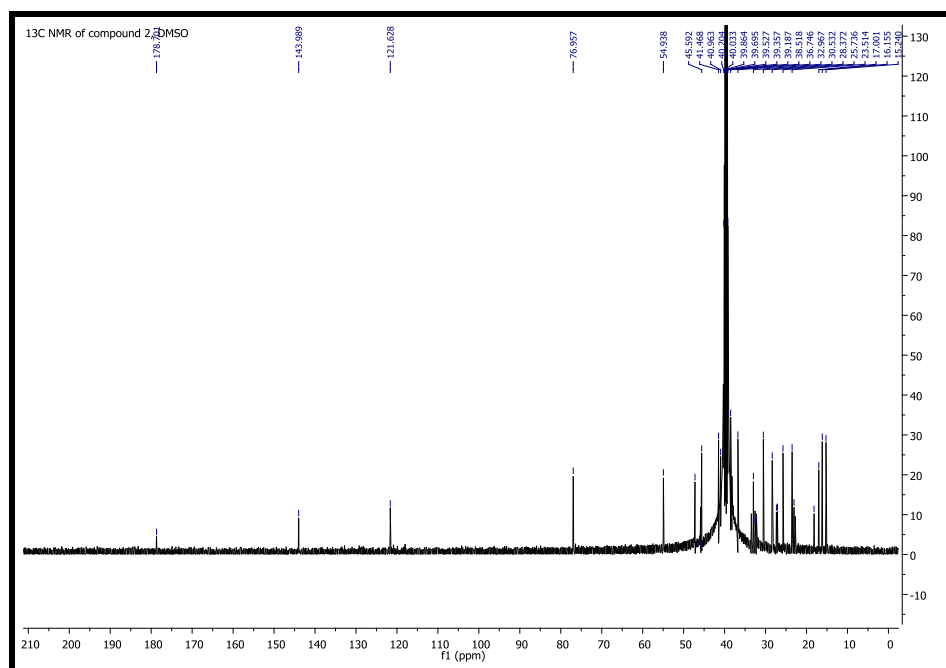
Fig.110:^{13}C NMR spectrum of compound 1 (oleanolic acid), 500MHz, DMSO

Compound 2
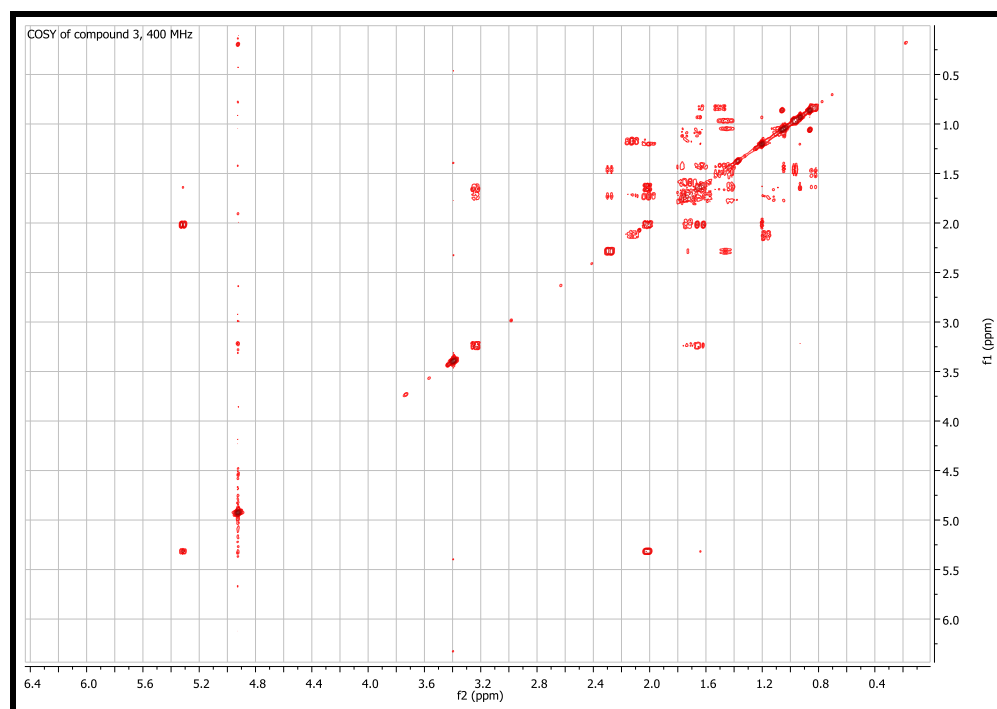
Fig.111: DQF-COSY spectrum of compound **2** (ursolic acid), 400MHz, CD$_4$O
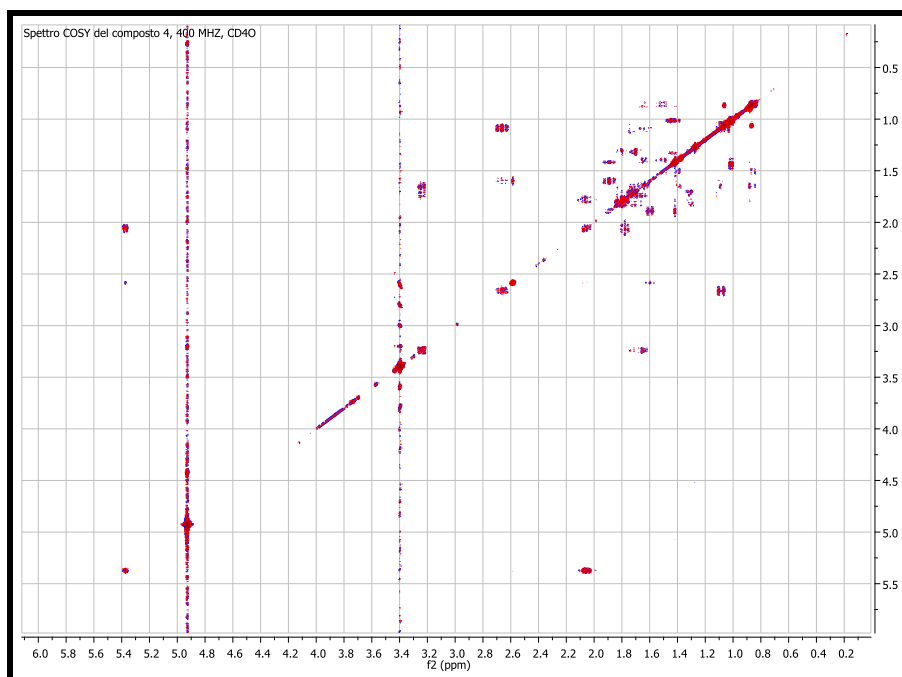
Compound 3

Fig.112: COSY spectrum of compound **3** (pomolic acid), 400MHz, CD$_4$O
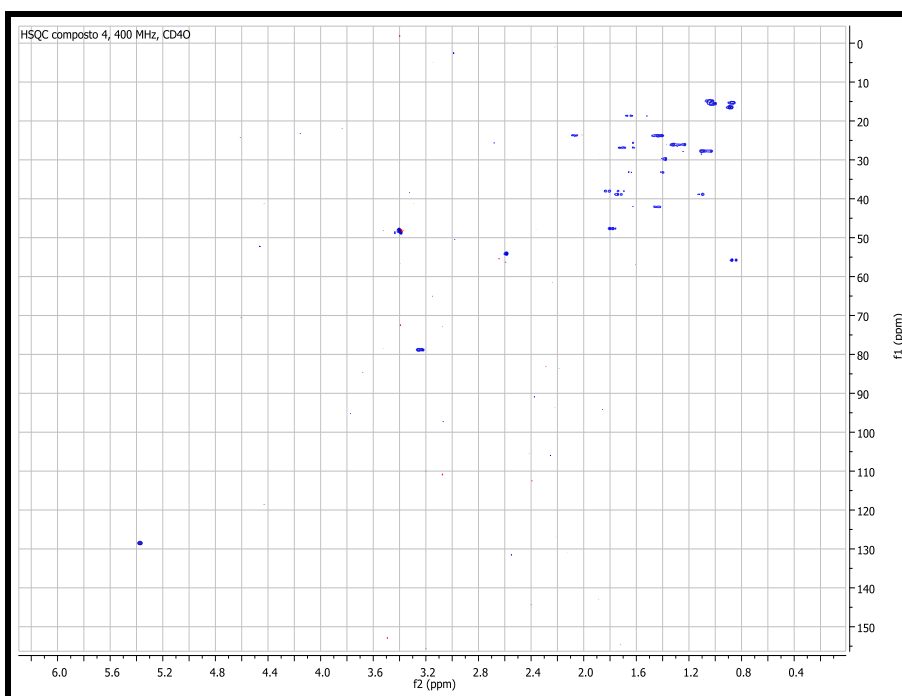
Fig.113: HSQC spectrum of compound **3** (pomolic acid), 400MHz, CD$_4$O
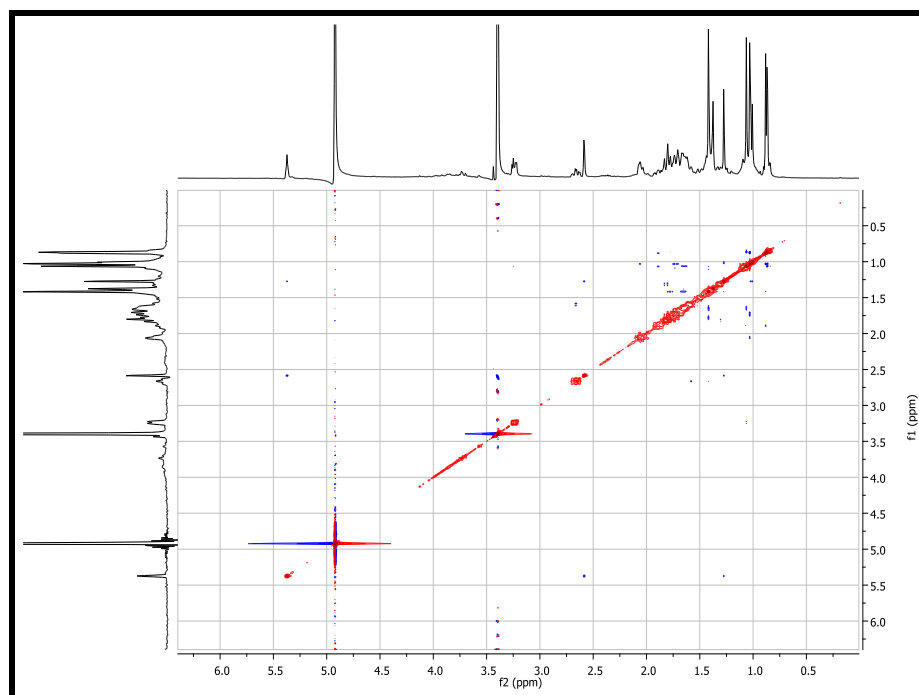
Fig.114: ^{1}H-^{1}H ROESY spectrum of compound **3** (pomolic acid), 400MHz, CD$_4$O

Compound 4
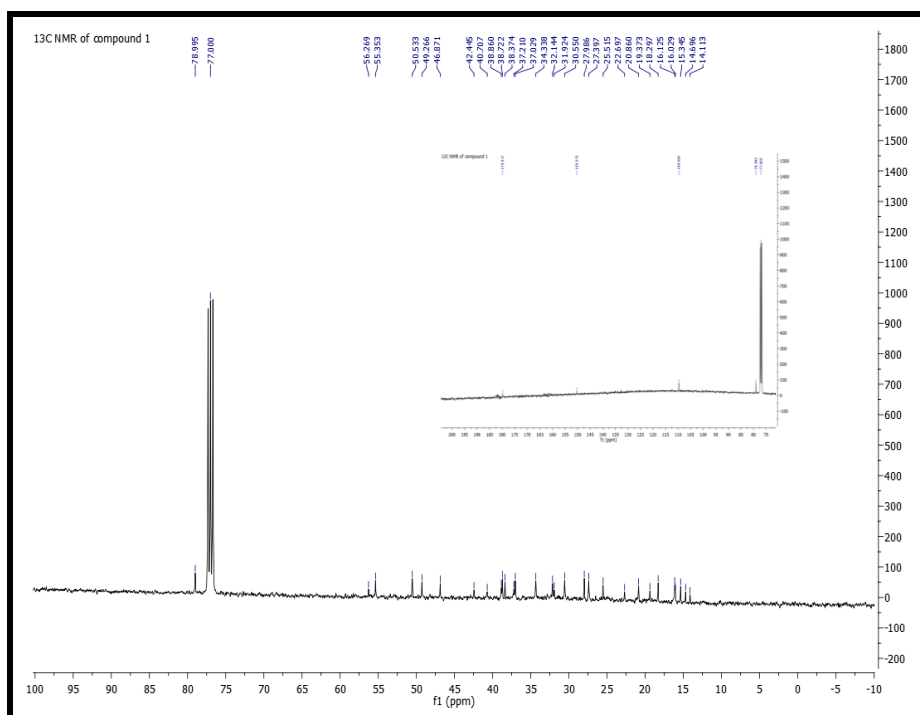
Fig.**115:** ^{13}C NMR spectrum of compound **4** (betulinic acid), 400MHz, CDCl$_3$
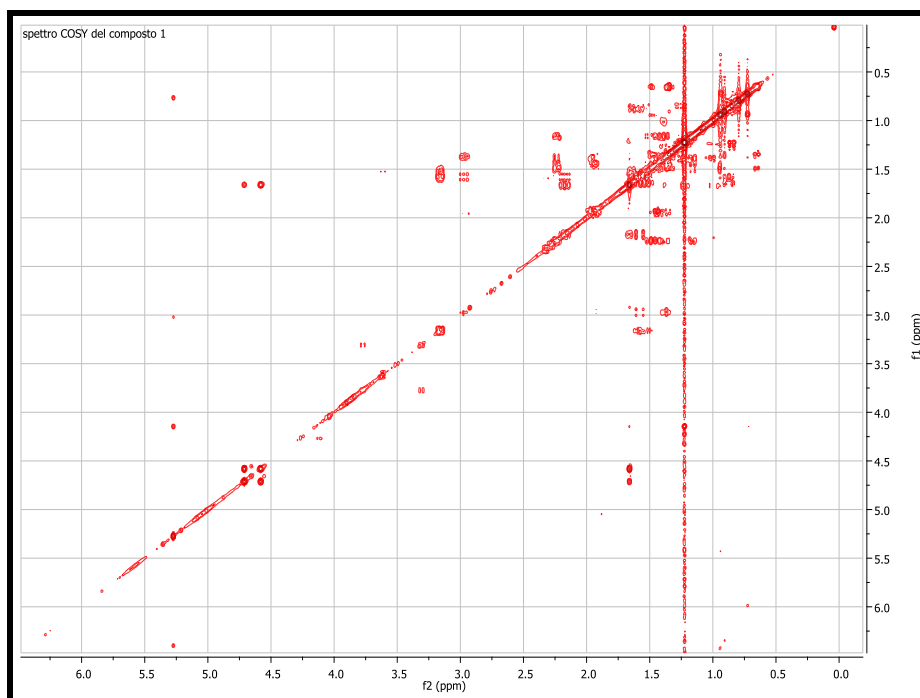
Fig.116: DQF-COSY spectrum of compound **4**, (betulinic acid), 400MHz, CDCl$_3$.

Fig.117: HSQC spectrum of compound **4**, (betulinic acid), 400MHz, CDCl₃.

Compound 5

Fig.118: COSY spectrum of compound **5** (stigmasterol), 400 MHz, CDCl₃
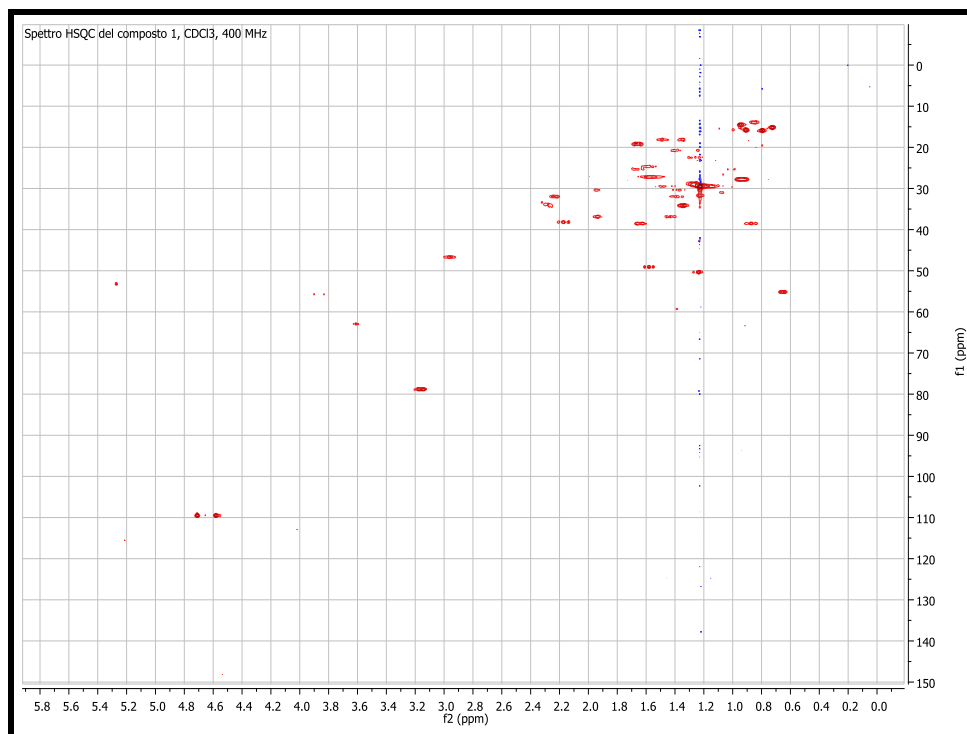
Fig.119: HSQC spectrum of compound **5** (stigmasterol), 400 MHz, CDCl₃
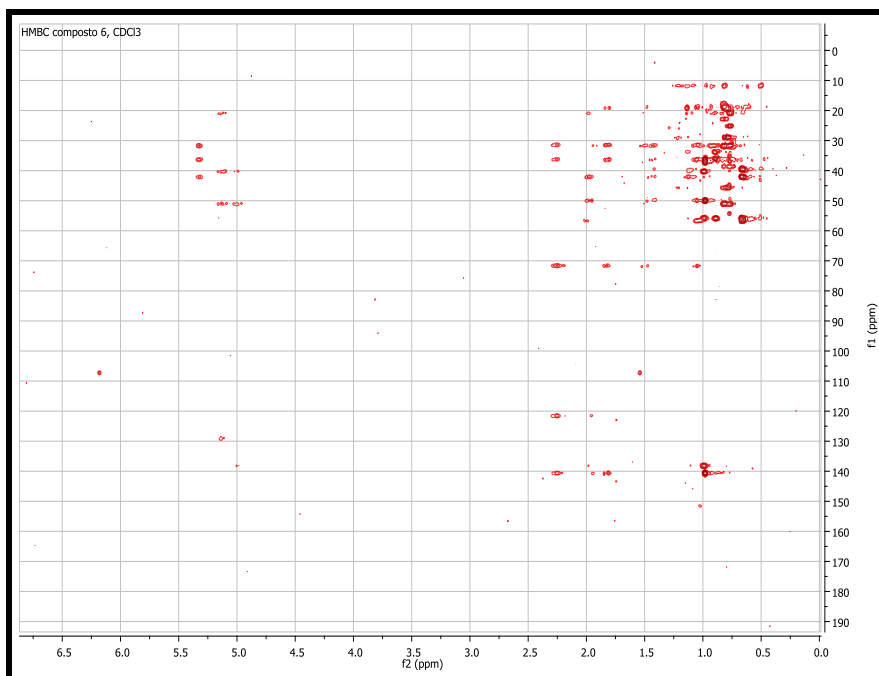
Fig.120: HMBC spectrum of compound **5**(stigmasterol), 400 MHz, CDCl$_3$
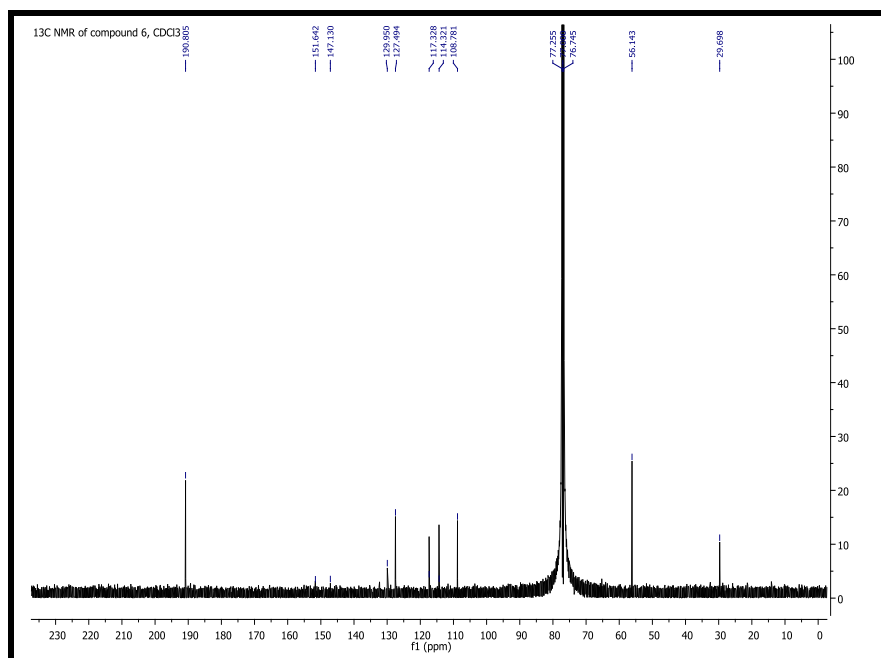
Compound 6

Fig.121: ^{13}C NMR spectrum of compound **6** (vanillin), 100MHz, CDCl$_3$

Compound 19
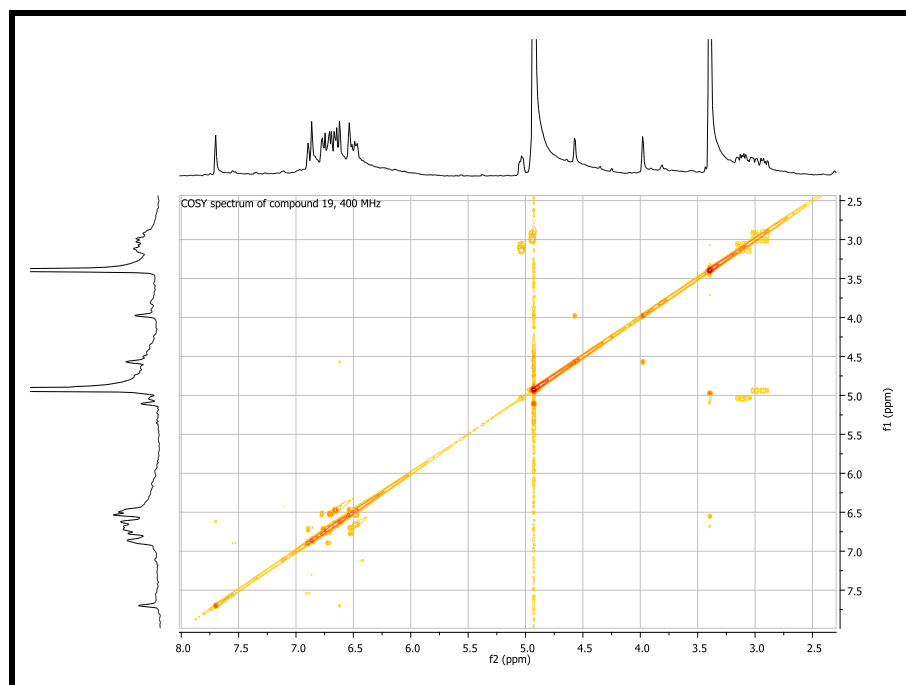
Fig.122: COSY spectrum of compound **19** (rabdosiin), 400 MHz, CD$_4$O
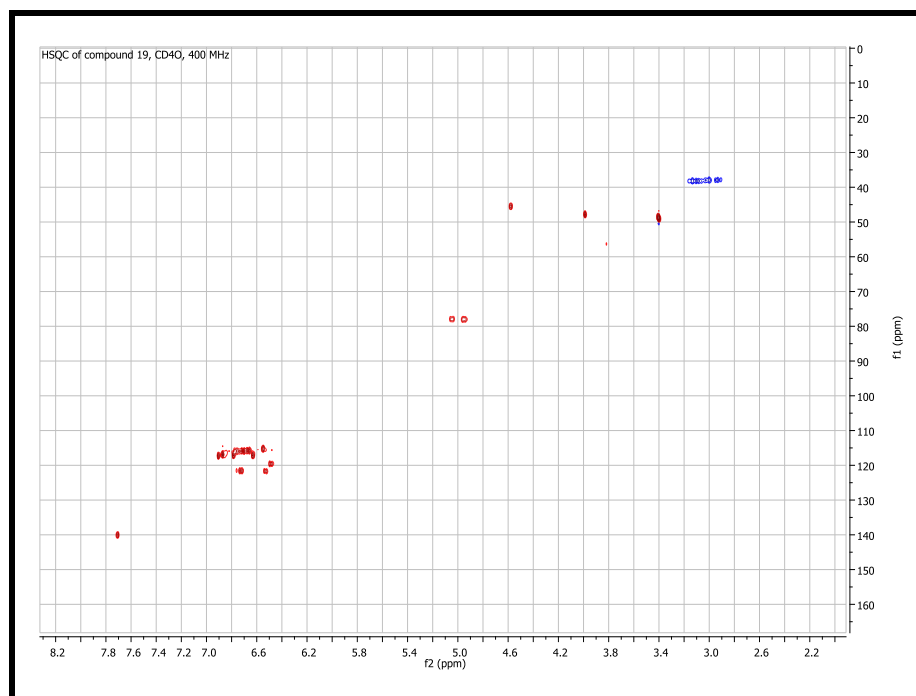
Fig.123: HSQC of compound **19** (rabdosiin), 400 MHz, CD$_4$O
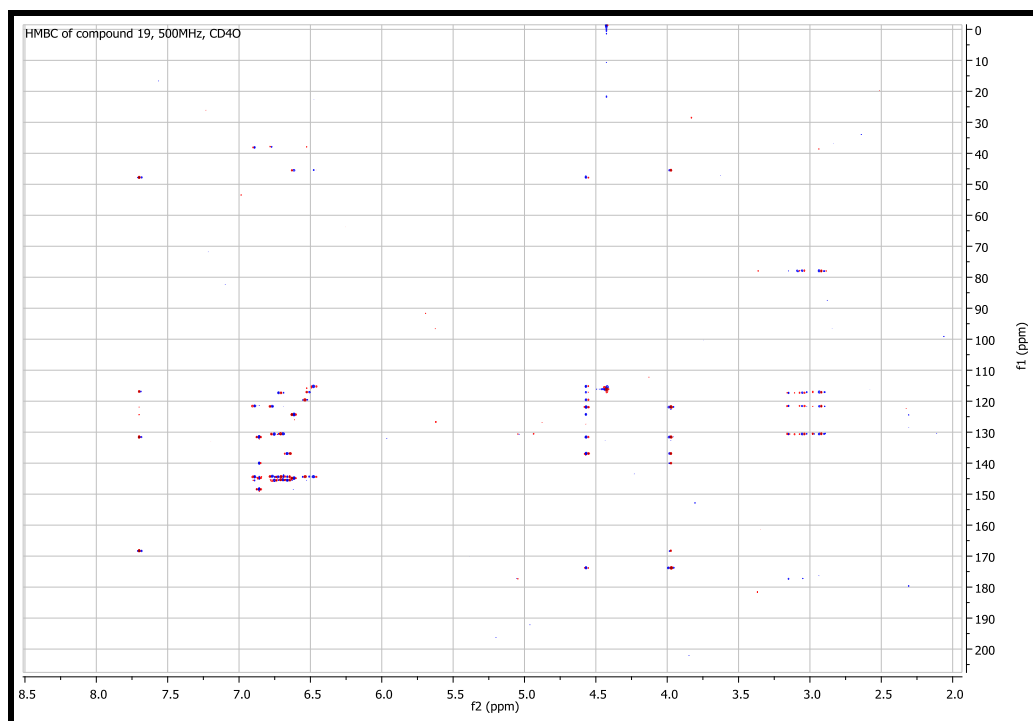
Fig.124: HMBC of compound **19** (rabdosiin), 500 MHz, CD$_4$O

7.2.6 Synthesis of compounds (Ferulic acid derivatives)

7.2.6.1 General procedure for the synthesis of 4′-ethyloxycarbonyloxy ferulate 11b-l

Ethyl chloroformate (0.76 ml, 8 mmol) and TEA (1.1 ml, 8 mmol) were added to a suspension of ferulic acid (0.737 g, 3.8 mmol) in DCM (10 ml) and stirred for 1 h at -15 °C until TLC analysis revealed a total consumption of starting material. Alcohol (8 mmol) and DMAP (0.030 g, 0.08 mmol) were then added and the mixture stirred at room temperature for 6 h. The solvent was evaporated under reduced pressure to afford the crude product. This product was purified by silica gel column chromatography using mixtures of *n*-hexane/ethyl acetate or toluene/ethyl acetate as eluents.

7.2.6.2 General procedure for the synthesis of ferulate 12b-l

To a solution of the each protected feruloyl ester **11b-l** (2.5 mmol) in DCM (10 ml) was added 80 equiv of piperidine (80 mmol) at 0 °C, and the reaction mixture was stirred at room temperature for 3h. The feruloyl ester was purified by VLC (silica gel) or Sephadex LH-20.

7.2.6.3 General procedure for the synthesis of amide of ferulic acid 13f

Ethyl chloroformate (0.76 ml, 8 mmol) and TEA (1.1 ml, 8 mmol) were added to a suspension of ferulic acid (0.737 g, 3.8 mmol) in DCM (10 ml) and stirred for 1 h at -15 °C until TLC analysis revealed a total consumption of starting material. Oleyl amine (17.4 ml, 80 mmol) and DMAP (0.030g, 0.08 mmol) were then added and the mixture stirred at room temperature for 6 h. On completion, the solvent was evaporated *in vacuum*, and the crude product purified by Sephadex LH 20 with MeOH as eluent to give N-oleylferuloylamide (**13f**).

7.2.6.4 General procedure for the synthesis of (*E*)-3,4-diethyloxycarbonyloxy caffeate 16f,g

Ethyl chloroformate (1.52 ml, 16.7 mmol) and TEA (2.2 ml, 16 mmol) were added to a suspension of caffeic acid (0.737 g, 3.8 mmol) in DCM (10 ml) and stirred for 1 h at -15 °C until TLC analysis revealed a total consumption of starting material. Alcohol (8 mmol) and DMAP (0.030 g, 0.08 mmol) were then added and the mixture stirred at room temperature for 6 h. The solvent was evaporated under reduced pressure to afford the crude product. This product was purified by VLC (silica gel) using mixtures of *n*-hexane/ethyl acetate or toluene/ethyl acetate as eluents.

7.2.6.5 General procedure for the synthesis of caffeate 17f, g

To a solution of the each protected caffeoyl ester **16f,g** (2.5 mmol) in DCM (10 ml) was added 80 equiv of piperidine (80 mmol) at 0 °C, and the reaction mixture was stirred at room temperature for 3h. The ester of caffeic acid was purified by VLC (silica gel) or Sephadex LH-20.

7.2.6.6 General procedure for the synthesis of N-caffeamide 18f

Ethyl chloroformate (1.52 ml, 16.7 mmol) and TEA (2.2 ml, 16 mmol) were added to a suspension of caffeic acid (0.737 g, 3.8 mmol) in DCM (10 ml) and stirred for 1 h at -15 °C until TLC analysis revealed a total consumption of starting material. Oleyl amine (17.4 ml, 80 mmol) and DMAP (0.030 g, 0.08 mmol) were then added and the mixture stirred at room temperature for 6 h. On completion, the solvent was evaporated *in vacuo*, and the crude product purified by Sephadex LH 20 with MeOH as eluent to give N-oleylcaffeamide (**18f**).

7.2.7 Characterization of the synthesized compounds

*(E)-4-Ethyloxycarbonyloxy-3-methoxy decyl cinnamate (**11b**)*. White solid, yield: 73%; column chromatography mobile phase: toluene/ethyl acetate (9.5 : 0.5); ^{1}H NMR (500 MHz, CDCl$_3$): δ_H 7.63 (d, 1H, J = 16 Hz, H-3), 7.01 (m, 3H, H-2′, H-5′, H-6′), 6.38 (d, 1H, J = 16 Hz, H-2), 4.32 (q, 2H, J = 7.5 Hz, OC$\underline{H_2}$-CH$_3$), 4.19 (t, 2H, J = 6.8 Hz, H-1″), 3.87 (s, 3H, OCH$_3$-3′), 1.69 (m, 2H, H-2″), 1.39 (t, 3H, J = 7.5 Hz, OCH$_2$-$\underline{CH_3}$), 1.39 (m, 2H, H-3″), 1.25 (m, 12H, H-4″-H-9″), 0.87 (t, 3H, J = 6.8, Hz, H-10″).

*(E)-4-Ethyloxycarbonyloxy-3-methoxy dodecyl cinnamate (**11c**)*. White semi-solid, yield: 75%; column chromatography mobile phase: toluene/ethyl acetate (9.5 : 0.5); ^{1}H NMR (500 MHz, CDCl$_3$): δ_H 7.63 (d, 1H, J = 16 Hz, H-3), 7.03 (m, 3H, H-2′, H-5′, H-6′), 6.38 (d, 1H, J = 16 Hz, H-2), 4.33 (q, 2H, J = 7.5 Hz, OC$\underline{H_2}$-CH$_3$), 4.19 (t, 2H, J = 6.8 Hz, H-1″), 3.89 (s, 3H, OCH$_3$-3′), 1.69 (m, 2H, H-2″), 1.36 (t, 3H, J = 7.5 Hz, OCH$_2$-$\underline{CH_3}$), 1.35 (m, 2H, H-3″), 1.26 (m, 16H, H-4″-H-11″), 0.87 (t, 3H, J = 6.8, Hz, H-12″).

*(E)-4-Ethyloxycarbonyloxy-3-methoxy esadecyl cinnamate (**11d**)*. White solid, yield, 70%; column chromatography mobile phase: toluene/ethyl acetate (9.5 : 0.5); ^{1}H NMR (500 MHz, CDCl$_3$): δ_H 7.64 (d, 1H, J = 16 Hz, H-3), 7.02 (m, 3H, H-2′, H-5′, H-6′), 6.32 (d, 1H, J = 16 Hz, H-2), 4.32 (q, 2H, J = 7.5 Hz, OC$\underline{H_2}$-CH$_3$), 4.20 (t, 2H, J = 6.8 Hz, H-1″), 3.89 (s, 3H, OCH$_3$-3′), 1.67 (m, 2H, H-2″), 1.39 (t, 3H, J = 7.5 Hz, OCH$_2$-$\underline{CH_3}$), 1.36 (m, 2H, H-3″), 1.26 (m, 24H, H-4″-H-15″), 0.88 (t, 3H, J = 6.8, Hz, H-16″).

*(E)-4-Ethyloxycarbonyloxy-3-methoxy octadecyl cinnamate (**11e**)*. White solid, yield: 79%; column chromatography mobile phase: toluene/ethyl acetate (9.5 : 0.5); ^{1}H NMR (500 MHz,

CDCl$_3$): δ_H 7.62 (d, 1H, J = 16 Hz, H-3), 7.10 (m, 3H, H-2′, H-5′, H-6′), 6.37 (d, 1H, J = 16 Hz, H-2), 4.30 (q, 2H, J = 7.5 Hz, OC<u>H</u>$_2$-CH$_3$),4.19 (t, 2H, J = 6.8 Hz, H-1″), 3.86 (s, 3H, OCH$_3$-3′), 1.69 (m, 2H, H-2″), 1.37 (t, 3H, J = 7.5 Hz, OCH$_2$-<u>CH</u>$_3$), 1.36 (m, 2H, H-3″), 1.25 (m, 28H, H-4″-H-17″), 0.87 (t, 3H, J = 6.8, Hz, H-18″).

(E)-4-Ethyloxycarbonyloxy-3-methoxy oleyl cinnamate (11f). White solid, yield: 68%; column chromatography mobile phase: toluene/ethyl acetate (9.5 : 0.5); ^{1}H NMR (500 MHz, CDCl$_3$): δ_H 7.65 (d, 1H, J = 16 Hz, H-3), 7.14 (m, 3H, H-2′, H-5′, H-6′), 6.41 (d, 1H, J = 16 Hz, H-2), 5.38 (m, 2H, H-9″, H-10″), 4.32 (q, 2H, J = 7.5 Hz, OC<u>H</u>$_2$-CH$_3$), 4.2 (t, 2H, J = 6.8 Hz, H-1″), 3.87 (s, 3H, OCH$_3$-3′), 2.10 (4H, H-8″, H11″), 1.80 (m, 2H, H-2″), 1.39 (t, 3H, J = 7.5 Hz, OCH$_2$-<u>CH</u>$_3$), 1.34 (m, 2H, H-3″), 1.26 (m, 4H, H-4″-H-5″), 1.29 (18H, H-6″, H-7″, H-12″-H-17″), 0.9 (t, 3H, J = 6.8, Hz, H-18″);

(E)-4-Ethyloxycarbonyloxy-3-methoxy-O-geranylgeranyl cinnamate (11g). White solid yield: 70 %; column chromatography mobile phase: toluene/ethyl acetate (9.5 : 0.5); ^{1}H NMR (500 MHz, CDCl$_3$): δ_H 7.63 (d, 1H, J = 16 Hz, H-3), 7.13 (br s, 1H, H-2′), 7.09 (m, 2H, H-5′, H-6′), 6.39 (d, 1H, J = 16 Hz, H-2), 5.43 (t, 2H, J = 7.0 Hz, H-2″), 5.09 (m, 1H, H-14″), 5.07 (4H, m, H-6″, H-10″), 4.70 (d, 2H, J =7.5 Hz, H-1″), 4.31 (q, 2H, J = 7.5 Hz, OC<u>H</u>$_2$-CH$_3$), 3.87 (s, 3H, OCH$_3$-3′), 2.16 (m, 2H, H-4″), 2.11(m, 2H, H-8″), 2.06 (m, 2H, H-12″), 1.98 (m, 6H, H-5″, H-9″, H-13″), 1.79 (s, 3H, H-20″), 1.67 (s, 3H, H-17″), 1.62 (s, 3H, H-16″), 1.59 (s, 6H, H-18″, H-19″), 1.38 (t, 3H, J = 7.5 Hz, OCH$_2$-<u>CH</u>$_3$).

2-Phenylethyl (E)-4-ethyloxycarbonyloxy-3-methoxy cinnamate (11h). White solid, yield: 79 %; column chromatography mobile phase: *n*-hexane/ethyl acetate (7 : 3); ^{1}H NMR (500 MHz, CDCl$_3$): δ_H 7.70 (d, 1H, J = 15.6 Hz, H-3), 7.36 (m, 5H, H-4″-H8″), 7.2 (m, 3H, H-2′, H-5′, H-

6′), 6.44 (d, 1H, J = 15.6 Hz, H-2), 4.51 (t, 2H, J = 6.8 Hz, H-1″), 4.39 (q, 2H, J = 7.5 Hz, O<u>CH$_2$</u>-CH$_3$), 4.0 (s, 3H, OCH$_3$-3′), 3.10 (t, 2H, J = 6.8 Hz, H-2″), 1.46(t, 3H, J = 7.5 Hz, OCH$_2$-<u>CH$_3$</u>).

*2-(p-Methyl-phenyl)ethyl (E)-4-ethyloxycarbonyloxy-3-methoxy cinnamate (**11i**).* White solid, yield: 76 %; column chromatography mobile phase: *n*-hexane/ethyl acetate (8.5 : 1.5); ^{1}H NMR (500 MHz, CDCl$_3$): δ_H 7.63 (d, 1H, J = 15.6 Hz, H-3), 7.15 (m, 7H, H-2′, H-5′, H-6′, H-4″-H-5″, H-7″, H8″), 6.39 (d, 1H, J = 15.6 Hz, H-2), 4.42 (t, 2H, J = 6.8 Hz, H-1″), 4.33 (q, 2H, J = 7.5 Hz, O<u>CH$_2$</u>-CH$_3$), 3.88 (s, 3H, OCH$_3$-3′), 2.99 (t, 2H, J = 6.8 Hz, H-2″), 2.34 (s, 3H, CH$_3$-6″), 1.39 (t, 3H, J = 7.5 Hz, OCH$_2$-<u>CH$_3$</u>).

*2-(o-Methylphenyl)ethyl (E)-4-ethyloxycarbonyloxy-3-methoxy cinnamate (**11j**).* White solid, yield: 79 %; column chromatography mobile phase: *n*-hexane/ethyl acetate (8.5 : 1.5); ^{1}H NMR (500 MHz, CDCl$_3$): δ_H 7.64 (d, 1H, J = 15.6 Hz, H-3), 7.16 (m, 7H, H-2′, H-5′, H-6′, H-5″-H8″), 6.38 (d, 1H, J = 15.6 Hz, H-2), 4.40 (t, 2H, J = 7 Hz, H-1″), 4.32 (q, 2H, J = 7.5 Hz, O<u>CH$_2$</u>-CH$_3$), 3.89 (s, 3H, OCH$_3$-3′), 3.03 (t, 2H, J = 7 Hz, H-2″), 2.39 (s, 3H, CH$_3$-4″), ″), 1.39 (t, 3H, J = 7.5 Hz, OCH$_2$-<u>CH$_3$</u>).

*2-(p-Chlorophenyl)ethyl (E)-4-ethyloxycarbonyloxy-3-methoxy cinnamate (**11k**).* White solid, yield: 80 %; column chromatography mobile phase: *n*-hexane/ethyl acetate (8.5 : 1.5); ^{1}H NMR (500 MHz, CDCl$_3$): δ_H 7.58 (d, 1H, J = 16 Hz, H-3), 7.27 (d, 2H, J = 8 Hz, H-5″, H-7″), 7.16 (d, 2H, J = 8 Hz, H-4″, H-8″), 7.08 (m, 2H, H-2′, H-6′), 7.12 (d, 1H, J = 8 Hz, H-5′), 6.32 (d, 1H, J = 16 Hz, H-2), 4.38 (t, 2H, J = 6.8 Hz, H-1″), 4.29 (q, 2H, J = 7.5 Hz, O<u>CH$_2$</u>-CH$_3$), 3.90 (s, 3H, OCH$_3$-3′), 2.96 (t, 2H, J = 6.8 Hz, H-2″), 1.36 (t, 3H, J = 7.5 Hz, OCH$_2$-<u>CH$_3$</u>).

2-(1-Naphthyl)ethyl (E)-4-ethyloxycarbonyloxy-3-methoxy cinnamate (11l). White solid, yield: 80 %; column chromatography mobile phase: *n*-hexane/ethyl acetate (8 : 2); ^{1}H NMR (500 MHz, CDCl$_3$): δ_H 8.15 (d, 1H, J = 8.5 Hz, H-11″), 7.88 (br d, 1H, J = 8 Hz, H-8″), 7.78 (br d, 1H, J = 7 Hz, H-6″), 7.61 (d, 1H, J = 16 Hz, H-3), 7.57 (m, 1H, H-10″), 7.50 (m, 1H, H-9″), 7.42 (m, 2H, H-4″,H-5″), 7.1 (m, 2H, H-2′, H-6′), 7.16 (d, 1H, J = 8, Hz, H-5′), 6.37 (d, 1H, J = 16 Hz, H-2), 4.57 (t, 2H, J = 7.5 Hz, H-1″), 4.33(q, 2H, J = 7.5 Hz, OC$\underline{H_2}$-CH$_3$), 3.89 (s, 3H, OCH$_3$-3′), 3.51 (t, 2H, J = 7.5 Hz, H-2″), 1.40 (t, 3H, J = 7.5 Hz, OCH$_2$-$\underline{CH_3}$).

Decyl ferulate (12b). White semi-solid, yield: 51%; VLC mobile phase: toluene/ethyl acetate (9.5 : 0.5); ^{1}H NMR (500 MHz, CDCl$_3$): δ_H 7.60 (d, 1H, J = 16 Hz, H-3), 7.06 (dd, 1H, J = 1.6, 8 Hz, H-6′), 7.02 (d, 1H, J = 1.6, Hz, H-2′), 6.90 (d, 1H, J = 8, Hz, H-5′), 6.28 (d, 1H, J = 16 Hz, H-2), 4.18 (t, 2H, J = 6.8 Hz, H-1″), 3.90 (s, 3H, OCH$_3$-3′), 1.69 (m, 2H, H-2″), 1.39 (m, 2H, H-3″), 1.25 (m, 12H, H-4″-H-9″), 0.87 (t, 3H, J = 6.8, Hz, H-10″); ^{13}C NMR (100 MHz, CDCl$_3$): δ_C 167.4 (C-1), 148.0 (C-3′), 146.9 (C-4′), 144.6 (C-3), 126.9 (C-1′), 122.9 (C-6′), 115.5 (C-2), 114.8 (C-5′), 109.4 (C-2′), 64.5 (C-1″), 55.8 (OCH$_3$), 31.8 (C-8″), 29.5 (C-5″ and C-6″), 29.2 (C-4″, C-7″), 28.7 (C-2″), 25.9 (C-3″), 22.6 (C-9″), 14.0 (C-10″); ESI mass (negative mode): 333 [M − H]⁻, 375 [M + ACN]⁻.

Dodecyl ferulate (12c). White solid, yield: 60%; m. p.: 55-56 °C; VLC mobile phase: toluene/ethyl acetate (9.5 : 0.5); ^{1}H NMR (500 MHz, CDCl$_3$): δ_H 7.60 (d, 1H, J = 16 Hz, H-3), 7.06 (dd, 1H, J = 1.6, 8 Hz, H-6′), 7.02 (d, 1H, J = 1.6, Hz, H-2′), 6.90 (d, 1H, J = 8, Hz, H-5′), 6.05 (s, 1H, OH), 6.28 (d, 1H, J = 16 Hz, H-2), 4.18 (t, 2H, J = 6.8 Hz, H-1″), 3.90 (s, 3H, OCH$_3$-3′), 1.69 (m, 2H, H-2″), 1.38 (m, 2H, H-3″), 1.26 (m, 16H, H-4″-H-11″), 0.87 (t, 3H, J = 6.8, Hz, H-12″); ^{13}C NMR (100 MHz, CDCl$_3$): δ_C 167.4 (C-1), 147.9 (C-3′), 146.8 (C-4′), 144.6

(C-3), 127.0 (C-1′), 123.0 (C-6′), 115.2 (C-2), 114.7 (C-5′), 109.3 (C-2′), 64.6 (C-1″), 55.9 (OCH$_3$), 31.9 (C-10″), 29.6, 29.5, 29.4, (C-5″- C-9″), 29.3 (C-4″), 28.7 (C-2″), 25.9 (C-3″), 22.6 (C-11″), 14.1 (C-12″); ESI mass (negative mode): 361 [M –H]⁻, 403 [M + ACN]⁻.

Hexadecyl ferulate (12d). White solid, yield: 65%; m. p.: 57-59 °C; VLC mobile phase: toluene/ethyl acetate (9.5 : 0.5); ^{1}H NMR (500 MHz, CDCl$_3$): δ_H 7.61 (d, 1H, J = 16 Hz, H-3), 7.07 (dd, 1H, J = 1.6, 8 Hz, H-6′), 7.03 (d, 1H, J = 1.6, Hz, H-2′), 6.91(d, 1H, J = 8, Hz, H-5′), 6.29 (d, 1H, J = 16 Hz, H-2), 5.90 (s, 1H, OH), 4.19 (t, 2H, J = 6.8 Hz, H-1″), 3.92 (s, 3H, OCH$_3$-3′), 1.69 (m, 2H, H-2″), 1.39 (m, 2H, H-3″), 1.26 (m, 24H, H-4″-H-15″), 0.88 (t, 3H, J = 6.8, Hz, H-16″); ^{13}C NMR (100 MHz, CDCl$_3$): δ_C 167.3 (C-1), 147.9 (C-3′), 146.8 (C-4′), 144.6 (C-3), 127.1 (C-1′), 123.0 (C-6′), 115.7 (C-2), 114.7 (C-5′), 109.3 (C-2′), 64.6 (C-1″), 55.9 (OCH$_3$), 31.9 (C-14″), 29.7, 29.6, 29.5, (C-5″- C-12″), 29.4 (C-13″), 29.3 (C-4″), 28.8 (C-2″), 26.0 (C-3″), 22.7 (C-15″), 14.1 (C-16″); ESI mass (negative mode): 417 [M –H]⁻, 459 [M + ACN]⁻.

Octadecyl ferulate. (12e). White solid, yield: 63 %; m. p.: 61-62 °C; VLC mobile phase: toluene/ethyl acetate (9.5 : 0.5); ^{1}H NMR (500 MHz, CDCl$_3$): δ_H 7.61 (d, 1H, J = 16 Hz, H-3), 7.07 (dd, 1H, J = 1.6, 8 Hz, H-6′), 7.03 (d, 1H, J = 1.6, Hz, H-2′), 6.91 (d, 1H, J = 8, Hz, H-5′), 6.29 (d, 1H, J = 16 Hz, H-2), 5.94 (s, 1H, OH), 4.19 (t, 2H, J = 6.8 Hz, H-1″), 3.92 (s, 3H, OCH$_3$-3′), 1.69 (m, 2H, H-2″), 1.40 (m, 2H, H-3″), 1.26 (m, 28H, H-4″-H-17″), 0.88 (t, 3H, J = 6.8, Hz, H-18″); ^{13}C NMR (100 MHz, CDCl$_3$): δ_C 167.3 (C-1), 147.9 (C-3′), 146.8 (C-4′), 144.6 (C-3), 127.1 (C-1′), 123.0 (C-6′), 115.7 (C-2), 114.7 (C-5′), 109.3 (C-2′), 64.6 (C-1″), 55.9 (OCH$_3$), 31.9 (C-16″), 29.7, 29.6, 29.5 (C-5″- C-14″), 29.4 (C-15″), 29.3 (C-4″), 28.8 (C-2″),

26.0 (C-3″), 22.7 (C-17″), 14.1 (C-18″); ESI mass (negative mode): 445 [M −H]⁻, 487 [M + ACN]⁻.

*Oleyl ferulate (**12f**)*. White solid, yield: 68 %; m. p.: 35-36 °C; VLC mobile phase: toluene/ethyl acetate (9.5 : 0.5); ¹H NMR (500 MHz, CDCl₃): δ_H 7.59 (d, 1H, *J* = 16 Hz, H-3), 7.03 (dd, 1H, *J* = 1.6, 8 Hz, H-6′), 6.97 (d, 1H, *J* = 1.6, Hz, H-2′), 6.91 (d, 1H, *J* = 8, Hz, H-5′), 6.27 (d, 1H, *J* = 16 Hz, H-2), 5.34 (m, 2H, H-9″, H-10″), 4.18 (t, 2H, *J* = 6.8 Hz, H-1″), 3.86 (s, 3H, OCH₃-3′), 2.0 (4H, H-8″, H11″), 1.68 (m, 2H, H-2″), 1.29 (m, 2H, H-3″), 1.26 (m, 4H, H-4″-H-5″), 1.25 (16H, H-6″, H-7″, H-12″-H-17″), 0.87 (t, 3H, *J* = 6.8, Hz, H-18″); ¹³C NMR (100 MHz, CDCl₃): δ_C 167.3 (C-1), 148.0 (C-3′), 146.8 (C-4′), 144.6 (C-3), 129.8 (C-10″), 129.6 (C-9″), 126.8 (C-1′), 122.8 (C-6′), 115.4 (C-2), 114.7 (C-5′), 109.4 (C-2′), 64.5 (C-1″), 55.7 (OCH₃), 31.8 (C-16″), 29.7, 29.6, 29.4, 29.3, 29.2, 29.1, 29.0 (C-4″-C-7″, C-12″- C-15″), 28.7 (C-2″), 27.1 (C-8″, C-11″), 26.0 (C-3″), 22.5 (C-17″), 14.0 (C-18″); ESI mass (negative mode): 443 [M −H]⁻, 485 [M + ACN]⁻.

*Geranylgeranyl ferulate (**12g**)*. White semi-solid,yield: 70 %; VLC mobile phase: *n*-hexan/ethyl acetate (8 : 2); ¹H NMR (500 MHz, CDCl₃): δ_H 7.61 (d, 1H, *J* = 16 Hz, H-3), 7.05 (dd, 1H, *J* = 1.6, 8 Hz, H-6′), 7.01 (d, 1H, *J* = 1.6, Hz, H-2′), 6.90 (d, 1H, *J* = 8, Hz, H-5′), 6.29 (d, 1H, *J* = 16 Hz, H-2), 5.43 (t, 2H, *J* = 7.0 Hz, H-2″), 5.09 (m, 1H, H-14″), 5.07 (4H, m, H-6″, H-10″), 4.70 (d, 2H, *J* =7.5 Hz, H-1″), 3.90 (s, 3H, OCH₃-3′), 2.16 (m, 2H, H-4″), 2.11(m, 2H, H-8″), 2.06 (m, 2H, H-12″), 1.98 (m, 6H, H-5″, H-9″, H-13″), 1.79 (s, 3H, H-20″), 1.67 (s, 3H, H-17″), 1.62 (s, 3H, H-16″), 1.59 (s, 6H, H-18″, H-19″); ¹³C NMR (100 MHz, CDCl₃): δ_C 167.2 (C-1), 147.9 (C-3′), 146.7 (C-4′), 144.7 (C-3), 142.7 (C-3″), 135.8 (C-7″), 135.0 (C-11″), 131.2 (C-15″), 127.0 (C-1′), 124.4, 124.1 (C-6″, C-10″), 123.4 (C-14″), 123.0 (C-6′), 119.3 (C-2″), 115.6 (C-2),

114.7 (C-5′), 109.3 (C-2′), 61.0 (C-1″), 55.9 (OCH$_3$), 39.7 (C-5″, C-9″, C-13″), 32.2 (C-4″), 26.7, 26.6 (C-8″, C-12″), 25.7 (C-17″), 23.5 (C-20″), 17.6 (C-16″), 16.0 (C-18″, C-19″); ESI mass (negative mode): 465 [M −H]⁻.

*2-Phenylethyl ferulate (**12h**)*. White semi-solid, yield: 67 %; Sephadex LH-20 (MeOH); ^{1}H NMR (400 MHz, CDCl$_3$): δ_H 7.68 (d, 1H, J = 15.6 Hz, H-3), 7.36 (m, 5H, H-4″-H8″), 7.11 (dd, 1H, J = 1.6, 8 Hz, H-6′), 7.09 (d, 1H, J = 1.6, Hz, H-2′), 6.99 (d, 1H, J = 8, Hz, H-5′), 6.35 (d, 1H, J = 15.6 Hz, H-2), 6.03 (s, 1H, OH), 4.50 (t, 2H, J = 6.8 Hz, H-1″), 3.90 (s, 3H, OCH$_3$-3′), 3.10 (t, 2H, J = 6.8 Hz, H-2″); ^{13}C NMR (100 MHz, CDCl$_3$): δ_C 167.2 (C-1), 148.0 (C-3′), 146.7 (C-4′), 144.9 (C-3), 137.9 (C-3″), 128.9 (C-4″, C8″), 128.5 (C-5″, C7″), 126.9 (C-1′), 126.5 (C-6″), 123.1 (C-6′), 115.3 (C-2), 114.7 (C-5′), 109.3 (C-2′), 64.8 (C-1″), 55.9 (OCH$_3$), 35.2 (C-2″); ESI mass (negative mode): 297 [M −H]⁻.

*2-(p-Methylphenyl)ethyl ferulate (**12i**)*. White semi-solid, yield: 62 %; Sephadex LH-20 (MeOH); ^{1}H NMR (400 MHz, CDCl$_3$): δ_H 7.60 (d, 1H, J = 15.6 Hz, H-3), 7.15 (m, 4H, H-4″-H-5″, H-7″-H8″), 7.06 (dd, 1H, J = 1.6, 8.4 Hz, H-6′), 7.03 (d, 1H, J = 1.6, Hz, H-2′), 6.90 (d, 1H, J = 8.4, Hz, H-5′), 6.35 (d, 1H, J = 15.6 Hz, H-2), 5.86 (s, 1H, OH), 4.40 (t, 2H, J = 6.8 Hz, H-1″), 3.93 (s, 3H, OCH$_3$-3′), 3.0 (t, 2H, J = 6.8 Hz, H-2″), 2.30 (s, 3H, CH$_3$-6″); ^{13}C NMR (100 MHz, CDCl$_3$): δ_C 167.2 (C-1), 147.9 (C-3′), 146.7 (C-4′), 144.9 (C-3), 136.0 (C-3″), 134.8 (C-6″), 129.1 (C-5″, C7″), 128.5 (C-4″, C8″), 127.0 (C-1′), 123.1 (C-6′), 115.3 (C-2), 114.7 (C-5′), 109.3 (C-2′), 65.0 (C-1″), 55.9 (OCH$_3$), 34.8 (C-2″), 21.0 (CH$_3$); ESI mass (negative mode): 311 [M −H]⁻.

*2-(o-Methylphenyl)ethyl ferulate (**12j**)*. White semi-solid, yield: 75 %; Sephadex LH-20 (MeOH); ^{1}H NMR (500 MHz, CDCl$_3$): δ_H 7.62(d, 1H, J = 15.6 Hz, H-3), 7.20 (m, 4H, H-5′-

H8″), 7.07 (dd, 1H, *J* = 1.5, 8.4 Hz, H-6′), 7.03 (d, 1H, *J* = 1.5, Hz, H-2′), 6.90 (d, 1H, *J* = 8.4, Hz, H-5′), 6.29 (d, 1H, *J* = 15.6 Hz, H-2), 5.93 (s, 1H, OH), 4.40 (t, 2H, *J* = 7 Hz, H-1″), 3.92 (s, 3H, OCH₃-3′), 3.03 (t, 2H, *J* = 7 Hz, H-2″), 2.39 (s, 3H, CH₃-4″); ¹³C NMR (100 MHz, CDCl₃): δ_C 167.2 (C-1), 148.0 (C-3′), 146.8 (C-4′), 144.9 (C-3), 136.4 (C-3″), 135.9 (C-4″), 130.3 (C-5″), 129.4 (C7″), 126.9 (C-1′), 126.7 (C-6″), 126.0 (C8″), 123.0 (C-6′), 115.4 (C-2), 114.7 (C-5′), 109.4 (C-2′), 64.0 (C-1″), 55.9 (OCH₃), 32.5 (C-2″), 19.4 (CH₃); ESI mass (negative mode): 311 [M –H]⁻.

*2-(p-Chlorophenyl)ethyl ferulate (**12k**)*. White solid, yield: 62 %; m. p.: 53-54 °C; Sephadex LH-20 (MeOH); ¹H NMR (400 MHz, CDCl₃): δ_H 7.59 (d, 1H, *J* = 16 Hz, H-3), 7.27 (d, 2H, *J* = 8 Hz, H-5″, H-7″), 7.18 (d, 2H, *J* = 8 Hz, H-4″, H-8″), 7.05 (dd, 1H, *J* = 1.6, 8.4 Hz, H-6′), 7.02 (d, 1H, *J* = 1.6, Hz, H-2′), 6.91 (d, 1H, *J* = 8.4, Hz, H-5′), 6.26 (d, 1H, *J* = 16 Hz, H-2), 4.39 (t, 2H, *J* = 6.8 Hz, H-1″), 3.90 (s, 3H, OCH₃-3′), 2.98 (t, 2H, *J* = 6.8 Hz, H-2″); ¹³C NMR (100 MHz, CDCl₃): δ_C 167.1 (C-1), 148.0 (C-3′), 146.8 (C-4′), 145.1 (C-3), 136.4 (C-3″), 132.3 (C-6″), 130.2 (C-5″, C-7″), 128.5 (C-4″, C-8″), 126.8 (C-1′), 123.0 (C-6′), 115.0 (C-2), 114.7 (C-5′), 109.4 (C-2′), 64.4 (C-1″), 55.9 (OCH₃), 34.5 (C-2″); ESI mass (negative mode): 331 [M –H]⁻.

*2-(1-Naphthyl)ethyl ferulate (**12l**).* Pale yellow solid, yield: 80 %; m. p.: 90-91 °C; VLC mobile phase: *n*-hexan/ethyl acetate (8.5 : 1.5); ¹H NMR (500 MHz, CDCl₃): δ_H 8.16 (d, 1H, *J* = 8.5 Hz, H-11″), 7.88 (br d, 1H, *J* = 8 Hz, H-8″), 7.78 (br d, 1H, *J* = 7 Hz, H-6″), 7.59 (d, 1H, *J* = 16 Hz, H-3), 7.57 (m, 1H, H-10″), 7.50 (m, 1H, H-9″), 7.40 (m, 2H, H-4″,H-5″), 7.06 (dd, 1H, *J* = 2, 8 Hz, H-6′), 7.01 (d, 1H, *J* = 2, Hz, H-2′), 6.92 (d, 1H, *J* = 8, Hz, H-5′), 6.29 (d, 1H, *J* = 16 Hz, H-2), 4.57 (t, 2H, *J* = 7.5 Hz, H-1″), 3.93 (s, 3H, OCH₃-3′), 3.51 (t, 2H, *J* = 7.5 Hz, H-2″); ¹³C NMR (100 MHz, CDCl₃): δ_C 167.2 (C-1), 148.0 (C-3′), 146.7 (C-4′), 145.0 (C-3), 133.8 (C-3″,

C-7″), 132.1 (C-12″), 128.8 (C-8″), 127.4 (C-4″), 126.9 (C-1′, C-6″), 126.1 (C-10″), 125.6 (C-5″), 125.5 (C-11″), 123.7 (C-9″), 123.0 (C-6′), 115.3 (C-2), 114.7 (C-5′), 109.4 (C-2′), 64.4 (C-1″), 55.9 (OCH$_3$), 32.3 (C-2″); ESI mass (negative mode): 347 [M –H]⁻.

N-oleylferulamide (13f). White solid, yield: 55%; m. p.: 50-51 °C; ^{1}H NMR (500 MHz, CDCl$_3$): δ_H 7.55 (d, 1H, J = 16 Hz, H-3), 7.05 (br d, 1H, J = 8 Hz, H-6′), 6.99 (br s, 1H, H-2′), 6.93 (d, 1H, J = 8, Hz, H-5′), 6.26 (d, 1H, J = 16 Hz, H-2), 5.74 (s, 1H, NH), 5.34 (m, 2H, H-9″, H-10″), 3.91 (s, 3H, OCH$_3$-3′), 3.37 (br s, 2H, H-1″), 2.0 (4H, H-8″, H11″), 1.56 (m, 2H, H-2″), 1.29 (m, 22H, H-3″-H-7″, H-12″-H17″), 0.88 (t, 3H, J = 7, Hz, H-18″); ^{13}C NMR (100 MHz, CDCl$_3$): δ_C 166.3 (C-1), 147.4 (C-3′), 146.7 (C-4′), 141.0 (C-3), 129.8 (C-10″), 129.7 (C-9″), 127.3 (C-1′), 122.0 (C-6′), 118.1 (C-2), 114.7 (C-5′), 109.7 (C-2′), 55.9 (OCH$_3$), 39.9 (C-1″), 32.6 (C-16″), 29.7, 29.6, 29.5, 29.4, 29.3, 29.2, (C-4″-C-7″, C-12″- C-15″), 28.2 (C-2″, C-3″), 27.0 (C-8″, C-11″), 22.7 (C-17″), 14.1 (C-18″); ESI mass (negative mode): 442 [M –H]⁻.

Oleyl 3,4-diethyloxycarbonyloxy caffeate (16f). White solid, yield: 90%; VLC mobile phase: toluene/ethyl acetate (9.5 : 0.5); ^{1}H NMR (500 MHz, CDCl$_3$): δ_H 7.61 (d, 1H, J = 16 Hz, H-3), 7.45 (d, 1H, J = 2, Hz, H-2′), 7.4 (dd, 1H, J = 2, 8.5 Hz, H-6′), 7.30 (d, 1H, J = 8.5, Hz, H-5′), 6.38 (d, 1H, J = 16 Hz, H-2), 5.36 (m, 2H, H-9″, H-10″), 4.32 (q, 2H, J = 7.5 Hz, OC$\underline{H_2}$-CH$_3$), 4.33 (q, 2H, J = 7.5 Hz, OC$\underline{H_2}$-CH$_3$), 4.19 (t, 2H, J = 7 Hz, H-1″), 2.01 (4H, H-8″, H11″), 1.69 (m, 2H, H-2″), 1.39 (t, 6H, J = 7.5 Hz, OCH$_2$-C$\underline{H_3}$), 1.38 (t, 6H, J = 7.5 Hz, OCH$_2$-C$\underline{H_3}$), 1.31 (m, 2H, H-3″), 1.27 (20H, H-4″-H-7″, H-12″-H-17″), 0.88 (t, 3H, J = 7, Hz, H-18″);

Geranylgeranyl 3,4-diethyloxycarbonyloxy caffeate (16g). White solid, yield: 87%; VLC mobile phase: toluene/ethyl acetate (9.5 : 0.5); ^{1}H NMR (500 MHz, CDCl$_3$): δ_H 7.62 (d, 1H, J = 16 Hz, H-3), 7.43 (d, 1H, J = 1.6, Hz, H-2′), 7.4 (dd, 1H, J = 1.6, 8.5 Hz, H-6′), 7.30 (d, 1H, J = 8.5, Hz,

H-5′), 6.39 (d, 1H, *J* = 16 Hz, H-2), 5.42 (t, 2H, *J* = 7.0 Hz, H-2″), 5.13 (m, 1H, H-14″), 5.11

(4H, m, H-6″, H-10″), 4.70 (d, 2H, *J* =7 Hz, H-1″), 4.32 (q, 2H, *J* = 7.5 Hz, OC$\underline{H_2}$-CH₃), 4.33 (q,

2H, *J* = 7.5 Hz, OC$\underline{H_2}$-CH₃), 2.16 (m, 2H, H-4″), 2.12(m, 2H, H-8″), 2.07 (m, 2H, H-12″), 1.98

(m, 6H, H-5″, H-9″, H-13″), 1.79 (s, 3H, H-20″), 1.68 (s, 3H, H-17″), 1.62 (s, 3H, H-16″), 1.60

(s, 6H, H-18″, H-19″), 1.39 (t, 6H, *J* = 7.5 Hz, OCH₂-C$\underline{H_3}$), 1.38 (t, 6H, *J* = 7.5 Hz, OCH₂-C$\underline{H_3}$),

Oleyl caffeate (17f). White solid, yield: 69%; m. p.: 68-69 °C; VLC mobile phase: *n*-hexane/ethyl acetate (7 : 3); ¹H NMR (500 MHz, CDCl₃): δ_H 7.59 (d, 1H, *J* = 16 Hz, H-3), 7.12

(d, 1H, *J* = 2, Hz, H-2′), 7.01 (dd, 1H, *J* = 2, 8.5 Hz, H-6′), 6.88 (d, 1H, *J* = 8.5, Hz, H-5′), 6.27

(d, 1H, *J* = 16 Hz, H-2), 6.18 (1H, OH), 5.93 (1H, OH), 5.34 (m, 2H, H-9″, H-10″), 4.20 (t, 2H, *J*

= 7 Hz, H-1″), 2.01 (4H, H-8″, H11″), 1.70 (m, 2H, H-2″), 1.31 (m, 2H, H-3″), 1.29 (m, 4H, H-

4″-H-5″), 1.27 (16H, H-6″, H-7″, H-12″-H-17″), 0.88 (t, 3H, *J* = 7, Hz, H-18″); ¹³C NMR (100

MHz, CDCl₃): δ_C 168.1 (C-1), 146.4 (C-3′), 145.1 (C-3), 143.8 (C-4′), 130.0 (C-10″), 129.8 (C-

9″), 127.5 (C-1′), 122.4 (C-6′), 115.6 (C-2′), 115.4 (C-2), 114.5 (C-5′), 65.0 (C-1″), 31.9 (C-16″),

29.8, 29.7, 29.5, 29.4, 29.3, 29.2, (C-4″-C-7″, C-12″- C-15″), 28.8 (C-2″), 27.2, 27.1 (C-8″, C-

11″), 26.0 (C-3″), 22.7 (C-17″), 14.1 (C-18″); ESI mass (negative mode): 429 [M –H]⁻.

Geranylgeranyl caffeate (17g). White solid, yield: 55 %; m. p.: 53-54 °C; Sephadex LH-20

(MeOH); ¹H NMR (500 MHz, CDCl₃): δ_H 7.59 (d, 1H, *J* = 16 Hz, H-3), 7.09 (d, 1H, *J* = 1.6, Hz,

H-2′), 6.98 (dd, 1H, *J* = 1.6, 8.5 Hz, H-6′), 6.87 (d, 1H, *J* = 8.5, Hz, H-5′), 6.26 (d, 1H, *J* = 16

Hz, H-2), 6.0 (s, 1H, OH), 5.43 (t, 2H, *J* = 7.0 Hz, H-2″), 5.13 (m, 1H, H-14″), 5.09 (4H, m, H-

6″, H-10″), 4.69 (d, 2H, *J* =7 Hz, H-1″), 2.16 (m, 2H, H-4″), 2.12 (m, 2H, H-8″), 2.07 (m, 2H,

H-12″), 1.98 (m, 6H, H-5″, H-9″, H-13″), 1.79 (s, 3H, H-20″), 1.68 (s, 3H, H-17″), 1.61 (s, 3H,

H-16″), 1.59 (s, 6H, H-18″, H-19″); ¹³C NMR (100 MHz, CDCl₃): δ_C 167.1 (C-1), 146.3 (C-3′),

144.8 (C-3), 143.8 (C-4′), 142.8 (C-3″), 135.9 (C-7″), 135.0 (C-11″), 131.3 (C-15″), 127.6 (C-1′), 124.4, 124.2 (C-6″, C-10″), 123.4 (C-14″), 122.4 (C-6′), 119.1 (C-2″), 115.7 (C-2′), 115.5 (C-2), 114.4 (C-5′),   61.3 (C-1″), 39.7 (C-5″, C-9″, C-13″), 32.2 (C-4″), 26.8, 26.6 (C-8″, C-12″), 25.7 (C-17″), 23.6 (C-20″), 17.7 (C-16″), 16.0 (C-18″, C-19″); ESI mass (negative mode): 465 [M –H]⁻

*N-oleylcaffeamide (**18f**).* White solid; yield: 75%; m. p.: 68-69 °C; ^{1}H NMR (500 MHz, CDCl$_3$): δ_H 7.49 (d, 1H, *J* = 15.5 Hz, H-3), 7.11 (br s, 1H, H-2′), 6.85 (m, 1H, H-6′), 6.81 (d, 1H, *J* = 8, Hz, H-5′), 6.40 (s, 1H, OH), 6.24 (d, 1H, *J* = 15.5 Hz, H-2), 5.36 (m, 2H, H-9″, H-10″), 3.34 (br s, 2H, , H-1″), 1.99 (4H, H-8″, H11″), 1.55 (m, 2H, H-2″), 1.26 (22 H, H-3″- H-7″, H-12″-H-17″), 0.88 (t, 3H, *J* = 6.5, Hz, H-18″); ^{13}C NMR (100 MHz, CDCl$_3$): δ_C 167.9 (C-1), 147.0 (C-3′), 144.4 (C-3), 142.7 (C-4′), 129.9 (C-10″), 129.8 (C-9″), 126.8 (C-1′), 121.5 (C-6′), 116.5 (C-2′), 115.5 (C-2), 114.7 (C-5′), 40.4 (C-1″), 31.9 (C-16″), 29.8, 29.7, 29.5, 29.4, 29.3, 29.2, (C-2″-C-7″, C-12″- C-15″), 27.2, 27.1 (C-8″, C-11″), 22.7 (C-17″), 14.1 (C-18″); ESI mass (negative mode): 428 [M –H]⁻.

7.2.8 ^{1}H NMR and ^{13}C NMR spectra of final compounds (12b-l, 13f, 17f-g, 18f)
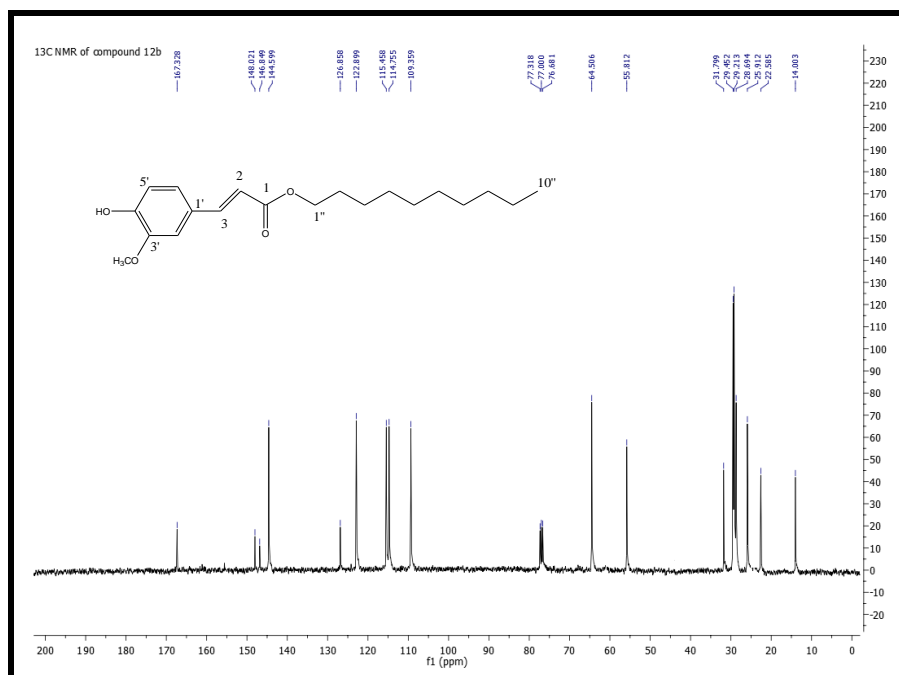
Fig. 125: ^{1}H NMR spectrum (400 MHz, CDCl$_3$) of decyl ferulate (**12b**)
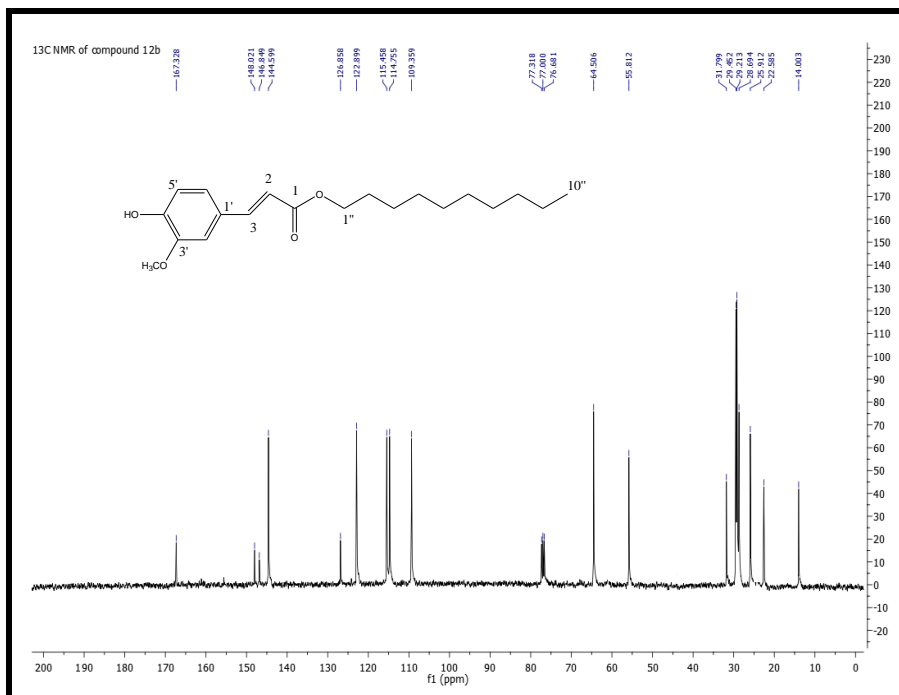
Fig.126: ^{13}C NMR spectrum (100 MHz, CDCl$_3$) of decyl ferulate (**12b**)
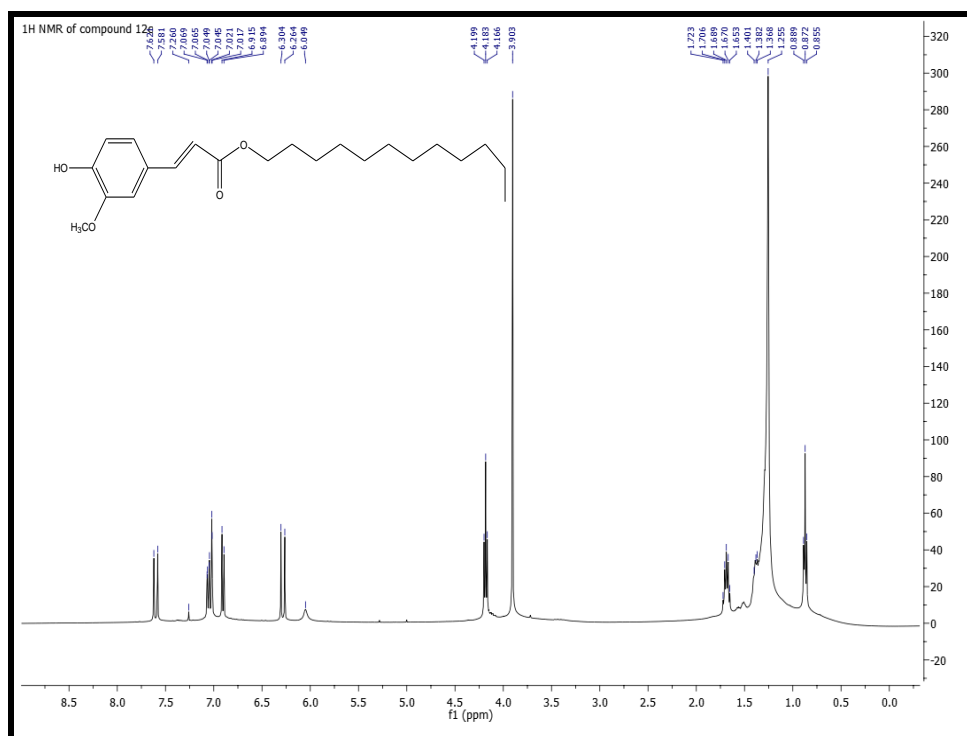
Fig. 127: ^{1}H NMR spectrum (400 MHz, CDCl$_3$) of dodecyl ferulate (**12c**)
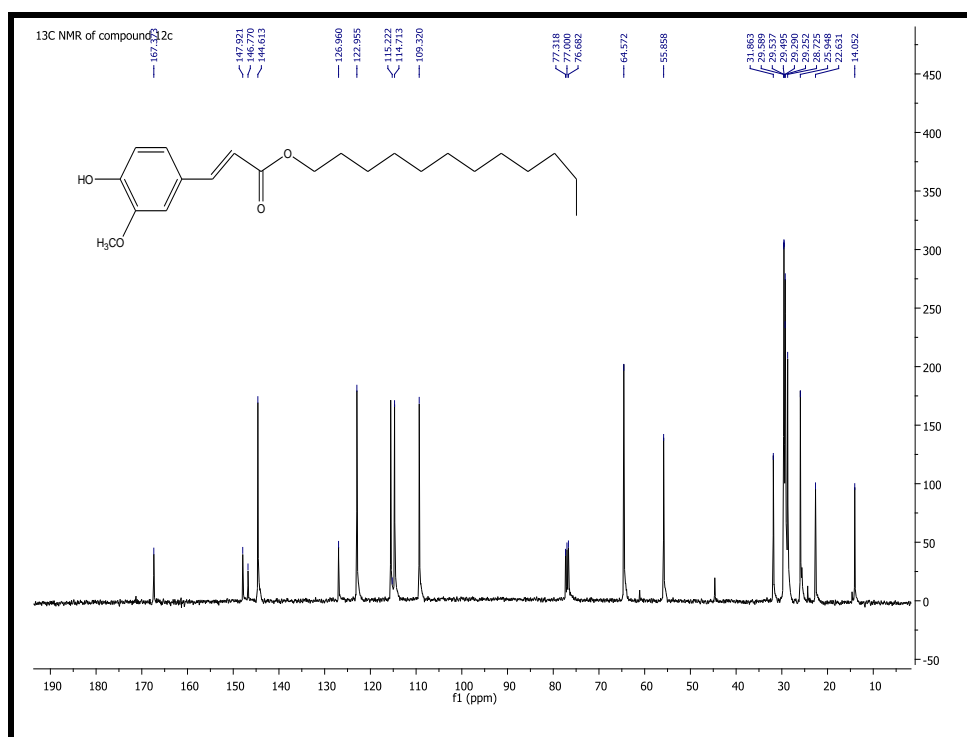
Fig.128: ^{13}C NMR spectrum (100 MHz, CDCl$_3$) of dodecyl ferulate (**12c**)
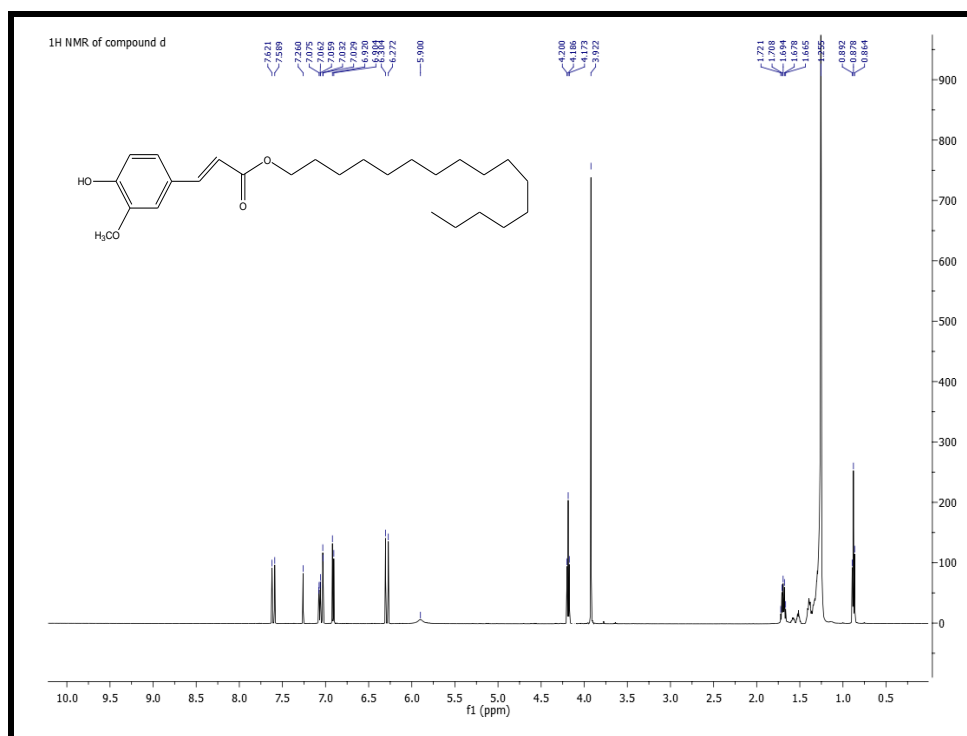
Fig.129: ^{1}H NMR spectrum (500 MHz, CDCl$_3$) of hexadecyl ferulate (**12d**)
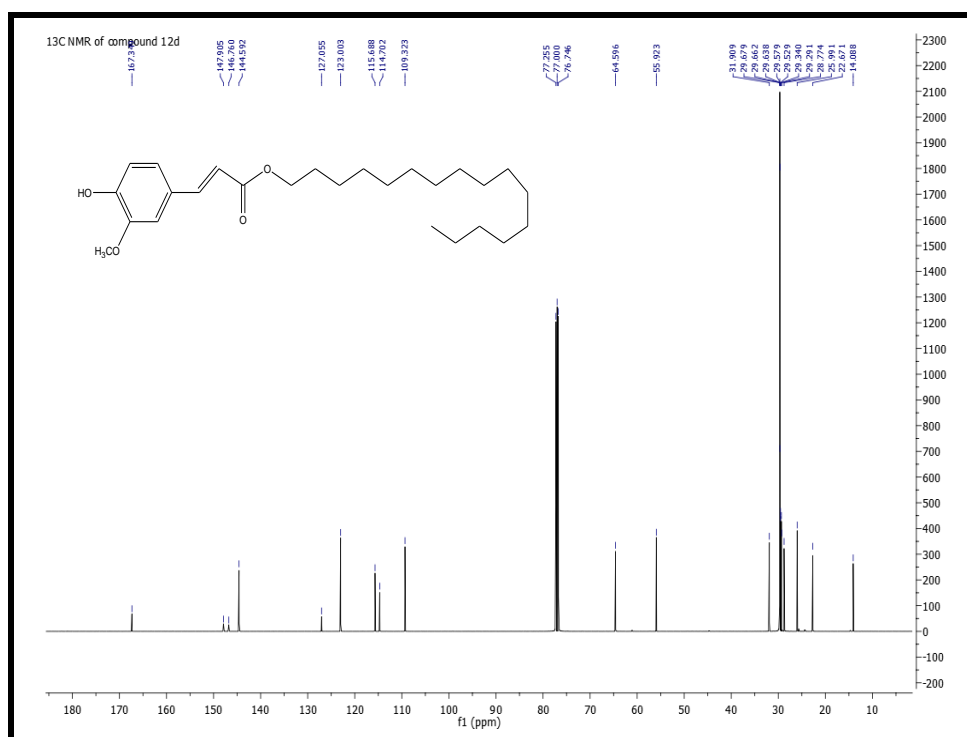
Fig.130: ^{13}C NMR spectrum (100 MHz, CDCl$_3$) of hexadecyl ferulate (**12d**)
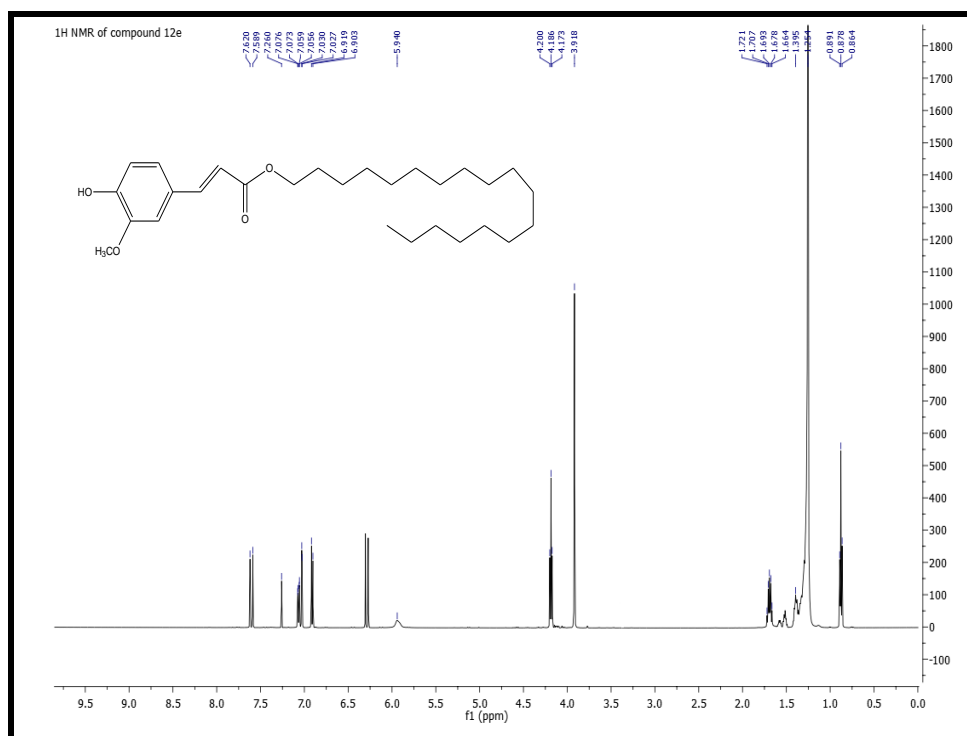
Fig. 131: ^{1}H NMR spectrum (500 MHz, CDCl$_3$) of octadecyl ferulate (**12e**)
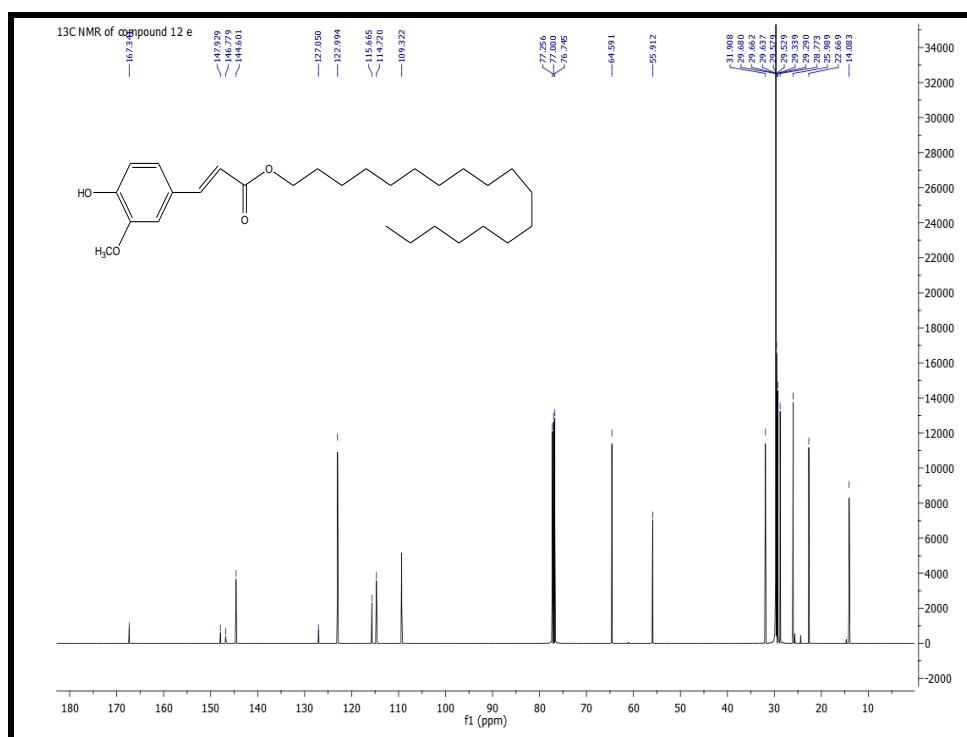
Fig. 132: ^{13}C NMR spectrum (100 MHz, CDCl$_3$) of octadecyl ferulate (**12e**)
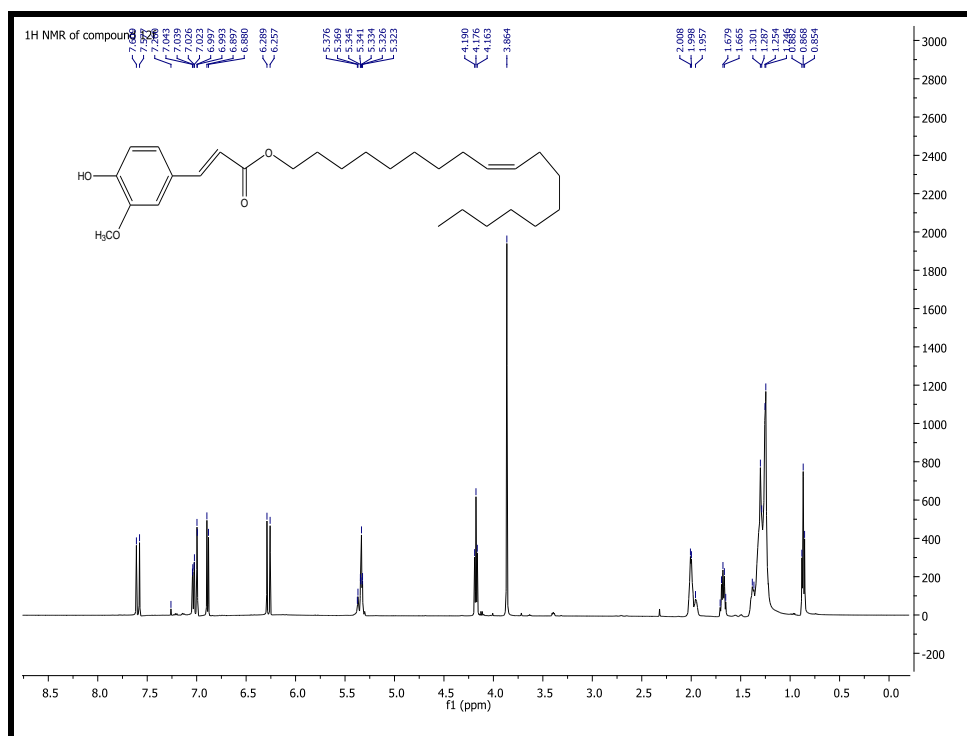
Fig. 133: ^{1}H NMR spectrum (500 MHz, CDCl$_3$) of oleyl ferulate (**12f**)
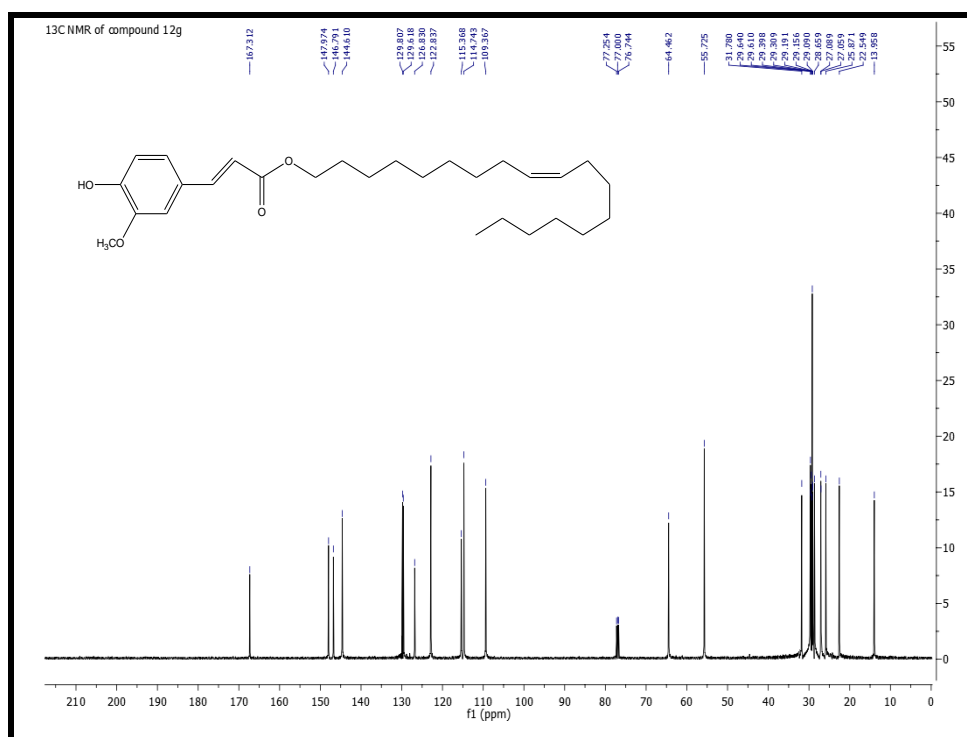
Fig. 134: ^{13}C NMR spectrum (100 MHz, CDCl$_3$) of oleyl ferulate (**12f**)
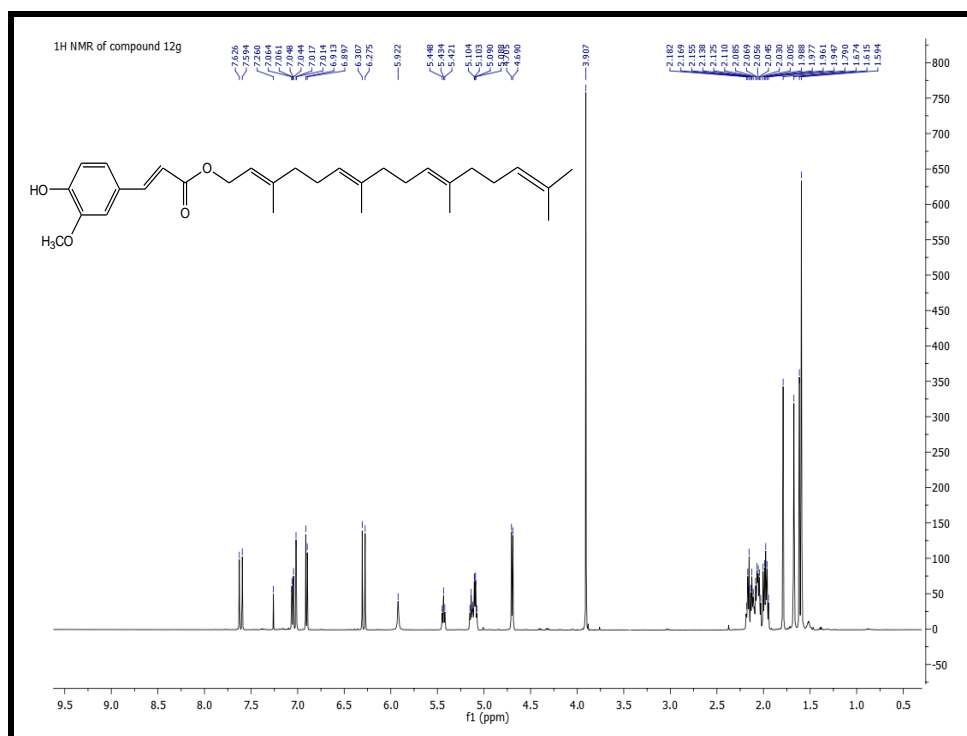
Fig. 135: ¹H NMR spectrum (500 MHz, CDCl₃) of geranylgeranyl ferulate (**12g**)
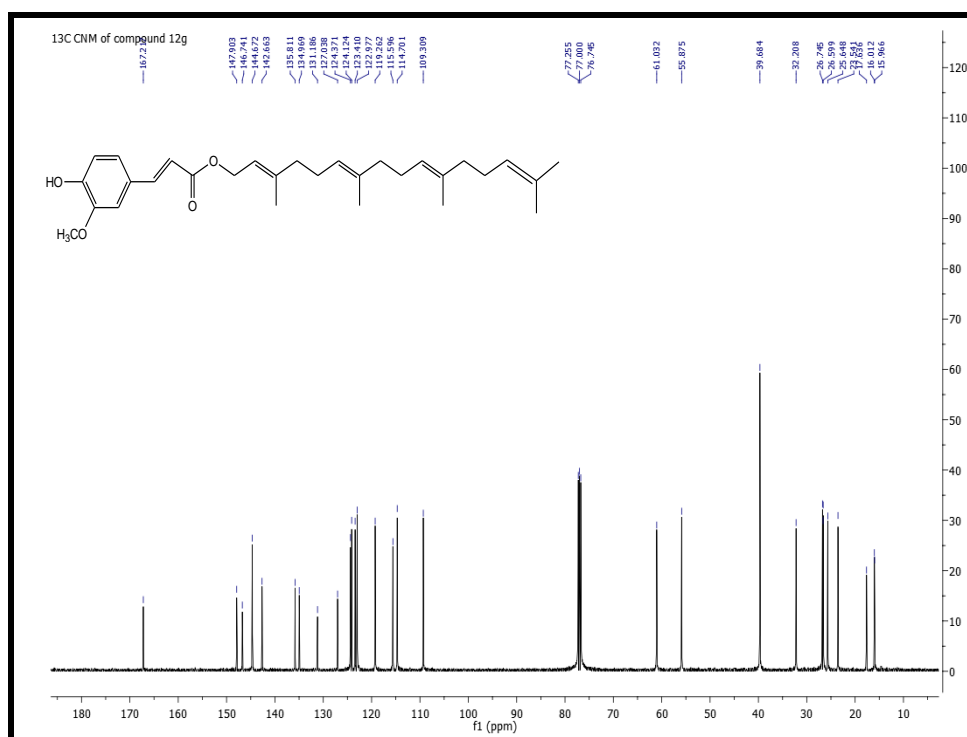
Fig. 136: ¹³C NMR spectrum (100 MHz, CDCl₃) of geranylgeranyl ferulate (**12g**)
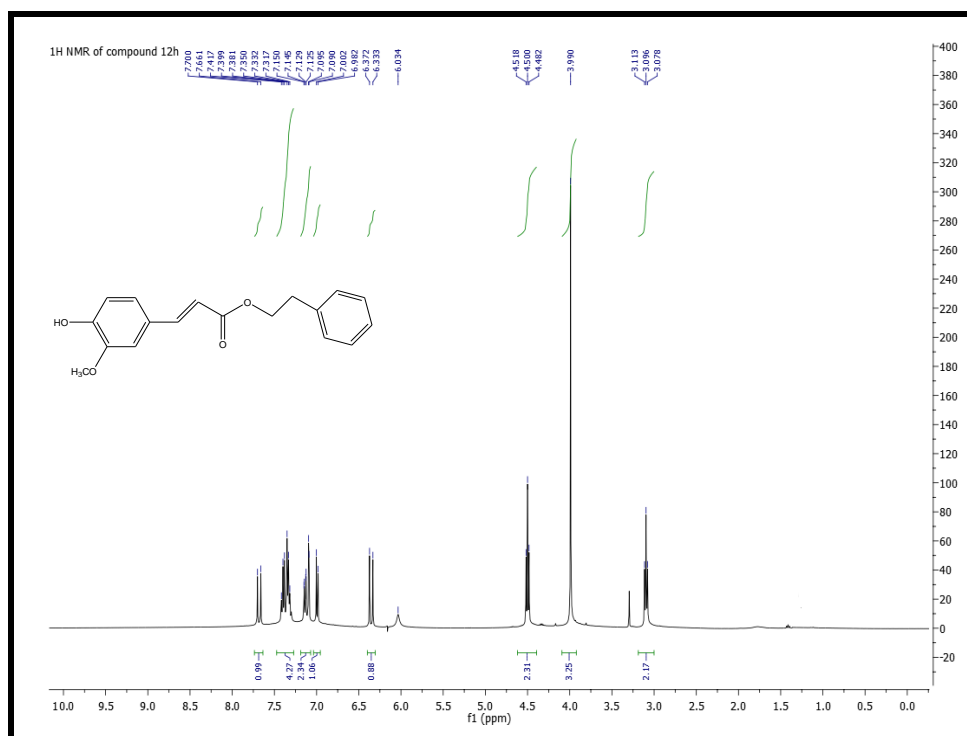
Fig. 137: ^{1}H NMR spectrum (400 MHz, CDCl$_3$) of 2-phenylethyl ferulate (**12h**)
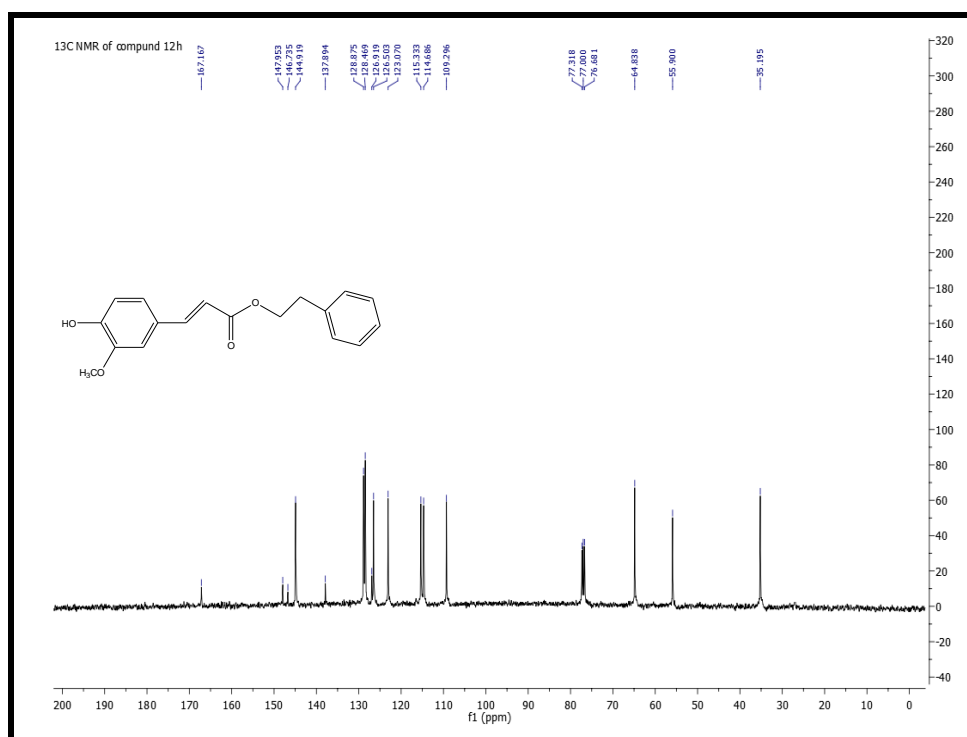
Fig 138: ^{13}C NMR spectrum (100 MHz, CDCl$_3$) of 2-phenylethyl ferulate (**12h**)
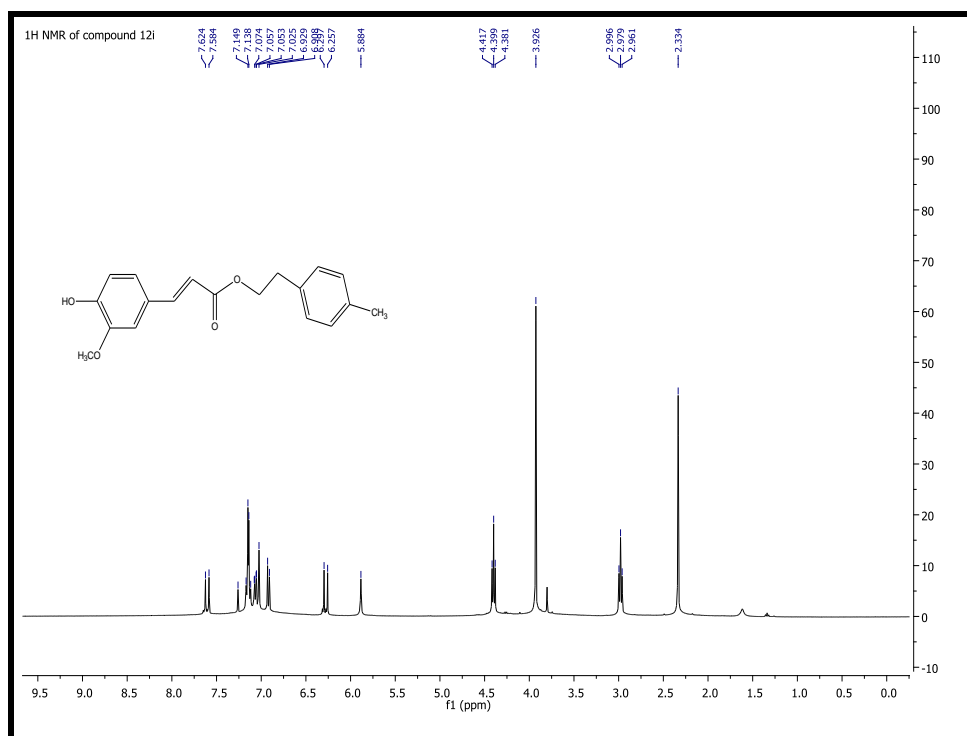
Fig. 139: ^{1}H NMR spectrum (400 MHz, CDCl$_3$) of 2-(*p*-methylphenyl)ethyl ferulate (**12i**)
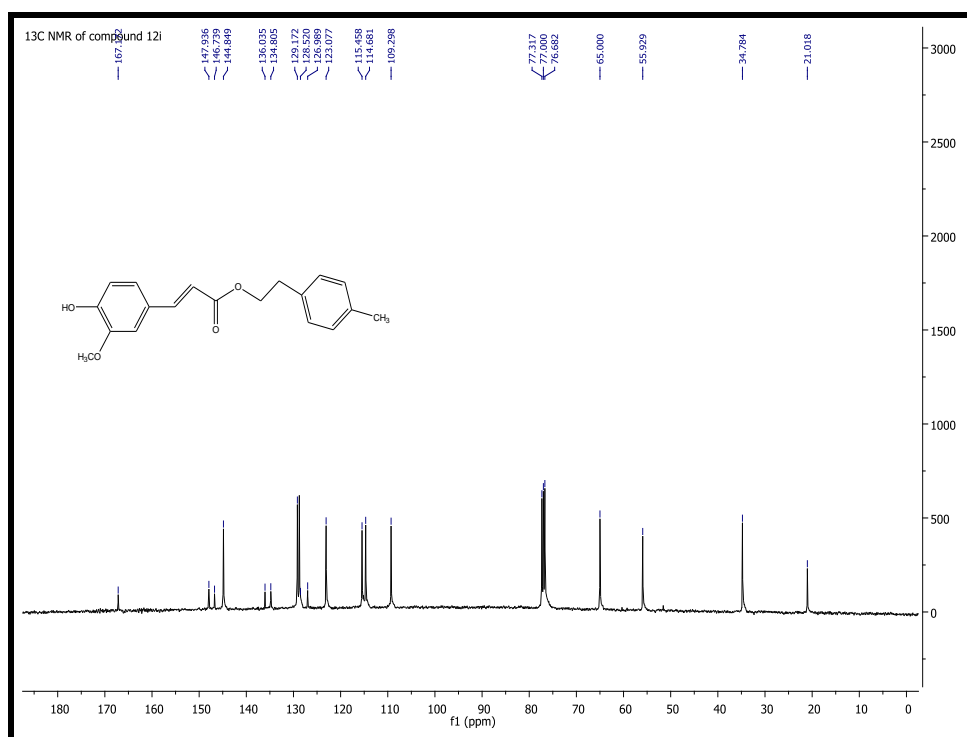
Fig.140: ^{13}C NMR spectrum (100 MHz, CDCl$_3$) of 2-(*p*-methylphenyl)ethyl ferulate (**12i**)

228
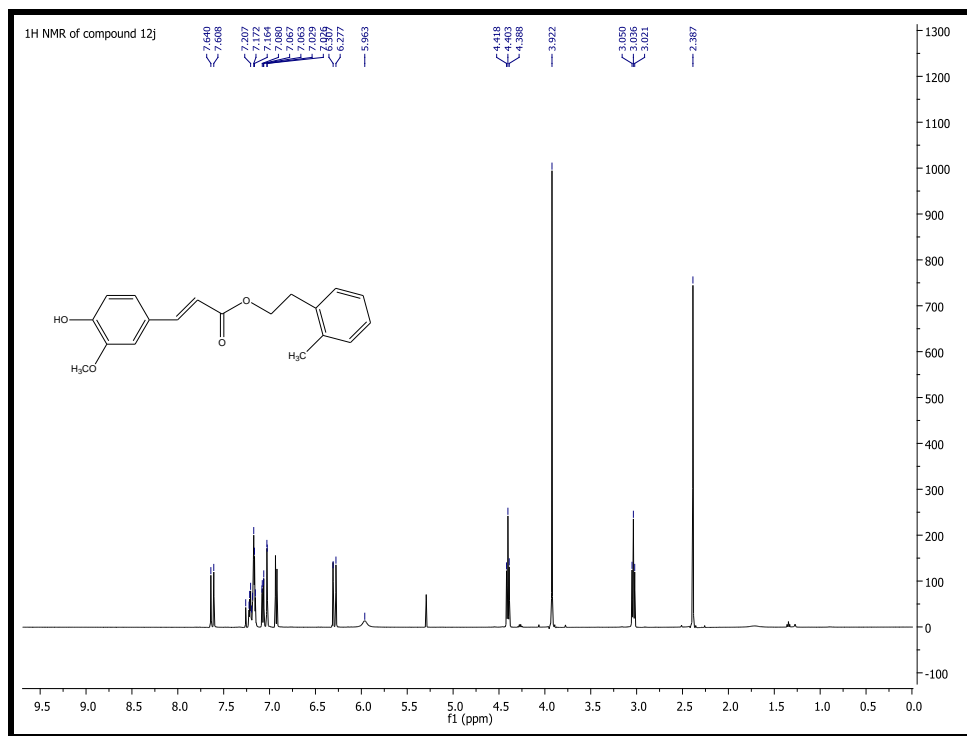
Fig. 141: ^{1}H NMR spectrum (500 MHz, CDCl$_3$) of 2-(*o*-methylphenyl) ethyl ferulate (**12j**)
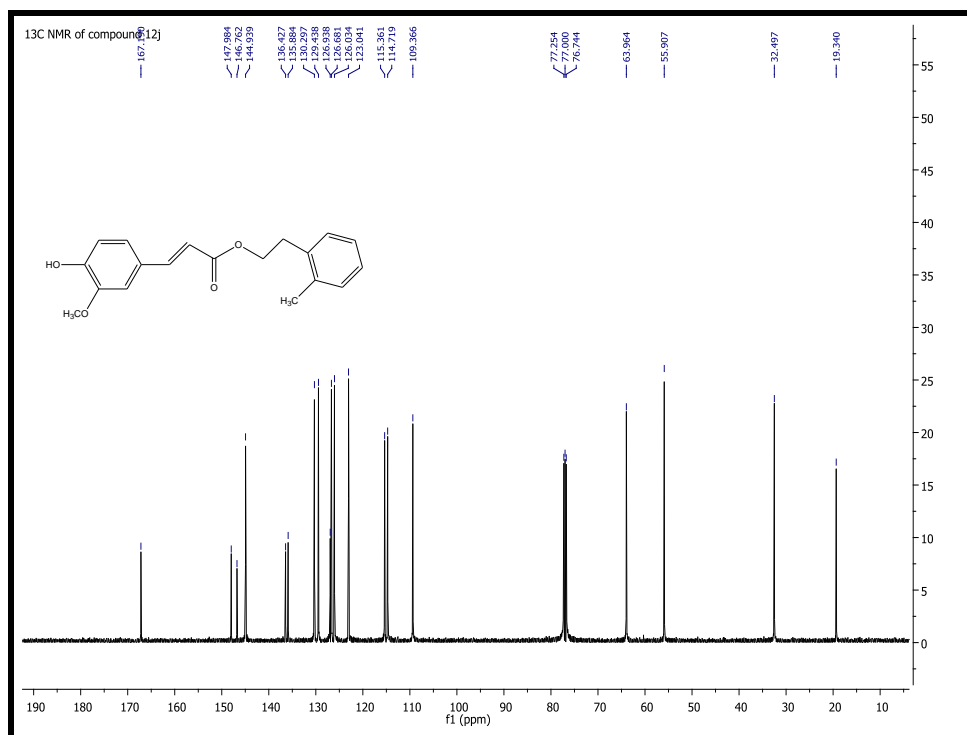
Fig. 142: ^{13}C NMR spectrum (100 MHz, CDCl$_3$) of 2-(*o*-methylphenyl) ethyl ferulate (**12j**)
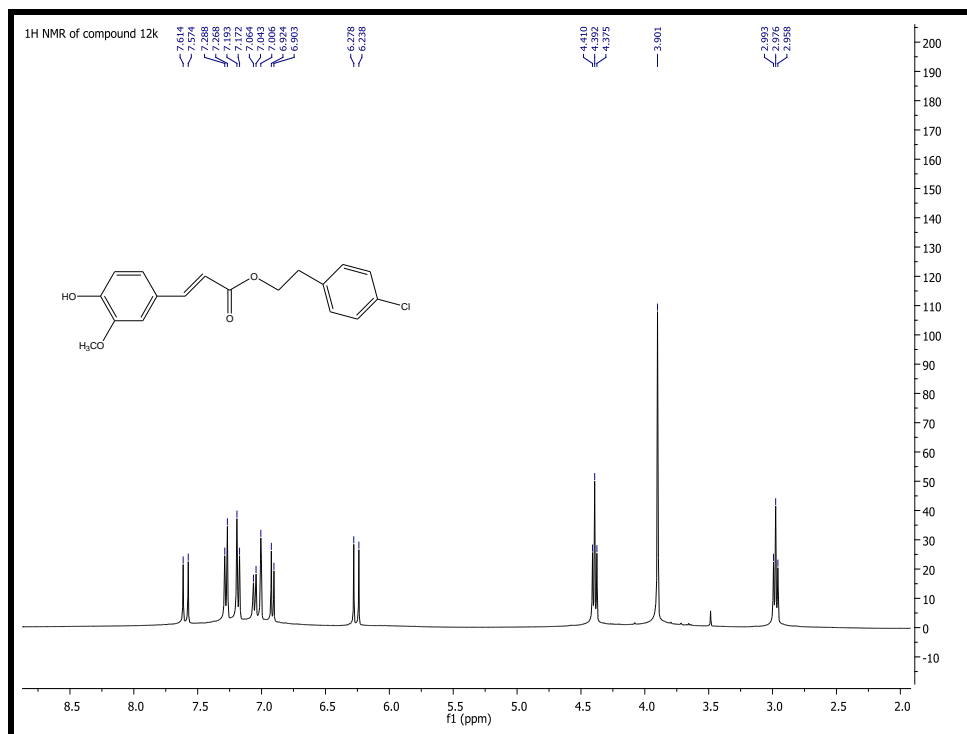
Fig. 143: ¹H NMR spectrum (400 MHz, CDCl₃) of 2-(*p*-chlorophenyl) ethyl ferulate (**12k**)
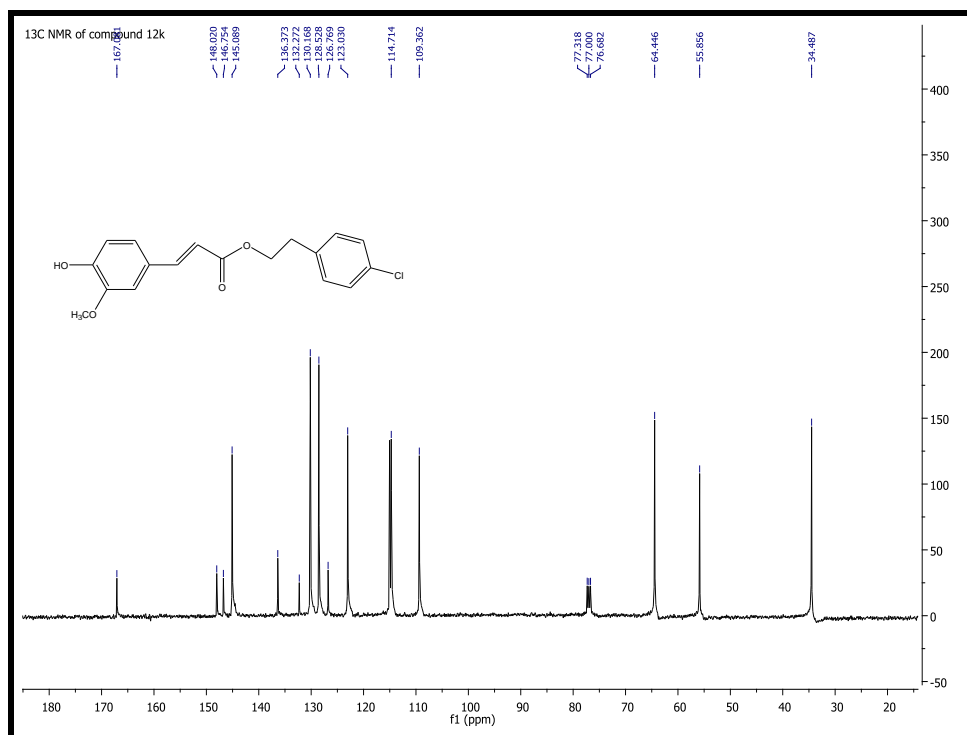
Fig. 144: ¹³C NMR spectrum (400 MHz, CDCl₃) of 2-(*p*-chlorophenyl) ethyl ferulate (**12k**)
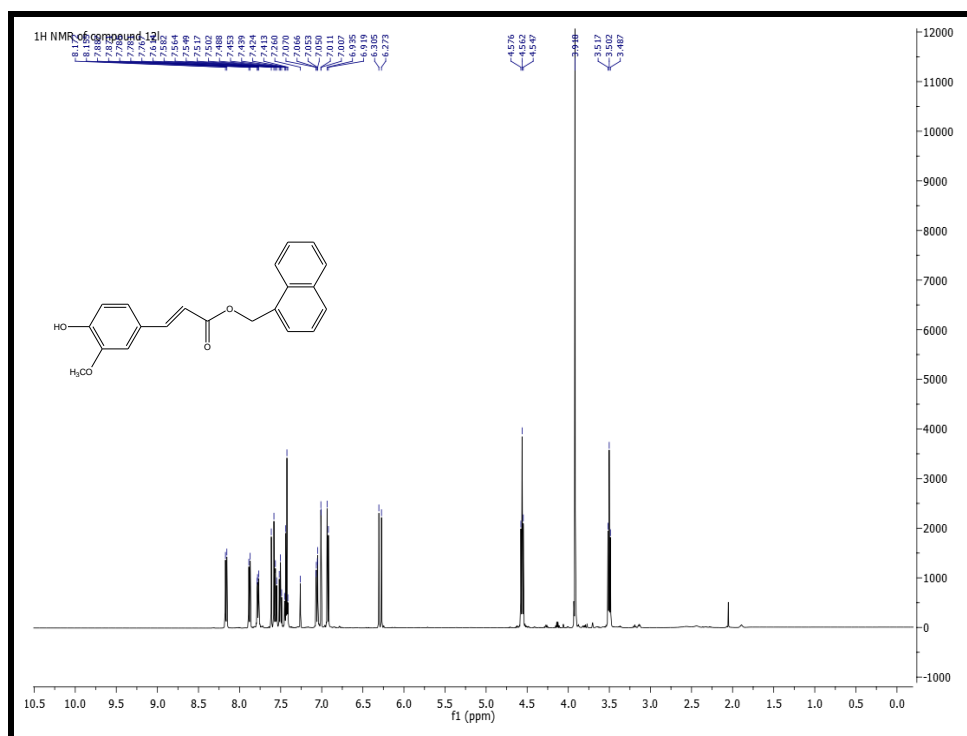
Fig. 145: ¹H NMR spectrum (500 MHz, CDCl₃) of 2-(1-naphthyl) ethyl ferulate (**12l**)
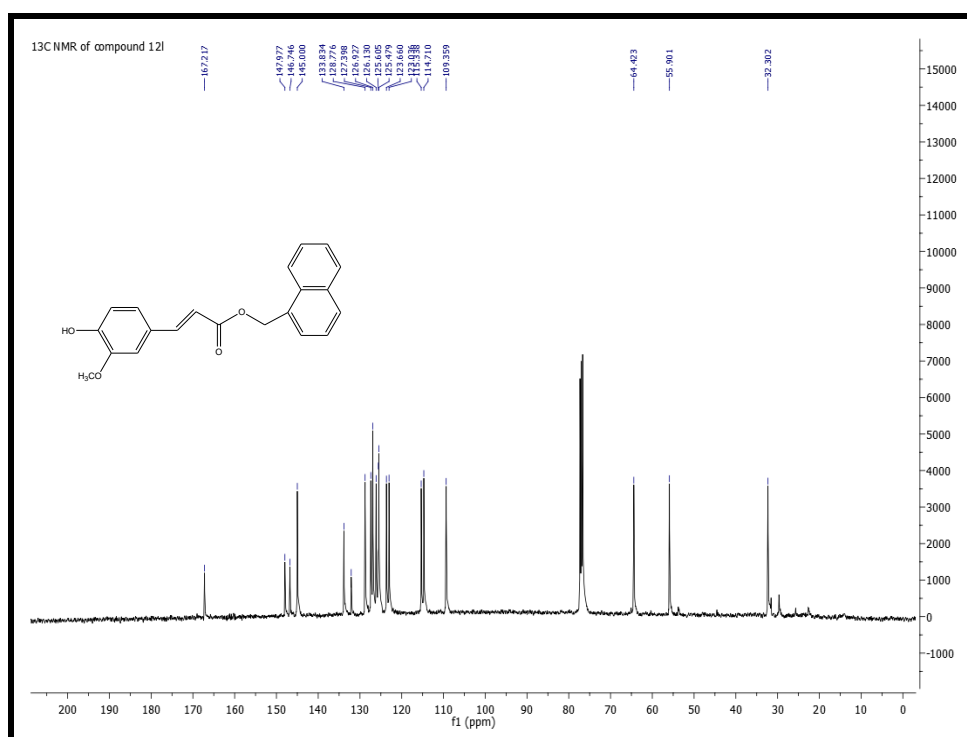
Fig.146: ¹³C NMR spectrum (100 MHz, CDCl₃) of 2-(1-naphthyl) ethyl ferulate (**12l**)
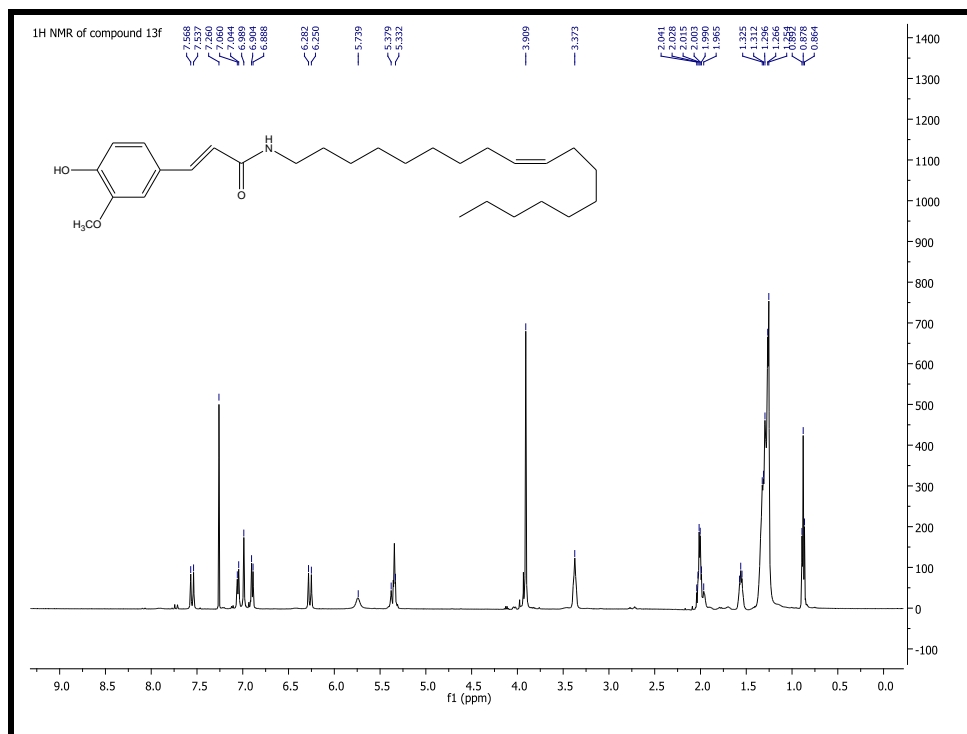
Fig. 147: ^{1}H NMR spectrum (500 MHz, CDCl$_3$) of N-oleylferulamide (**13f**)
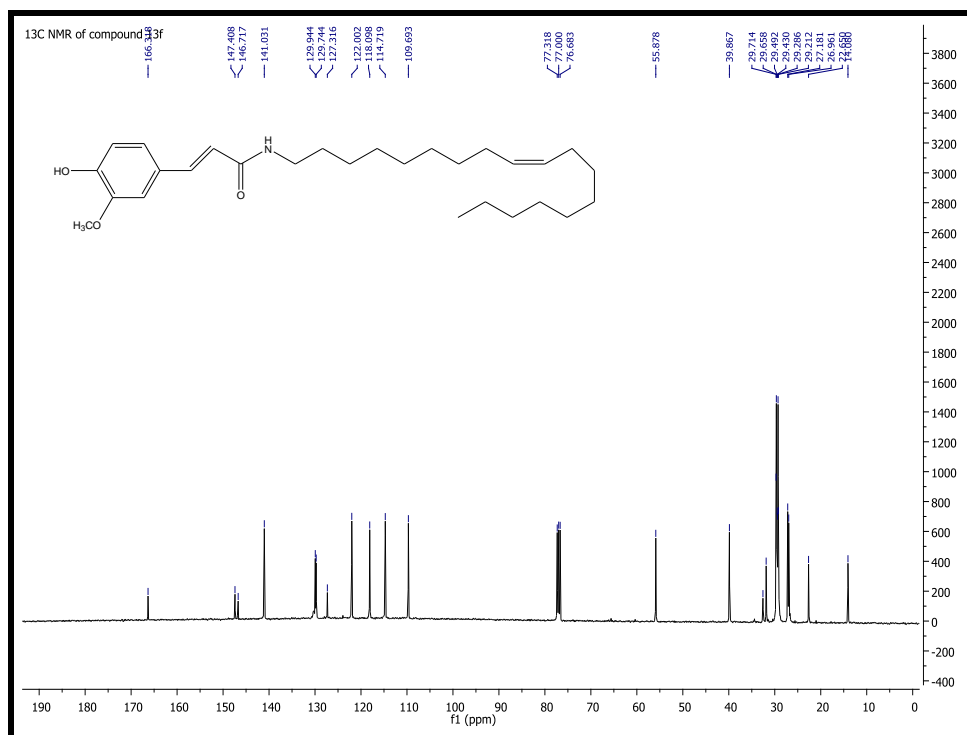
Fig. 148: ^{13}C NMR spectrum (100 MHz, CDCl$_3$) of N-oleylferulamide (**13f**)
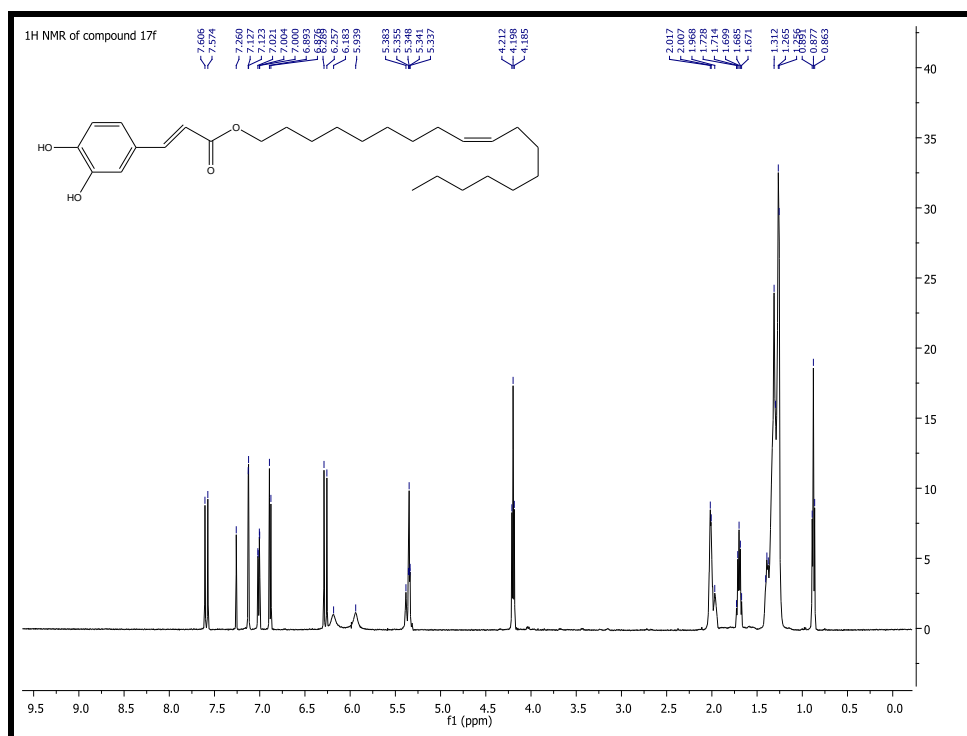
Fig. 149: ^{1}H NMR spectrum (500 MHz, CDCl$_3$) of oleyl caffeate (**17f**)
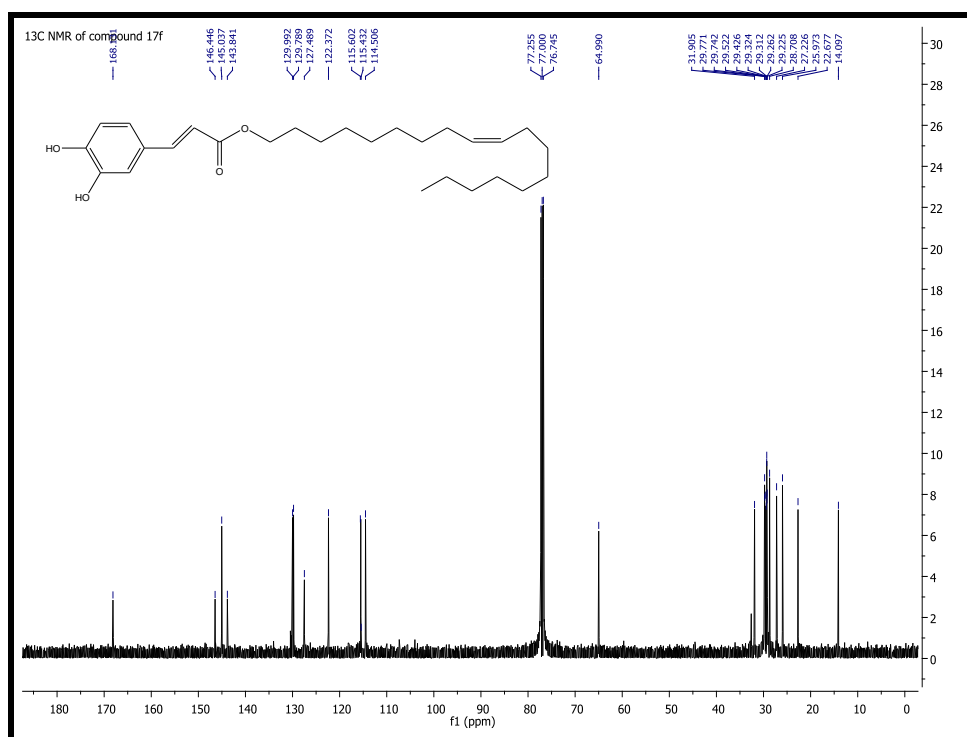
Fig. 150: ^{13}C NMR spectrum (100 MHz, CDCl$_3$) of oleyl caffeate (**17f**)
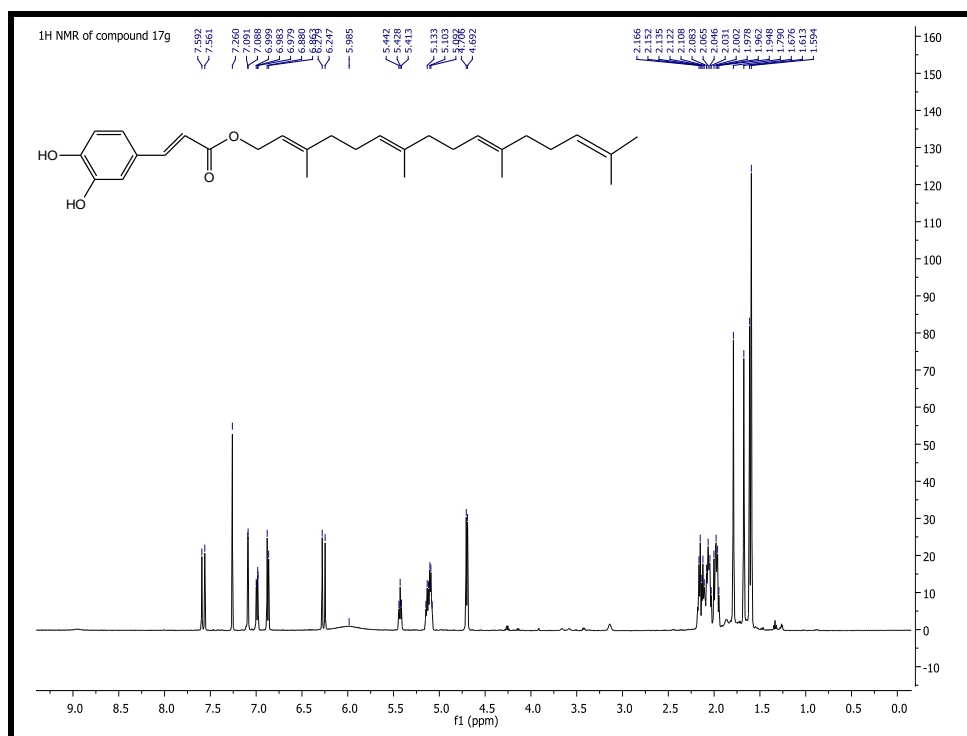
Fig. 151: ^{1}H NMR spectrum (500 MHz, CDCl$_3$) of geranylgeranyl caffeate (**17g**)
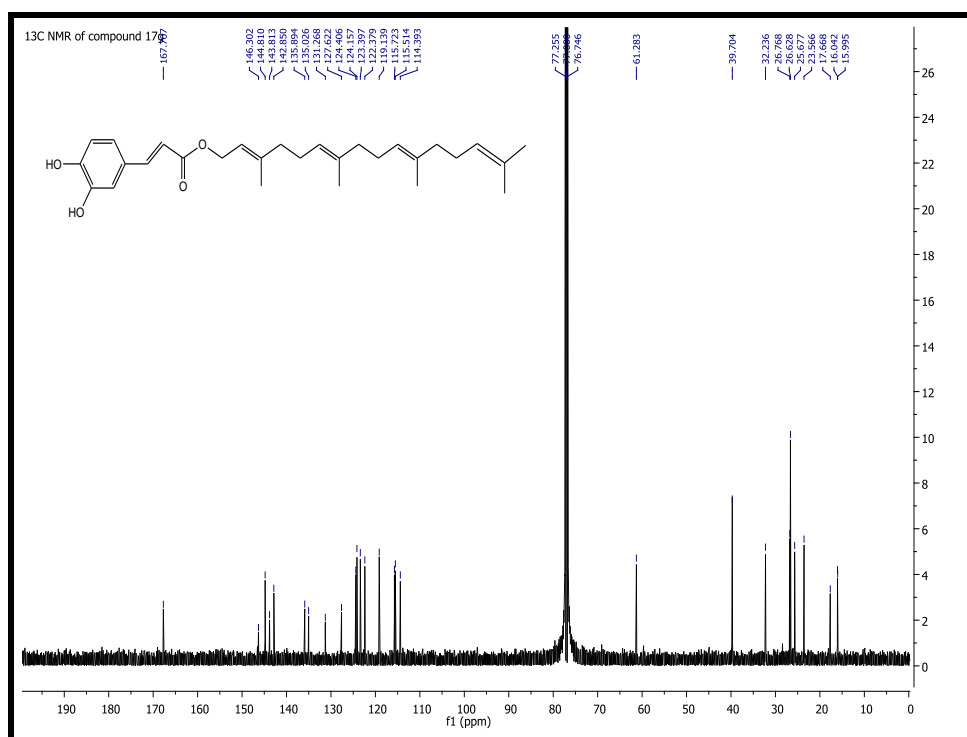
Fig. 152: ^{13}C NMR spectrum (100 MHz, CDCl$_3$) of geranylgeranyl caffeate (**17g**)
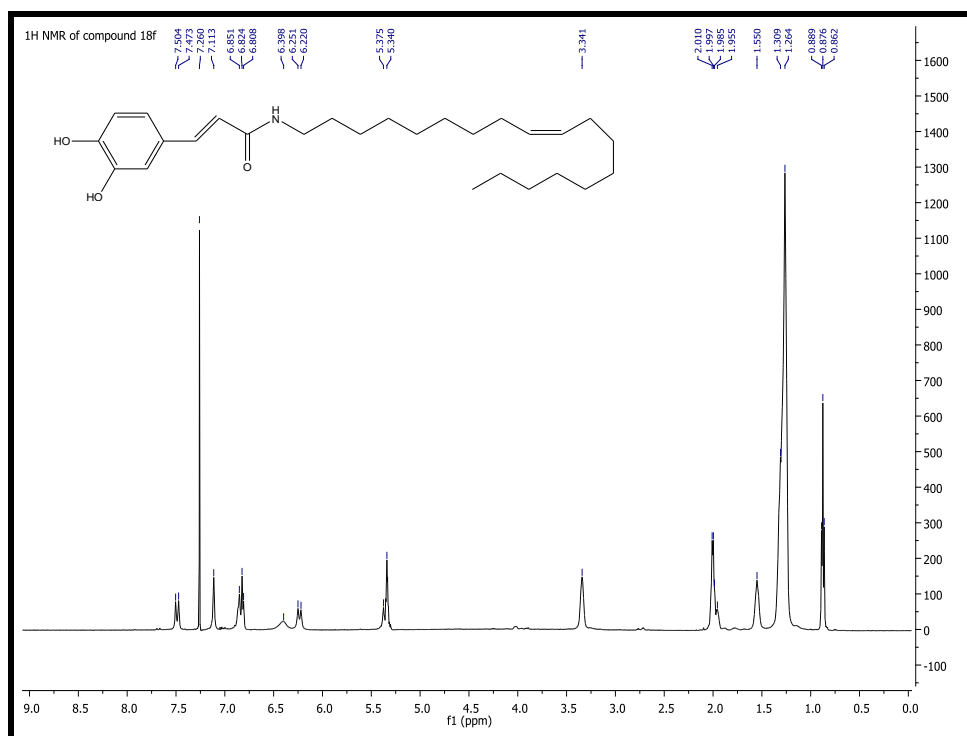
Fig. 153: ¹H NMR spectrum (500 MHz, CDCl₃) of N-oleylcaffeamide (**18f**)
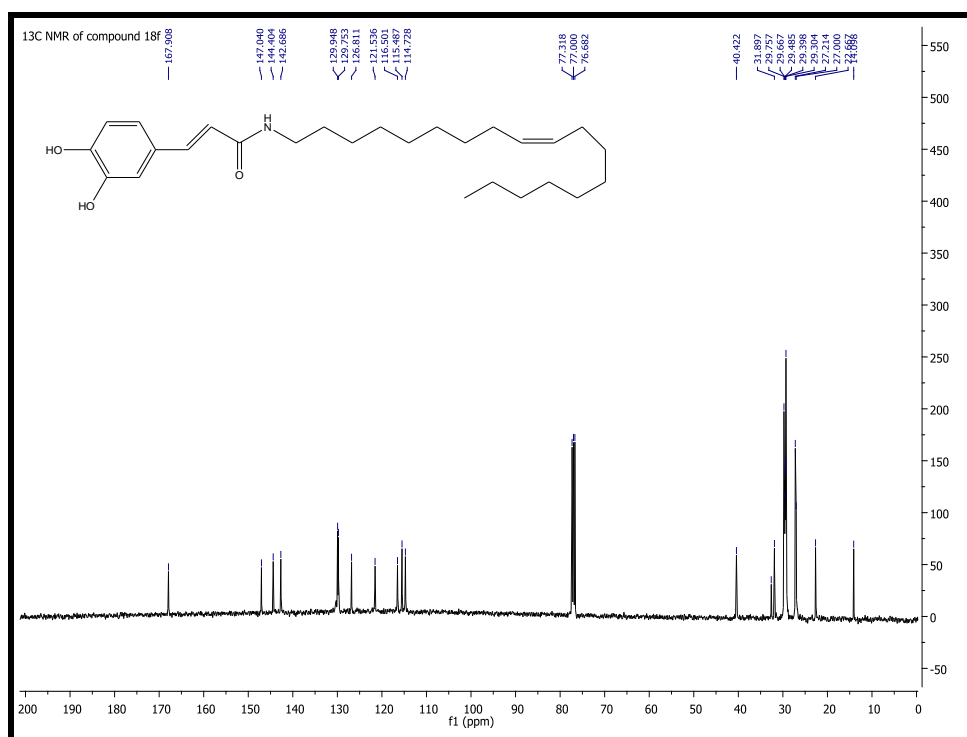
Fig. 154: ¹³C NMR spectrum (100 MHz, CDCl₃) of N-oleylcaffeamide (**18f**)

7.3 Methodology of isolation for *Tinospora cordifolia*

7.3.1 Plant material-

Dried stem bark powder of *T. cordifolia* was procured in August, 2014 from Vedshree Ayurvedic Medical, Nashik (India). Plant material was identified by Dr. N V Malpure (Dept. of Botany, SSGM College of Science, Kopargaon, India). The voucher specimen was deposited in the Herbarium of the Department of Life and Environmental Science, Drug Sciences Section, University of Cagliari.

7.3.2 Extraction method

300 g of completely dried and powdered stem bark were subjected to extraction. Extraction was successively carried out using DCM at room temperature. Repetitive cycles of percolation (during the day) and maceration (during the night) were implemented. Solvents were evaporated under reduced pressure using rotatory evaporator. 5.4 g of DCM extract was obtained at the end of percolation

7.3.3 Isolation of secondary metabolites from DCM extract

The CH_2Cl_2 extract (5.4 g) was subjected to vacuum-liquid chromatography (VLC) (silica gel, 100 g, 40 - 63 µm) using a step gradient of *n*-hexane/EtOAc/MeOH (7.5 : 2.5 : 0 : 0 to 0 : 0 : 7.5 : 2.5, 200 ml each) to yield 10 fractions (F1-F10). A portion of F1 of VLC (395 mg) was purified by CC over silica gel, eluted with DCM/Ethyl Acetate (9.9:0.1), to yield 9 subfractions (F1.1-F1.9). F1.3 (48 mg) was further purified by CC over silica gel, eluted with Hexane: Ethyl acetate (9.5:0.5) to yield **Lupenone (21),** (11.6 mg). F1.9 was identified as **β-sitosterol (25)**, (15.5 mg).

F3 of VLC (300 mg) was purified by CC over sephadex LH-20 with MeOH as eluent yielding 4 subfractions (F3.1-F3.4). F3.4 (200 mg) was further purified by CC over silica gel, eluted with DCM: Ethyl acetate (9.9:0.1) to give 8 subfractions (F3.4.1-F3.4.8). F3.4.1 was compound identified as **β-asarone (28),** (30 mg, a white solid). F3.4.3 (16.7 mg) was purified by sephadex LH 20 with methanol as eluent to give **Lupeol (22),** (6.8 mg). F3.4.6 (45 mg) was

purified by CC over silica gel, eluted with Hexane: Ethyl acetate (8:2) to give **Stigmasterol (24),** (12 mg).

F8 of VLC (142.8 mg) was subjected to CC over silica gel, eluted with DCM: MeOH (9.75:0.25) to give 4 subfractions (F8.1-F8.4). Methanol soluble portion of F8.2 was purified over sephadex LH-20 using Methanol as eluent to obtain **Balanophonin (31),**(7.3 mg). Methanol soluble portion of F8.4 (27 mg) was purified be CC over sephadex LH-20 to obtain white oily solid, identified as **N-trans-feruloyltyramine (29),** (5 mg).

F4 of VLC (200 mg) was purified by CC over Sephadex LH-20 followed by purification by CC over silica gel, eluted with Hexane: ethyl acetate (9: 1) to give two subfractions (F4.1-F4.2). F4.2 was chromatographed by RP-HPLC using MeOH/ H_2O/ Trifluroacetic acid (50: 50: 0.5, Flow 3ml/min) to yield **11-oxo- β- amyrine (23),** (t_R 14 min, 3.1 mg).

F6 was purified by CC over sephadex LH-20 to yield **columbine (26)** and **vanillin (27).**
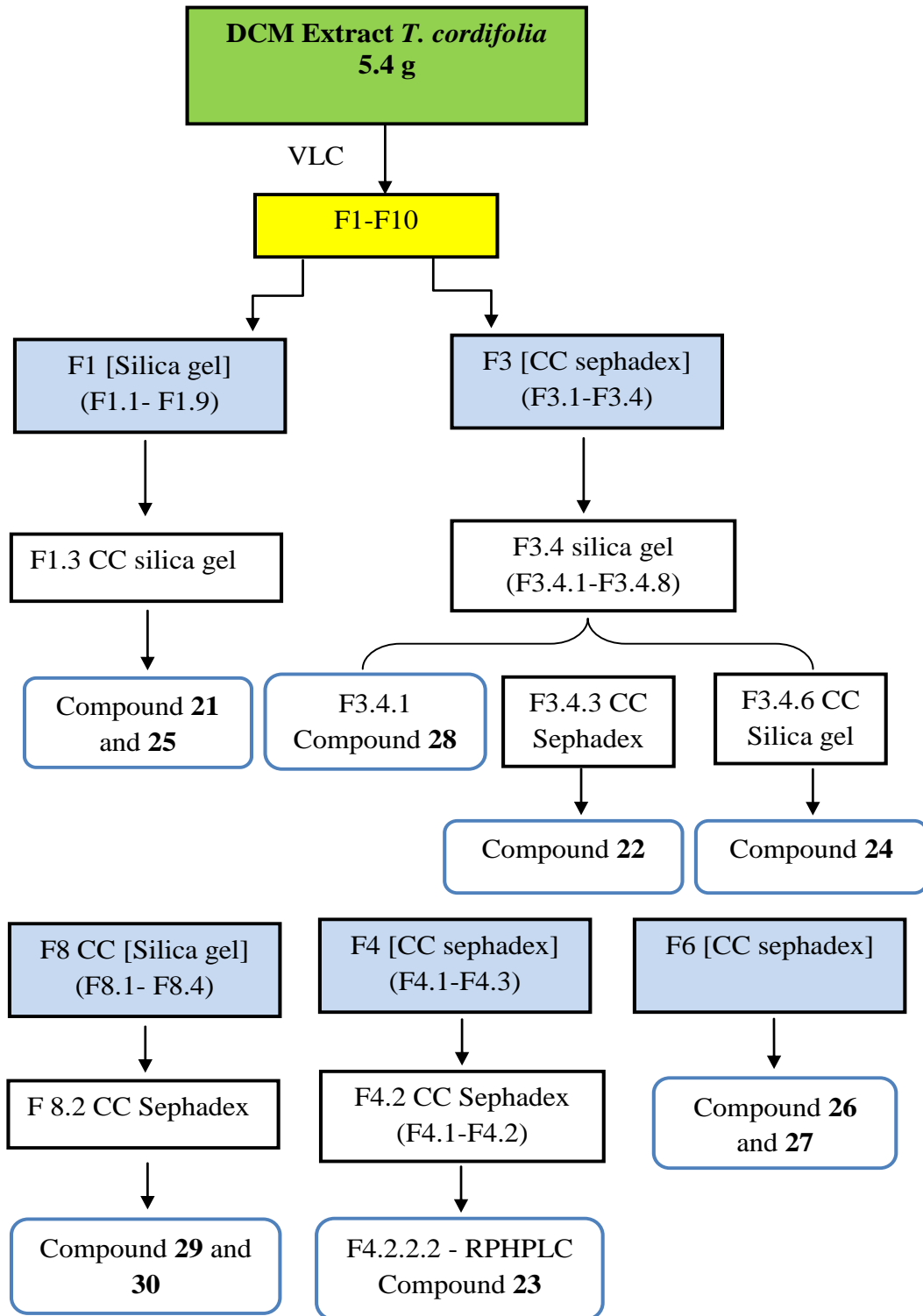
Fig.155: Scheme of isolation of secondary metabolites from DCM extract of *T. cordifolia*

7.3.4 ESI MS and NMR spectra of compounds Isolated from *T. cordifolia*
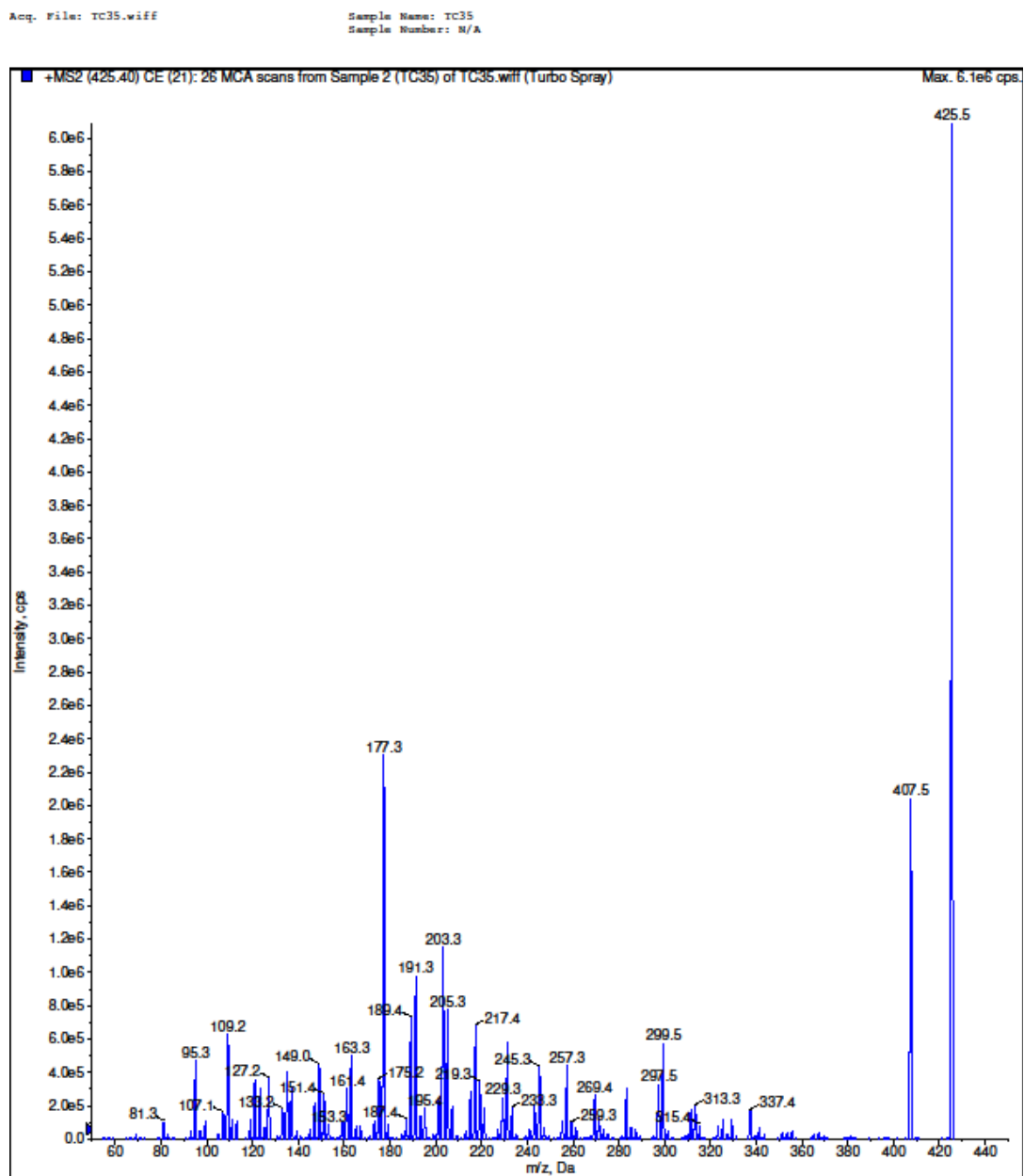
Compound 21

Fig.156: Mass spectrum of compound **21** (lupenone) measured with ESI source in positive mode
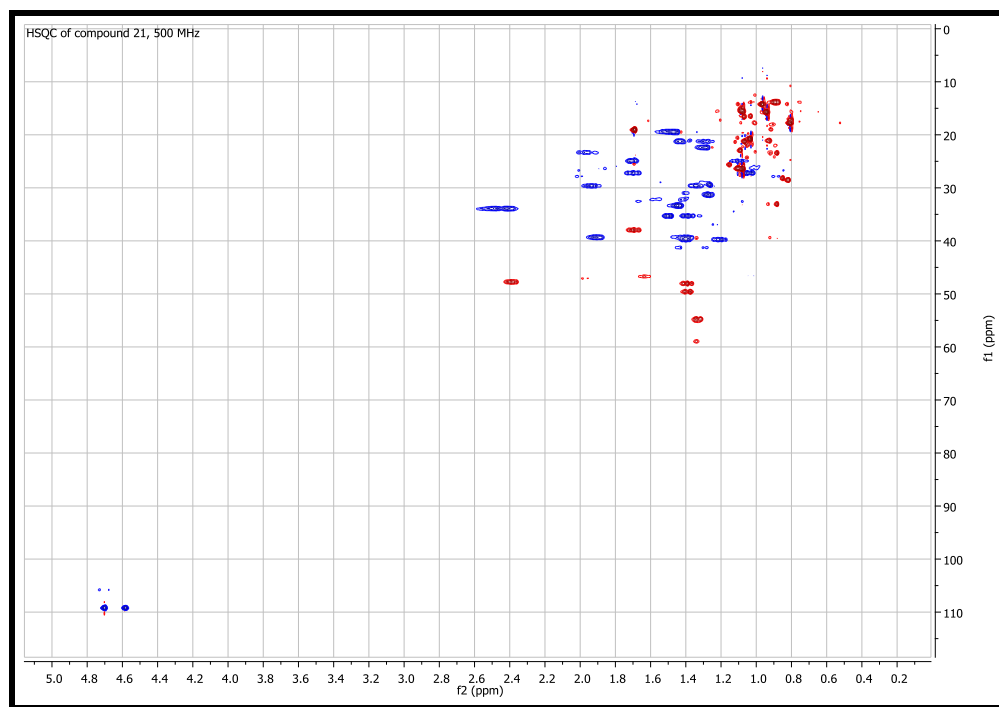
Fig.157: HSQC spectrum of compound **21** (lupenone), 500 MHz, CDCl$_3$
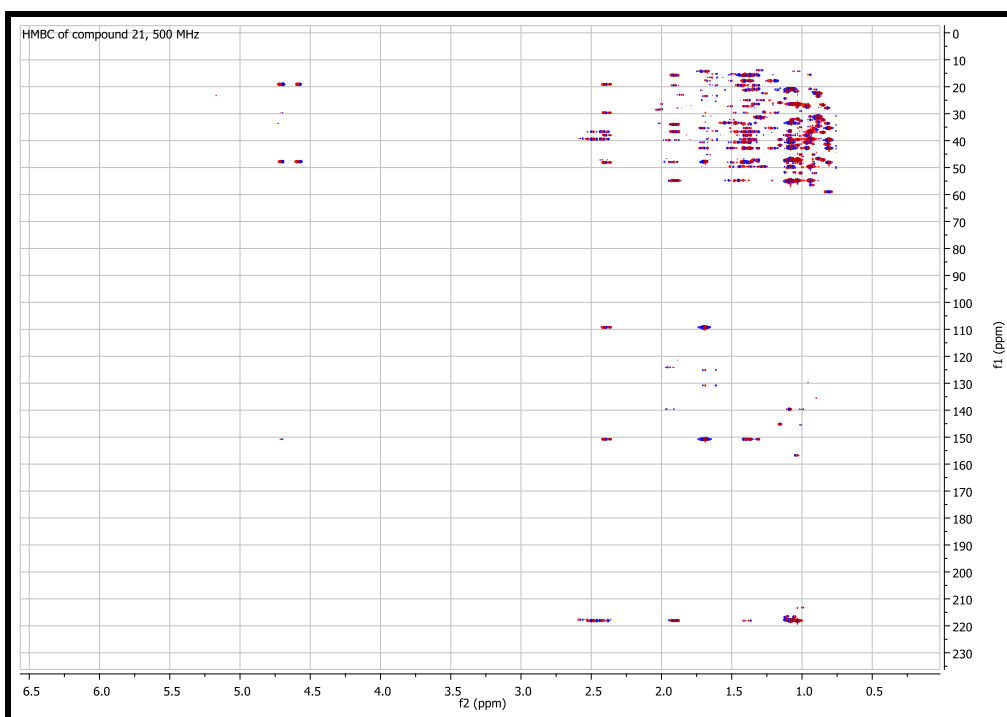
Fig.158: HMBC spectrum of compound **21** (lupenone), 500 MHz, CDCl$_3$
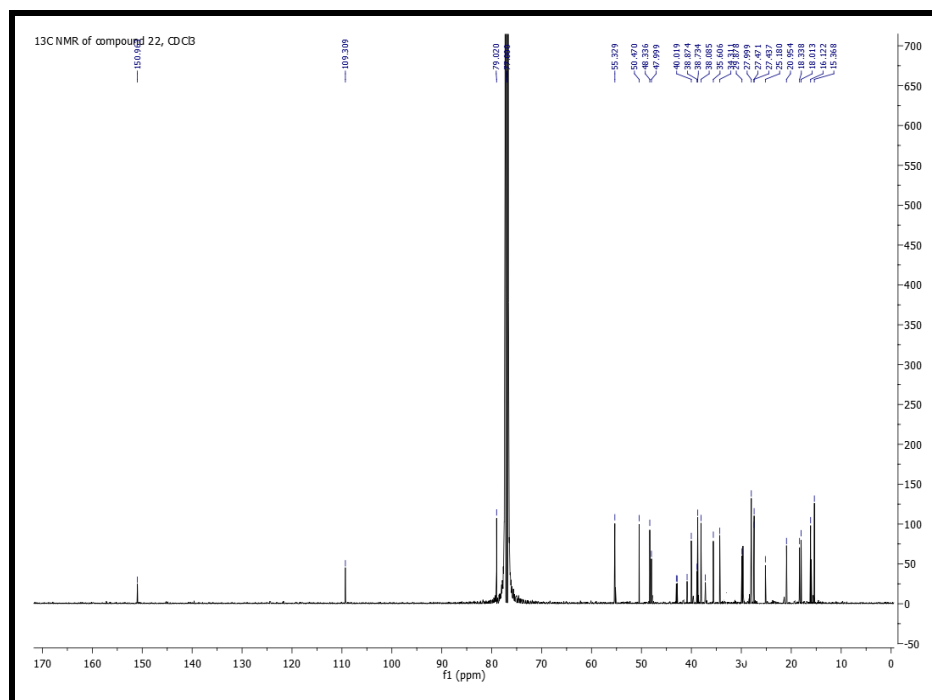
Compound 22

Fig.159: ^{13}C NMR spectrum of compound **22** (lupeol), 500 MHz, CDCl$_3$
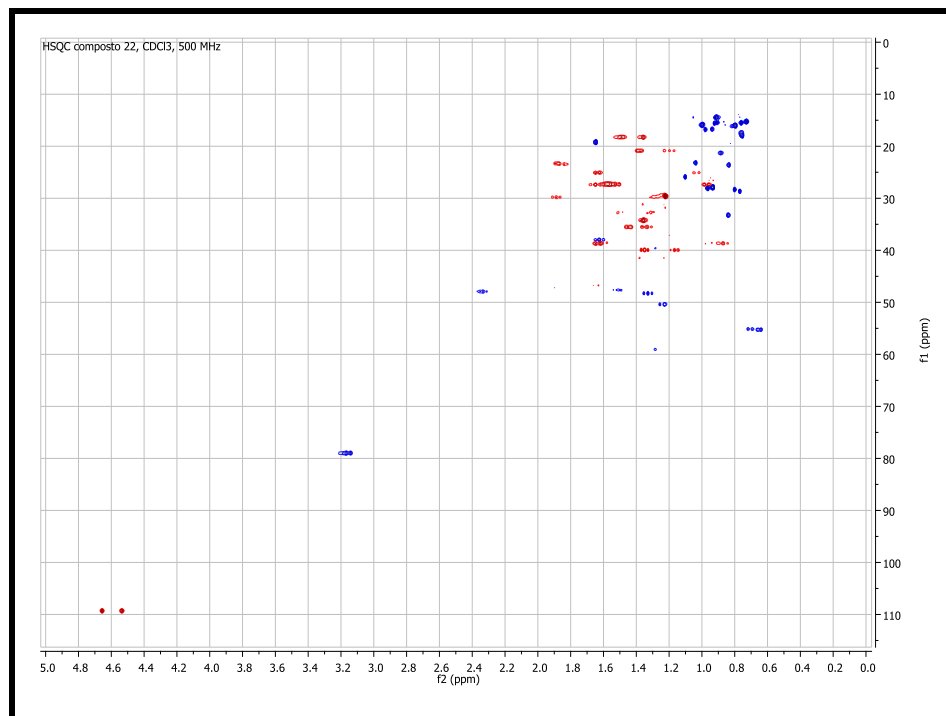
Fig160: HSQC spectrum compound **22** (lupeol), 500 MHz CDCl$_3$
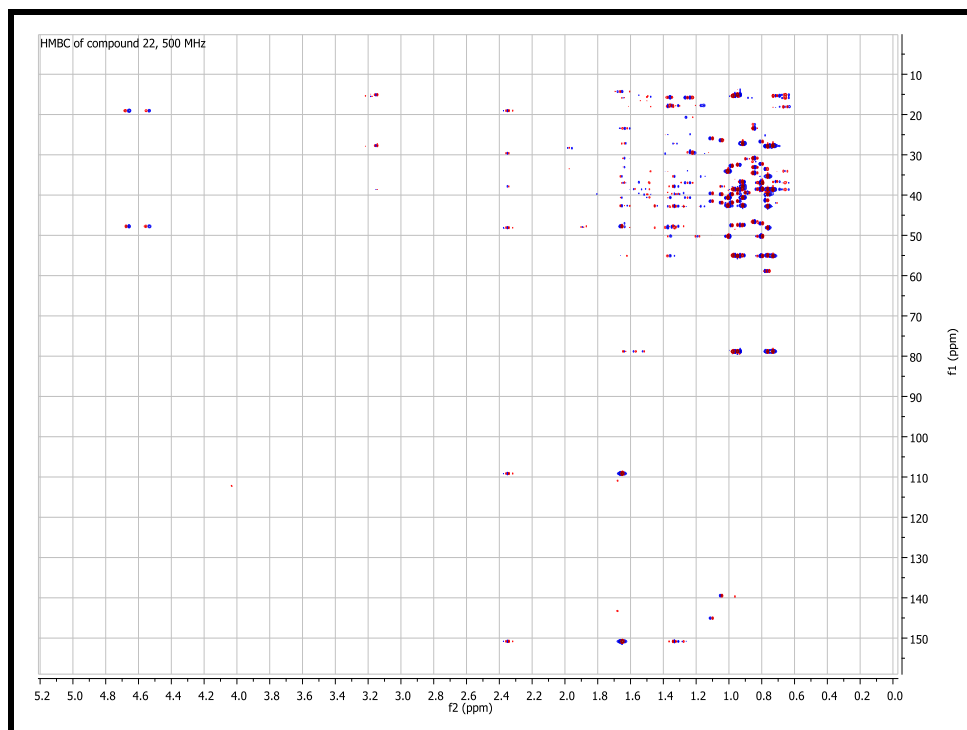
Fig.161: HMBC spectrum of compound **22** (lupeol), 500 MHz, CDCl$_3$

Compound 23
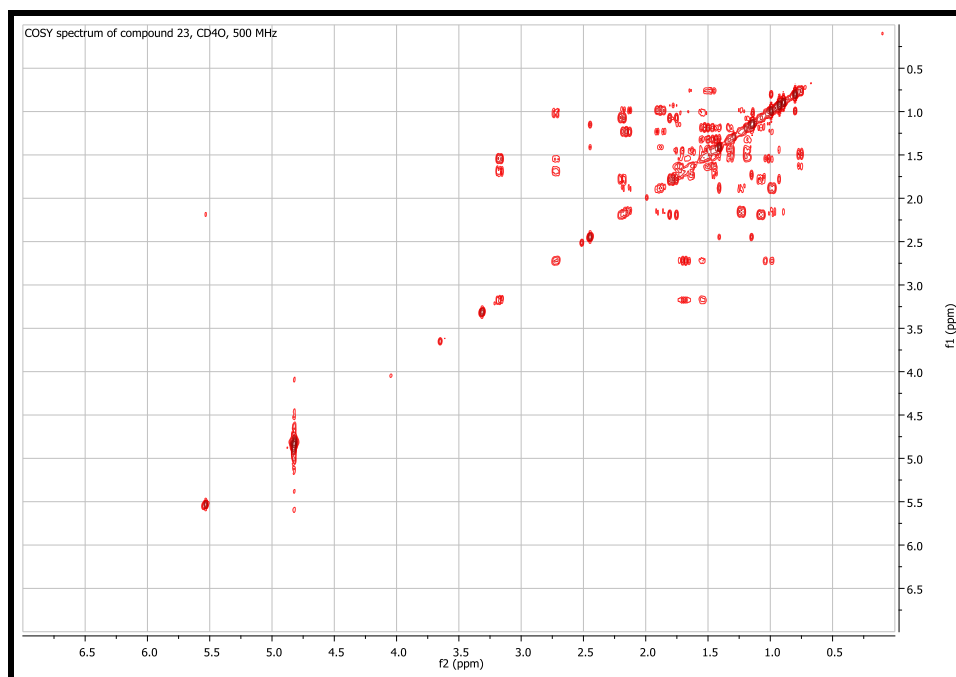
Fig.162: COSY spectrum of compound **23** (11-oxo-β-amyrin), 500 MHz, CD$_4$O
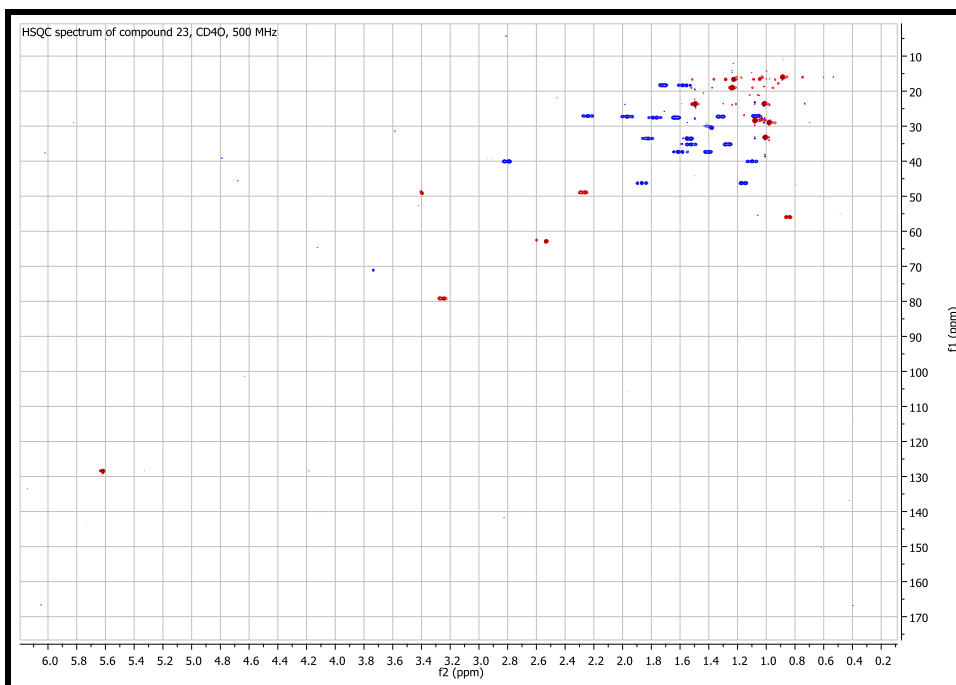
Fig.163: HSQC spectrum of compound **23** (11-oxo-β-amyrin), 500 MHz, CD$_4$O
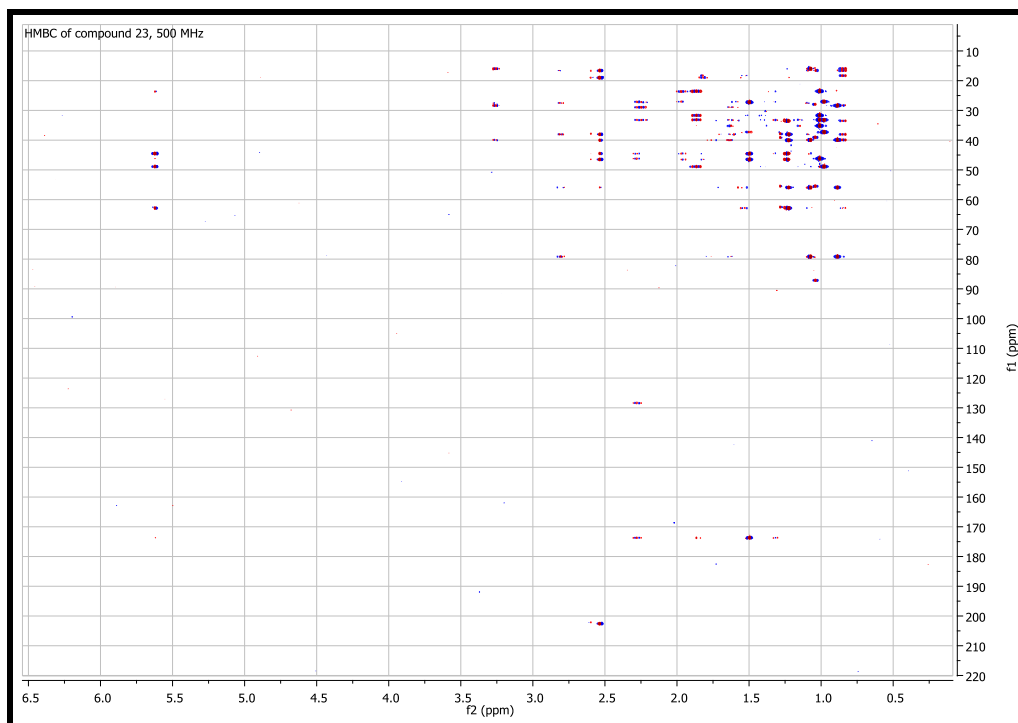
Fig.164: HMBC spectrum of compound **23** (11-oxo-β-amyrin), 500 MHz, CD$_4$O
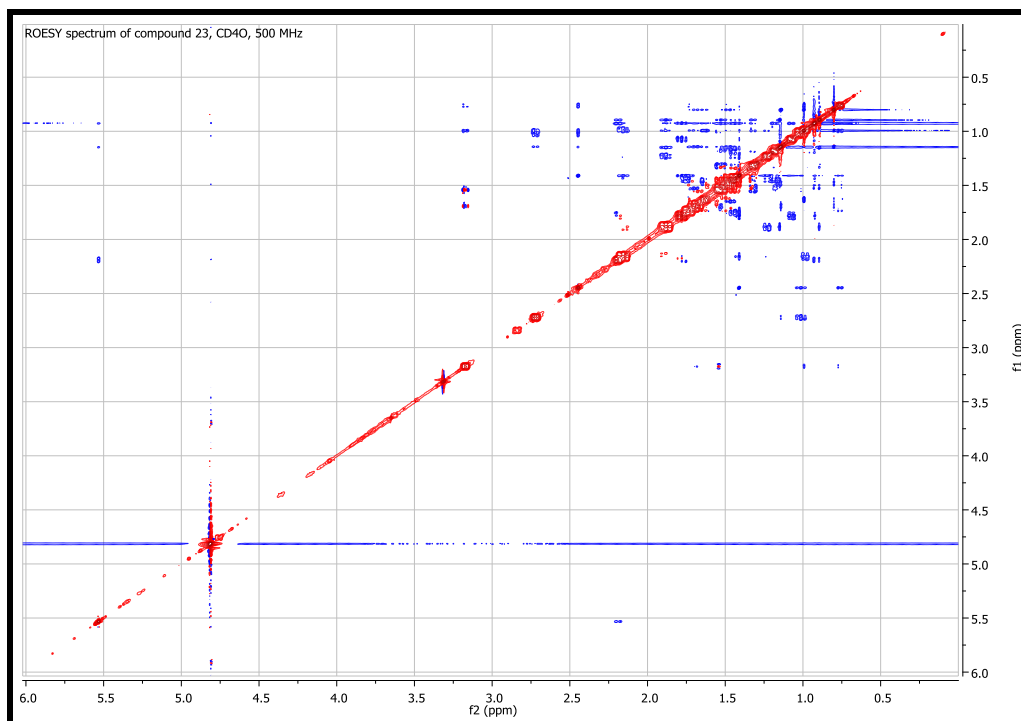
Fig. 165: ROESY spectrum of compound **23** (11-oxo-β-amyrin), 500 MHz, CD$_4$O

Compound 24
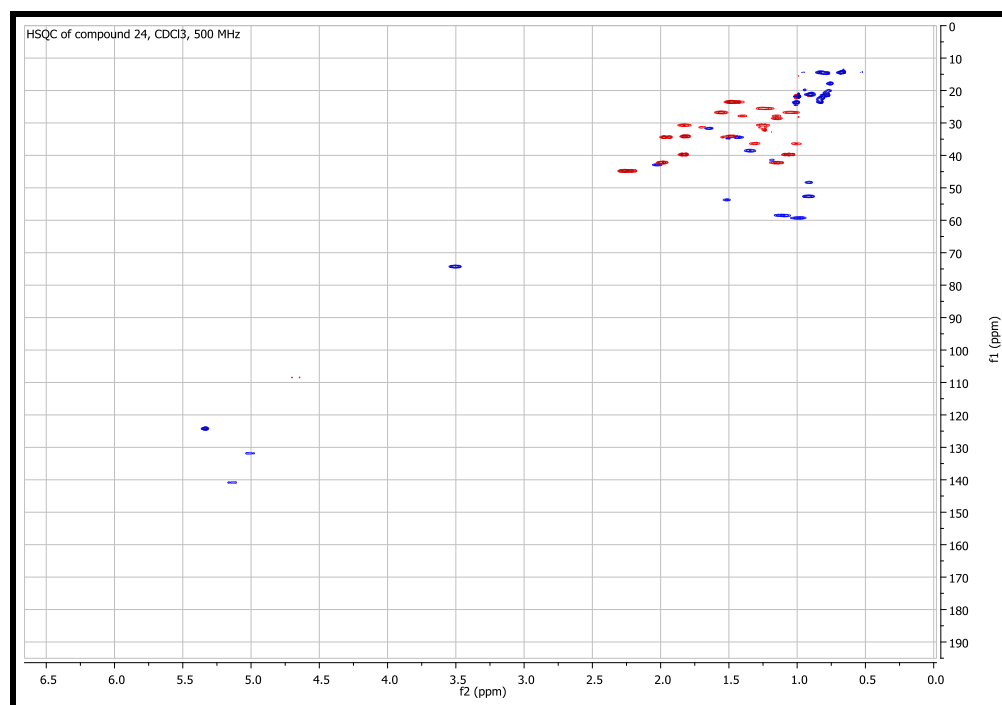
Fig. 166: HSQC spectrum of compound **24** (stigmasterol), 500 MHz, CDCl$_3$
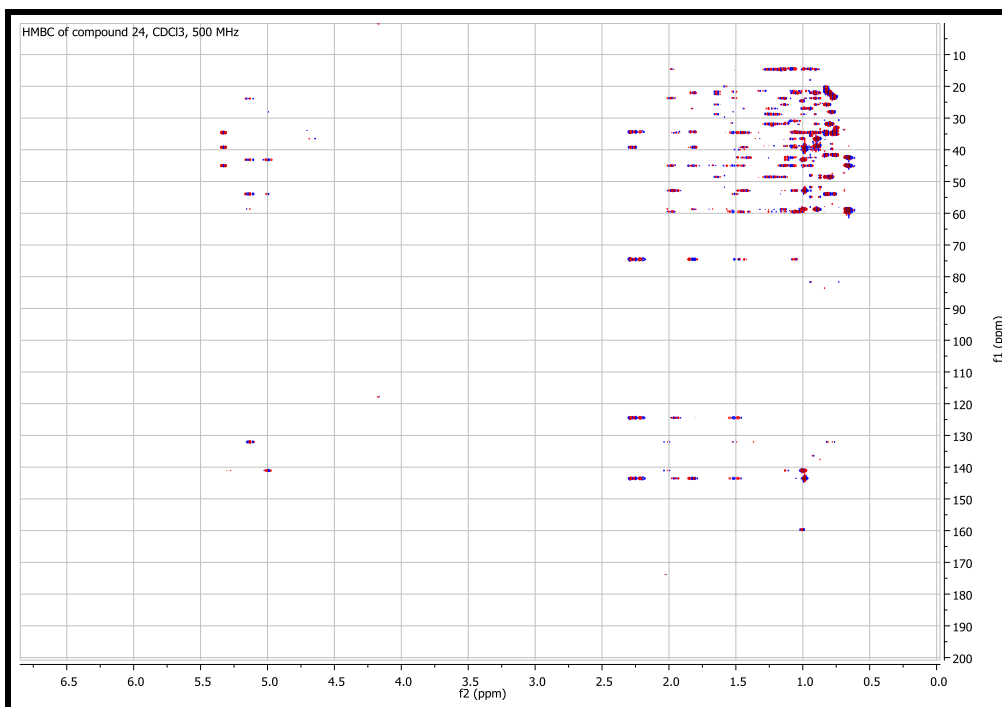
Fig. 167: HMBC spectrum of compound **24** (stigmasterol) 500 MHz, CDCl$_3$
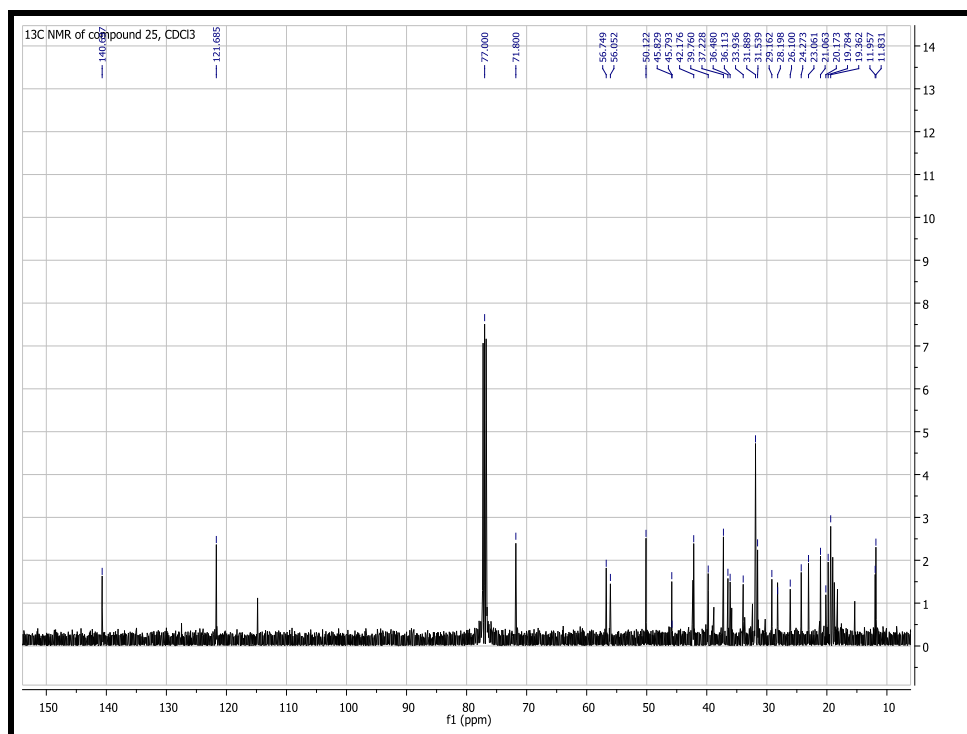
Compound 25

Fig.168: ^{13}C NMR spectrum of compound **25** (β-sitosterol), 100 MHz, CDCl$_3$

Compound 26
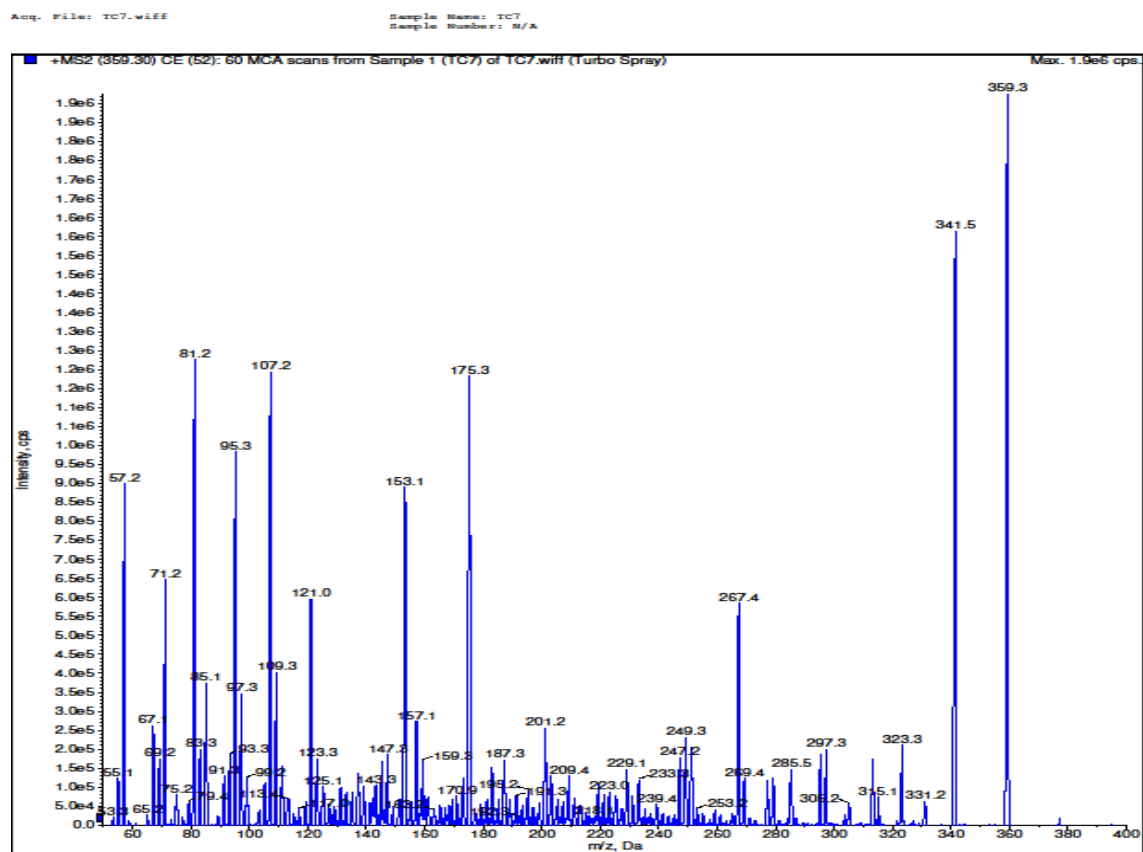
Fig.169: Mass spectrum of compound **26** (Columbine) measured with ESI source in positive mode
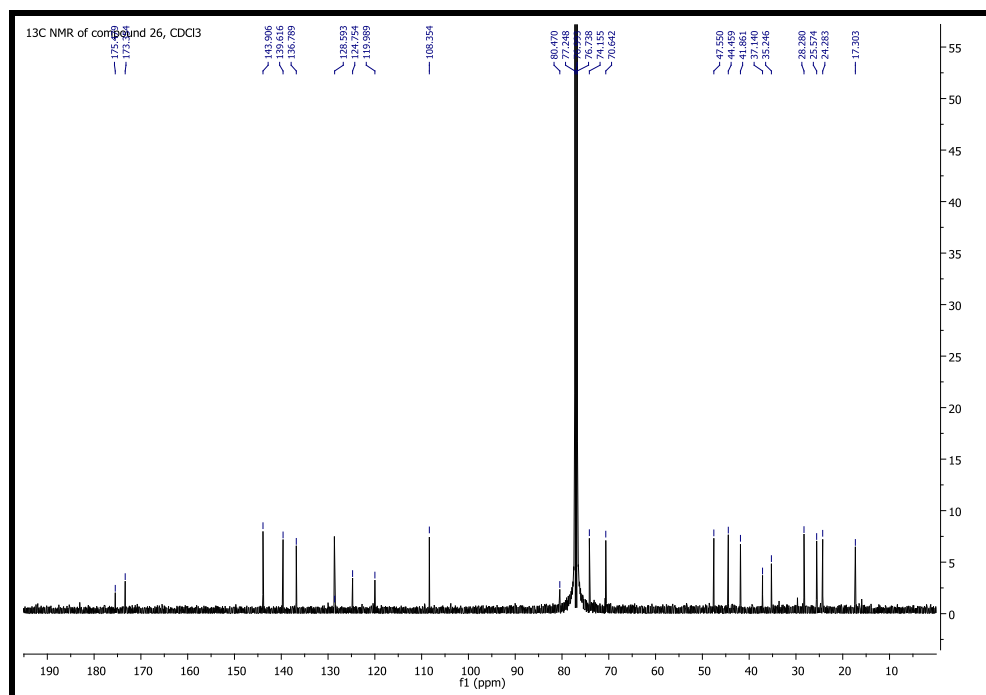
Fig. 170: ^{13}C NMR spectrum of compound **26** (columbin), 100 MHz, CDCl$_3$
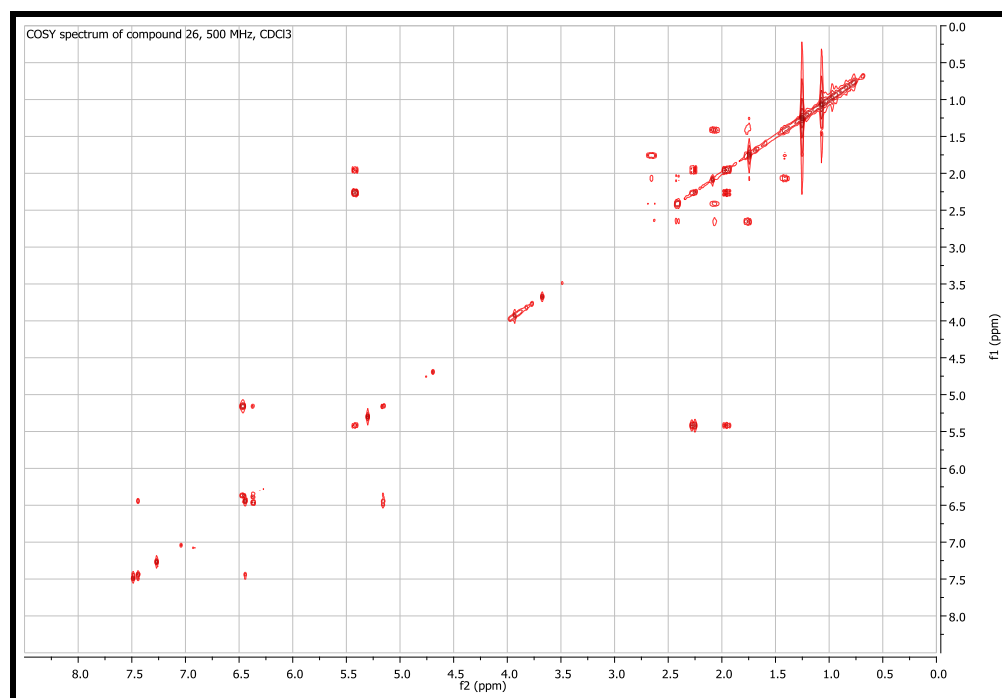
Fig. 171: COSY spectrum of compound **26** (columbin), 500 MHz, CDCl$_3$
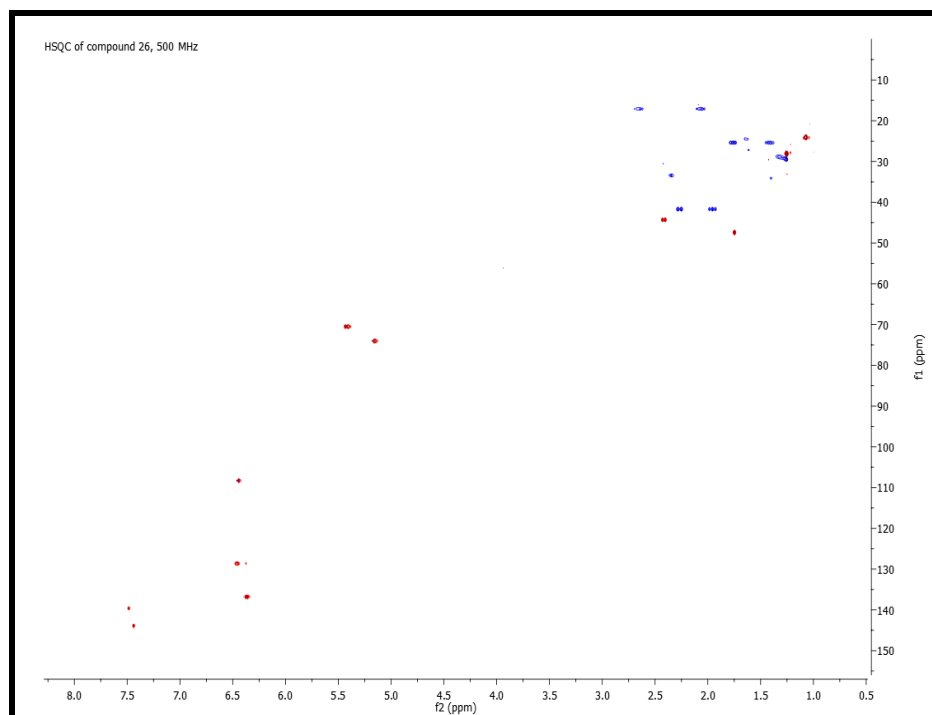
Fig. 172: HSQC spectrum of compound **26** (columbin), 500 MHz, CDCl$_3$
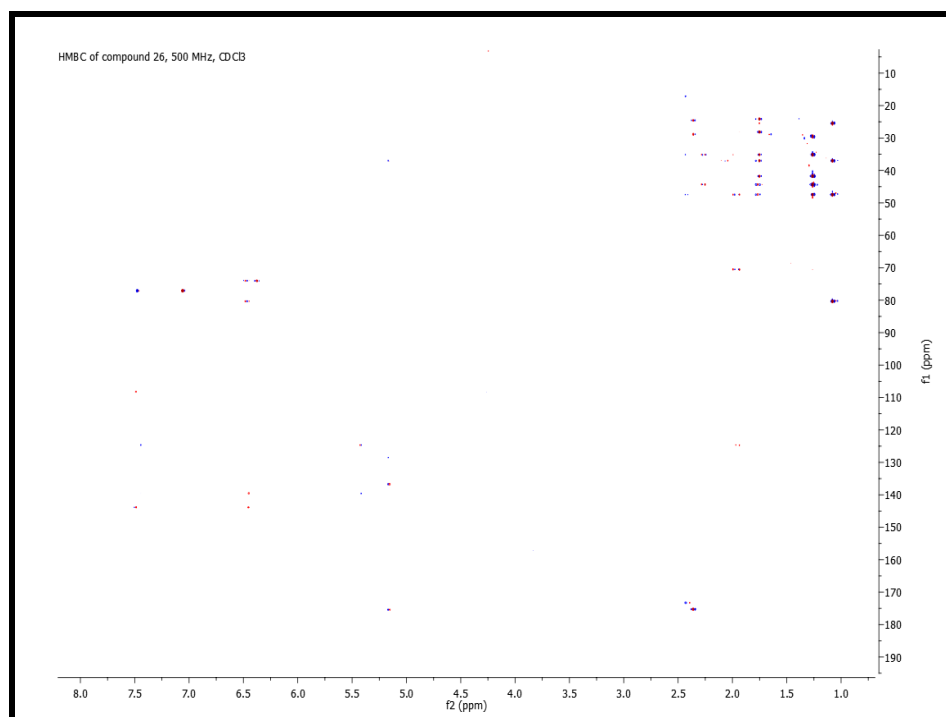
Fig. 173: HMBC spectrum of compound **26** (columbin), 500 MHz, CDCl$_3$
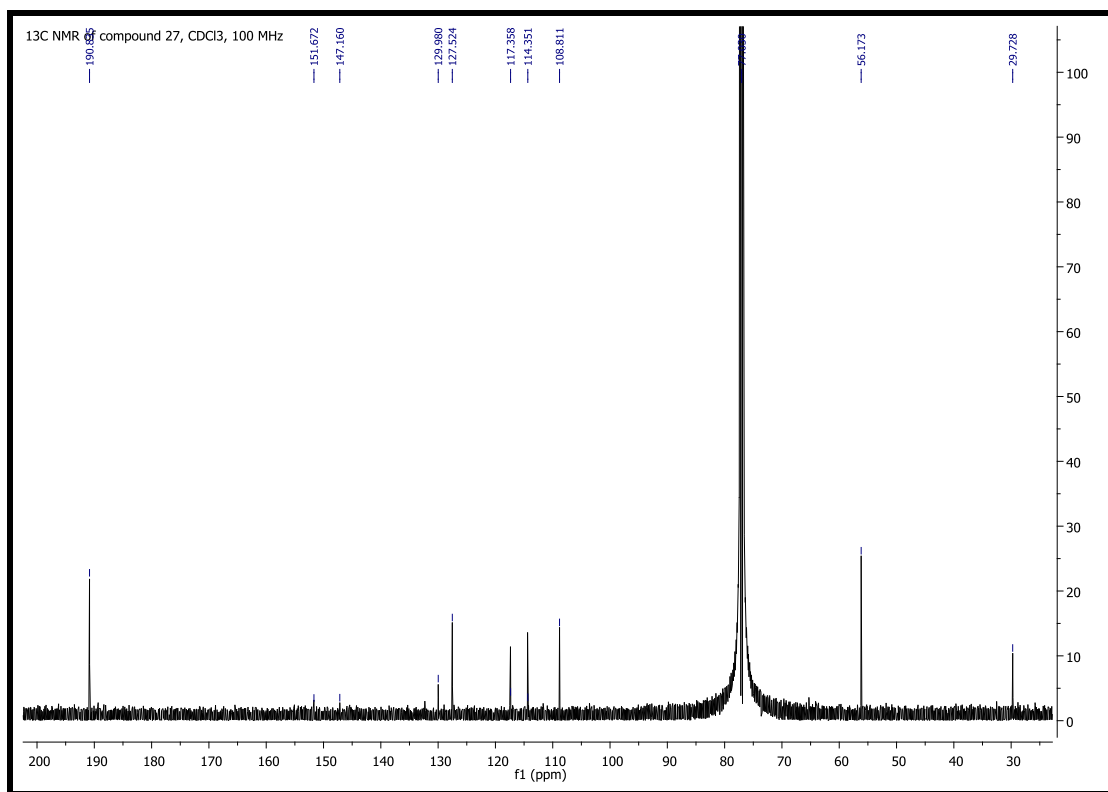
Compound 27

Fig. 174: ^{13}C NMR spectrum of compound **27** (vanillin), 100 MHz, CDCl$_3$
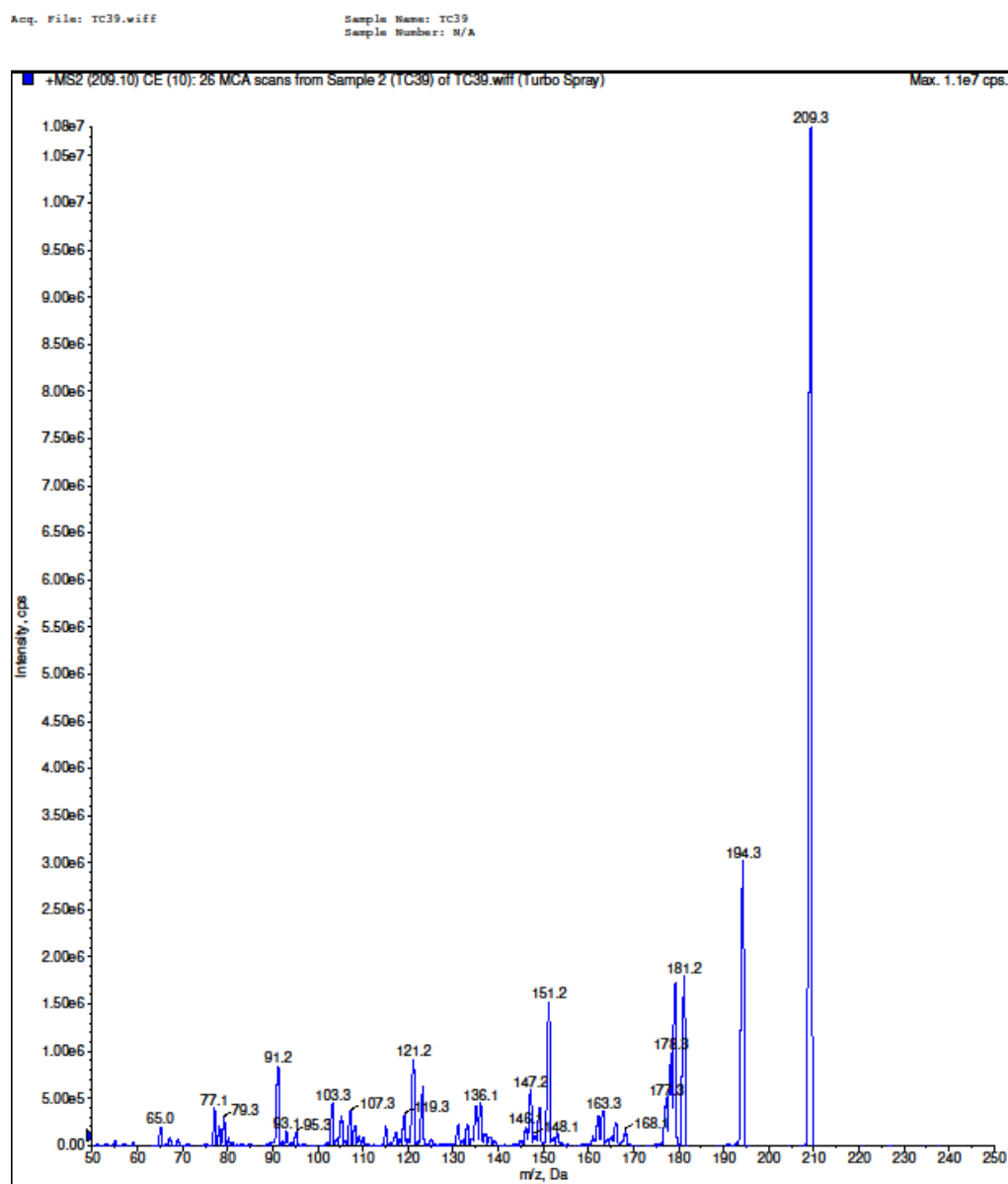
Compound 28

Fig.175: Mass spectrum of compound **28** (β-asarone) measured with ESI source in positive mode
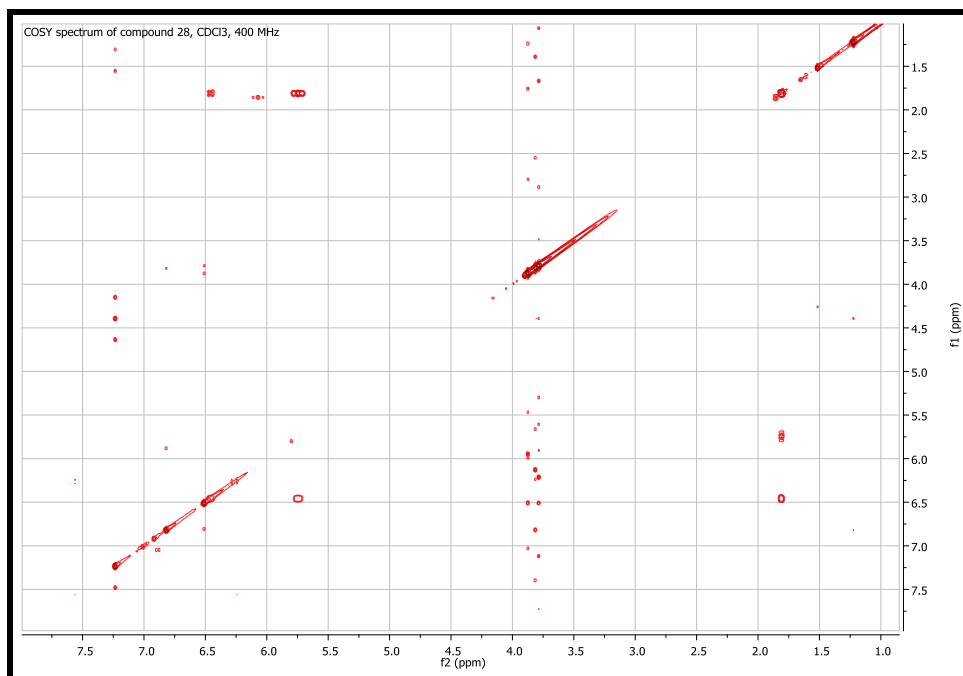
Fig.176: COSY spectrum of compound **28** (β-asarone), 400MHz, CDCl₃
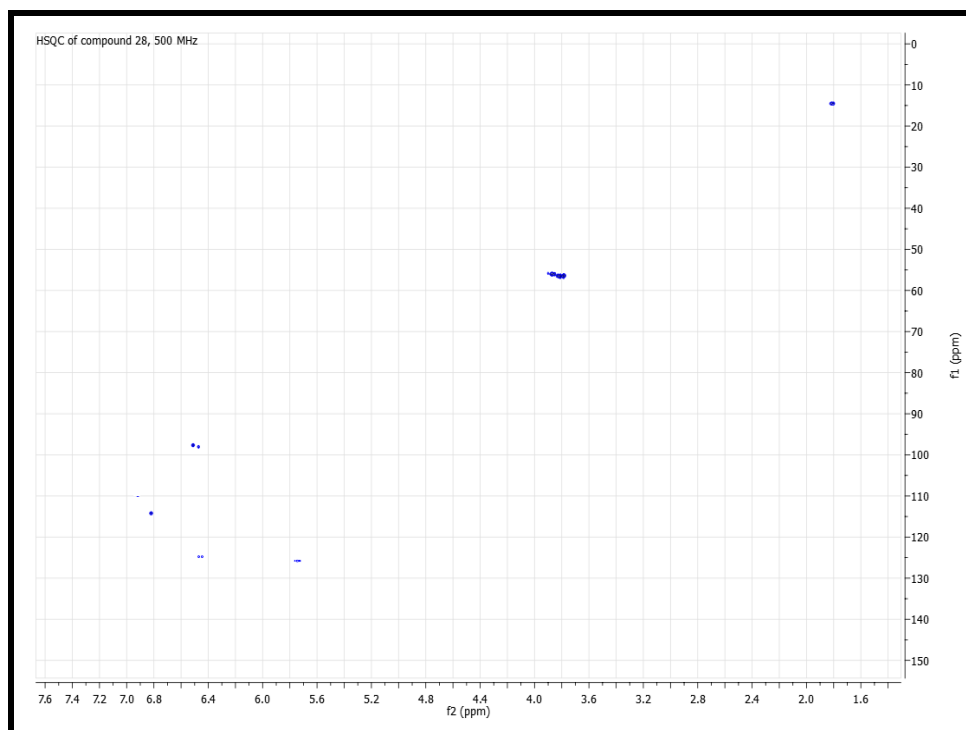
Fig.177: HSQC spectrum of compound **28** (β-asarone), 400MHz, CDCl₃
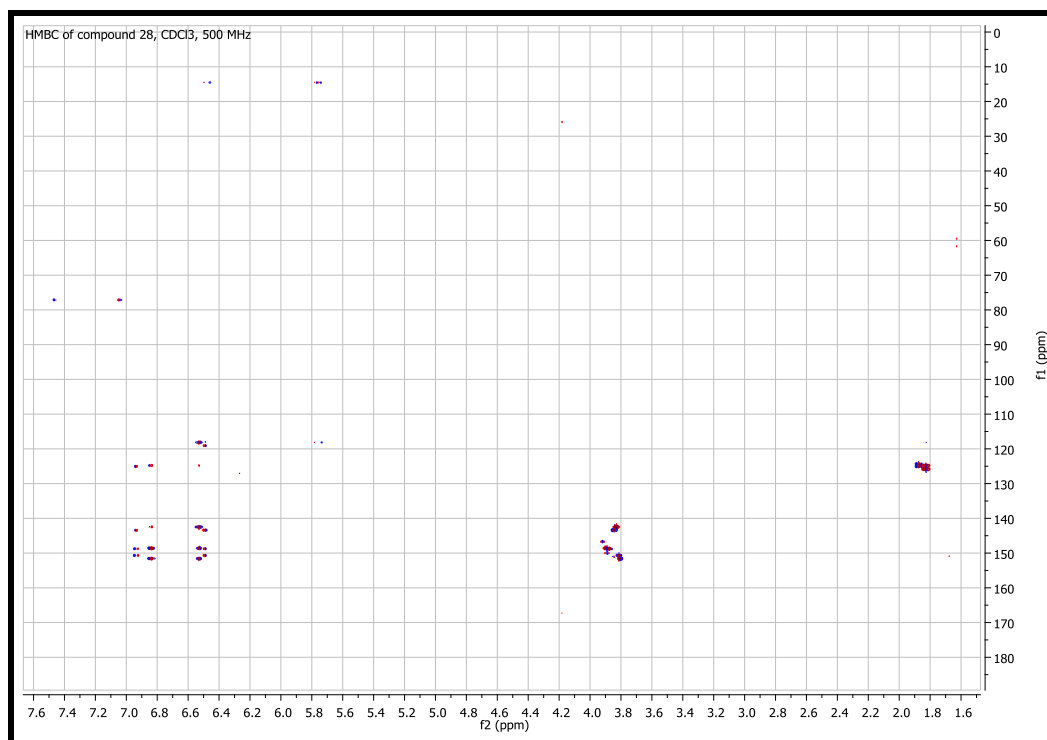
Fig.178: HMBC spectrum of compound **28** (β-asarone), 400MHz, CDCl$_3$

Compound 29

COSY spectrum of compound 29, aceton-d6, 500 MHz
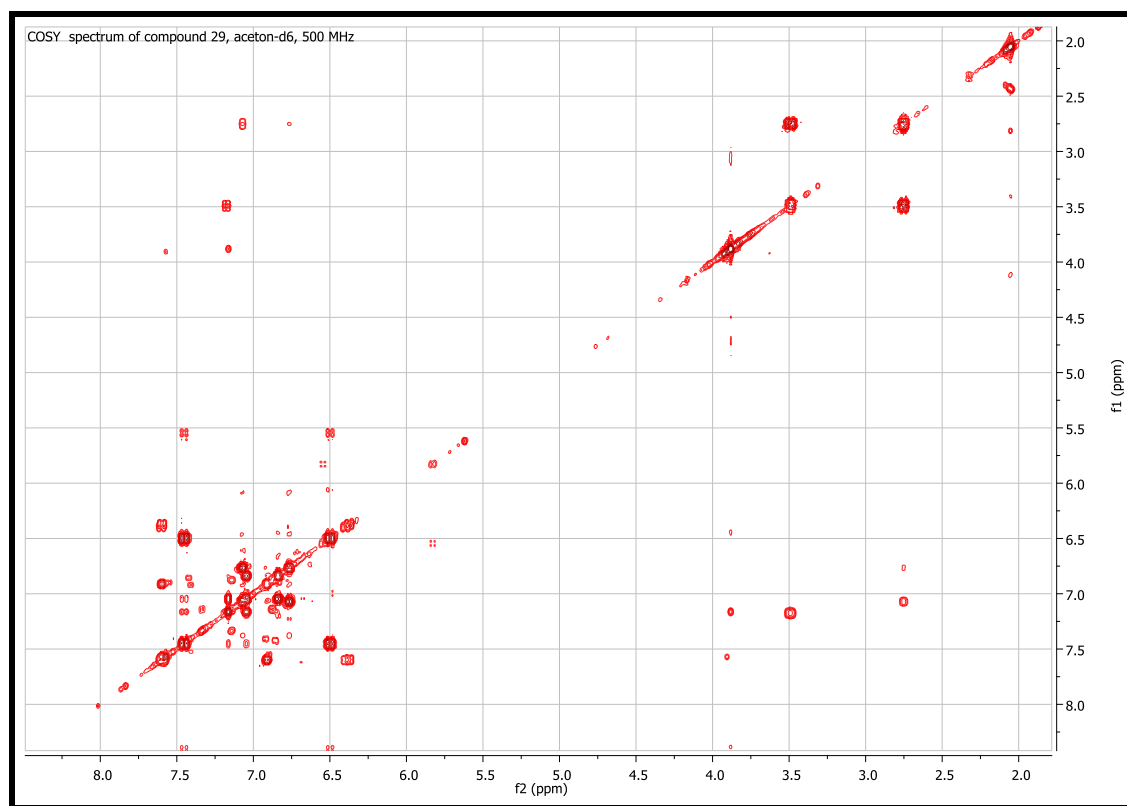
Fig.179: COSY spectrum of compound **29** (N-*trans*-feruloyltyramine), 500MHz, aceton- d$_6$
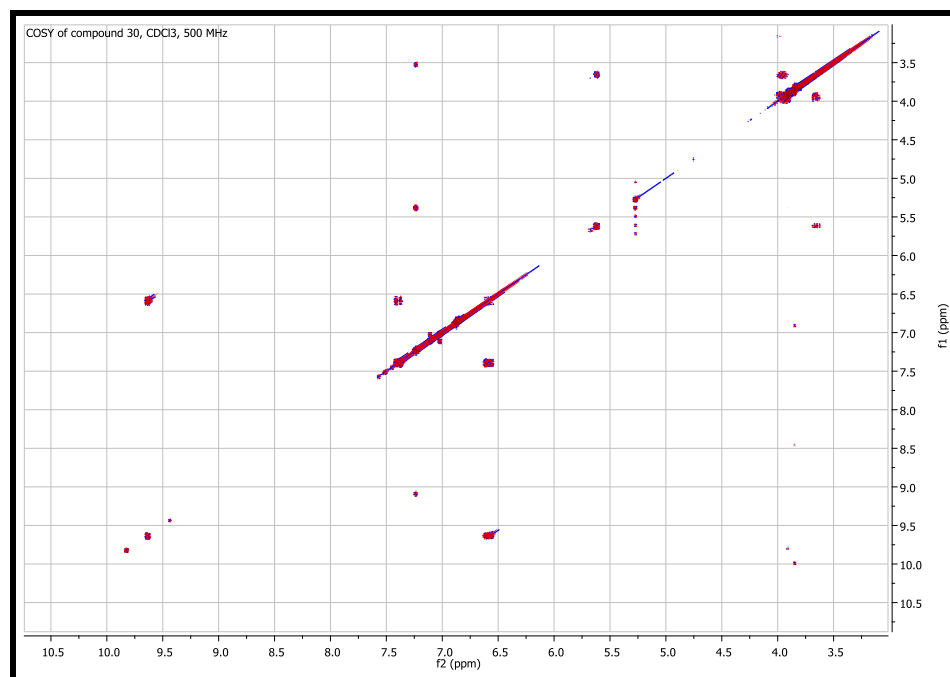
Compound 30

Fig.180: COSY spectrum of compound **30** [(+)-balanophonin], 500MHz, CDCl₃
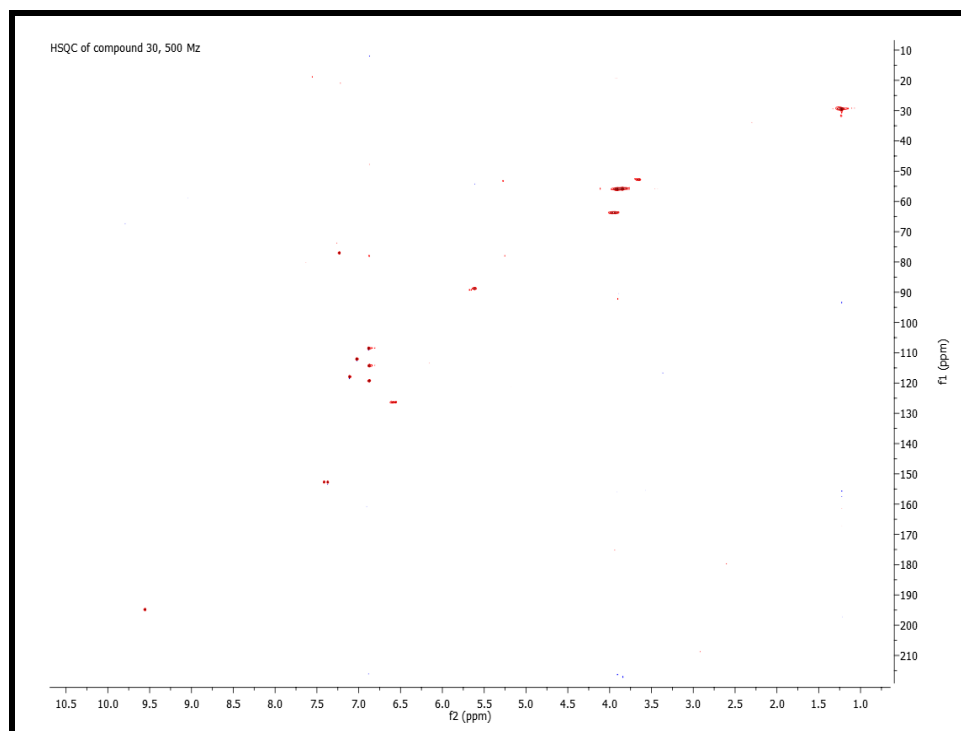
Fig.181: HSQC spectrum of compound **30** [(+)-balanophonin], 500MHz, CDCl₃
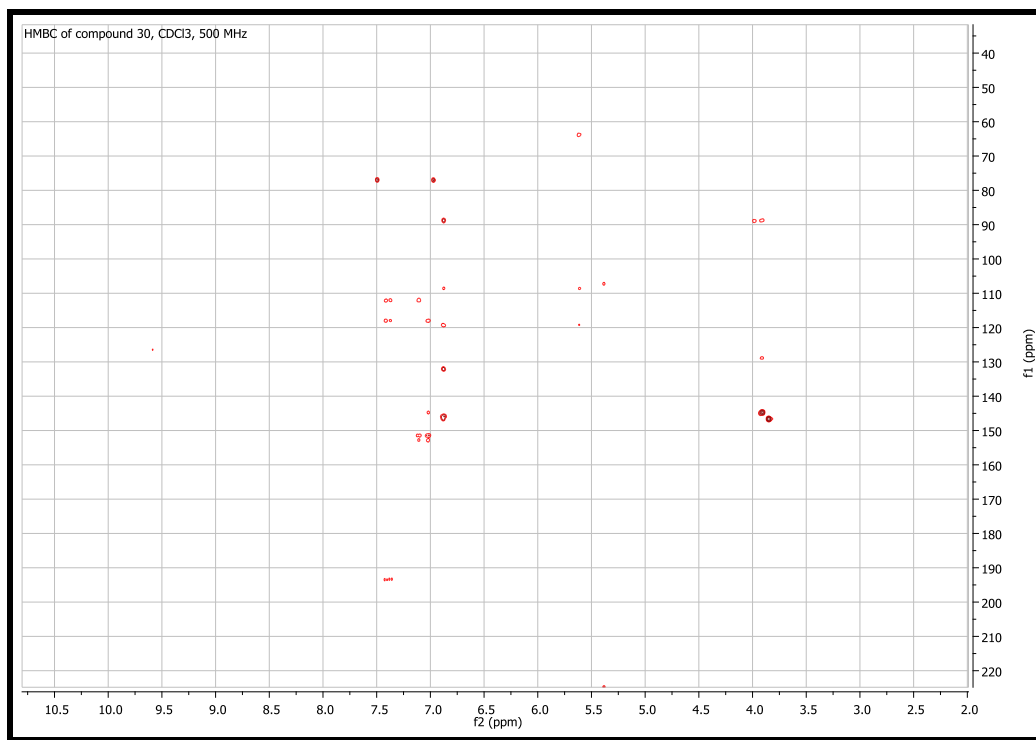
Fig.182: HMBC spectrum of compound **30** [(+)-balanophonin], 500MHz, CDCl$_3$
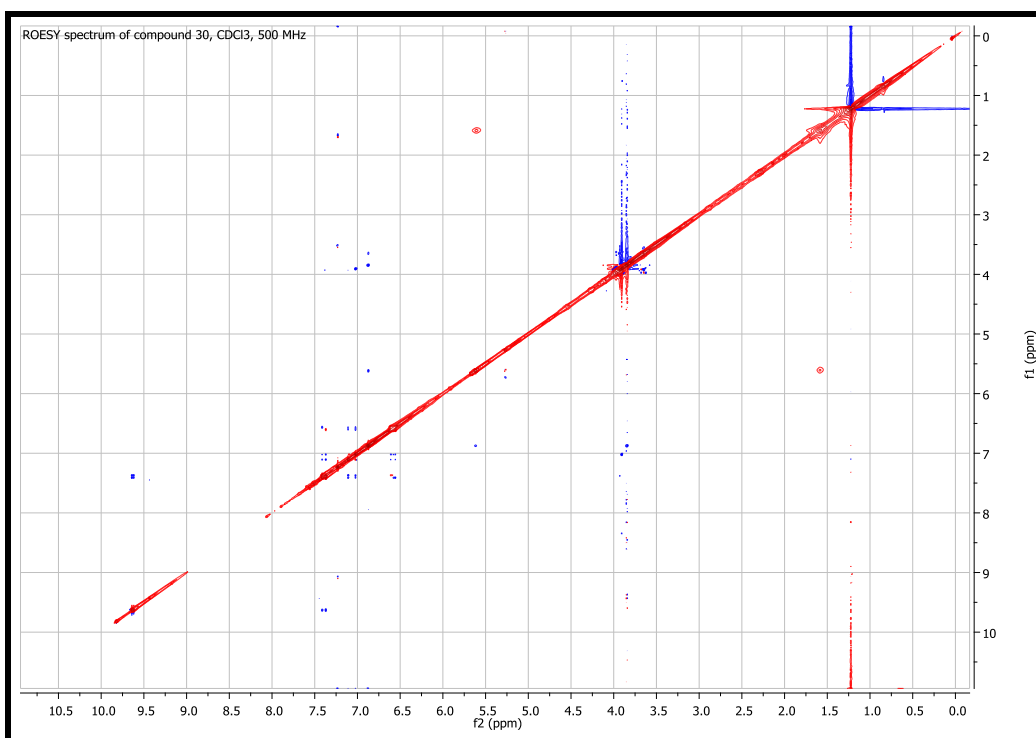
Fig.183: ROESY spectrum of compound **30** [(+)-balanophonin], 500MHz, CDCl$_3$

7.4 Methodology of isolation for *Bupleurum fruticosum* L.

7.4.1 Plant material

Dried leaves of *B. fruticosum* were collected from Sardinia (South Italy) in August, 2014 The voucher specimen was deposited in the Herbarium of the Department of Life and Environmental Science, Drug Sciences Section, University of Cagliari.

7.4.2 Extraction method

Dried leaves of *B. fruticosum* (460 g) were subjected for percolation. Extraction was carried out using DCM at room temperature. Repetitive cycles of percolation (during the day) and maceration (during the night) were implemented. Solvents were evaporated under reduced pressure using rotatory evaporator. 23.5 g of DCM extract was obtained at the end of percolation.

7.4.3 Isolation of secondary metabolites from DCM extract

The CH_2Cl_2 extract (23.5 g) was subjected to vacuum-liquid chromatography (VLC) (silica gel, 100 g, 40 - 63 µm) using a step gradient of *n*-hexane/EtOAc/MeOH (7.5 : 2.5 : 0 : 0 to 0 : 0 : 7.5 : 2.5, 500 ml each) to yield 6 main fractions (F1-F6).

F3 (300 mg) was purified by sephadex to remove chlorophyll like impurities. Resulting fractions were further purified by SPE RP-18 column using Acetonitrile to give **Compound 34** (57.8 mg).

Another portion of F3 (1.4 g) was subjected to CC over silica gel, eluted with DCM: Ethyl acetate (9:1) to give 8 subfractions (F3.1-F3.8). F3.3 (60 mg) was purified by CC over sephadex, eluted with methanol to give a fraction. This fraction was purified again by SPE RP-18 column using Acetonitrile: H_2O (8.5: 1.5) to give **Compound 38** (7.9 mg), a yellow colour semisolid. F3.4 was purified by sephadex, eluted with methanol, followed by SPE RP-18 coloumn to give a compound, identified as **Compound 40** (12.4 mg). Optical rotation of BF 18 was measured in $CHCl_3$ at 25 °C using a Perkin-Elmer 241 polarimeter and found as (-) 17. F3.8 (120 mg) was purified by sephadex, eluted with Methanol to give **Compound 32** (66.7 mg). F3.2 was subjected to CC over sephadex, eluted with Methanol to give **Compound 34** (10.5 mg).

F1 (1g) was subjected to CC over silica gel, eluted with Hexane: Ethyl acetate (9:1) to give 8 subtractions (F1.1-F1.8). F1.3 was identified as compound **Compound 35** (11.1 mg). F1.7 (250 mg) was purified over sephadex to remove chlorophyll like impurities to give a fraction. This fraction (70 mg) was further subjected to CC over silica gel, eluted with Toluene: Ethyl acetate (9:1) to give colourless oily compound. This oil was identified as **Compound 33** (16.9 mg).

Another portion of F1 (1 g) was subjected to CC over silica gel, eluted with Toluene: Ethyl acetate (9.75:0.25) to give 8 subfractions (F1.1-F1.8). F1.4 was purified by sephadex, eluted with methanol, to give white semisolid compound. This compound was identified as **Compound 36** (2.8 mg). F1.6 was subjected to CC over sephadex using Methanol as eluent to give **Compound 35** (9.8 mg).

F4 (2.6g) was subjected to CC over silica gel, eluted with DCM: MeOH (9.75: 0.25) to give 8 subfractions (F4.1-F4.8). F4.2 was purified by sephadex, eluted with Methanol, followed by RP-HPLC using Acetonitrile: H_2O (6:4, flow 2.5ml/min) to give **Compound 39**, a white transparent solid (t_R = 6.3min, 2.3 mg). F4.8 was purified by CC over silica gel using Hexane: Ethyl acetate (60:40) as elunet to give **Compound 31** (110 mg), transparent oil.

F2 (1g) was subjected to CC over silica gel, eluted with Hexane: Ethyl acetate (8:2) to give 8 subfractions (F2.1-F2.8). F2.6 was purified by sephadex, eluted with methanol, followed by RP-HPLC using DCM: Ethyl acetate (9.75: 0.25, flow 2.5ml/min) to give **Compound 37** (t_R = 6.5min, 1.5 mg).
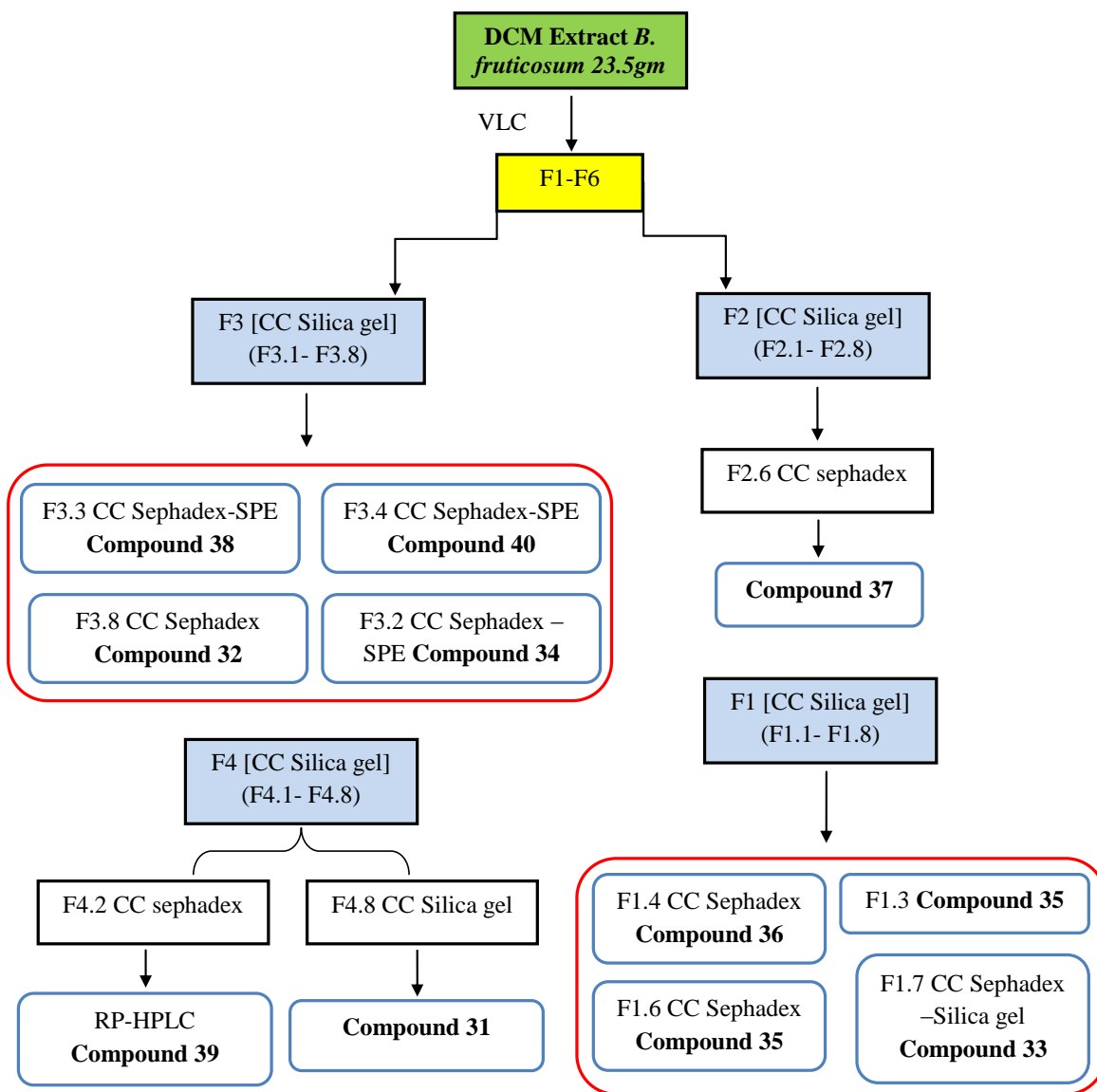
Fig.184: Scheme of isolation of secondary metabolites from DCM extract of *B.fruticosum*

7.4.4 Spectral data of compounds Isolated from *B. fruticosum*

Compound 33
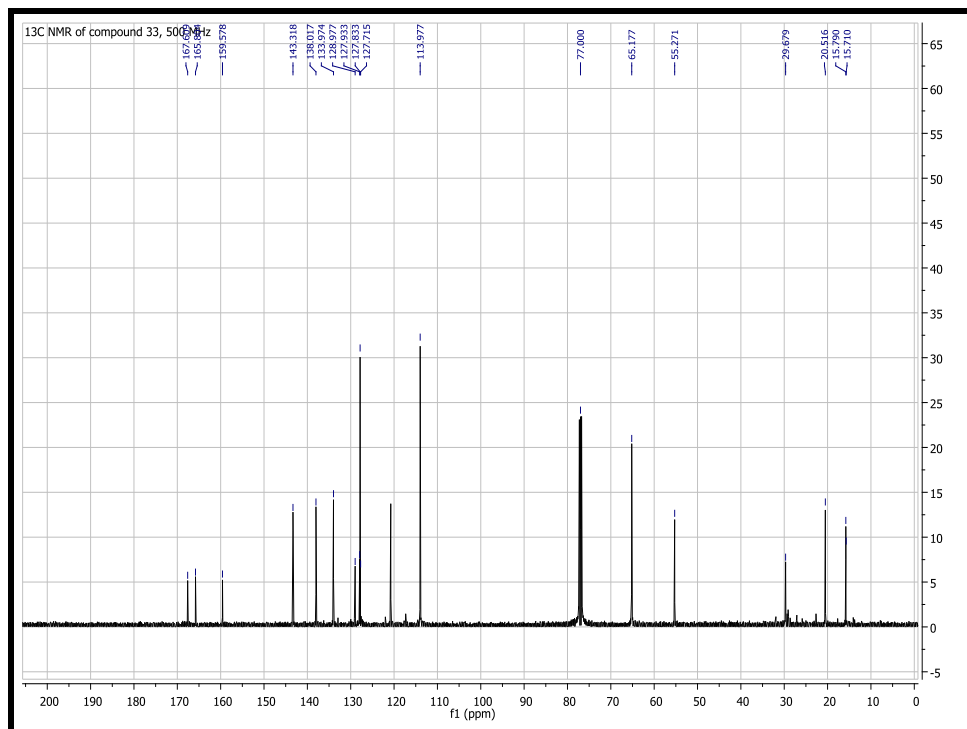
Fig. 185: ^{13}C NMR spectrum of compound **33**, 500 MHz, CDCl$_3$

Compound 34
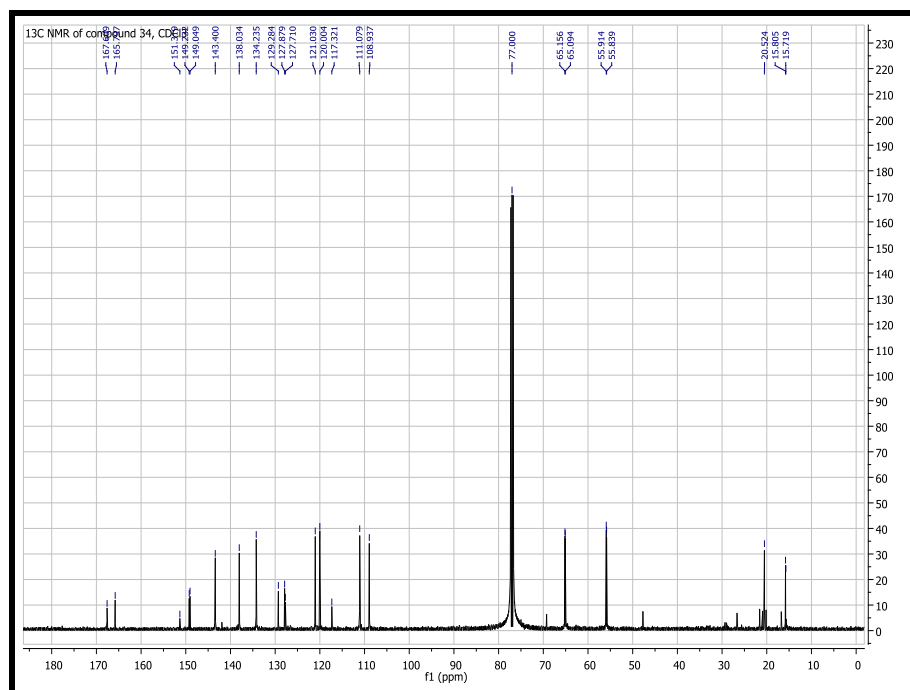
Fig.186: ^{13}C NMR spectrum of compound **34**, 100 MHz, CDCl$_3$
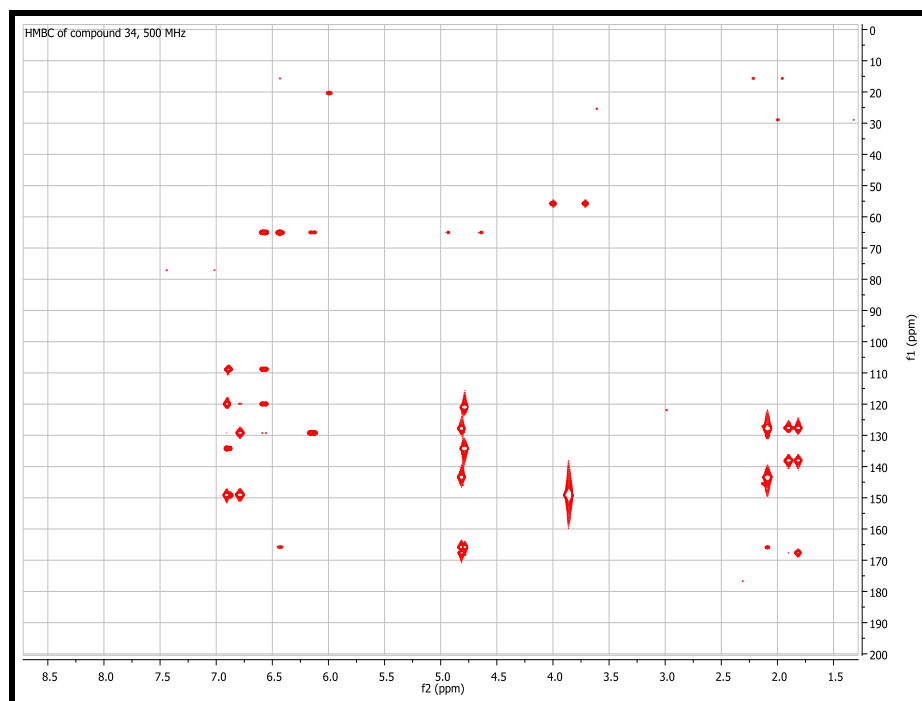
Fig.187: HMBC spectrum of compound **34**, 500 MHz, CDCl$_3$

Compound 35
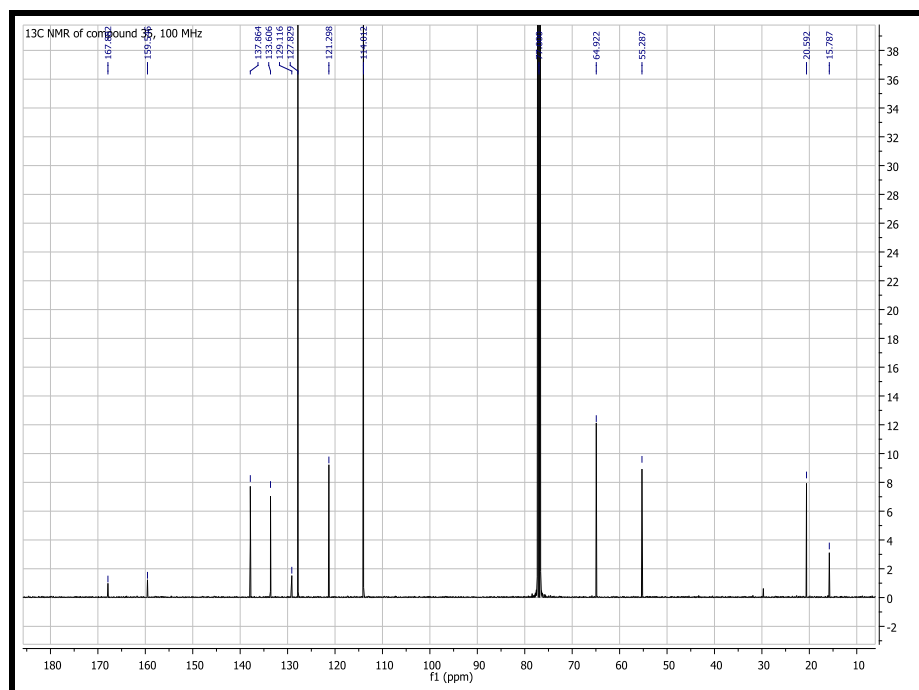
Fig.188: ^{13}C NMR spectrum of compound **35**, 100 MHz, CDCl$_3$
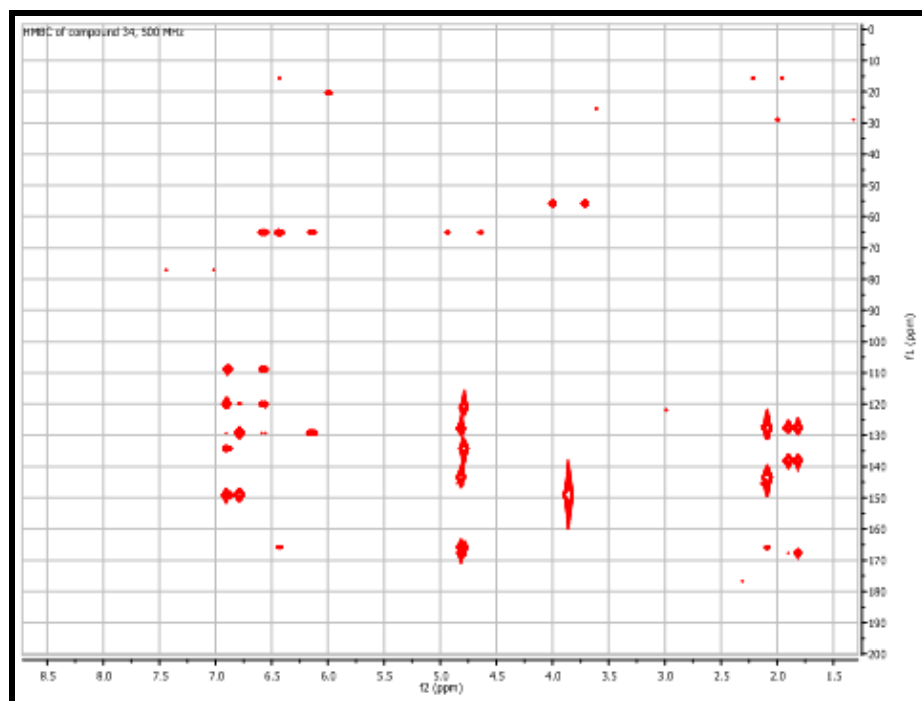
Fig.189: HSQC spectrum of compound **35**, 500 MHz, CDCl$_3$
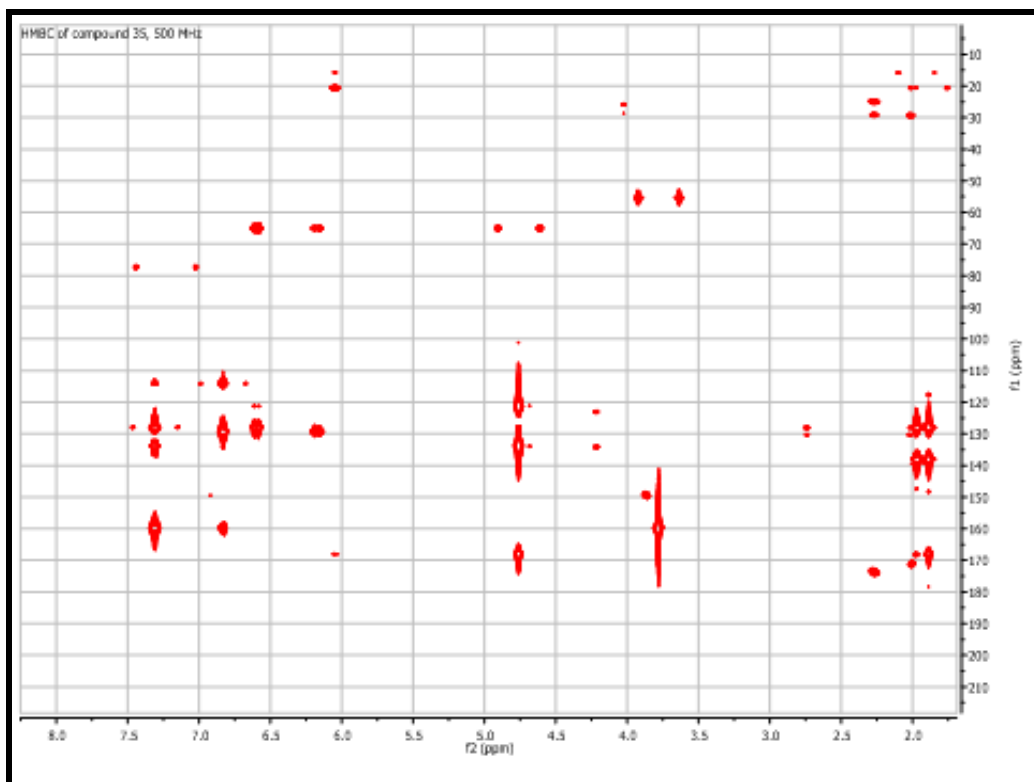
Fig.190: HMBC spectrum of compound **35**, 500 MHz, CDCl$_3$

Compound 36
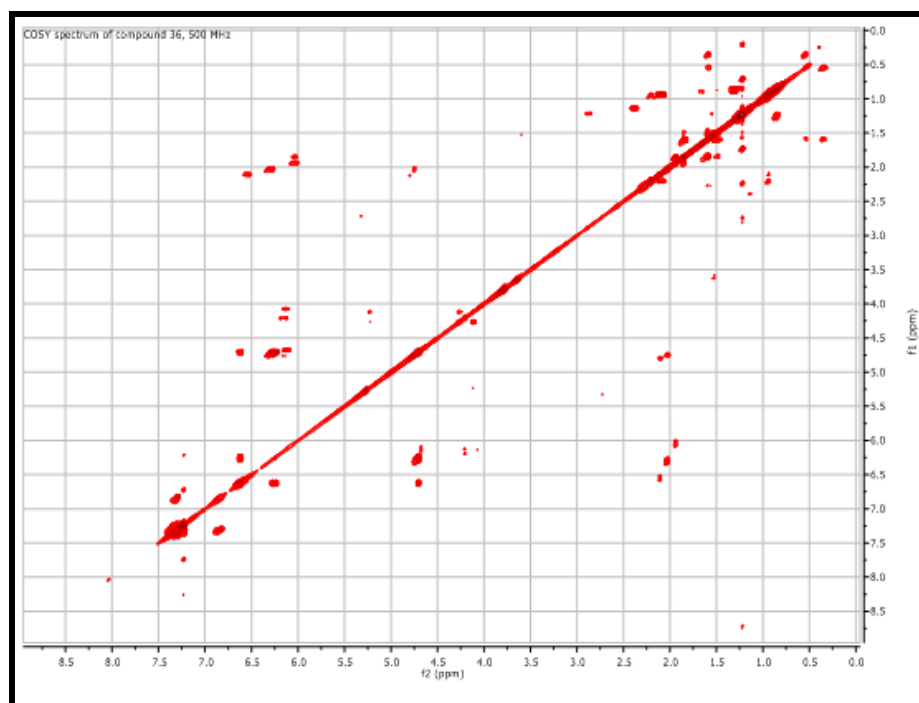
Fig.191: COSY spectrum of compound **36**, 500 MHz, CDCl$_3$
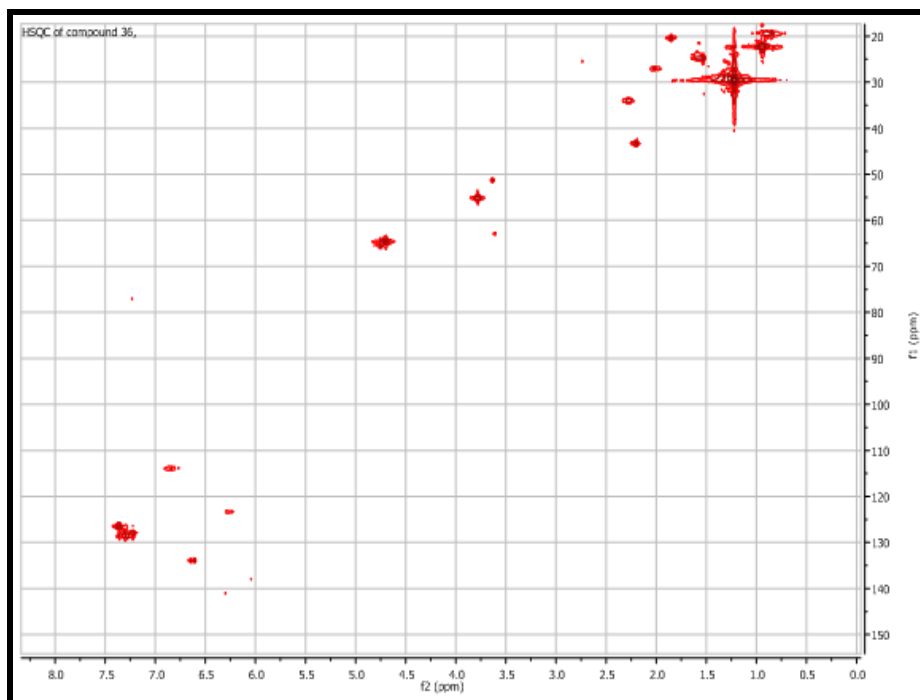
Fig.192: HSQC spectrum of compound **36**, 500 MHz, CDCl$_3$
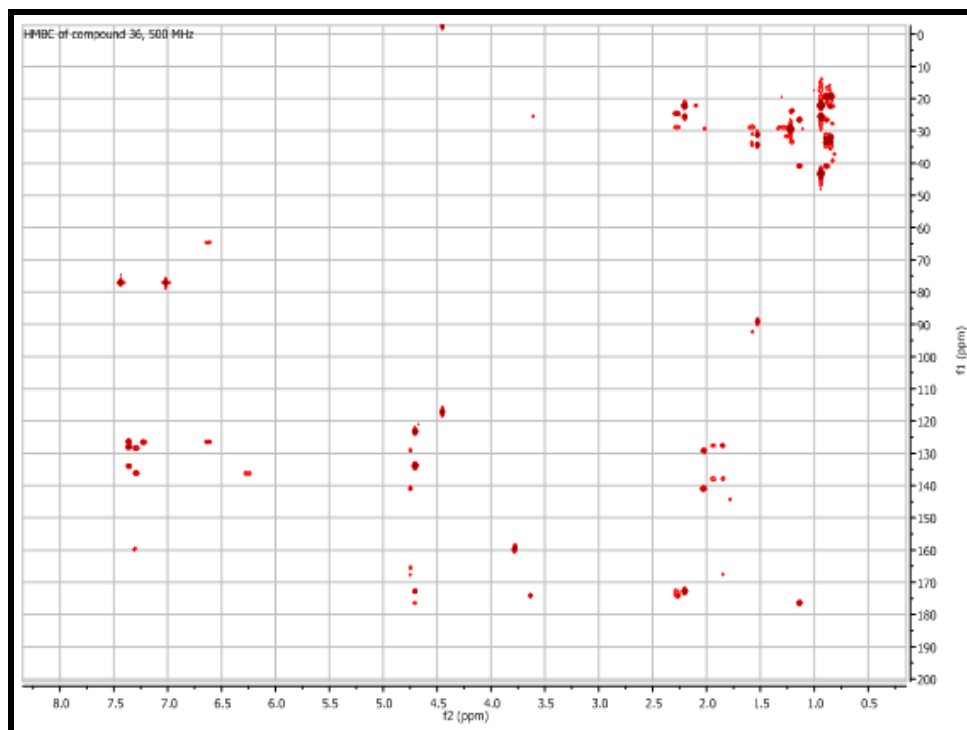
Fig.193: HMBC spectrum of compound **36**, 500 MHz, CDCl₃

Compound 37
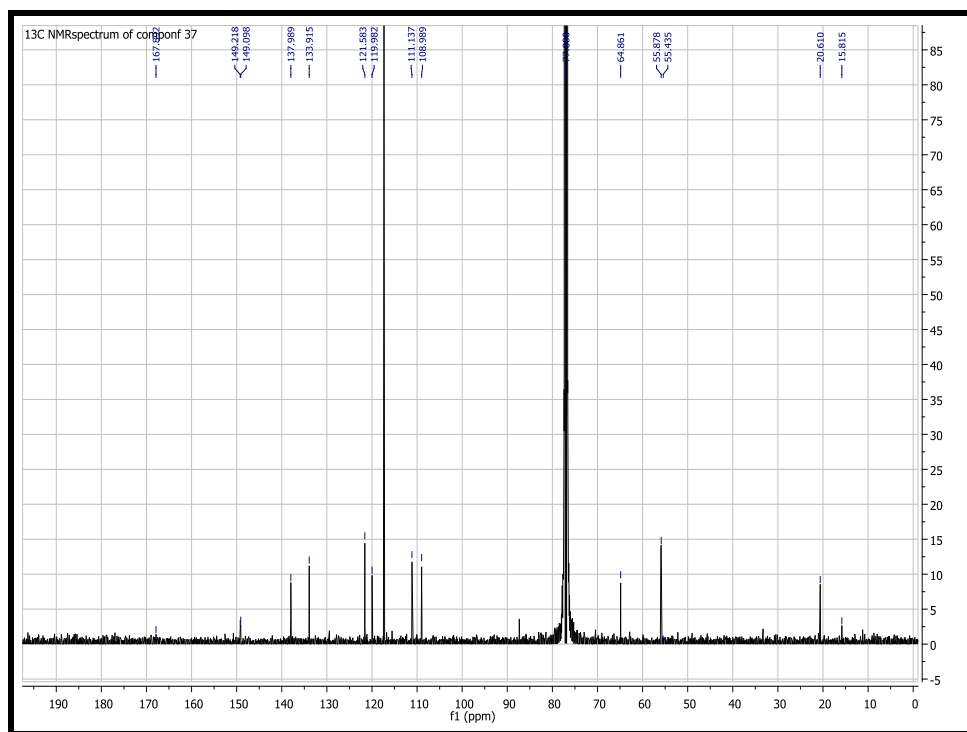
Fig.194: ^{13}C NMR spectrum of compound **37**, 100 MHz, CDCl$_3$

Compound 38
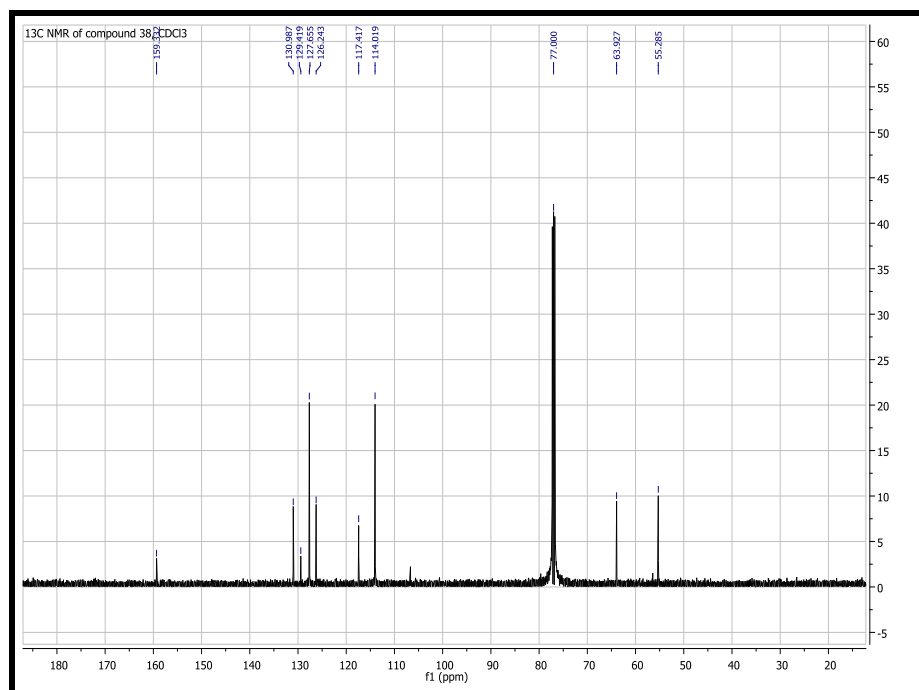
Fig.195: ^{13}C NMR spectrum of compound **38**, 100 MHz, CDCl$_3$
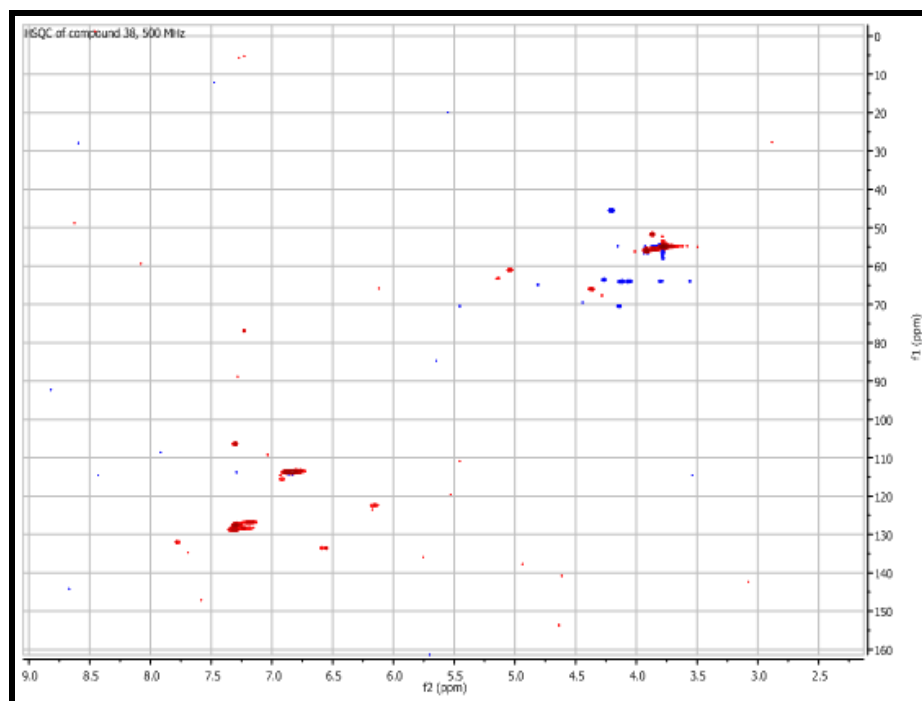
Fig.196: HSQC spectrum of compound **38**, 500 MHz, CDCl$_3$
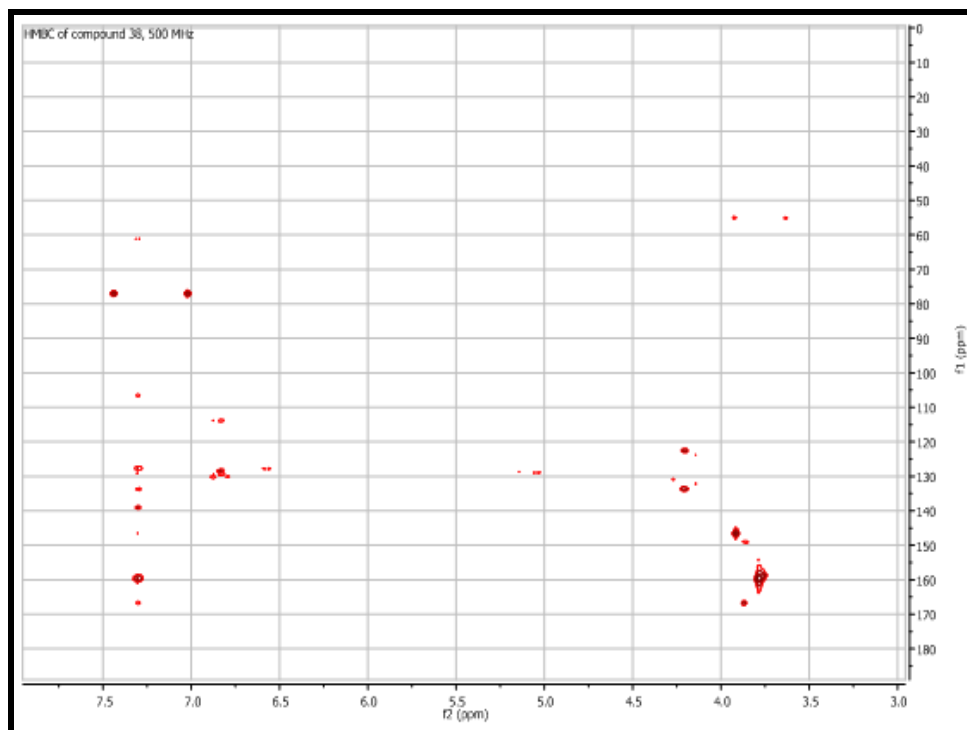
Fig.197: HMBC spectrum of compound **38**, 500 MHz, CDCl$_3$

Compound 39
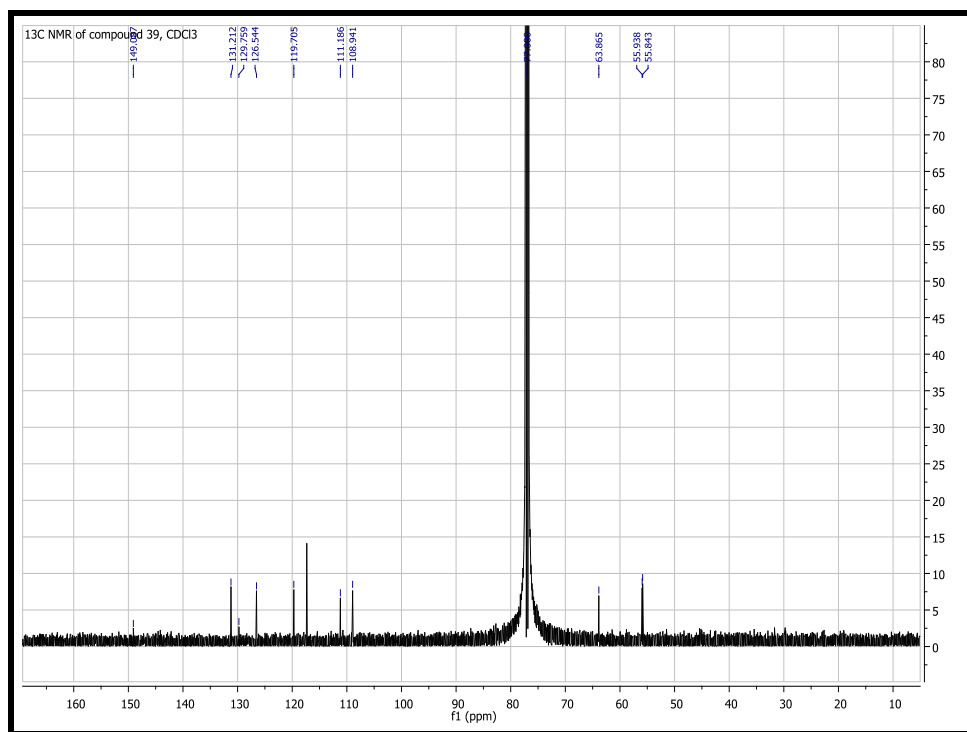
Fig.198: ^{13}C NMR spectrum of compound **39**, 100 MHz, CDCl$_3$

7.5 Methodology of isolation for *Withania somnifera*

7.5.1 Extraction and isolation method

Methanol extract of *W. somnifera* was procured from Natural Remedies, Banglore, India. 20 g of this extract was dissolved in DCM. DCM soluble portion (1.2 g) was subjected to CC over silica gel, eluted with Toluene: Ethyl acetate (9.5:0.5). 10 fractions (F1-F10) were obtained.

F9 (370 mg) was further purified by CC over silica gel, eluted with Hexane: Ethyl acetate (4:6) to give 9 subfractions (F9.1-F9.9). Hexane soluble portion of F9.4 (75 mg) was subjected to CC over sephadex LH-20, eluted with Methanol, to get a more pure fraction (F9.4.1), which was further chromatographed by RP-HPLC using Acetonitrile:Water (7:3) to yield new compound (2.1 mg, t_R 9.2 min). We gave name **Withasomniferolide A (41)** to the newly isolated compound. F9.7 (19 mg) was purified further by CC over sephadex LH-20 to obtain a more pure fraction, which was further chromatographed by RP-HPLC using Acetonitril: Water (7:3) to yield another new compound (1.8 mg, t_R 12 min). We gave a name **Withasomniferolide B (42)** to newly isolated compound.

F9.5 was a mixture of 3 compounds. The ESI MS spectrum (negative mode) revealed three ion peaks at *m/z* 501, 473 and 445 (Fig. 97). MS/MS spectrum of the three ion peaks, each showing a loss of a methyl group, (Fig. 98: A, B, and C), clearly demonstrated that peaks at *m/z* 473 and 445 did not originate from that at *m/z* 501. Therefore, the compound was a mixture of three long chain alkyl ferulates differing each other only by the number of the methylene groups and was identified as mixture of **octadecyl ferulate (44), eicosanyl ferulate (45)** and **docosanyl ferulate** (**46**). It was impossible to separate the compounds from the mixture hence we have synthesized the three ferulates. Method of synthesis is described below.

F9.3 was purified by CC over sephadex LH-20 to give compound 43. Compound 43 was identified as **1,5-di-*O*-feruloylpentanediol.** Also, we have synthesized this compound to confirm the structure.

F9.6 (18 mg) was purified by CC over silica gel, eluted with Hexane: Ethyl acetate (1:1) to get a fraction which was further chromatographed by RP-HPLC using Acetonitrile: Water (6:4). A white solid compound (t_R 7.6 min) was obtained, identified as **Withanolide B (47)**.

F9.9 was eluted with Ethyl acetate (100%). A solid precipitate was observed at the bottom. A white coloured compound was obtained on filtration, identified as **Withanolide A (48)**.

F10 (60 mg) was dissolved in Tertiary butyl ether. Soluble portion of F10 was further partitioned between hexane soluble and hexane insoluble fractions. Hexane insoluble fraction was chromatographed by RP-HPLC using Acetonitrile: H_2O: TFAA (5:5:0.05) to give a compound identified as **Withaferin A (49)** (t_R 5.4min).

.
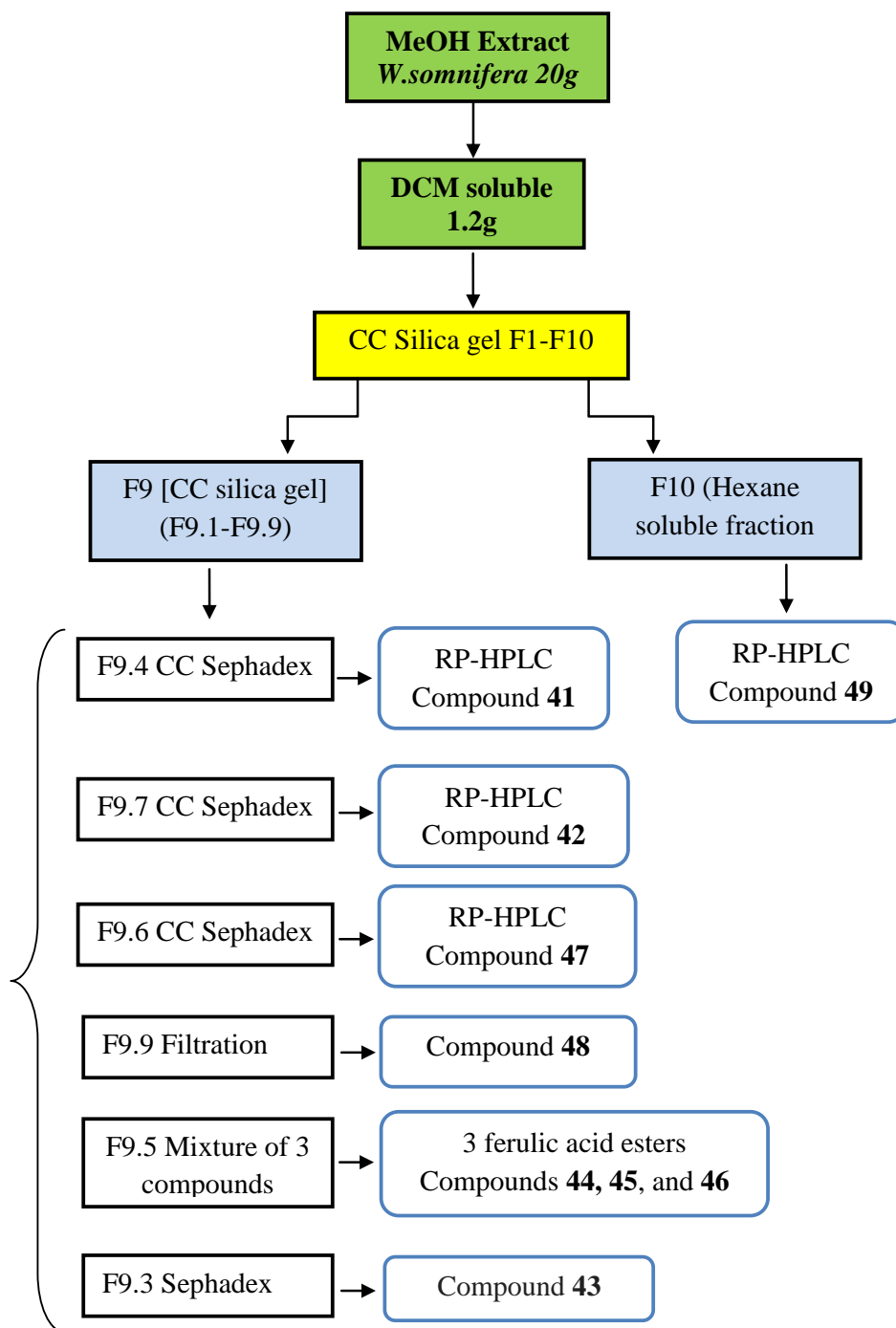
Fig.199: Scheme of isolation of secondary metabolites from DCM extract of *W.somnifera*

7.5.2 General procedure for the synthesis of 1,5-di-*O*-feruloylpentanediol (43)

Ethyl chloroformate (1.45 ml, 15.2 mmol) and TEA (2.1 ml, 15.2 mmol) were added to a suspension of ferulic acid (1.47 g, 7.6 mmol) in DCM (10 ml) and stirred for 1 h at -15 °C until TLC analysis revealed a total consumption of starting material. Pantandiol (7.6 mmol) and DMAP (0.030 g, 0.08 mmol) were then added and the mixture stirred at room temperature for 6 h. The solvent was evaporated under reduced pressure to afford the crude product. This product was purified by silica gel column chromatography using mixtures of Hexane/ethyl acetate as eluents.

To a solution of the protected feruloyl ester (2.5 mmol) in DCM (10 ml) was added 80 equiv of piperidine (80 mmol) at 0 °C, and the reaction mixture was stirred at room temperature for 3h. The feruloyl ester was purified by VLC (silica gel) using Toluene: Ethyl acetate (9.5:0.5) as eluents.

7.5.3 General procedure for the synthesis of ferulates (44-46)

Ethyl chloroformate (0.83 ml, 8.7 mmol) and TEA (1.2 ml, 8.7 mmol) were added to a suspension of ferulic acid (0.8 g, 4.1 mmol) in DCM (10 ml) and stirred for 1 h at -15 °C until TLC analysis revealed a total consumption of starting material. Alcohol (8.7 mmol) and DMAP (0.030 g, 0.08 mmol) were then added and the mixture stirred at room temperature for 6 h. The solvent was evaporated under reduced pressure to afford the crude product. This product was purified by silica gel column chromatography using mixtures of toluene/ethyl acetate as eluents.

To a solution of the each protected feruloyl ester (2.5 mmol) in DCM (10 ml) was added 80 equiv of piperidine (80 mmol) at 0 °C, and the reaction mixture was stirred at room temperature for 3h. The feruloyl ester was purified by VLC (silica gel) using Toluene: Ethyl acetate (9.5:0.5) as eluents.

7.6 Biological assay

7.6.1 HIV inhibition assay

7.6.1.1 Expression and purification of recombinant DNA

HIV-1 RT group M subtype B. Heterodimeric RT was expressed essentially as described [229]. Briefly, E. coli strain M15 containing the p6HRT-prot vector was grown to an optical density at 600 nm of 0.7 and induced with 1.7 mM isopropyl β-D-1-thiogalactopyranoside (IPTG) for 4 h. Protein purification was carried out with a BioLogic LP system (Biorad), using a combination of immobilized metal affinity and ion exchange chromatography. Cell pellets were resuspended in lysis buffer (50 mM sodiumphosphate buffer pH 7.8, containing 0.5 mg/ml lysozyme), incubated on ice for 20 min, and after adding NaCl to a final concentration of 0.3 M, were sonicated and centrifuged at 30,000×g for 1 h. The supernatant was loaded onto a Ni^{2+}-NTA-Sepharose column pre-equilibrated with loading buffer (50 mM sodium phosphate buffer pH 7.8, containing 0.3M NaCl, 10% glycerol, and 10 mM imidazole) and washed thoroughly with wash buffer (50 mM sodium phosphate buffer pH 6.0, containing 0.3 M NaCl, 10% glycerol, and 80 mM imidazole). RT was eluted with an imidazole gradient in wash buffer (0 – 0.5 M). Fractions were collected; protein purity was checked by SDS-PAGE and found to be higher than 90%. The 1:1 ration between the p66/p51 subunits was also verified. Enzyme-containing fractions were pooled and diluted 1:1 with 50 mM sodium phosphate buffer pH 7.0, containing 10% glycerol; and then loaded into a Hi-trap heparin HP GE (Healthcare Lifescience) pre-equilibrated with 10 column volumes of loading buffer(50 mM sodium phosphate buffer pH 7.0, containing 10% glycerol and 150 mM NaCl). The column was then washed with loading buffer and the RT was eluted with Elute Buffer 2 (50 mM Sodium Phosphate pH 7.0, 10% glycerol, 1M NaCl). Fractions were collected; protein was dialyzed and stored in buffer containing 50 mM TrisHCl pH 7.0, 25 mM NaCl, 1 mM EDTA, and 50% glycerol. Catalytic activities and protein concentrations were determined. Enzyme-containing fractions were pooled and aliquots were stored at −80ºC.

7.6.1.2 HIV-1 DNA polymerase-independent RNase H activity determination

HIV RT-associated RNase H activity was measured as described [261] using the RNase H inhibitor RDS1759 as a control. In 100 µ L reaction volume containing 50 mM Tris-HCl buffer pH 7.8, 6 mM MgCl2, 1 mM dithiothreitol (DTT), 80 mM KCl, 0.25 μM hybrid RNA/DNA 5'- GAUCUGAGCCUGGGAGCU-Fluorescin-3' (HPLC, dry, QC: Mass Check) (available from Metabion) 5'-Dabcyl-AGCTCCCAGGCTCAGATC-3'(HPLC, dry, QC: Mass Check), increasing concentrations of inhibitor, whose dilution were made in water, and 20 ng of wt RT according to a linear range of dose-response curve. The reaction mixture was incubated for 1 h at 37ºC, stopped by addition of EDTA and products were measured with a multilabel counter plate reader Victor 3 (Perkin Elmer model 1420-051) equipped with filters for 490/528 nm (excitation/emission wavelength).

7.6.1.3 HIV-1 RNA-dependent DNA polymerase activity determination

RNA-dependent DNA polymerase (RDDP) activity was measured as described [262] using the NNRTI Efavirenz as a control. in 25 µ L volume containing 60 mM Tris-HCl buffer pH 8.1, 8 mM MgCl2, 60 mM KCl, 13 mM DTT, 2.5 µ M poly(A)-oligo (dT),100 μM dTTP, increasing concentrations of inhibitor, whose dilution were made in water, and 6 ng of wt RT according to a linear range of dose-response curve. After enzyme addition, the reaction mixture was incubated for 30 min at 37ºC and the stopped by addition of EDTA. Reaction products were detected by picogreen addition and measured with a multilabel counter plate reader Victor 3 (Perkin Elmer model 1420-051) equipped with filters for 502/523 nm (excitation/emission wavelength).

7.6.2 Molecular modeling

Ligand **18f** was docked onsidering the global minimum energy conformation and the conformations within 5 kcal/mol and with different RMSD values from the global minimum as determined by molecular mechanics conformational analysis performed with Macromodel software [263]. In practical, theoretical 3D model of the compound was built by means of Maestro GUI. The molecule was then submitted to a conformational search of 1000 steps with an energy window for saving structure of 21 kJ/mol (5.02 kcal/mol). The algorithm used was the Monte Carlo method followed by an energy minimization carried out using the MMFFs,[264] the GB/SA water implicit solvation model [265] and the Polak-Ribier Conjugate Gradient (PRCG) method for 5000 iterations, converging on gradient with a threshold of 0.05 kJ(molÅ)$^{-1}$.

Docking experiment

The docking experiments were performed as described in our previous works [229,230] applying QM- Polarized Ligand Docking (QMPLD) [266]. In order to better take into account the induced fit phenomena, the most energy favoured generated complexes were fully optimized using AMBER* united atoms force field [267] in GB/SA implicit water [229], setting 10000 steps interactions analysis with Polak-Ribier Conjugate Gradient (PRCG) method and a convergence criterion of 0.1 kJ/(molÅ). The resulting complexes were considered for the binding modes graphical analysis with Pymol [268] and Maestro [269].

7.6.3 The Yonetani-Theorell analysis

The Yonetani-Theorell analysis was performed as described previously [237,261].

7.6.4 Isobologram analysis

Isobologram analysis was carried out as previously described [270].

7.6.5 Inhibition of HRV replication assay

7.6.5.1 Cells and viruses

The cytotoxic and antiviral activity of the compounds was studied on HeLa cells (Ohio strain) grown in DMEM with 1% non-essential amino acids, 200 µg/ml streptomycin, 200 units/ml penicillin G and 10% fetal calf serum (GIBCO Laboratories INC). Cell lines were kept at 37ºC in a humidified atmosphere with 5% CO_2. Rhinoviruses HRV14 (group B) and HRV39 (group A), were purchased from the American Type Culture Collection (ATCC). For all the above mentioned viruses, working stocks were prepared as cellular lysates using DMEM with 2% heat inactivated fetal calf serum.

7.6.5.2 Cytotoxic activity

The cytotoxicity of the test compounds was evaluated by measuring the effect produced on cell morphology and cell growth in vitro. Cell monolayers were prepared in 24-well tissue culture plates and exposed to various concentrations of the compounds. Plates were checked by light microscopy after 24, 48 and 72 h. Cytotoxicity was scored as morphological alterations (e.g., rounding up, shrinking, and detachment). The viability of the cells was determined by a tetrazolium-based colorimetric method using 3-(4,5-dimethylthiazol-2-yl)-2,5-diphenyltetrazolium bro-mide (MTT), as previously described [271,272]. The 50% cytotoxic dose (CC_{50}) is the concentration of the compound that reduced the absorbance of the control sample by 50%.

7.6.5.3 Inhibition of virus multiplication

The Rhinovirus inhibition assay was evaluated by a one-step viral infection of cell monolayers, followed by virus yield titration in an agar-plaque assay. HeLa cell monolayers were prepared in multiwell plates and were infected by the Rhinoviruses at a MOI of 1 [273]. Next, serial dilutions of the test compounds were added and after 24–36 h of incubation at 33ºC and 3% CO_2, when the cytopathic effect in the control cells was almost total, the monolayers were frozen and thawed and the viruses in the supernatant were titrated by the plaque assay method. The antiviral

activity assay on the Rhinoviruses was carried out by the 50% plaque reduction assay in HeLa cells as previously described [274]. The compound concentration required to inhibit virus plaque formation by 50% is expressed as the 50% inhibitory concentration (CC_{50}), and calculated by dose–response curves and linear regression.

7.6.6 GABA_A modulation activity

Whole-cell patch-clamp recordings

Electrophysiological whole-cell patch-clamp recordings were carried out on dentate gyrus granule cells obtained from coronal hippocampal slices of deeply anesthetized (chloroform) Sprague-Dawley rats. Briefly, brains were removed from the skull and quickly transferred to a modified artificial cerebrospinal fluid (mACSF) containing (in mM): 220 sucrose, 2 KCl, 0.2 $CaCl_2$, 6 $MgSO_4$, 26 $NaHCO_3$, 1.3 NaH_2PO_4, and 10 D-glucose (pH 7.4, set by aeration with 95% O_2 and 5% CO_2). Coronal slices (thickness 300 μm) that included the hippocampal formation were cut in ice-cold mACSF with the use of a Leica VT1200S vibratome (Leica, Heidelberg, Germany). Slices were then transferred immediately to a nylon net submerged in standard ACSF containing (in mM): 126 NaCl, 3 KCl, 2 $CaCl_2$, 1 $MgCl_2$, 26 $NaHCO_3$, 1.25 NaH_2PO_4, and 10 D-glucose (pH 7.4, set by aeration with 95% O_2 and 5% CO_2), for at least 40 min at a controlled temperature of 35°C. After subsequent incubation for 30 min at room temperature, hemi-slices were transferred to the recording chamber, which was constantly perfused with ACSF at a flow rate of ~2 ml/min. For all recordings, temperature of ACSF was then set at 32°C. The granule cells present in dentate gyrus were visualized under IR microscope, identified and selected on the basis of their round shape of their cell body. Recording pipettes were prepared from borosilicate glass using a Flaming Brown micropipette puller (Molecular Devices, Novato, CA). Resistance of the pipettes ranged from 2.5 to 4.5 MΩ when they were filled with an internal solution containing (in mM): 140 CsCl, 2 MgCl, 2 CaCl, 10 EGTA, 10 HEPES, 2 ATP-Na (pH 7.3 with CsOH 5N). We analyzed only recordings with access resistance of <25 MΩ. Series resistance was not compensated, and cells were excluded from further analysis if access resistance changed by >25% during the course of the recording. Membrane currents were recorded with the use of an Axopatch 200-B amplifier (Axon Instruments), filtered at 2 kHz, and digitized at 5 kHz, For patch-clamp experiments, we used pClamp 9.2 software (Molecular Devices, Union City, CA), which allowed us to measure various characteristics of the neuronal membrane and to detect current differences. For all experiments, electrically evoked GABA_AR-mediated currents (IPSCs) were recorded in ACSF containing the ionotropic glutamate receptor antagonist kynurenic acid (1 mM). After a stable baseline was reached, IPSCs

were recorded for at least 3 min before the bath application of the different compounds. Clampfit 9.2 software was used in order to calculate the amplitude of GABAergic sIPSCs. Statistical analysis was performed using the software Graph Pad Prism 7.0 (Graph Pad Software Inc., San Diego, California, USA).

7.6.7 Antioxidant assay

Antioxidant potential of MeOH extract of *O. sanctum, T. cordifolia, B. fruticosum* and DCM extract of *O. sanctum* and *B. fruticosum* was measured by four different methods. This assay was carried out at faculty of Sciences, University of Porto, Portugal.

7.6.7.1 DPPH assay

1,1-Diphenyl-2-picrylhydrazyl radical scavenging activity was measured as described in literature with slight modifications [275] [276].

Preparation of solutions-

a) DPPH solution- 13.5 mg in 5 ml of Ethanol (Stock solution)
b) Prepare Working solution using 500 µl of stock solution (a) in 25 ml of Ethannol, to have the absorbance 0.7±0.001, measured at 512 nM
c) Test solutions- Different concentrations of test solution to determine IC_{50}
d) Standard- 100 µM solution of Caffeic Acid and Trolox as a reference standard.

Stock solution was prepared by dissolving 13.5 mg of DPPH in 5 ml of ethanol. Working solution (b) for DPPH was prepared using 500 µl of stock solution prepared above, diluted in 25 ml of ethanol, to have the absorbance of 0.7±0.001 measured at 512 nM. 100 µM of standard solution of caffeic acid and Trolox were prepared. Test solutions of the extract with different concentration were prepared. Triplicates of blank, control, test sample, reference standard were prepared as mention below. Absorbance was recorded at 45th minute using multimode microplate reader at 512 nM. IC_{50} was calculated using formula given below.

$$IC_{50} = (A_c - A_s)/A_c * 100$$

A_c- Absorbance of control
A_s- Absorbance of sample (Absorbance of sample must be corrected by subtracting the absorbance of blank)

Blank- 20 µl test solution+180 µl Ethanol

Control- 20 µl Ethanol+ 180 µl DPPH working solution (b)

Sample- 20 µl Test solution+180 µl DPPH working solution (b)

Reference Standard- 20 µl of 100 µM standard solution (Caffeic acid and Trolox in separate well) + 180 µl DPPH working solution.

7.6.7.2 ABTS method

2,2 -Azino-bis(3-ethylbenzthiazoline-6-sulphonic acid) radical-scavenging activity was measured as described in literature with slight mdifications [275] [277].

Preparation of solutions-

a) ABTS solution (7 mM) 2,2-Azino-bis (3-ethylbenzothiazoline-6-sulfonic acid) diammonum salt. MW- 548.68. Dissolve 38.4 mg of ABTS in 10 ml of water.

b) $K_2S_2O_8$ solution, 40.5 mg in 1 ml of water.

c) Stock solution- Prepare stock solution by addition of 163 µl of solution (b) in ABTS solution prepared in step (a). Keep this solution protected from light for at least 16 hrs before using and not to be used after 48 hrs.

d) Working solution- 475 µl of Stock solution (c)+ upto 20 ml of Ethanol to have the absorbance of 0.72±0.001, measured at 734 nM

e) Standard Solutions- 100 µM solution of Caffeic Acid and Trolox as a referecne standard.

7 mM of ABTS working solution ((3-ethylbenzothiazoline-6-sulfonic acid) diammonum salt) was prepared by dissolving 38.48 mg of ABTS in 10 ml of water (a). 40.5 mg of potassium persulphate was dissolved in 1 ml of water (b). Stock solution (c) was prepared by addition of 163 µl of solution (b) to the ABTS solution prepared in step (a). The stock solution was kept protected from light for 16 hours to generate free radicals. Working solution was prepared using 475 µl of stock solution (c) diluted upto 20 ml by ethanol to have an absorbance 0.72 ±0.001, measured at 734 nM.100µM of standard solution of caffeic acid and trolox were prepared as reference standard. Triplicates of blank, control, test sample, reference standard were prepared as given below,

Blank- 20 µl test solution+180 µl Ethanol

Control- 20 µl Ethanol+ 180 µl ABTS working solution (d)

Sample- 20 µl Test solution+180 µl ABTS working solution (d)

Reference Standard- 20 µl of 100µM standard solution (Caffeic acid and Trolox in separate well) + 180 µl ABTS working solution.

Abosrbance was recorded at 15th minute using micro plate reader at 734 nM and IC_{50} value was calculated using the formula as follow,

$$IC_{50}= (A_c-A_s)/A_c * 100$$

A_c- Absorbance of control

A_s- Absorbance of sample (Absorbance of sample must be corrected by subtracting the absorbance of blank)

7.6.7.3 Iron (Fe^{2+}) chelation method

Iron chelation potential was measured as described in literature with slight modifications [278].

Preparation of solutions-

a) Ammonium acetate buffer solution, P^H 6.7- Dissolve 1.542 g of Ammonium acetate in 100 ml water.
b) Ferrozine solution (492.5g/mole)- Dissolve 12.31 mg in 5 ml of Water.
c) Ammonium Iron (II) Sulphate solution- Dissolve7.84 in 10ml of water.
d) Working solution -100ul of Ammonium Iron sulphate solution (c) + 10 ml of buffer
e) Reference standard- EDTA 100uM

Ammonium acetate buffer (pH 6.7) was prepared by dissolving 1.542 g in 100 ml of water. 12.31 mg of ferrozine dissolved in 5 ml of water to get 492.5g/mol (b). Ammonium iron sulphate solution (c) was prepared by dissolving 7.84 g in 10 ml of water. Working solution (d) was prepared by dilution of 100 µl of solution (c) with 10 ml of water. 100µM of EDTA solution

was used as a reference standard. Triplicates of Blank, control and test sample were prepared as given below,

Blank- 4 µl Ethanol/DMSO + 200 µl of Working solution (d), incubate for 10 minutes then add 4 µl of Ferrozine solution (b) and again incubate for 10 minutes, measure the absorbance at 562 nM

Control- 4 µl of EDTA solution 100 µM (e) + 200 µl Working solution (d), incubate for 10 minutes then add 4 µl of Ferrozine solution (b) and again incubate for 10 minutes, measure the absorbance at 562 nM

Test Sample- 4 µl Test solution+200 µl of Working solution (d), incubate for 10 minutes then add 4 µl of Ferrozine solution (b) and again incubate for 10 minutes, measure the absorbance at 562 nM.

Absorbance was recorded after 2nd incubation and percentage chelation was calculated by formula given below,

$$\% \text{ chelation} = (A_b - A_s)/A_b * 100$$

A_b- Absorbance of Blank

A_s – Absorbance of Sample

7.6.7.4 Galvinoxyl free radical method

Preparation of solutions-

a)   Stock solution-Galvinoxyl solution (5 mM)- Dissolve 10.5 mg in 5 ml of Ethanol

b)   Take 100 µl of (i) and dilute upto 5ml in Ethanol

c)   GO Working solution- Dilute 82.5 µl of solution (b) with 500 µl of Ethanol to have absorbance less than 1 (Approximately between 0.9 to 0.99).

5 mM of Galvinoxyl solution (a) was prepared by dissolving 10.5 mg in 5ml of ethanol. 100 µl of GO solution (a) was diluted upto 5ml in ethanol (b). GO working solution (c) was prepared using 500 µl of solution (b) diluted with ethanol to have the absorbance not more than 1 (approximately between 0.9 to 0.99), measured at 428 nM. Triplicates of blank, control and test sample were prepared as below,

Blank- 20 µl test solution+180 µl Ethanol

Control- 20 µl Ethanol+ 180 µl GO working solution (c)

Sample- 20 µl Test solution+180 µl GO working solution (c)

Absorbance was recorded at 30th minute using micro plate reader at 428 nM and IC_{50} value was calculated using the formula below,

$$IC_{50}= (A_c-A_s)/A_c * 100$$

Ac- Absorbance of control

As- Absorbance of sample (Absorbance of sample must be corrected by subtracting the absorbance of blank).

REFERENCES

[1]   Awang DVC **(2009)**. Tyler's herbs of choice: the therapeutic use of phytomedicinals: CRC Press.

[2]   Farnsworth NR, Akerele O, Bingel AS, Soejarto DD, Guo Z (**1985**). Medicinal plants in therapy. Bulletin of the world health organization;63 (6):965.

[3]   Lu Y, Hernandez P, Abegunde D, Edejer T **(2011)**. The world medicines situation 2011. Medicine expenditures. World Health Organization, Geneva. 1-34.

[4]   Katiyar C, Gupta A, Kanjilal S, Katiyar S (**2012**). Drug discovery from plant sources: An integrated approach. AYU (An international quarterly journal of research in Ayurveda);33 (1):10.

[5]   Cragg GM, Newman DJ, Snader KM (**1997**). Natural products in drug discovery and development. Journal of Natural Products;60 (1):52-60.

[6]   De Smet PAGM (**1997**). The role of plant-derived drugs and herbal medicines in healthcare. Drugs;54 (6):801-40.

[7]   Ekka NR, Namdeo KP, Samal PK (**2008**). Standardization strategies for herbal drugs-an overview. Research Journal of Pharmacy and Technology;1 (4):310-2.

[8]   Folashade O, Omoregie H, Ochogu P (**2012**). Standardization of herbal medicines-A review. International Journal of Biodiversity and Conservation;4 (3):101-12.

[9]   Lambert J, Srivastava J, Vietmeyer N **(1997)**. Medicinal plants: rescuing a global heritage: World Bank Publications.

[10]   Calixto JB (**2000**). Efficacy, safety, quality control, marketing and regulatory guidelines for herbal medicines (phytotherapeutic agents). Brazilian Journal of Medical and Biological Research;33 (2):179-89.

[11]   Grünwald J (**1995**). The European phytomedicines market: figures, trends, analysis. HerbalGram;34:60-5.

[12]   Balick MJ, Cox PA **(1996)**. Plants, people, and culture: the science of ethnobotany: Scientific American Library.

[13]   Veeresham C (**2012**). Natural products derived from plants as a source of drugs. Journal of Advanced Pharmaceutical Technology & Research;3 (4):200-1.

[14]   Newman DJ, Cragg GM, Snader KM (**2003**). Natural products as sources of new drugs over the period 1981-2002. Journal of Natural Products;66 (7):1022-37.

[15]   Ngo LT, Okogun JI, Folk WR (**2013**). 21st century natural product research and drug development and traditional medicines. Natural product reports;30 (4):584-92.

[16]   Harvey AL (**2008**). Natural products in drug discovery. Drug discovery today;13 (19):894-901.

[17]   Butler MS (**2004**). The role of natural product chemistry in drug discovery. Journal of Natural Products;67 (12):2141-53.

[18]   Kingston DGI (**2000**). Recent Advances in the Chemistry of Taxol 1, 2. Journal of Natural Products;63 (5):726-34.

[19]   Deleu D, Hanssens Y, Northway MG (**2004**). Subcutaneous Apomorphine. Drugs & aging;21 (11):687-709.

[20]   USFDA **(2008)**. CDER new molecular Entity (NME) drug and new biologic approvals in calendar year 2004.

[21]   Koumis T, Samuel S (**2005**). Tiotropium bromide: a new long-acting bronchodilator for the treatment of chronic obstructive pulmonary disease. Clinical therapeutics;27 (4):377-92.

[22]   Newman DJ, Cragg GM (**2012**). Natural products as sources of new drugs over the 30 years from 1981 to 2010. Journal of natural products;75 (3):311-35.

[23]   Denis JN, Greene AE, Guenard D, Gueritte-Voegelein F, Mangatal L, Potier P (**1988**). Highly efficient, practical approach to natural taxol. Journal of the American Chemical Society;110 (17):5917-9.

[24]   Holton RA, Biediger RJ, Boatman PD **(1995)**. Semisynthesis of taxol and taxotere: CRC Press: Boca Raton, FL.

[25]   Lee K-H, Xiao Z (**2005**). Podophyllotoxins and analogs. Anticancer agents from natural products:71-88.

[26]   Pinney KG, Pettit GR, Trawick ML, Jelinek C, Chaplin DJ, Cragg GM, Kingston DGI, Newman DJ**)**. Antitumor Agents from Natural Products. Boca Raton, FL: CRC Press, Taylor and Francis Group.

[27]   Krentz AJ, Bailey CJ (**2005**). Oral antidiabetic agents. Drugs;65 (3):385-411.

[28]   Robbers JE, Tyler VE **(1999)**. Tyler's herbs of choice. The therapeutic use of phytomedicinals: Haworth Press Inc.

[29]   Schulz V, Hänsel R, Tyler VE **(2001)**. Rational phytotherapy: a physician's guide to herbal medicine: Psychology Press.

[30]   World Health O (**2004**). WHO guidelines on safety monitoring of herbal medicines in pharmacovigilance systems.

[31]   Evaluation study report on Ayurvedic dispensaries of Delhi Govt, **(Sept. 2006)**. In: Delhi PdGoncto, New Delhi: Delhi secretariat

[32]   Houghton PJ, Mukherjee PK **(2009)**. Evaluation of herbal medicinal products: Perspectives on quality, safety and efficacy: Pharmaceutical press.

[33]   Heyn B **(1990)**. Ayurveda: The Indian Art of Natural Medicine and Life Extension: Inner Traditions/Bear & Co.

[34]   Ninivaggi FJ (**2008**). Ayurveda: A Comprehensive Guide to Traditional Indian Medicine for the West. Westport, CT: Praeger Press.

[35]   Mukherjee PK, Wahile A (**2006**). Integrated approaches towards drug development from Ayurveda and other Indian system of medicines. Journal of ethnopharmacology;103 (1):25-35.

[36]   Subhose V, Srinivas P, Narayana A (**2004**). Basic principles of pharmaceutical science in Ayurveda. Bulletin of the Indian Institute of History of Medicine (Hyderabad);35 (2):83-92.

[37]   Sharma S (**1979**). Realms of ayurveda. New Delhi: Arnold-Heinemann.

[38]   Heinrich M, Gibbons J, Simon Williamson EM **(2004)**. Fundamentals of pharmacognosy and phytotheraphy: Edinburgh, GB: Churchill Livingstone.

[39]   Loon G V **(2003)**. Charak Samhita, handbook on Ayurveda.

[40]   Jaiswal YS, Williams LL (**2016**). A glimpse of Ayurveda-The forgotten history and principles of Indian traditional medicine. Journal of Traditional and Complementary Medicine.

[41]   Lad V **(1984)**. Ayurveda: The science of self-healing: A practical guide: Lotus press.

[42]   Montagnier L (**2010**). 25 years after HIV discovery: prospects for cure and vaccine. Virology;397 (2):248-54.

[43]   Papadopulos-Eleopulos E, Turner VF, Papadimitriou J, Page B, Causer D, Alfonso H, Mhlongo S, Miller T, Maniotis A, Fiala C (**2004**). A critique of the Montagnier evidence for the HIV/AIDS hypothesis. Medical hypotheses;63 (4):597-601.

[44] Gallo RC, Montagnier L (**2003**). The discovery of HIV as the cause of AIDS. New England Journal of Medicine;349 (24):2283-5.

[45] Barre-Sinoussi F, Chermann JC, Rey F, Nugeyre MT, Chamaret S, Gruest J, Dauguet C (**2004**). Isolation of T-lymphotropic retrovirus from a patient at risk for acquired immune defficiency syndrome (AIDS). Revista de investigación clínica;56 (2):126-9.

[46] Sharp PM, Hahn BH (**2011**). Origins of HIV and the AIDS pandemic. Cold Spring Harbor perspectives in medicine;1 (1):a006841.

[47] Faria NR, Rambaut A, Suchard MA, Baele G, Bedford T, Ward MJ, Tatem AJ, Sousa JoD, Arinaminpathy N, Pépin J (**2014**). The early spread and epidemic ignition of HIV-1 in human populations. Science;346 (6205):56-61.

[48] Tebit DM, Arts EJ (**2011**). Tracking a century of global expansion and evolution of HIV to drive understanding and to combat disease. The Lancet infectious diseases;11 (1):45-56.

[49] Clavel Fo, Guetard D, Brun-Vezinet F, Chamaret S, Rey M-A, Santos-Ferreira MO, Laurent AG, Dauguet C, Katlama C, Rouzioux C (**1986**). Isolation of a new human retrovirus from West African patients with AIDS. Science;233 (4761):343-6.

[50] Chakrabarti L, Guyader M, Alizon M, Daniel MD, Desrosiers RC, Tiollais P, Sonigo P (**1987**). Sequence of simian immunodeficiency virus from macaque and its relationship to other human and simian retroviruses. Nature;328 (6130):543-7.

[51] Huet T, Cheynier Rm, Meyerhans A, Roelants G, Wain-Hobson S (**1990**). Genetic organization of a chimpanzee lentivirus related to HIV-1.

[52] Hirsch VM, Olmsted RA, Murphey-Corb M, Purcell RH, Johnson PR (**1989**). An African primate lentivirus (SIVs) closely related to HIV-2.

[53]   Müller B, Heilemann M (**2013**). Shedding new light on viruses: super-resolution microscopy for studying human immunodeficiency virus. Trends in microbiology;21 (10):522-33.

[54]   Frankel AD, Young JAT (**1998**). HIV-1: fifteen proteins and an RNA. Annual review of biochemistry;67 (1):1-25.

[55]   WHO (**March, 1986**). Acquired Immunodeficiency syndrome (AIDS) WHO/CDC case definition for surveillance, Weekly Epidemiological Record. World Health Organization.

[56]   De Clercq E, Li G (**2016**). Approved Antiviral Drugs over the Past 50 Years. Clinical Microbiology Reviews;29 (3):695-747.

[57]   Daluge SM, Good SS, Faletto MB, Miller WH, St Clair MH, Boone LR, Tisdale M, Parry NR, Reardon JE, Dornsife RE (**1997**). 1592U89, a novel carbocyclic nucleoside analog with potent, selective anti-human immunodeficiency virus activity. Antimicrobial agents and chemotherapy;41 (5):1082-93.

[58]   De Clercq E (**2012**). Tenofovir: quo vadis anno 2012 (where is it going in the year 2012)? Medicinal research reviews;32 (4):765-85.

[59]   Kang D, Fang Z, Li Z, Huang B, Zhang H, Lu X, Xu H, Zhou Z, Ding X, Daelemans D (**2016**). Design, Synthesis, and Evaluation of Thiophene [3, 2-d] pyrimidine Derivatives as HIV-1 Non-nucleoside Reverse Transcriptase Inhibitors with Significantly Improved Drug Resistance Profiles. Journal of Medicinal Chemistry;59 (17):7991-8007.

[60]   Arts EJ, Hazuda DJ (**2012**). HIV-1 antiretroviral drug therapy. Cold Spring Harbor perspectives in medicine;2 (4):a007161.

[61]   Baba M, Tanaka H, De Clercq E, Pauwels R, Balzarini J, Schols D, Nakashima H, Perno CF, Walker RT, Miyasaka T (**1989**). Highly specific inhibition of human immunodeficiency virus type 1 by a novel 6-substituted acyclouridine derivative. Biochemical and biophysical research communications;165 (3):1375-81.

[62]   Miyasaka T, Tanaka H, Baba M, Hayakawa H, Walker RT, Balzarini J, De Clercq E (**1989**). A novel lead for specific anti-HIV-1 agents: 1-[(2-hydroxyethoxy) methyl]-6-(phenylthio) thymine. Journal of Medicinal Chemistry;32 (12):2507-9.

[63]   Das K, Ding J, Hsiou Y, Clark AD, Moereels H, Koymans L, Andries K, Pauwels R, Janssen PAJ, Boyer PL (**1996**). Crystal structures of 8-Cl and 9-Cl TIBO complexed with wild-type HIV-1 RT and 8-Cl TIBO complexed with the Tyr181Cys HIV-1 RT drug-resistant mutant. Journal of molecular biology;264 (5):1085-100.

[64]   Ding J, Das K, Moereels H, Koymans L, Andries K, Janssen PAJ, Hughes SH, Arnold E (**1995**). Structure of HIV-1 RT/TIBO R 86183 complex reveals similarity in the binding of diverse nonnucleoside inhibitors. Nature Structural & Molecular Biology;2 (5):407-15.

[65]   Tantillo C, Ding J, Jacobo-Molina A, Nanni RG, Boyer PL, Hughes SH, Pauwels R, Andries K, Janssen PAJ, Arnold E (**1994**). Locations of anti-AIDS drug binding sites and resistance mutations in the three-dimensional structure of HIV-1 reverse transcriptase: implications for mechanisms of drug inhibition and resistance. Journal of molecular biology;243 (3):369-87.

[66]   Tuaillon E, Gueudin M, Lemée Vr, Gueit I, Roques P, Corrigan GE, Plantier J-C, Simon Fo, Braun Jp (**2004**). Phenotypic susceptibility to nonnucleoside inhibitors of virion-associated reverse transcriptase from different HIV types and groups. Journal of Acquired Immune Deficiency Syndromes;37 (5):1543-9.

[67]   Boyd M A KN, Moore C L, Nwizu C, Losso M H, Mohapi L, Martin A, Kerr S, Sohn A H, Teppler H, Van de Steen O, Molina J M, Emery S, Cooper DA (**2013**). Ritonavir-boosted lopinavir plus nucleoside or nucleotide reverse transcriptase inhibitors versus ritonavir-boosted lopinavir plus raltegravir for treatment of HIV-1 infection in adults with virological failure of a standard first-line ART regimen (SECOND-LINE): a randomised, open-label, non-inferiority study. The Lancet;381 (9883):2091-9.

[68] Sato M, Motomura T, Aramaki H, Matsuda T, Yamashita M, Ito Y, Kawakami H, Matsuzaki Y, Watanabe W, Yamataka K (**2006**). Novel HIV-1 integrase inhibitors derived from quinolone antibiotics. Journal of Medicinal Chemistry;49 (5):1506-8.

[69] Shimura K, Kodama E, Sakagami Y, Matsuzaki Y, Watanabe W, Yamataka K, Watanabe Y, Ohata Y, Doi S, Sato M (**2008**). Broad antiretroviral activity and resistance profile of the novel human immunodeficiency virus integrase inhibitor elvitegravir (JTK-303/GS-9137). Journal of virology;82 (2):764-74.

[70] Manzardo C, Gatell JM (**2013**). Stribild® (elvitegravir/cobicistat/emtricitabine/tenofovir disoproxil fumarate): a new paradigm for HIV-1 treatment. AIDS reviews;16 (1):35-42.

[71] Murrell DE, Moorman JP, Harirforoosh S (**2015**). Stribild: a review of component characteristics and combination drug efficacy. Eur Rev Med Pharmacol Sci;19 (5):904-14.

[72] Messiaen P, Wensing AMJ, Fun A, Nijhuis M, Brusselaers N, Vandekerckhove L (**2013**). Clinical use of HIV integrase inhibitors: a systematic review and meta-analysis. PloS one;8 (1):e52562.

[73] Cahn P, Pozniak AL, Mingrone H, Shuldyakov A, Brites C, Andrade-Villanueva JF, Richmond G, Buendia CB, Fourie J, Ramgopal M (**2013**). Dolutegravir versus raltegravir in antiretroviral-experienced, integrase-inhibitor-naive adults with HIV: week 48 results from the randomised, double-blind, non-inferiority SAILING study. The Lancet;382 (9893):700-8.

[74] Lalezari JP, Henry K, O'Hearn M, Montaner JSG, Piliero PJ, Trottier Bi, Walmsley S, Cohen C, Kuritzkes DR, Eron Jr JJ (**2003**). Enfuvirtide, an HIV-1 fusion inhibitor, for drug-resistant HIV infection in North and South America. New England Journal of Medicine;348 (22):2175-85.

[75] Kuritzkes DR (**2009**). HIV-1 Entry inhbitors: An overview. Current Opinion in HIV and AIDS;4 (2):82.

[76]   Tramontano E (**2006**). HIV-1 RNase H: recent progress in an exciting, yet little explored, drug target. Mini reviews in medicinal chemistry;6 (6):727-37.

[77]   Corona A, Masaoka T, Tocco G, Tramontano E, Le Grice SFJ (**2013**). Active site and allosteric inhibitors of the ribonuclease H activity of HIV reverse transcriptase. Future medicinal chemistry;5 (18):2127-39.

[78]   Tramontano E, Di Santo R (**2010**). HIV-1 RT-associated RNase H function inhibitors: recent advances in drug development. Current medicinal chemistry;17 (26):2837-53.

[79]   Schatz O, Cromme FV, Naas T, Lindemann D, Mous J, Le Grice SFJ (**1990**). Inactivation of the RNase H domain of HIV-1 reverse transcriptase blocks viral infectivity. Gene regulation and AIDS. Portfolio, Houston, Tex:293-404.

[80]   Jacobo-Molina A, Ding J, Nanni RG, Clark AD, Lu X, Tantillo C, Williams RL, Kamer G, Ferris AL, Clark P (**1993**). Crystal structure of human immunodeficiency virus type 1 reverse transcriptase complexed with double-stranded DNA at 3.0 A resolution shows bent DNA. Proceedings of the National Academy of Sciences;90 (13):6320-4.

[81]   Kohlstaedt LA, Wang J, Friedman JM, Rice PA, Steitz TA (**1992**). Crystal structure at 3.5 A resolution of HIV-1 reverse transcriptase complexed with an inhibitor. Science;256 (5065):1783-90.

[82]   Huang H, Chopra R, Verdine GL, Harrison SC (**1998**). Structure of a covalently trapped catalytic complex of HIV-1 reverse transcriptase: implications for drug resistance. Science;282 (5394):1669-75.

[83]   Sarafianos SG, Das K, Tantillo C, Clark AD, Ding J, Whitcomb JM, Boyer PL, Hughes SH, Arnold E (**2001**). Crystal structure of HIV-1 reverse transcriptase in complex with a polypurine tract RNA: DNA. The EMBO journal;20 (6):1449-61.

[84]   Sarafianos SG, Marchand B, Das K, Himmel DM, Parniak MA, Hughes SH, Arnold E (**2009**). Structure and function of HIV-1 reverse transcriptase: molecular mechanisms of polymerization and inhibition. Journal of molecular biology;385 (3):693-713.

[85]   Pettersen EF, Goddard TD, Huang CC, Couch GS, Greenblatt DM, Meng EC, Ferrin TE (**2004**). UCSF Chimera-a visualization system for exploratory research and analysis. Journal of computational chemistry;25 (13):1605-12.

[86]   Davies J, Jordan SR (**1991**). Domain of HIV-1 Reverse Transcriptase.

[87]   Parniak MA, Sluis-Cremer N (**2000**). Inhibitors of HIV-I reverse transcriptase. Advances in pharmacology;49:67-109.

[88]   Ilina T, LaBarge K, Sarafianos SG, Ishima R, Parniak MA (**2012**). Inhibitors of HIV-1 reverse transcriptase-associated ribonuclease H activity. Biology;1 (3):521-41.

[89]   Fletcher RS, Syed K, Mithani S, Dmitrienko GI, Parniak MA (**1995**). Carboxanilide derivative non-nucleoside inhibitors of HIV-1 reverse transcriptase interact with different mechanistic forms of the enzyme. Biochemistry;34 (13):4346-53.

[90]   Borkow G, Fletcher RS, Barnard J, Arion D, Motakis D, Dmitrienko GI, Parniak MA (**1997**). Inhibition of the ribonuclease H and DNA polymerase activities of HIV-1 reverse transcriptase by N-(4-tert-butylbenzoyl)-2-hydroxy-1-naphthaldehyde hydrazone. Biochemistry;36 (11):3179-85.

[91]   Himmel DM, Sarafianos SG, Dharmasena S, Hossain MM, McCoy-Simandle K, Ilina T, Clark Jr AD, Knight JL, Julias JG, Clark PK (**2006**). HIV-1 reverse transcriptase structure with RNase H inhibitor dihydroxy benzoyl naphthyl hydrazone bound at a novel site. ACS chemical biology;1 (11):702-12.

[92]   Budihas SR, Gorshkova I, Gaidamakov S, Wamiru A, Bona MK, Parniak MA, Crouch RJ, McMahon JB, Beutler JA, Le Grice SFJ (**2005**). Selective inhibition of HIV-1 reverse transcriptase-associated ribonuclease H activity by hydroxylated tropolones. Nucleic acids research;33 (4):1249-56.

[93]   Loya S, Tal R, Kashman Y, Hizi A (**1990**). Illimaquinone, a selective inhibitor of the RNase H activity of human immunodeficiency virus type 1 reverse transcriptase. Antimicrobial agents and chemotherapy;34 (10):2009-12.

[94]   Esposito F, Zinzula L, Tramontano E **(2007)**. Antiviral drug discovery: HIV-1 RNase H, the next hit target. Communicating Current Research and Educational Topics and Trends in Applied Microbiology: Citeseer.

[95]   World Health Organisation (**1989**). Report of a WHO informal consultation on traditional medicine and AIDS: in vitro screening for anti-HIV activity, Geneva, 6-8 February 1989.

[96]   Kurapati KRV, Atluri VS, Samikkannu T, Garcia G, Nair MPN (**2015**). Natural products as anti-HIV agents and role in HIV-associated neurocognitive disorders (HAND): A brief overview. Frontiers in microbiology;6.

[97]   Dharmaratne HRW, Tan GT, Marasinghe GPK, Pezzuto JM (**2002**). Inhibition of HIV-1 reverse transcriptase and HIV-1 replication by *Calophyllum* coumarins and xanthones. Planta medica;68 (01):86-7.

[98]   Shikishima Y, Takaishi Y, Honda G, Ito M, Takeda Y, Kodzhimatov OK, Ashurmetov O, Lee K-H (**2001**). Chemical Constituents of *Prangos tschimganica*; Structure Elucidation and Absolute Configuration of Coumarin and Furanocoumarin Derivatives with Anti-HIV Activity. Chemical and pharmaceutical bulletin;49 (7):877-80.

[99]   Min BS, Jung HJ, Lee JS, Kim YH, Bok SH, Ma CM, Nakamura N, Hattori M, Bae KH (**1999**). Inhibitory effect of triterpenes from *Crataegus pinatifida* on HIV-1 protease. Planta medica;65 (04):374-5.

[100]   Min BS, Miyashiro H, Hattori M (**2002**). Inhibitory effects of quinones on RNase H activity associated with HIV-1 reverse transcriptase. Phytotherapy Research;16 (S1):57-62.

[101]   Abd-Elazem IS, Chen HS, Bates RB, Huang RCC (**2002**). Isolation of two highly potent and non-toxic inhibitors of human immunodeficiency virus type 1 (HIV-1) integrase from *Salvia miltiorrhiza*. Antiviral research;55 (1):91-106.

[102]   Orhan DDea (**2010**). Antibacterial, antifungal, and antiviral activities of some flavonoids. Microbiological research;165 (6):496-504.

[103] Havsteen BH (**2002**). The biochemistry and medical significance of the flavonoids. Pharmacology & therapeutics;96 (2):67-202.

[104] Ohtake N, Nakai Y, Yamamoto M, Sakakibara I, Takeda S, Amagaya S, Aburada M (**2004**). Separation and isolation methods for analysis of the active principles of Sho-saiko-to (SST) oriental medicine. Journal of Chromatography B;812 (1):135-48.

[105] Asres K, Seyoum A, Veeresham C, Bucar F, Gibbons S (**2005**). Naturally derived anti-HIV agents. Phytotherapy Research;19 (7):557-81.

[106] Tewtrakul S, Nakamura N, Hattori M, Fujiwara T, Supavita T (**2002**). Flavanone and flavonol glycosides from the leaves of *Thevetia peruviana* and their HIV-1 reverse transcriptase and HIV-1 integrase inhibitory activities. Chemical and pharmaceutical bulletin;50 (5):630-5.

[107] Sabde S, Bodiwala HS, Karmase A, Deshpande PJ, Kaur A, Ahmed N, Chauthe SK, Brahmbhatt KG, Phadke RU, Mitra D (**2011**). Anti-HIV activity of Indian medicinal plants. Journal of natural medicines;65 (3-4):662-9.

[108] Rege AA, Ambaye RY, Deshmukh RA (**2010**). In-vitro testing of anti-HIV activity of some medicinal plants. Indian Journal of Natural products and resources;1 (2):193-9.

[109] Rege AA, Chowdhary AS (**2014**). Evaluation of *Ocimum sanctum* and *Tinospora cordifolia* as probable HIV protease inhibitors. International Journal of Pharmaceutical Sciences Review and Research;25:315-8.

[110] Kashman Y, Gustafson KR, Fuller RW, Cardellina 2nd JH, McMahon JB, Currens MJ, Buckheit Jr RW, Hughes SH, Cragg GM, Boyd MR (**1992**). The calanolides, a novel HIV-inhibitory class of coumarin derivatives from the tropical rainforest tree, *Calophyllum lanigerum*. Journal of Medicinal Chemistry;35 (15):2735-43.

[111] Singh IP, Bodiwala HS (**2010**). Recent advances in anti-HIV natural products. Natural product reports;27 (12):1781-800.

[112] Li F, Goila-Gaur R, Salzwedel K, Kilgore NR, Reddick M, Matallana C, Castillo A, Zoumplis D, Martin DE, Orenstein JM (**2003**). PA-457: a potent HIV inhibitor that disrupts core condensation by targeting a late step in Gag processing. Proceedings of the National Academy of Sciences;100 (23):13555-60.

[113] Robinson WE, Cordeiro M, Abdel-Malek S, Jia Q, Chow SA, Reinecke MG, Mitchell WM (**1996**). Dicaffeoylquinic acid inhibitors of human immunodeficiency virus integrase: inhibition of the core catalytic domain of human immunodeficiency virus integrase. Molecular pharmacology;50 (4):846-55.

[114] Mazumder A, Raghavan K, Weinstein J, Kohn KW, Pommier Y (**1995**). Inhibition of human immunodeficiency virus type-1 integrase by curcumin. Biochemical Pharmacology;49 (8):1165-70.

[115] Bolmstedt AJ, O'Keefe BR, Shenoy SR, McMahon JB, Boyd MR (**2001**). Cyanovirin-N defines a new class of antiviral agent targeting N-linked, high-mannose glycans in an oligosaccharide-specific manner. Molecular pharmacology;59 (5):949-54.

[116] Boyd MR, Gustafson KR, McMahon JB, Shoemaker RH, O'Keefe BR, Mori T, Gulakowski RJ, Wu L, Rivera MI, Laurencot CM (**1997**). Discovery of cyanovirin-N, a novel human immunodeficiency virus-inactivating protein that binds viral surface envelope glycoprotein gp120: potential applications to microbicide development. Antimicrobial agents and chemotherapy;41 (7):1521-30.

[117] Jacobs SE, Lamson DM, George KS, Walsh TJ (**2013**). Human rhinoviruses. Clinical Microbiology Reviews;26 (1):135-62.

[118] Palmenberg AC, Rathe JA, Liggett SB (**2010**). Analysis of the complete genome sequences of human rhinovirus. Journal of Allergy and Clinical Immunology;125 (6):1190-9.

[119] Palmenberg AC, Spiro D, Kuzmickas R, Wang S, Djikeng A, Rathe JA, Fraser-Liggett CM, Liggett SB (**2009**). Sequencing and analyses of all known human rhinovirus genomes reveal structure and evolution. Science;324 (5923):55-9.

[120] Lamson D, Renwick N, Kapoor V, Liu Z, Palacios G, Ju J, Dean A, George KS, Briese T, Lipkin WI (**2006**). MassTag polymerase-chain-reaction detection of respiratory pathogens, including a new rhinovirus genotype, that caused influenza-like illness in New York State during 2004-2005. Journal of Infectious Diseases;194 (10):1398-402.

[121] Albuquerque MCM, Varella RB, Santos N (**2012**). Acute respiratory viral infections in children in Rio de Janeiro and Teresópolis, Brazil. Revista do Instituto de Medicina Tropical de SÃo Paulo;54 (5):249-55.

[122] Rossmann MG, Bella J, Kolatkar PR, He Y, Wimmer E, Kuhn RJ, Baker TS (**2000**). Cell recognition and entry by rhino-and enteroviruses. Virology;269 (2):239-47.

[123] Wang L, Smith DL (**2005**). Capsid structure and dynamics of a human rhinovirus probed by hydrogen exchange mass spectrometry. Protein science;14 (6):1661-72.

[124] Van de Stolpe A, Van der Saag PT (**1996**). Intercellular adhesion molecule-1. Journal of Molecular Medicine;74 (1):13-33.

[125] Bochkov YA, Gern JE (**2016**). Rhinoviruses and Their Receptors: Implications for Allergic Disease. Current allergy and asthma reports;16 (4):1-11.

[126] Bella J, Kolatkar PR, Marlor CW, Greve JM, Rossmann MG (**1999**). The structure of the two amino-terminal domains of human intercellular adhesion molecule-1 suggests how it functions as a rhinovirus receptor. Virus research;62 (2):107-17.

[127] Dustin M L RR, Bhan A K, Dinarello C A, Springer T A (**1986**). Induction by IL 1 and interferon-g: tissue distribution, biochemistry, and function of a natural adherence molecule (ICAM-1). Journal of Immunology;137:245–54

[128] Greve JM, Davis G, Meyer AM, Forte CP, Yost SC, Marlor CW, Kamarck ME, McClelland A (**1989**). The major human rhinovirus receptor is ICAM-1. Cell;56 (5):839-47.

[129] Hoover-Litty H, Greve JM (**1993**). Formation of rhinovirus-soluble ICAM-1 complexes and conformational changes in the virion. Journal of virology;67 (1):390-7.

[130] Rossmann MG (**1994**). Viral cell recognition and entry. Protein science;3 (10):1712-25.

[131] Russell DW, Schneider WJ, Yamamoto T, Luskey KL, Brown MS, Goldstein JL (**1984**). Domain map of the LDL receptor: sequence homology with the epidermal growth factor precursor. Cell;37 (2):577-85.

[132] Brown MS, Goldstein JL (**1979**). Receptor-mediated endocytosis: insights from the lipoprotein receptor system. Proceedings of the National Academy of Sciences;76 (7):3330-7.

[133] Jeon H, Blacklow SC (**2005**). Structure and physiologic function of the low-density lipoprotein receptor. Annu. Rev. Biochem.;74:535-62.

[134] Bella J, Rossmann MG (**1999**). Review: rhinoviruses and their ICAM receptors. Journal of structural biology;128 (1):69-74.

[135] Mäkelä MJ, Puhakka T, Ruuskanen O, Leinonen M, Saikku P, Kimpimäki M, Blomqvist S, Hyypiä T, Arstila P (**1998**). Viruses and bacteria in the etiology of the common cold. Journal of clinical microbiology;36 (2):539-42.

[136] Winther B, Alper CM, Mandel EM, Doyle WJ, Hendley JO (**2007**). Temporal relationships between colds, upper respiratory viruses detected by polymerase chain reaction, and otitis media in young children followed through a typical cold season. Pediatrics;119 (6):1069-75.

[137] Turner BW, Cail WS, Hendley JO, Hayden FG, Doyle WJ, Sorrentino JV, Gwaltney JM (**1992**). Physiologic abnormalities in the paranasal sinuses during experimental rhinovirus colds. Journal of Allergy and Clinical Immunology;90 (3):474-8.

[138] Henquell C, Mirand A, Deusebis A-L, Regagnon C, Archimbaud C, Chambon M, Bailly J-L, Gourdon F, Hermet E, Dauphin J-Bt (**2012**). Prospective genotyping of human rhinoviruses in children and adults during the winter of 2009-2010. Journal of Clinical Virology;53 (4):280-4.

[139] Murali S, Langston AA, Nolte FS, Banks G, Martin R, Caliendo AM (**2009**). Detection of respiratory viruses with a multiplex polymerase chain reaction assay (MultiCode-PLx Respiratory Virus Panel) in patients with hematologic malignancies. Leukemia & lymphoma;50 (4):619-24.

[140] Corne JM, Marshall C, Smith S, Schreiber J, Sanderson G, Holgate ST, Johnston SL (**2002**). Frequency, severity, and duration of rhinovirus infections in asthmatic and non-asthmatic individuals: a longitudinal cohort study. The Lancet;359 (9309):831-4.

[141] Gern JE (**2010**). The ABCs of rhinoviruses, wheezing, and asthma. Journal of virology;84 (15):7418-26.

[142] Thibaut HJ, De Palma AM, Neyts J (**2012**). Combating enterovirus replication: state-of-the-art on antiviral research. Biochemical Pharmacology;83 (2):185-92.

[143] Pevear DC, Tull TM, Seipel ME, Groarke JM (**1999**). Activity of pleconaril against enteroviruses. Antimicrobial agents and chemotherapy;43 (9):2109-15.

[144] Webster ADB (**2005**). Pleconaril-an advance in the treatment of enteroviral infection in immuno-compromised patients. Journal of Clinical Virology;32 (1):1-6.

[145] Hayden FG, Andries K, Janssen PA (**1992**). Safety and efficacy of intranasal pirodavir (R77975) in experimental rhinovirus infection. Antimicrobial agents and chemotherapy;36 (4):727-32.

[146] Hayden FG, Hipskind GJ, Woerner DH, Eisen GF, Janssens M, Janssen PA, Andries K (**1995**). Intranasal pirodavir (R77, 975) treatment of rhinovirus colds. Antimicrobial agents and chemotherapy;39 (2):290-4.

[147] Rotbart HA (**2000**). Antiviral therapy for enteroviruses and rhinoviruses. Antiviral Chemistry and Chemotherapy;11 (4):261-71.

[148] Heinz BA, Vance LM (**1995**). The antiviral compound enviroxime targets the 3A coding region of rhinovirus and poliovirus. Journal of virology;69 (7):4189-97.

[149] Patick AK, Ford C, Binford S, Fuhrman S, Brothers M, Meador J, Webber SE, Okano K, Zalman L, Worland S (**1997**). Evaluation of the antiviral activity and cytotoxicity of peptidic inhibitors of human rhinovirus 3C protease, a novel target for antiviral intervention. Antiviral research;34 (2):A75.

[150] Hayden FG, Turner RB, Gwaltney JM, Chi-Burris K, Gersten M, Hsyu P, Patick AK, Smith GJ, Zalman LS (**2003**). Phase II, randomized, double-blind, placebo-controlled studies of ruprintrivir nasal spray 2-percent suspension for prevention and treatment of experimentally induced rhinovirus colds in healthy volunteers. Antimicrobial agents and chemotherapy;47 (12):3907-16.

[151] Patick AK, Brothers MA, Maldonado F, Binford S, Maldonado O, Fuhrman S, Petersen A, Smith GJ, Zalman LS, Burns-Naas LA (**2005**). In vitro antiviral activity and single-dose pharmacokinetics in humans of a novel, orally bioavailable inhibitor of human rhinovirus 3C protease. Antimicrobial agents and chemotherapy;49 (6):2267-75.

[152] Kawatkar SP, Gagnon M, Hoesch V, Tiong-Yip C, Johnson K, Ek M, Nilsson E, Lister T, Olsson L, Patel J (**2016**). Design and structure-activity relationships of novel inhibitors of human rhinovirus 3C protease. Bioorganic & medicinal chemistry letters;26 (14):3248-52.

[153] Johnston GAR (**2005**). GABAA receptor channel pharmacology. Current pharmaceutical design;11 (15):1867-85.

[154] Somogyi P, Tamas G, Lujan R, Buhl EH (**1998**). Salient features of synaptic organisation in the cerebral cortex. Brain research reviews;26 (2):113-35.

[155] Jin H, Wu H, Osterhaus G, Wei J, Davis K, Sha D, Floor E, Hsu C-C, Kopke RD, Wu J-Y (**2003**). Demonstration of functional coupling between γ-aminobutyric acid (GABA) synthesis and vesicular GABA transport into synaptic vesicles. Proceedings of the National Academy of Sciences;100 (7):4293-8.

[156] Cherubini E, Conti F (**2001**). Generating diversity at GABAergic synapses. Trends in neurosciences;24 (3):155-62.

[157] Deken SL, Wang D, Quick MW (**2003**). Plasma membrane GABA transporters reside on distinct vesicles and undergo rapid regulated recycling. The Journal of neuroscience;23 (5):1563-8.

[158] Owens DF, Kriegstein AR (**2002**). Is there more to GABA than synaptic inhibition? Nature Reviews Neuroscience;3 (9):715-27.

[159] Mehta AK, Ticku MK (**1999**). An update on GABA A receptors. Brain research reviews;29 (2):196-217.

[160] Bormann J (**1988**). Electrophysiology of GABAA and GABAB receptor subtypes. Trends in neurosciences;11 (3):112-6.

[161] Cossart R, Bernard C, Ben-Ari Y (**2005**). Multiple facets of GABAergic neurons and synapses: multiple fates of GABA signalling in epilepsies. Trends in neurosciences;28 (2):108-15.

[162] Burt DR, Kamatchi GL (**1991**). GABAA receptor subtypes: from pharmacology to molecular biology. The FASEB journal;5 (14):2916-23.

[163] Nutt D (**2006**). GABAA receptors: subtypes, regional distribution, and function. Journal of clinical sleep medicine: JCSM: official publication of the American Academy of Sleep Medicine;2 (2):S7-11.

[164] Bormann J, Feigenspan A **(2001)**. GABAC receptors: structure, function and pharmacology. In: Pharmacology of GABA and Glycine Neurotransmission: Springer. pp. 271-96.

[165] Cutting GR, Lu L, O'Hara BF, Kasch LM, Montrose-Rafizadeh C, Donovan DM, Shimada S, Antonarakis SE, Guggino WB, Uhl GR (**1991**). Cloning of the gamma-aminobutyric acid (GABA) rho 1 cDNA: a GABA receptor subunit highly expressed in the retina. Proceedings of the National Academy of Sciences;88 (7):2673-7.

[166] Feigenspan A, Bormann J (**1998**). GABA-gated Cl_2 channels in the rat retina. Progress in retinal and eye research;17 (1):99-126.

[167] Chen K, Li H-Z, Ye N, Zhang J, Wang J-J (**2005**). Role of GABA B receptors in GABA and baclofen-induced inhibition of adult rat cerebellar interpositus nucleus neurons in vitro. Brain research bulletin;67 (4):310-8.

[168] Benarroch EE (**2012**). GABAB receptors: structure, functions, and clinical implications. Clinical implications of Neuroscience research;78:578-84

[169] Bowery NG (**2006**). GABA B receptor: a site of therapeutic benefit. Current opinion in pharmacology;6 (1):37-43.

[170] Bowery NG, Bettler B, Froestl W, Gallagher JP, Marshall F, Raiteri M, Bonner TI, Enna SJ (**2002**). International Union of Pharmacology. XXXIII. Mammalian γ -aminobutyric acid B receptors: structure and function. Pharmacological reviews;54 (2):247-64.

[171] Ulrich D, Bettler B (**2007**). GABA B receptors: synaptic functions and mechanisms of diversity. Current opinion in neurobiology;17 (3):298-303.

[172] Khare CP **(2007)**. Indian Medicinal Plants: an illustrated dictionary Library of congress Control Number: 2007922446 ISBN: 978-0-387-70637-5 Springer-Verlag Berlin. Heidelberg, Springer science+ Business Media, LLC.

[173] Baby J, Nair VM (**2013**). Ethanopharmacological and phytochemical aspects of *Ocimum sanctum* Linn-the elixir of life. British Journal of Pharmaceutical Research;3 (2):273.

[174] The Ayurvedic Pharmacopeia of India **(2007)**. In: Ayush New Delhi: Govt. of India, pp. 19-20, 7-9,170-6.

[175] Meher A (**2012**). Antitussive evaluation of formulated polyherbal cough syrup. Journal of Drug Delivery and Therapeutics;2 (5).

[176] Koche D, Imran S, Shirsat R, Bhadange D (**2011**). Comparative phytochemical and nutritional studies of leaves and stem of three lamiaceae members. Research Journal of Pharmaceutical, Biological and Chemical Sciences;2 (3):1-4.

[177] Deshmukh V, Kshirsagar M (**2009**). Honey based medication in the management of cough: efficacy and safety. Paediatrics Today;12 (9):229-36.

[178] Suanarunsawat T, Songsak T (**2005**). Anti-hyperglycaemic and anti-dyslipidaemic effect of dietary supplement of white *Ocimum Sanctum* Linnean before and after STZ-induced diabetes mellitus. International Journal of Diabetes and Metabolism;13 (1):18.

[179] Ahmed MM, Singh KP (**2011**). Traditional knowledge of kidney stones treatment by Muslim Maiba (herbalists) of Manipur, India. Notulae Scientia Biologicae;3 (2):12.

[180] Kuhn MA, Winston D **(2007)**. Winston & Kuhn's Herbal Therapy and Supplements: A Scientific and Traditional Approach: Lippincott Williams & Wilkins.

[181] Nguyen H, Lemberkovics E, Tarr K, Mathe I, Petri G (**1993**). A comparative study on formation of flavonoid, tannin, polyphenol contents in ontogenesis of *Ocimum basilicum* L.(Part II). Acta Agronomica Hungarica;42:41-50.

[182] Nörr H, Wagner H (**1992**). New constituents from *Ocimum sanctum*. Planta medica;58 (06):574-.

[183] Skaltsa H, Philianos S, Singh M (**1987**). Phytochemical study of the leaves of *Ocimum sanctum*. Fitoterapia;8:286.

[184] Sukari MA, Rahmani M, Lee GB, Takahashi S (**1995**). Constituents of stem barks of *Ocimum sanctum*. Fitoterapia;66 (6):552-3.

[185] Karthikeyan K, Gunasekaran P, Ramamurthy N, Govindasamy S (**1999**). Anticancer activity of *Ocimum sanctum*. Pharmaceutical biology;37 (4):285-90.

[186] Jyoti S, Satendra S, Sushma S, Anjana T, Shashi S (**2007**). Antistressor activity of *Ocimum sanctum* (Tulsi) against experimentally induced oxidative stress in rabbits. Methods and findings in experimental and clinical pharmacology;29 (6):411-6.

[187] Mandal S, Das DN, De K, Ray K, Roy G, Chaudhuri SB, Sahana CC, Chowdhuri MK (**1993**). *Ocimum sanctum* Linn-a study on gastric ulceration and gastric secretion in rats. Indian journal of physiology and pharmacology;37 (1):91-2.

[188] Rajeshwari S (**1992**). *Ocimum sanctum*-The Indian home remedy. Current Medical Scene. March-April (published by, Cipla Ltd., Bombay Central, Bombay).

[189] Uma Devi P, Ganasoundari A, Vrinda B, Srinivasan KK, Unnikrishnan MK (**2000**). Radiation protection by the ocimum flavonoids orientin and vicenin: mechanisms of action. Radiation Research;154 (4):455-60.

[190] Sultana N, Ata A (**2008**). Oleanolic acid and related derivatives as medicinally important compounds. Journal of enzyme inhibition and medicinal chemistry;23 (6):739-56.

[191] Neeraja PV, Margaret E (**2013**). Amruthavalli (*Tinospora cordifolia*): Multipurpose rejuvenator. International Journal of Pharmceutical, Chemical and Biological Sciences;3:233-41.

[192] Stanely Mainzen Prince P, Menon VP (**2003**). Hypoglycaemic and hypolipidaemic action of alcohol extract of *Tinospora cordifolia* roots in chemical induced diabetes in rats. Phytotherapy Research;17 (4):410-3.

[193] Patel MB, Mishra S (**2011**). Hypoglycemic activity of alkaloidal fraction of *Tinospora cordifolia*. Phytomedicine;18 (12):1045-52.

[194] Sudha P, Zinjarde SS, Bhargava SY, Kumar AR (**2011**). Potent α amylase inhibitory activity of Indian Ayurvedic medicinal plants. BMC complementary and alternative medicine;11 (1):1.

[195] Bishayi B, Roychowdhury S, Ghosh S, Sengupta M (**2002**). Hepatoprotective and immunomodulatory properties of *Tinospora cordifolia* in CCl4 intoxicated mature albino rats. The Journal of toxicological sciences;27 (3):139-46.

[196] Rai M, Gupta SS (**1967**). Experimental evaluation of *Tinospora cordifolia* (Guduchi) for dissolution of urinary calculi. J Res Ind Med;2 (1).

[197] Kalikar MV, Thawani VR, Varadpande UK, Sontakke SD, Singh RP, Khiyani RK (**2008**). Immunomodulatory effect of *Tinospora cordifolia* extract in human immuno-deficiency virus positive patients. Indian journal of pharmacology;40 (3):107.

[198] Sharma V, Pandey D (**2010**). Beneficial effects of *Tinospora cordifolia* on blood profiles in male mice exposed to lead. Toxicology international;17 (1):8.

[199] Ashour ML, Wink M (**2011**). Genus Bupleurum: a review of its phytochemistry, pharmacology and modes of action. Journal of Pharmacy and Pharmacology;63 (3):305-21.

[200] Wyk B-EV, Wink M (**2004**). Medicinal plants of the world: an illustrated scientific guide to important medicinal plants and their uses. Portland: Timber;480.

[201] Menale B, De Castro O, Cascone C, Muoio R (**1991**). Ethnobotanical investigation on medicinal plants in the Vesuvio National Park (Campania, Southern Italy). Journal of ethnopharmacology;192:320-49.

[202] Dugo D TA, Verzera A, Rapisarda A (**2000**). L'olio essenziale delle foglie di piante tipiche della flora mediterranea, Essenze, Derivati Agrumari 70:201–5

[203] Bertoli A, Pistelli L, Morelli I, Fraternale D, Giamperi L, Ricci D (**2004**). Volatile constituents of micropropagated plants of *Bupleurum fruticosum* L. Plant science;167 (4):807-10.

[204] Lorente I, Ocete MA, Zarzuelo A, Cabo MM, Jimenez J (**1989**). Bioactivity of the essential oil of *Bupleurum fruticosum*. Journal of Natural Products;52 (2):267-72.

[205] Manunta A, Morelli I, Picci V (**1987**). L'huile essentielle de *Bupleurum fruticosum* L.[bupleurol, inhibition bacteriostatique]. Plantes Medicinales e Phytotherapie.

[206] Weiner MA, Weiner J (**1994**). Ashwagandha (Indian ginseng). Herbs that heal:70-2.

[207] Sharma PC, Yelne MB, Dennis TJ, Joshi A **(2001)**. Database on Medicinal Plants Used in Ayurveda & Siddha: Central Council for Research in Ayurveda & Siddha, Deptt. of ISM & H, Min. of Health & Family Welfare, Government of India.

[208] Berghe WV, Sabbe L, Kaileh M, Haegeman G, Heyninck K (**2012**). Molecular insight in the multifunctional activities of Withaferin A. Biochemical Pharmacology;84 (10):1282-91.

[209] Mohan R, Hammers H, Bargagna-Mohan P, Zhan X, Herbstritt C, Ruiz A, Zhang L, Hanson A, Conner B, Rougas J (**2004**). Withaferin A is a potent inhibitor of angiogenesis. Angiogenesis;7 (2):115-22.

[210] Bargagna-Mohan P, Hamza A, Kim Y-e, Ho YKA, Mor-Vaknin N, Wendschlag N, Liu J, Evans RM, Markovitz DM, Zhan C-G (**2007**). The tumor inhibitor and antiangiogenic agent withaferin A targets the intermediate filament protein vimentin. Chemistry & biology;14 (6):623-34.

[211] Choudhary MI, Nawaz SA, Lodhi MA, Ghayur MN, Jalil S, Riaz N, Yousuf S, Malik A, Gilani AH (**2005**). Withanolides, a new class of natural cholinesterase inhibitors with calcium antagonistic properties. Biochemical and biophysical research communications;334 (1):276-87.

[212] Ahmad M, Saleem S, Ahmad AS, Ansari MA, Yousuf S, Hoda MN, Islam F (**2005**). Neuroprotective effects of *Withania somnifera* on 6-hydroxydopamine induced Parkinsonism in rats. Human & experimental toxicology;24 (3):137-47.

[213] Kulkarni SK, George B (**1996**). Anticonvulsant Action of *Withania somnifera* (Aswaganda) Root Extract against Pentylenetetrazole-induced Kindling in Mice. Phytotherapy Research;10 (5):447-9.

[214] Orrù A, Marchese G, Casu G, Casu MA, Kasture S, Cottiglia F, Acquas E, Mascia MP, Anzani N, Ruiu S (**2014**). *Withania somnifera* root extract prolongs analgesia and suppresses hyperalgesia in mice treated with morphine. Phytomedicine;21 (5):745-52.

[215] Kulkarni SK, Dhir A (**2008**). *Withania somnifera*: an Indian ginseng. Progress in neuro-psychopharmacology and biological psychiatry;32 (5):1093-105.

[216] Sarker SD, Latif Z, Gray AI (**2006**). Natural products isolation, (Methods in Biotechnology; 20). Totowa, New Jersey: Humana Press, pp. 4-10.

[217] Harborne AJ (**1998**). Phytochemical methods a guide to modern techniques of plant analysis: Springer Science & Business Media.

[218] Seebacher W, Simic N, Weis R, Saf R, Kunert O (**2003**). Complete assignments of 1H and 13C NMR resonances of oleanolic acid, ursolic acid and their 11-oxo derivatives. Magnetic Resonance in Chemistry;41 (8):636-8.

[219] Cheng J-J, Zhang L-J, Cheng H-L, Chiou C-T, Lee IJ, Kuo Y-H (**2010**). Cytotoxic hexacyclic triterpene acids from *Euscaphis japonica*. Journal of Natural Products;73 (10):1655-8.

[220] Ikuta A, Itokawa H (**1988**). Triterpenoids of *Paeonia japonica* callus tissue. Phytochemistry;27 (9):2813-5.

[221] Sright JLC, McInnes AG, Shimizu S, Smith DG, Walter JA, Idler D, Khalil W (**1978**). Identification of C-24 alkyl epimers of marine sterols by ^{13}C nuclear magnetic resonance spectroscopy. Canadian Journal of Chemistry;56 (14):1898-903.

[222] A.F. Erasmuson RJF, N. C. Franca, H. E. Gottlieb, E. Wenker (**1977**). ^{13}C Nuclear Magnetic Resonance Spectroscopy of Vanillin Derivatives J.C.S. Perkin I:492-4.

[223] Barakat HH, Nawwar MAM, Buddrus J, Linscheid M (**1987**). Niloticol, a phenolic glyceride and two phenolic aldehydes from the roots of *Tamarix nilotica*. Phytochemistry;26 (6):1837-8.

[224] Nkengfack AE, Vouffo TW, Vardamides JC, Kouam J, Fomum ZT, Meyer M, Sterner O (**1997**). Phenolic metabolites from Erythrina species. Phytochemistry;46 (3):573-8.

[225] Corona A, Di Leva FS, Thierry S, Pescatori L, Crucitti GC, Subra F, Delelis O, Esposito F, Rigogliuso G, Costi R (**2014**). Identification of highly conserved residues involved in inhibition of HIV-1 RNase H function by diketo acid derivatives. Antimicrobial agents and chemotherapy;58 (10):6101-10.

[226] Akihisa T, Ogihara J, Kato J, Yasukawa K, Ukiya M, Yamanouchi S, Oishi K (**2001**). Inhibitory effects of triterpenoids and sterols on human immunodeficiency virus-1 reverse transcriptase. Lipids;36 (5):507-12.

[227] Zhang J, Liu X, De Clercq E (**2009**). Capsid (CA) protein as a novel drug target: recent progress in the research of HIV-1 CA inhibitors. Mini reviews in medicinal chemistry;9 (4):510-8.

[228] Nakamura K, Nakajima T, Aoyama T, Okitsu S, Koyama M (**2014**). One-pot esterification and amidation of phenolic acids. Tetrahedron;70 (43):8097-107.

[229] Corona A, Meleddu R, Esposito F, Distinto S, Bianco G, Masaoka T, Maccioni E, Menéndez-Arias L, Alcaro S, Le Grice SFJ (**2016**). Ribonuclease H/DNA Polymerase HIV-1 Reverse Transcriptase Dual Inhibitor: Mechanistic Studies on the Allosteric Mode of Action of Isatin-Based Compound RMNC6. PloS one;11 (1):e0147225.

[230] Meleddu R, Cannas V, Distinto S, Sarais G, Del Vecchio C, Esposito F, Bianco G, Corona A, Cottiglia F, Alcaro S (**2014**). Design, Synthesis, and Biological Evaluation of 1,3-Diarylpropenones as Dual Inhibitors of HIV-1 Reverse Transcriptase. ChemMedChem;9 (8):1869-79.

[231] Paris KA, Haq O, Felts AK, Das K, Arnold E, Levy RM (**2009**). Conformational landscape of the human immunodeficiency virus type 1 reverse transcriptase non-nucleoside inhibitor binding pocket: lessons for inhibitor design from a cluster analysis of many crystal structures. Journal of medicinal chemistry;52 (20):6413-20.

[232] Barnett-Norris J, Guarnieri F, Hurst DP, Reggio PH (**1998**). Exploration of biologically relevant conformations of anandamide, 2-arachidonylglycerol, and their analogues using conformational memories. Journal of medicinal chemistry;41 (24):4861-72.

[233] Sauton N, Lagorce D, Villoutreix BO, Miteva MA (**2008**). MS-DOCK: accurate multiple conformation generator and rigid docking protocol for multi-step virtual ligand screening. BMC bioinformatics;9 (1):1.

[234] Plewczynski D, Michał Łaźniewski, Augustyniak, R, Ginalski K (**2011**). Can we trust docking results? Evaluation of seven commonly used programs on PDBbind database. Journal of computational chemistry;32 (4):742-55.

[235] Perola E, Walters WP, Charifson PS (**2004**). A detailed comparison of current docking and scoring methods on systems of pharmaceutical relevance. Proteins: Structure, Function, and Bioinformatics;56 (2):235-49.

[236] Corona A, Meleddu R, Esposito F, Distinto S, Bianco G, Masaoka T, Maccioni E, Menendez-Arias L, Alcaro S, Le Grice SFJ (**2016**). Ribonuclease H/DNA Polymerase HIV-1 Reverse Transcriptase Dual Inhibitor: Mechanistic Studies on the Allosteric Mode of Action of Isatin-Based Compound RMNC6. PloS one;11 (1):e0147225.

[237] Yonetani T (**1982**). The Yonetani-Theorell graphical method for examining overlapping subsites of enzyme active centers. Methods in enzymology;87:500-9.

[238] M. Nishizawa MT, K.Hayashi. (**1990**). Phytochemistry;29:2645-9.

[239] Tadrent W, Alabdul Magid A, Kabouche A, Harakat D, Voutquenne-Nazabadioko L, Kabouche Z (**2016**). A new sulfonylated flavonoid and other bioactive compounds isolated from the aerial parts of *Cotula anthemoides* L. Natural Product Research:1-9.

[240] Oguakwa JU, Galeffi C, Nicoletti M, Messana I, Marini-Bettolo GB (**1986**). Research on African Medicinal Plants. XI1 8-Hydroxycolumbin, A New Furanoid Diterpene from *Chasmanthera dependens*. Planta medica;52 (03):198-9.

[241] Patra A, Mitra AK (**1981**). Constituents of *Acorus calamus*: structure of acoramone. Carbon-13 NMR spectra of cis-and trans-asarone. Journal of natural products;44 (6):668-9.

[242] Wu Y-C, Chang G-Y, Ko F-N, Teng C-M (**1995**). Bioactive constitutents from the stems of *Annona montana.* Planta medica;61 (02):146-9.

[243] Mitsumasa Haruna TK, Kazuo Ito, Hiroyuki Murata (**1982**). Balanophonin, a new neo-lignan from *Balanophora japonica* Makino. Chemical and pharmaceutical bulletin;30 (4):1525-7.

[244] Barrero AF, HaÃdour A, Munoz-Dorado M, Akssira M, Sedqui A, Mansour I (**1998**). Polyacetylenes, terpenoids and flavonoids from *Bupleurum spinosum*. Phytochemistry;48 (7):1237-40.

[245] Liu K, Lota ML, Casanova J, Tomi F (**2009**). The essential oil of *Bupleurum fruticosum* L. from Corsica: a comprehensive study. Chemistry & biodiversity;6 (12):2244-54.

[246] G.M. Massanet FMG, Z.D. Joerge, L.G. Casalvaquez (**1997**). Phytochemistry;44:173-9.

[247] L. Pistelli ARB, A. Bertoli, I. Morelli, A. Marsili (**1995**). J. Nat. Prod;58:112-6.

[248] P. Bremner ST, H. Birkmayer, B.L. Fiebickh, M. Heinrich (**2004**). Planta Medica;70:914-8.

[249] Kawazu K, Ohigashi H, Mitsui T (**1968**). The piscicidal constituents of *Calophyllum inophyllum* linn. Tetrahedron letters;9 (19):2383-5.

[250] Su B-N, Takaishi Y, Duan H-Q, Chen B (**1999**). Phenylpropanol derivatives from *Morina chinensis*. Journal of natural products;62 (10):1363-6.

[251] Zhu M, Song Y, Cao Y (**2007**). A fast and convenient heck reaction in water under microwave irradiation. Synthesis;2007(06):853-6.

[252] Feliciano AS, Medarde M, Lopez JL, Del Corral JMM, Barrero AF (**1986**). Two new cinnamyl isovalerate derivatives from *Juniperus thurifera* leaves. Journal of natural products;49 (4):677-9.

[253] Satoh A, Utamura H, Nakade T, Nishimura H (**1995**). Absolute configuration of a new mosquito repellent,(+)-eucamalol and the repellent activity of its epimer. Bioscience, biotechnology, and biochemistry;59 (6):1139-41.

[254] Da Costa L, Roche M, Scheers E, Coluccia A, Neyts J, Terme T, Leyssen P, Silvestri R, Vanelle P (**2016**). VP1 crystal structure-guided exploration and optimization of 4, 5-dimethoxybenzene-based inhibitors of rhinovirus 14 infection. European journal of medicinal chemistry;115:453-62.

[255] Roche M, Lacroix C, Khoumeri O, Franco D, Neyts J, Terme T, Leyssen P, Vanelle P (**2014**). Synthesis, biological activity and structure-activity relationship of 4, 5-dimethoxybenzene derivatives inhibitor of rhinovirus 14 infection. European journal of medicinal chemistry;76:445-59.

[256] Guillén-Villar RC, Vargas-A•lvarez Y, Vargas R, Garza J, Matus MH, Salas-Reyes M, Domínguez Z (**2015**). Study of the oxidation mechanisms associated to new dimeric and trimeric esters of ferulic acid. Journal of Electroanalytical Chemistry;740:95-104.

[257] Minguzzi S, Barata LES, Shin YG, Jonas PF, Chai H-B, Park EJ, Pezzuto JM, Cordell GA (**2002**). Cytotoxic withanolides from *Acnistus arborescens*. Phytochemistry;59 (6):635-41.

[258] Katagiri Y, Mizutani J, Tahara S (**1997**). Ferulic acid esters of unsaturated higher alcohols from *Lupinusluteus* roots. Phytochemistry;46 (2):347-52.

[259] Neogi P, Kawai M, Butsugan Y, Mori Y, Suzuki M (**1988**). Withacoagin, a new withanolide from *Withania coagulans* roots. Bulletin of the Chemical Society of Japan;61 (12):4479-81.

[260] Esposito F, Sanna C, Del Vecchio C, Cannas V, Venditti A, Corona A, Bianco A, Serrilli AM, Guarcini L, Parolin C (**2013**). *Hypericum hircinum* L. components as new single-molecule inhibitors of both HIV-1 reverse transcriptase-associated DNA polymerase and ribonuclease H activities. Pathogens and disease;68 (3):116-24.

[261] Meleddu R, Distinto S, Corona A, Bianco G, Cannas V, Esposito F, Artese A, Alcaro S, Matyus P, Bogdan D (**2015**). (3Z)-3-(2-[4-(aryl)-1, 3-thiazol-2-yl] hydrazin-1-ylidene)-2, 3-dihydro-1H-indol-2-one derivatives as dual inhibitors of HIV-1 reverse transcriptase. European journal of medicinal chemistry;93:452-60.

[262] Xu L, Grandi N, Del Vecchio C, Mandas D, Corona A, Piano D, Esposito F, Parolin C, Tramontano E (**2015**). From the traditional Chinese medicine plant *Schisandra chinensis* new scaffolds effective on HIV-1 reverse transcriptase resistant to non-nucleoside inhibitors. Journal of Microbiology;53 (4):288-93.

[263] Mohamadi F, Richards NGJ, Guida WC, Liskamp R, Lipton M, Caufield C, Chang G, Hendrickson T, Still WC (**1990**). MacroModel-an integrated software system for modeling organic and bioorganic molecules using molecular mechanics. Journal of computational chemistry;11 (4):440-67.

[264] Halgren TA (**1996**). Merck molecular force field. II. MMFF94 van der Waals and electrostatic parameters for intermolecular interactions. Journal of computational chemistry;17 (5-6):520-52.

[265] Still WC, Tempczyk A, Hawley RC, Hendrickson T (**1990**). Semianalytical treatment of solvation for molecular mechanics and dynamics. Journal of the American Chemical Society;112 (16):6127-9.

[266] Schrödinger L. QMPolarized protocol NY, USA.

[267] McDonald DQ, Still WC (**1992**). AMBER torsional parameters for the peptide backbone. Tetrahedron letters;33 (50):7743-6.

[268] PyMOL MGSS, LLC.

[269] Schrödinger LLC. MG (**2013**). New York, USA.

[270] Tintori C, Corona A, Esposito F, Brai A, Grandi N, Ceresola ER, Clementi M, Canducci F, Tramontano E, Botta M (**2016**). Inhibition of HIV-1 Reverse Transcriptase Dimerization by Small Molecules. ChemBioChem;17 (8):683-8.

[271] Denizot F, Lang R (**1986**). Rapid colorimetric assay for cell growth and survival: modifications to the tetrazolium dye procedure giving improved sensitivity and reliability. Journal of immunological methods;89 (2):271-7.

[272] Jensen NP, Ager AL, Bliss RA, Canfield CJ, Kotecka BM, Rieckmann KH, Terpinski J, Jacobus DP (**2001**). Phenoxypropoxybiguanides, prodrugs of DHFR-inhibiting diaminotriazine antimalarials. Journal of medicinal chemistry;44 (23):3925-31.

[273] Bernard AM, Cabiddu MG, De Montis S, Mura R, Pompei R (**2014**). Synthesis of new compounds with promising antiviral properties against group A and B Human Rhinoviruses. Bioorganic & medicinal chemistry;22 (15):4061-6.

[274] Laconi S, Madeddu MA, Pompei R (**2011**). Study of the biological activity of novel synthetic compounds with antiviral properties against human rhinoviruses. Molecules;16 (5):3479-87.

[275] Zeljković SĆ, Topčagić, A., Požgan, F., Štefane, B., Tarkowski, P., & Maksimović, M. (**2015**). Antioxidant activity of natural and modified phenolic extracts from Satureja montana L. Industrial Crops and Products;76:1094-9.

[276] Brand-Williams W, Cuvelier M-E, Berset C (**1995**). Use of a free radical method to evaluate antioxidant activity. LWT-Food science and Technology;28 (1):25-30.

[277] Scalzo J, Politi A, Pellegrini N, Mezzetti B, Battino M (**2005**). Plant genotype affects total antioxidant capacity and phenolic contents in fruit. Nutrition;21 (2):207-13.

[278] Dinis TCP, Madeira VtMC, Almeida LM (**1994**). Action of phenolic derivatives (acetaminophen, salicylate, and 5-aminosalicylate) as inhibitors of membrane lipid peroxidation and as peroxyl radical scavengers. Archives of biochemistry and biophysics;315 (1):161-9.

Publications and Presentations

Publications

1) **Vijay P. Sonar** , Angela Corona , Simona Distinto , Elias Maccioni , Rita Meleddu , Benedetta Fois , Costantino Floris , Nilesh V. Malpure , Stefano Alcaro , Enzo Tramontano , Filippo Cottiglia. Natural product inspired esters and amides of ferulic and caffeic acid as dual inhibitors of HIV-1 reverse transcriptase. European Journal of Medicinal chemistry, 130 (2017):248-260.

Oral presentation

1) **Vijay Sonar**. Discovery of Natural Ester of Ferulic acid as a Single Inhibitor of HIV-1 RT and Synthesis of its Dual Inhibitor Analogues. MuTaLig cost action CA15135 WG meeting 2016, Budapest, Hungary (November, 2016).

Poster presentation

1) **V. Sonar**, E. Tramontano, A. Corona, F. Esposito, C. Floris, E. Maccioni, S. Distinto, Filippo Cottiglia. Bioguided Isolation of Triterpenoids and Phenylpropanoids from the Leaves of *Ocimum sanctum* Inhibiting the HIV-1 RT associated RNase H function. 5th meeting of the Paul Ehrlich MedChem Euro-PhD network, Cracovia, Poland (July, 2015).

2) **V. Sonar**, S. Ruiu , A. Orrù , C. Floris , N. Anzani , F. Cottiglia. Withanolides and Alkaloids from *Withania somnifera* roots with binding affinity to opioid, cannabinoids and GABAergic receptors. 63rd, International congress and annual meeting of the society for medicinal plant and natural product research, Budapest, Hungary (August, 2015).